MITOCHONDRIA AS A CRITICAL NEXUS POINT IN MEDIATING THC-INDUCED

TROPHOBLAST DYSFUNCTION: AN IN VITRO STUDY

BY:

O'LLENECIA S. WALKER

B.Sc., York University, 2005

M.Sc., York University, 2007

A Thesis Submitted to the School of Graduate Studies in Partial Fulfillment of the Requirements

for the Degree Doctor of Philosophy

DESCRIPTIVE NOTES

DOCTOR OF PHILOSOPHY (2020), McMaster University, Hamilton, Ontario (Medical Sciences)

DISSERTATION TITLE:	Mitochondria as a critical nexus point in mediating THC-induced trophoblast dysfunction: An in vitro study
AUTHOR:	O'Llenecia S. Walker, BSc, MSc (York University)
DISSERTATION ADVISOR:	Dr. Sandeep Raha
NUMBER OF PAGES:	xxvi, 220

LAY ABSTRACT

Cannabis is commonly used by pregnant women. Fetal exposure to cannabis and its components can impair fetal growth and neurological development. These negative fetal outcomes may be the result of poor placental formation, due to placental cell exposure to cannabis and its psychoactive component, delta-9-tetrahydrocannabinol (THC). Importantly, THC can also target intracellular organelles, like the mitochondria which are known as the "powerhouses" of the cell. Few studies have investigated the direct effects of THC on placental development. The purpose of this study was to determine how THC exposure to placental cells may alter their function. We found that THC impaired processes that allow placental attachment to the uterus and form a protective barrier, and compromised mitochondrial function, which are important for placental formation. These findings serve to inform scientists and doctors, thus stimulating the creation of new ideas and methods to further explore the impact of THC on pregnancy outcomes.

ABSTRACT

The etiology of many gestational disorders is still unknown. However, insufficient trans-placental passage of nutrients and wastes due to poor placentation is characteristic of several pathologies and may be due, in part, to altered function of placental mitochondria. Mitochondrial activity is essential in pregnancy because it sustains the metabolic activity of the placenta throughout gestation. Exposure to stressors that perturb processes governing placentation, including maternal drug use, can negatively impact fetal development.

Cannabis use is prevalent during pregnancy. The psychoactive constituent, delta-9-tetrahydrocannbinol (THC), can cross the placenta to affect placental and fetal physiology. Importantly, cannabinoid receptors have been reported on trophoblast cells, and on mitochondria which are abundant in placentae. It has been reported that THC may target the mitochondria in various tissue types, including placental tissue, and alter its function. However, few studies have addressed the physiological control of mitochondria within the placenta, an organ that is critical for fetal growth and pregnancy maintenance.

I investigated the role of mitochondria in trophoblast differentiation and syncytialization using rotenone, a complex I inhibitor. Subsequently, I investigated the role of THC on two important aspects of placentation – invasion and syncytialization – using placental trophoblast cells HTR8/SVneo and BeWo, respectively. In response to rotenone and THC, there was increased ROS production, oxidative stress, and altered transcriptional markers favouring mitochondrial fragmentation. Treatment with 20μM THC for 48 hours led to reduced mitochondrial respiration, ATP production and loss of mitochondrial membrane polarity. Critically, these THC-induced mitochondrial changes occurred concomitant with evidence of reduced trophoblast invasion and syncytialization. Furthermore, THC exposure reduced levels of human chorionic gonadotropin, human placental lactogen and insulin-like growth factor 2, which are growth factors necessary for

fetal development. Placental mitochondrial dysfunction, particularly when THC-induced, may be critical in a range of gestational disorders which have important implications for maternal and fetal/offspring health.

PREFACE

Chapter 3 has been published

Walker OS, Ragos R, Wong MK, Adam M, Cheung A, Raha S. Reactive oxygen species from mitochondria impacts trophoblast fusion and the production of endocrine hormones by syncytiotrophoblasts. *PLoS One* 15:2, e0229332 (2020).

I conducted most of the experiments and statistical analyses. I wrote the manuscript which was further refined by Dr. Sandeep Raha.

Chapter 4 has been published

Walker OS, Ragos R, Gurm H, Lapierre M, May LL, Raha S. Delta-9-tetrahydrocannabinol disrupts mitochondrial function and inhibits syncytialization in human placental BeWo cells. *Physiological Reports* 8:13, e14476 (2020).

I designed and conducted the experiments and performed the data analyses. I wrote the manuscript which was revised by Dr. Sandeep Raha.

Chapter 5 is under review (*Scientific Reports*)

Walker OS, Gurm H, Sharma R, Verma N, May LL, Raha S. Delta-9-tetrahydrocannabinol inhibits invasion of HTR8/SVneo human extravillous trophoblast cells and negatively impacts mitochondrial function.

I designed and conducted all the experimental testing and subsequent analyses. I wrote the manuscript with revisions by Dr. Sandeep Raha.

DEDICATION

I dedicate this dissertation to my sons, Julian (age 7) and Jackson (age 4). You both are the reason I began this academic journey, and it is for *you* that I saw it to its completion. I love you guys.

ACKNOWLEDGEMENTS

My supervisor, Dr. Sandeep Raha, from the beginning you had faith in me and my resolve to complete my doctoral studies. Thank you for helping me think more critically about my data. You have been incredibly supportive of me both academically and personally, and for that I am forever grateful.

To the Medical Science program and the School of Graduate Studies, thank you for addressing all my inquiries throughout the process of obtaining my degree.

My committee members Dr. Alison C. Holloway and Dr. Ali Ashkar, thank you for your insights, directions for change, academic and personal support. Thank you, Dr. Thomas J. Hawke, for your academic support and advisement.

To my Raha lab family, Holloway and Obeid/Timmons lab cousins, both past and present, thank you for creating a jovial, and supportive atmosphere. A special thank you to my undergraduate learners whom I have mentored but inadvertently taught me so much. An extra special thank you is extended to Linda May. In addition to your help with the OCR data acquisition, you have been and continue to be a phenomenal researcher, teacher of all things complicated and best of all a great friend.

♥ To my Mom, Dad, and brother, Remon, thank you for encouraging me to return to school to pursue my PhD following a 9 year academic hiatus, and steadfastly supporting me throughout the various ups and downs; I love you dearly. Thank you to my sons, Julian & Jackson, for letting me do my "homework" and being my dutiful audience when practicing for a lecture or presentation; I love you my BooBears. To my friends Barkha, Dorcas, Leah, Maria, Natasha, Talwinderjit, Gregory, Hashim, Nnamdi and Stephen, thank you all for your "cheerleader-like" encouragement throughout my academic journey; one love. My best friend, fellow foodie and fiancé, Kevin, thank you for your love, support, and unwavering belief in me during my studies; I love you. ♥

TABLE OF CONTENTS

DESCRIPTIVE NOTES ii

LAY ABSTRACT iii

ABSTRACT iv

PREFACE vi

DEDICATION vii

ACKNOWLEDGEMENTS viii

TABLE OF CONTENTS ix

LIST OF FIGURES xv

LIST OF TABLES xviii

LIST OF ABBREVIATIONS AND SYMBOLS xix

DECLARATION OF ACADEMIC ACHIEVEMENT xxvi

1.   CHAPTER ONE: INTRODUCTION 1

    1.1   PLACENTA 1

        1.1.1   Anatomy and physiology of human placental development 1

        1.1.2   Invasion 2

            1.1.2.1   Invasion and spiral artery remodelling 2

            1.1.2.2   MMPs and their inhibitors 4

        1.1.3   Syncytialization 7

            1.1.3.1   Human endogenous retroviruses 8

            1.1.3.2   Syncytin-1 and syncytin-2 in human placentation 8

            1.1.3.3   Role of syncytins in proliferation 10

            1.1.3.4   Role of syncytins in immunity 10

            1.1.3.5   Role of syncytins in PE and IUGR 11

            1.1.3.6   Function of some of the major hormones produced by syncytiotrophoblasts . 12

    1.2   MITOCHONDRIA 15

        1.2.1   Mitochondrial morphology 15

        1.2.2   Mitochondrial function 17

        1.2.3   Mitochondrial proton leak 19

        1.2.4   Oxidative stress 20

LIST OF FIGURES

Chapter 6

Appendix A

Appendix B

LIST OF TABLES

LIST OF ABBREVIATIONS AND SYMBOLS

11-OH-THC	11-hydroxy-Δ^9-tetrahydrocannabinol
2-AG	2-arachidonoylglycerol
AC	adenylyl cyclase
ADP	adenosine diphosphate
AEA	arachidonoyl ethanolamine; anandamide
ANOVA	analysis of variance
ANT	adenine nucleotide translocase
ASCT2	alanine, serine, cysteine-preferring transporter 2
ATP	adenosine triphosphate
BCA	bicinchoninic acid
BHO	butane hash oil
BSA	bovine serum albumin
Ca^{2+}	calcium
cAMP	cyclic adenosine monophosphate
CB1	cannabinoid receptor 1
CB2	cannabinoid receptor 2
CBD	cannabidiol
cDNA	complimentary deoxyribonucleic acid
CO_2	carbon dioxide
CT	cytotrophoblasts
CuZn	copper zinc
CYP	cytochromes P450 enzymes
DAG	diacylglycerol

DAGL	diacylglycerol lipase
DAPI	4',6-diamidino-2-phenylindole
DCFDA	2',7'-dichlorofluorescin diacetate
ddH$_2$O	double distilled water
DMSO	dimethyl sulfoxide
DNA	deoxyribonucleic acid
DPBS	Dulbecco's phosphate buffered saline
DRP1	dynamin-related protein 1
eCB	endocannabinoid
ECM	extracellular matrix
ECS	endocannabinoid system
eEVT	endothelial extravillous trophoblasts
EGF	epidermal growth factor
ELISA	enzyme-linked immunoprecipitation assay
EMT	endocannabinoid membrane transporter
ETC	electron transport chain
EVT	extravillous trophoblast
FAAH	fatty acid amide hydrolase
FADH$_2$	flavin adenine dinucleotide + hydrogen
Fe	iron
FeS	iron sulphur
Fis1	fission protein 1
FLAT	FAAH-like anandamide transporter protein
FMN	flavin mononucleotide

FSK	forskolin
G1/S/G2/M	cell cycle phases gap 1, DNA synthesis, gap 2, mitosis
GAPDH	glyceraldehyde 3-phosphate dehydrogenase
GCM1	glial cell missing 1
GDP	guanosine diphosphate
GFR	growth factor reduced
GPCR	G protein-coupled receptor
GP-NAE	glycerophospho-N-acylethanolamine
GSH	glutathione
GSK-3β	glycogen synthase kinase 3 beta
GSSG	glutathione disulfide
GTP	guanosine triphosphate
GTPase	guanosine triphosphate hydrolase
H^+	hydrogen ion
H_2O	water
H_2O_2	hydrogen peroxide
hCG	human chorionic gonadotropin
HERV	human endogenous retrovirus
HERV-FRD	syncytin-2
HERV-W	syncytin-1
HNE	hydroxynonenal
hPGH	human placental growth hormone
hPL	human placental lactogen
HSP	heat shock protein

iEVT	interstitial extravillous trophoblasts
IFN	interferon
IGF1	insulin-like growth factor
IL	interleukin
IMM	inner mitochondrial membrane
IMS	intermembrane space
IUGR	intrauterine growth restriction
JAK-STAT	Janus kinase-signal transducer and activator of transcription
JC-1	tetraethylbenzimidazolylcarbocyanine iodide
kDa	kilodalton
LDH	lactate dehydrogenase
LIF	leukemia inhibitory factor
LPS	lipopolysaccharide
MAGL	monoacylglycerol lipase
MAPK	mitogen-activated protein kinase
Mdivi-1	mitochondrial division inhibitor 1
MeOH	methanol
Mff	mitochondrial fission factor
MFN	mitofusin
MFSD2	major facilitator superfamily domain containing 2
Mid49	mitochondrial dynamics protein of 49 kDa
Mid51	mitochondrial dynamics protein of 51 kDa
MMP	matrix metalloproteinase
Mn	manganese

mRNA	messenger ribonucleic acid
mtCB1	mitochondrial cannabinoid receptor 1
MTS	3-(4,5-dimethylthiazol-2-yl)-5-(3-carboxymethoxyphenyl)-2- (4-sulfophenyl)-2H-tetrazolium
NAC	N-acetyl cysteine
NADH	nicotinamide adenine dinucleotide + hydrogen
NaOH	sodium hydroxide
NAPE	N-acyl phosphatidylethanolamine
NAT	N-acyltransferase
NDUFS2	NADH:ubiquinone oxidoreductase core subunit S2
NICU	neonatal intensive care unit
NSAIDs	non-steroidal anti-inflammatory drugs
O_2	molecular oxygen
OMM	outer mitochondrial membrane
OPA1	optic atrophy 1
OXPHOS	oxidative phosphorylation
$P450_{scc}$	cytochrome cholesterol side-chain cleavage enzyme
pAEA	phospho-N-arachidonoylethanolamine
PBS-T	phosphate buffered saline with tween
PE	preeclampsia
PFA	paraformaldehyde
PHA	phytohemagglutinin
P_i	inorganic phosphate
PKA	protein kinase A

PLC	phospholipase C
PLD	phospholipase D
PND	post-natal day
PVDF	polyvinylidene fluoride
RCC1	respiratory chain complex 1
RDR	retroviral mammalian type D receptor
RIPA	radioimmunoprecipitation assay
RNA	ribonucleic acid
ROS	reactive oxygen species
ROT	rotenone
RT-PCR	reverse transcription polymerase chain reaction
sAC	soluble adenylyl cyclase
SEM	standard error of the mean
siRNA	small interfering ribonucleic acid
SLC1A5	solute-linked carrier family A1 member 5
SOD	superoxide dismutase
ST	syncytiotrophoblasts
TBHP	tert-Butyl hydroperoxide
TBS	tris buffered saline
TBS-T	tris buffered saline with tween
THC	Δ-9-tetrahydrocannabinol
THC-A	tetrahydrocannabinolic acid
THC-COOH	11-nor-9-carboxy-Δ-9-tetrahydrocannabinol
TIMP	tissue inhibitor of matrix metalloproteinase

TNF	tumour necrosis factor
UCPs	uncoupling proteins
UGT	uridine-diphosphate glucuronosyltransferases
VEGF	vascular endothelial growth factor
Wnt	Wingless/Integrated
$\Delta\Delta$Ct	comparative Ct method
$\Delta\Psi$m	mitochondrial membrane potential

DECLARATION OF ACADEMIC ACHIEVEMENT

O'Llenecia S. Walker (OSW) and Dr. Sandeep Raha (SR) planned and executed this research with guidance from Dr. Alison C. Holloway (ACH) and Dr. Ali Ashkar (AA). All laboratory experiments were performed by OSW with the assistance of Harmeet Gurm, Rehginald Ragos, Mariah Lapierre, Navkiran Verma, and Reeti Sharma. Linda L. May performed the Seahorse Oxygen Consumption Rate protocols. Data analyses were performed by OSW and SR. OSW also prepared an invited review article[1]. OSW wrote this dissertation with the assistance of SR, ACH and AA.

1. CHAPTER ONE: INTRODUCTION

1.1 PLACENTA

1.1.1 Anatomy and physiology of human placental development

Placentation is a complex event. As a transient organ formed from maternal and embryonic tissues, the placenta exhibits multiple functions which are critical for the establishment and maintenance of pregnancy. The placenta, composed of several cell types, is a vital connecting organ between the maternal decidua and the embryo/fetus[2]. It supports the developing fetus by supplying nutrients, eliminating waste products from the fetus, and allowing gas exchange via the maternal blood supply. The placenta also protects the fetal allograft from maternal immune rejection, as the fetus presents with foreign paternal antigens[3]. The fetal cells in direct contact with the mother in the uterus are trophoblast cells, which are derived from the trophectoderm, the outer layer surrounding the pre-implantation embryo/blastocyst which gives rise to the various cytotrophoblast subpopulations (Figure 1A). Although maternal and fetal circulations do not mix, transient exchange of cells occurs, particularly during parturition[3]. To ensure sufficient delivery of maternal nutrients and oxygen to the placenta, a substantial increase in uterine blood flow is needed for normal fetal growth. This is achieved by invasion of trophoblast cells through the endometrial stroma and into arteries. Fully developed terminal villi are the functional unit of materno-fetal oxygen exchange and nutrient transport. Maternal blood is thus in direct contact with trophoblast cells (hemochorial placentation). Trophoblast invasion is always accompanied by dramatic changes to the uterine mucosa known as decidualization (cellular and vascular changes of the uterine epithelium), which in part helps to control the depth of trophoblast invasion[2–4].

1.1.2 Invasion

1.1.2.1 Invasion and spiral artery remodelling

Trophoblast invasion is a tightly regulated balance of competing mechanisms with multiple overlapping control systems. For successful invasion to occur, trophoblast cells must transform the maternal spiral arteries, tolerate hypoxia, proliferate and undergo apoptosis, differentiate, attach to and digest the extracellular matrix (ECM)[5] and interact with the maternal immune system[3].

During early human pregnancy, extravillous trophoblasts (EVTs) plug the maternal vessels generating hypoxic conditions and later displace maternal endothelial cells resulting in spiral artery remodelling[2,6]. EVTs from anchoring villi invade the decidualized endometrium and inner third of the myometrium (interstitial trophoblasts; iEVTs, which fuse and terminally differentiate to form giant cells) and migrate in a retrograde direction along the spiral arteries (endovascular trophoblasts; eEVTs) transforming them into large diameter vessels of low resistance[2,4]. This structural transformation is characterized by a gradual loss of the smooth muscle layer in the arterial walls which are subsequently replaced with amorphous fibrinoid material in which trophoblast cells are embedded (Figure 1B). These physiological changes are necessary for a successful pregnancy[2].
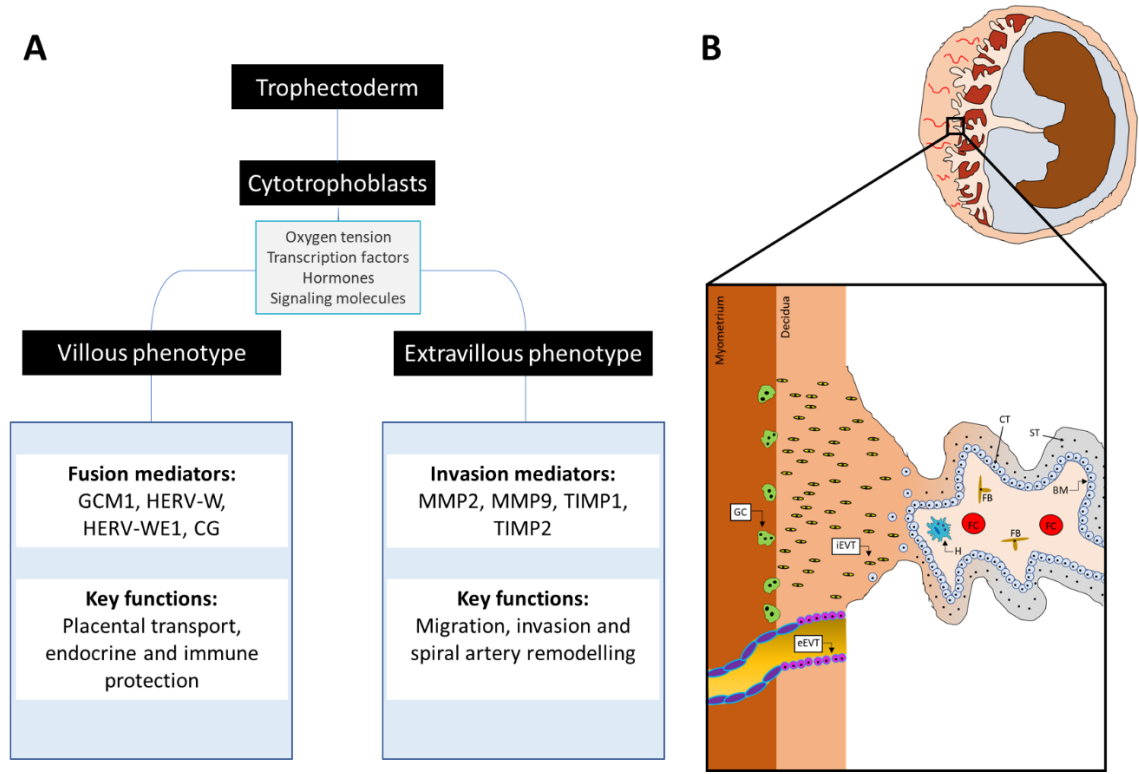
Figure 1. Schematic depiction of placenta formation and key mediators involved.

A. Main cytotrophoblast differentiation pathways and select transcriptional/functional mediators regulating trophoblast syncytialization and invasion. These differentiation events are tightly regulated by the interplay of oxygen tension, various transcription factors, hormones, and other signaling/growth factors. **B.** The placental villi are covered by villous trophoblast cells. Proliferation and differentiation of mononucleated cytotrophoblasts (CTs) by fusion gives rise to the overlying multinucleated syncytiotrophoblast (ST) layer. The core of each villus contains fetal capillaries (FC), fibroblasts (FB) and Hofbauer cells (H; fetal macrophages) which confers some protection to the fetus from vertical infections. The ST covers the floating villi which are bathed in maternal blood and creates the critical part of the materno-fetal interface. CT proliferation and detachment from the basement membrane and migration to the decidua gives rise to EVTs. Interstitial EVTs (iEVTs) invade and degrade the maternal decidua which is replaced by fibrinoid material. iEVTs move as far as the inner third of the myometrium where they terminally differentiate and fuse giving rise to placental-bed giant cells (GCs) and is the final differentiation step of the invasive pathway. Endothelial EVTs (eEVTs) form a plug in the maternal spiral arteries in early pregnancy to prevent premature blood flow. Once circulation is established, they replace the endothelial cells in the spiral arteries in a retrograde manner, destroying the smooth muscle layer, converting them to low-resistance, high-capacity arteries; this ensures proper oxygen and nutrient delivery to the fetus throughout gestation[2].

Failure of trophoblast invasion and spiral artery remodelling has been documented in preeclampsia (PE) and intrauterine growth restriction (IUGR) leading to significant maternal and perinatal morbidity[7]. Despite the importance of trophoblast invasion and vascular transformation, the exact mechanisms underlying these processes are still under investigation. Some of the physiological changes reported to control invasion and spiral artery remodelling include changes in expression of cell adhesion molecules, matrix metalloproteinases (MMPs) and their tissue inhibitors (TIMPs) and various cytokines, growth factors and their receptors[5,8].

Many elements of trophoblast invasion are similar to events that occur during tumor cell invasion[5,8]. The phenotypic change from carcinoma in situ to one that is invasive occurs when tumor cells acquire the ability to penetrate an epithelial basement membrane and invade the underlying stroma[9]. Likewise, after a brief adherent stage, cytotrophoblast cells penetrate the basement membrane of the uterine epithelial cells and invade the stroma and its associated arteries. These similarities suggest that the two invasive processes may share certain common mechanisms[8,10]. However, unlike tumor invasion, trophoblast invasion is tightly regulated, restricted spatially to the endometrium and inner third of the myometrium, and temporally to early pregnancy[5,10,11]. The direction of invasion seems to be determined by the expression of integrins within the decidual matrix surrounding the trophoblasts and the ability of these cells to produce MMP[8].

1.1.2.2 MMPs and their inhibitors

Transformation of the approximately 140 spiral arteries[5] and decidual adherence is precisely regulated by signaling events, autocrine and paracrine stimuli, specific protein recognition and immunological tolerance[5]. This event is influenced by promoting (cytokines, growth factors, MMPs) and inhibiting factors (TIMPs)[12]. The gelatinases (gelatinase A: MMP2: 72-kDa and

gelatinase B: MMP9: 92-kDa) which degrade collagen type IV, the main component of the basement membrane, are expressed by trophoblast cells and are therefore regarded as key enzymes in the trophoblast invasion process[10]. Several studies have shown that MMP2 and MMP9 synthesis and activation are required for the degradation of ECM components during trophoblast invasion[13–16] (Figure 1A).

MMPs are members of the metzincin superfamily of zinc-dependent endopeptidases that share homologous catalytic domains defined by a zinc-binding motif within the catalytic domain and an invariant downstream met-turn[17] that provides the hydrophobic base for the zinc binding site[17–20]. The approximately 23 mammalian MMPs are secreted and membrane-tethered extracellular enzymes, described as ECM-remodelling enzymes, that degrade protein components of the ECM[19]. With a diverse substrate repertoire, along with non-proteolytic functions[17], MMPs are crucial for extracellular remodeling and modulate various physiological (e.g. placentation) and pathophysiological (e.g. cancer) processes[12]. The MMP pro-domain contains a cysteine residue that binds zinc in the active site and maintains the MMP as an inactive zymogen[18]. Activation involves enzymes that cleave the cysteine residue[18]. MMP activity is balanced by endogenous inhibitors such as α-macroglobulin, in plasma, and TIMPs[18]. The four mammalian TIMPs tightly bind active MMPs in a non-covalent 1:1 stoichiometric interaction that involves the N-terminal TIMP inhibitory domain wedging into the MMP active site chelating the zinc ligand and displacing the water molecule required for peptide bond hydrolysis[17,20,21].

The importance of MMPs is further highlighted by the fact that aberrant MMP downregulation underlies numerous pathological disorders, including PE and IUGR; while upregulation leads to placenta accreta, increta or percreta (depending on the depth of invasion)[5] and tumour invasiveness[22]. Nissi et al (2013) report that a high ratio of serum MMP2/TIMP2, determined by enzyme-linked immunoprecipitation assay (ELISA), was associated with

miscarriage in the study patients (from 7-11 weeks gestation)[23]. Additionally, an in vivo study conducted by Plaks et al (2013) using MMP9-null mice demonstrates a phenotypic connection between MMP9 insufficiency and early manifestations of PE[7]. Plaks et al (2013) report reduced serum levels of total vascular endothelial growth factor (VEGF; involved in placental vascularization) by embryonic day 12.5 (E12.5) and gestational proteinuria (E13.5, peaking at E18.5), both of which returned to normal by post-natal day 10 (PND10). Furthermore, there were significant increases in systolic blood pressure in the MMP9-null mice throughout gestation which was associated with fetal demise in this cohort[7]. Results of studies carried out in late pregnancy are consistent with these findings from early pregnancy. Expression of different MMPs (MMP2, -8, -9, and -11) were downregulated in placental tissues from human pregnancies complicated with PE at >35 weeks of gestation compared to uncomplicated pregnancies[24,25]. Additionally, and importantly, Shokry et al (2009) further report that the expression of MMP9 was absent or markedly reduced in preeclamptic placentae[25]. The collective findings of aberrant MMP and TIMP expression can be related to insufficient trophoblast invasion and subsequently poor placentation.

In addition to MMPs and TIMPs, it is known that migration and invasion of EVTs is regulated by several growth factors and cytokines. The signal transducers and activators of transcription (STATs) are members of a ubiquitously expressed family of transcription factors activated in response to growth factors and cytokines[26]. An important candidate pathway mediating cytokine signal transduction in trophoblasts is the Janus kinase-signal transducer and activator of transcription (JAK-STAT) pathway. Several cytokines which are present in the decidua (e.g. interleukin 6 and 11; IL-6, IL-11, and leukemia inhibitory factor; LIF) have been described to use JAK-STAT pathways for signalling and may therefore influence invasiveness[8]. The current literature on functions of STAT3 in human trophoblast cells indicates its involvement in regulation of invasiveness[8]. Upon ligand-receptor binding (e.g. cytokine receptor activation), receptor

subunits can undergo JAK-mediated phosphorylation. STAT3 can bind on the receptors' phosphorylated sites which subsequently leads to its activation. Once phosphorylated, STAT3 will dissociate from the receptor complex, and its phosphorylated site allows STAT3 to homodimerize. The STAT3 homodimer can translocate to the nucleus where it can carryout its specific functions[8]. TIMP1 expression is directly influenced by STAT3, as the TIMP1 promoter was shown to contain STAT3 recognition elements[27,28]. Additionally, the MMP9 promoter region also contains multiple binding sites for STAT3[29], which when activated leads to increased MMP9 transcription and secretion[29] and downregulation of TIMP1 and is correlated to an invasive phenotype[8]. Furthermore, increasing evidence demonstrates that STATs also regulate other MMPs[26]. Together, the data suggests that JAK-STAT activation leads to a shift in the balance of the MMP9/TIMP1 ratio such that invasion can occur. When JAK-STAT signaling is inhibited, transcription of invasion promoting genes is reduced[6], which may provoke pathological processes such as disorders related to poor placentation[8].

1.1.3 Syncytialization

Cell fusion is an essential process which occurs during mammalian development for the purposes of fertilization, placentation (Figure 1), skeletal muscle development and osteoclast formation[30]. In the placenta, cell fusion follows cell adhesion by receptor-ligand interactions, various signalling molecules and alpha helical bundles formed by fusogenic proteins which brings the membranes of cytotrophoblasts into close proximity resulting in membrane fusion and the formation of the syncytiotrophoblast[31]. Among the many proteins involved in fusion events, syncytin proteins form similar alpha helical bundles[31] that allow the merging of two plasma membranes and are encoded by human endogenous retroviral (HERV) genes[30]. Syncytin proteins,

syncytin-1 and syncytin-2, belong to the HERV family and were initially identified in human placentae due to their fusogenic activities[31–33].

1.1.3.1 Human endogenous retroviruses

Infection of a host cell by exogenous retroviruses will cause the integration of retroviral DNA into the host cell's genome. Endogenous retroviral elements make up approximately 8% of the human genome[30,34]. Two retroviral proteins, syncytin-1 (HERV-W; ERVW-1) and syncytin-2 (HERV-FRD), were initially identified in human placenta. Syncytin proteins are mostly expressed in the trophoblastic layer, which is critical for normal placental function. Syncytin-1 is a glycoprotein with cell fusogenic activity. It binds to its receptor SLC1A5/ASCT2/RDR (a neutral amino acid transporter and type D mammalian retrovirus receptor) and promotes cytotrophoblast fusion to form the multinucleated syncytium[35,36]. The syncytin-2 receptor is a member of the carbohydrate transporter super family major facilitator superfamily domain containing 2 (MFSD2)[35,37]. Both syncytin proteins are involved in cell fusion, apoptosis, and immunosuppression in the human placenta. Altered expression of the syncytin proteins have been reported in placental pathologies[36].

1.1.3.2 Syncytin-1 and syncytin-2 in human placentation

Syncytin-1 was first identified in the syncytiotrophoblast of human placental villi[38]. Mi et al (2000) demonstrated that when syncytin-1 was transfected into COS cells (CV-1 in origin and carrying the SV40 genetic material), syncytia formed consisting of many aggregated nuclei surrounded by an extended cytoplasm[38]. When BeWo cells (trophoblast-derived choriocarcinoma cell line) were induced to fuse with 50 µM forskolin (FSK) and form syncytiotrophoblast-like cells,

a five-fold increase in BeWo cell fusion was correlated with increased ERVW-1 transcription[38]. Following the discovery of syncytin-1, Blond et al (2000) demonstrated that transfection of different cell lines with syncytin-1 resulted in syncytia formation via the interaction of syncytin-1 and its receptor, SLC1A5[32]. Therefore, a role for syncytin-1 in placental cytotrophoblast fusion along with its fusogenic properties in vitro is demonstrated[38].

Syncytin-2 interacts with a different receptor (MFSD2) than syncytin-1[30]. The amino acid sequence of syncytin-2 was analyzed and, like syncytin-1, it was demonstrated to have an immunosuppressive extracellular domain which may confer protection to the developing fetus against the maternal immune system[38].

After the identification of the fundamental fusogenic role of syncytins, notably syncytin-1, upstream components in this signaling pathway have since been identified, such as cAMP/PKA[39]. Primarily cAMP, MAPK, and Wnt signaling pathways orchestrate syncytialization of trophoblasts via the activation of glial cell missing 1 (GCM1) transcription factor which leads to the expression of syncytin-1, subsequently leading to fusion[6]. The ability of human trophoblasts to differentiate and fuse into a multinucleated syncytium while acquiring active endocrine functions is controlled by several factors, including hormones and cytokines[40]. Various cytokines (e.g. LIF) have been demonstrated to increase FSK-induced syncytialization of BeWo cells, via cAMP activation (triggered by first messenger activation of G_s-coupled G protein-coupled receptors) and is associated with activation of STAT3[40,41]. This was further demonstrated as JAK inhibition led to a reduction in FSK-induced BeWo cell fusion[40]. Although JAK-STAT signaling is described to increase trophoblast syncytialization, how it functions downstream to this effect remains to be fully elucidated.

1.1.3.3 Role of syncytins in proliferation

Syncytin 1 may be involved in the fusion of cytotrophoblasts and the proliferation of the cytotrophoblasts via cell cycle control mechanisms. Huang et al (2013) studied the role of syncytin-1 in trophoblast proliferation[42]. Syncytin-1 knockdown by siRNA significantly inhibited BeWo cell growth and DNA synthesis in vitro. At 72 hours post-transfection in syncytin-1 knockdown BeWo cells compared to control groups, there was a greater percentage of cells arrested in the G1 phase of the cell cycle and a decreased percentage of cells in the S and G2/M phases[42]. Because mononucleated cytotrophoblasts exit the cell cycle to differentiate into the multinucleated syncytiotrophoblast, they lose their proliferative capacity. When syncytin-1 protein expression is reduced, cell cycle arrest may occur in cytotrophoblasts. This will prevent adequate proliferation and lead to the absence of continuous fusion with the overlying syncytiotrophoblast, subsequently impairing proper formation of the syncytiotrophoblast layer[42]. These independent properties of syncytin 1 (fusogenic and non-fusogenic) can maintain a balance between the cytotrophoblast population and the overlying syncytiotrophoblast layer during human placental development[42].

1.1.3.4 Role of syncytins in immunity

The literature describes an immune regulatory function of syncytin-1 in vitro. Pro-inflammatory T helper 1 (Th1) cytokines (e.g. TNFα, IFNɣ and IL2) exert harmful effects on the developing fetus and are thus downregulated throughout gestation[43]. Indeed, Tolosa et al (2012) reported that lipopolysaccharide/phytohemagglutinin (LPS/PHA)-stimulated Th1 cytokine responses (specifically TNFα and IFNɣ) and chemokine CXCL10 were inhibited by a syncytin-1 recombinant ectodomain in a human blood culture system[43]. Additionally, BeWo cells treated with corticotropin-releasing hormone (CRH) increased secreted exosomal syncytin-1 protein expression

but not cellular syncytin-1[43]. Exosomes are small vesicles (30-100nm) responsible for intercellular communication and several biological processes[44]. In addition to syncytin-1, syncytin-2 is also detected at the surface of exosomes produced by placenta-derived villous trophoblasts[43,44]. Decreased syncytin-2 in serum-derived exosomes were found in PE patients when compared to control women[44]. These results suggest that the presence of syncytin-1 and -2 in placental exosomes might provide a mechanism by which syncytins reach and interact with target cells of the maternal immune system during pregnancy[43,44].

1.1.3.5 Role of syncytins in PE and IUGR

The potential role of syncytin-1 and -2 in placental pathologies, such as PE and IUGR, have been investigated. PE affects approximately 5-8% of all pregnancies[45]. PE is characterized by impaired spiral artery remodelling and insufficient placental circulation resulting in oxidative stress, hypoxia and endothelial dysfunction[46]. Several reports have demonstrated decreased expression and aberrant localization of syncytin-1 and -2 in PE placentae when compared to healthy controls[43,47–49]. In PE placentae, Chiang et al (2009) demonstrated reduced levels of GCM1, syncytin-1 and placental growth factor, all of which are crucial for the formation of the syncytiotrophoblast and placental vasculogenesis[48]. Hypoxia activates glycogen synthase kinase 3 beta (GSK-3β) in PE placentae, which subsequently phosphorylates GCM1, promotes its ubiquitination, subsequent degradation by the SCF^{FBW2} E3 ligase. Thus, the GCM1 target genes, i.e. syncytin-1 and syncytin-2, are likewise reduced[48]. The data also indicate an inverse correlation with disease severity and the expressions of syncytin-1 and -2 in isolated primary trophoblast cells from PE placentae[47]. Further, Vargas et al (2011) report a more dramatic decrease in syncytin-2 compared with syncytin-1in PE placentae[47].

The role of syncytin-1 and -2 in IUGR has also been studied. Biswas et al (2008) demonstrated that the surface area of chorionic villi, placental weights and volumes were significantly reduced in IUGR placentae compared to controls[50]. Despite decreases in placental weight, the placental to fetal weight ratio was unchanged. Thus, their findings of lower surface area of the chorionic villi, forming the materno-fetal interface, in IUGR compared to control placentae suggest that less oxygen and nutrients reached the fetuses of the IUGR group thus causing the intrauterine growth restriction[50]. Additionally, Ruebner et al (2010) report reduced levels of both syncytin-1 and -2 in IUGR placentae which may contribute to placental dysfunction in IUGR due to malformation of the interface[35]. Although dysregulation of syncytin-1 and -2 in PE placental pathology has been well documented, the role of syncytins in IUGR requires further investigation.

1.1.3.6 Function of some of the major hormones produced by syncytiotrophoblasts

The human placenta (fetal membranes and decidua) can be classified as an endocrine organ because of its ability to produce and secrete hormones which maintain and ensure the success of pregnancy. Placental hormones play critical roles during several gestational events, including implantation, placentation, vascular transformation, immune-protection, milk production and labour. These hormones can enter the fetal and maternal circulations to act upon their targets, or they may be produced and act locally within the uterus. Aberrant production of these hormones may impede these processes and negatively affect gestational outcomes[51,52].

While there are various structures from which the hormones of pregnancy are derived (i.e. relaxin derived from the corpus luteum[53], cortisol produced in the adrenal glands)[54], the focus here will be on the major hormones produced by the syncytial barrier and is summarized in Table 1.

Table 1. Major hormones produced by syncytiotrophoblasts

Hormone	Source(s)	Description	Key Functions
Human chorionic gonadotropin (hCG)	‣Syncytiotrophoblast, ‣EVTs, ‣Some tumour types[51,55]	‣Heterodimeric glycoprotein secreted mostly into the maternal circulation, ‣Peak concentrations at gestational week 10, falling progressively thereafter[51]	‣Maintains the viability of the corpus luteum, which releases progesterone, in early pregnancy, ‣Prevents myometrial contractions, ‣Stimulates cytotrophoblasts fusion into the syncytium[51,55]
Estrogen	‣Initially: corpus luteum, ‣Subsequently, syncytiotrophoblast[51]	‣Steroid hormone that increases throughout gestation and peaks at term, ‣Found in maternal and fetal circulations[51,56]	‣Facilitates implantation of the blastocyst, promotes decidualization and syncytialization, facilitates vascular remodelling and angiogenesis, promotes mammary gland development, ‣The peak at term stimulates myometrial contractions[51,56]
Progesterone	‣Weeks 1-8: corpus luteum (via hCG stimulation), ‣After ~week 8 to the end of gestation: syncytiotrophoblast[51]	‣Steroid hormone, ‣Progesterone = "Pro" "Gestation", ‣Produced in the mitochondria of syncytiotrophoblast from maternal cholesterol, ‣Found in maternal and fetal circulations, ‣Increases to a peak at ~ the last 4 weeks of gestation[4,51]	‣Promotes decidualization, ‣Increase uterine receptivity[57] ‣Prevents myometrial contractions, ‣Promotes mammary gland development and lipogenesis[51] ‣Promotes immunotolerance (e.g. reduced cytolytic activity of uterine natural killer cells)[51,58]
Human placental lactogen (hPL; also known as human chorionic somatomammotropin)	‣Syncytiotrophoblast, ‣EVT[51]	‣Polypeptide hormone released into both maternal and fetal circulations,	‣Regulates aspects of fetal and maternal metabolism, ‣Stimulates the production of insulin-like growth factors, insulin and pulmonary surfactant[51]

		‣Detected in the placenta at ~ the 2nd gestational week, ‣Progressively increases throughout gestation[51]	
Human placental growth hormone (hPGH)	‣Syncytiotrophoblast, ‣EVT[51]	‣Polypeptide hormone released into maternal circulation, ‣Levels detected at ~15-20 weeks gestation with significant increases into the third trimester[51]	‣Works with hPL to stimulate IGF production, ‣Promotes gluconeogenesis, lipolysis and anabolism, effectively increasing nutrient availability for fetal development[51] ‣Via autocrine mechanisms, stimulates in vitro invasion of primary EVTs via JAK/STAT activation[6]
Insulin-like growth factors (IGFs) I and II	‣Liver[59] ‣Syncytiotrophoblast, ‣Fetal tissues[4] ‣EVTs[60]	‣Polypeptide hormone, ‣Gradual increase in maternal circulation throughout gestation[51]	‣Regulates fetal and placental growth[61] ‣Promotes invasion[60] ‣Promotes cytotrophoblast proliferation and syncytialization[51]
Leptin	‣Adipocytes, ‣Syncytiotrophoblasts, ‣EVTs[51]	‣Peptide hormone, adipokine, ‣Released into maternal and fetal circulations[51]	‣Promotes cytotrophoblast proliferation and invasion, ‣Facilitates blastocyst implantation, ‣Mediates gestational immunomodulation, ‣Keeps myometrium quiet[51]
Adiponectin	‣Adipocytes, ‣Trophoblasts?[62]	‣Adipokine ‣Released into maternal circulation[62]	‣Promotes syncytialization[63] ‣Promotes migration and invasion of EVTs, ‣Reduces endocrine function of term syncytiotrophoblasts via reducing hCG, progesterone and hPL secretion[62]

1.2 MITOCHONDRIA

1.2.1 Mitochondrial morphology

Mitochondria are double membrane bound organelles with a corresponding intermembrane space. Each cell contains hundreds to thousands of mitochondria[64]. Although most of our genetic material is found tightly packaged on chromosomes in the nucleus, mitochondria contain their own circular DNA, thus making them semiautonomous. The central compartment is the matrix. The inner mitochondrial membrane (IMM) is arranged in folds, cristae, which increase the surface area available for energy production via the electron transport chain (ETC) and F_0-F_1 ATP synthase[65] in a process known as oxidative phosphorylation (OXPHOS). The outer mitochondrial membrane (OMM) houses porins which facilitate movement of ions in and out of the mitochondria (Figure 2A). The matrix contains free DNA and free ribosomes which facilitate lipid and protein synthesis and enzymes required for the Kreb's cycle[65–67].

Mitochondria are dynamic organelles that constantly undergo fission (fragmentation) and fusion (merging) to maintain a large functional mitochondrial network[68]. The list of proteins that facilitate fission and fusion is ever expanding but is primarily regulated by a few major constituents – namely guanosine triphosphatases (GTPases). Mitofusin-1 and -2 (MFN1 and MFN2) mediate fusion of the OMM and optic atrophy 1 (OPA1) promotes fusion of the IMM (Figure 2B). Dynamin-related protein 1 (DRP1) is a large cytoplasmic GTPase that controls fission of both mitochondrial membranes by translocating to the mitochondria and interacting with adaptor proteins (e.g. fission protein 1; Fis1). Once bound to the mitochondrial membrane, DRP1 assembles on the mitochondrion and constricts it to mediate fission[66,68,69]. DRP1 is recruited to mitochondrial membranes by accessory proteins Mid49, Mid51, and Mff. Posttranslational modifications to DRP1, including phosphorylation at specific serine residues, SUMOylation, and ubiquitinylation regulate mitochondrial recruitment and GTPase activity (Figure 2C). Protein

kinase A (PKA) phosphorylation of DRP1 at serine 637 inhibits DRP1 and allows mitochondrial fusion. Dephosphorylation of DRP1 at serine 637 via the calcium-dependent phosphatase, calcineurin, mediates DRP1 activation and recruitment to the mitochondria (Figure 2)[69]. Calcineurin conveys information about metabolic stimuli related to calcium changes into alterations in mitochondrial morphology[70].
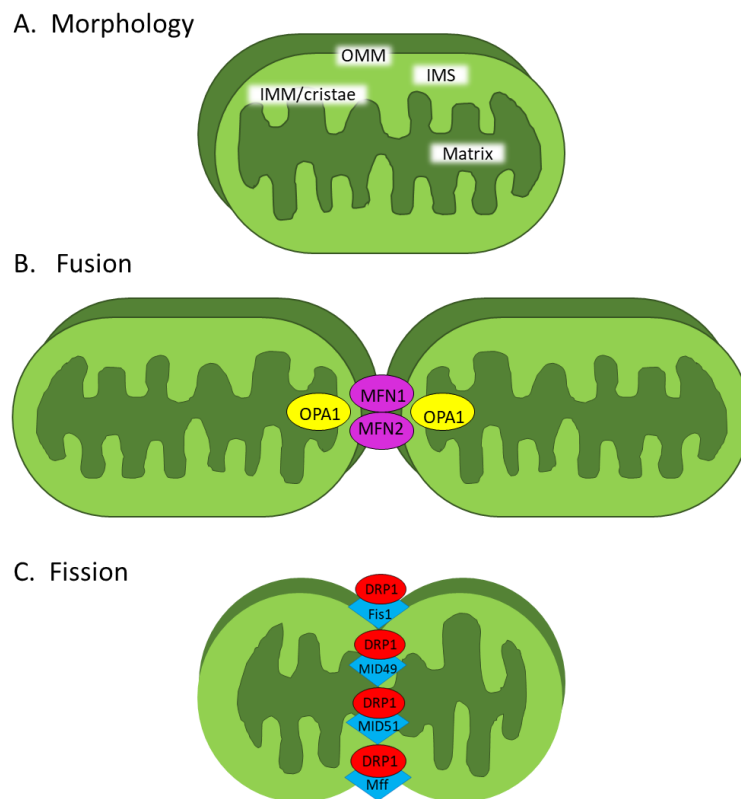
Figure 2. Dynamic equilibrium of mitochondrial fission and fusion.
A. Mitochondrial morphology. **B.** MFN1 and MFN2 tether mitochondrial outer membranes to mediate fusion. OPA1 drives fusion of the inner mitochondrial membrane. **C.** DRP1 assembles around mitochondria along accessory proteins Fis1, MID49, MID51 and Mff to mediate fission. Figure by OSW.

1.2.2 Mitochondrial function

Mitochondria are responsible for producing the majority of cellular adenosine triphosphate (ATP), the primary molecule used for chemical energy in the cell. The number of mitochondria found within a cell is therefore an indicator of the cell's rate of metabolic activity[71]; cells which are very metabolically active, such as placental trophoblasts[72,73], will contain many mitochondria[71]. Mitochondria also contain the major enzymes required for oxidation of carbohydrates, fats, and proteins. Each of these substrates can be catabolized to acetyl-coA which enters the Kreb's cycle in the matrix. Carbohydrates undergo glycolysis in the cytosol, converting them to pyruvate via pyruvate dehydrogenase. Fatty acids are converted to acetyl-coA via beta oxidation in the mitochondrial matrix. Various enzymes convert amino acids into pyruvate, acetyl-coA or directly into Kreb's cycle intermediates. In the Kreb's cycle, the two-carbon acetyl group of acetyl-coA is transferred to the four-carbon oxaloacetate, forming six-carbon citrate. Citrate is oxidized back to oxaloacetate, via a series of seven enzymatic reactions resulting in the production two molecules of carbon dioxide and the transfer of electrons to the cofactors NADH and FADH2 which shuttle the free energy to the ETC; the oxaloacetate is free to re-enter the cycle. The mitochondrial respiratory chain consists of multi-subunit protein complexes (I-IV) that are embedded in the IMM, arranged spatially in order of their redox potentials and carry out the final catabolic reactions (Figure 3)[65].

Electron transfer to oxygen facilitates the generation of the mitochondrial membrane potential ($\Delta\Psi$m) via proton pumping into the intermembrane space. This electrochemical gradient drives ATP synthesis via complex V (ATP synthase) in the last step of OXPHOS[65]. Complex I (NADH-ubiquinone oxidoreductase) oxidizes NADH with coenzyme Q, the electron acceptor, and couples this reaction to the pumping of four protons (H^+) from the matrix across the IMM. This generates the $\Delta\Psi$m, which if dissipated via pharmacological uncouplers will lead to extensive fission[74]. Coenzyme Q diffuses through the IMM to arrive at complex III (ubiquinone:cytochrome

c reductase) which oxidizes coenzyme Q and shuttles the electrons to cytochrome c, again coupled to the translocation of four protons, increasing the $\Delta\Psi$m. FADH2 carries electrons to complex II (succinate dehydrogenase) and catalyzes the oxidation of succinate to fumarate in the Kreb's cycle. Complex II contains covalently bound FAD and with iron-sulfur (FeS) clusters it facilitates the transfer of electrons to coenzyme Q. While complex II is a component of the ETC, no protons are transported to the intermembrane space in this pathway. At complex IV (cytochrome c oxidase), four molecules of cytochrome c each donate one electron to the enzymes iron/copper active site which catalyzes the production of water and the associated pumping of protons into the intermembrane space. The final reaction involves ATP synthase harnessing the energy of the proton gradient to form ATP via the phosphorylation of adenosine diphosphate (ADP; Figure 3)[64,65,67].

Mitochondria also participate in retrograde signaling that regulates nuclear gene expression, buffers intracellular calcium levels, and produce reactive oxygen species (ROS); under normal and pathological conditions, this retrograde communication serves to indicate mitochondrial status to the nucleus and the cell[75,76]. ROS produced by mitochondria, as a normal by-product of aerobic respiration, regulates cellular signaling pathways important in various aspects of cell biology[64,76]. Electrons derived from ETC complexes I and III, react readily with molecular oxygen to form superoxide in the mitochondrial matrix and the intermembrane space, respectively. The two primary sites for producing superoxide in the ETC are the flavin mononucleotide (FMN) group of complex I and the ubiquinone of complex III[76].
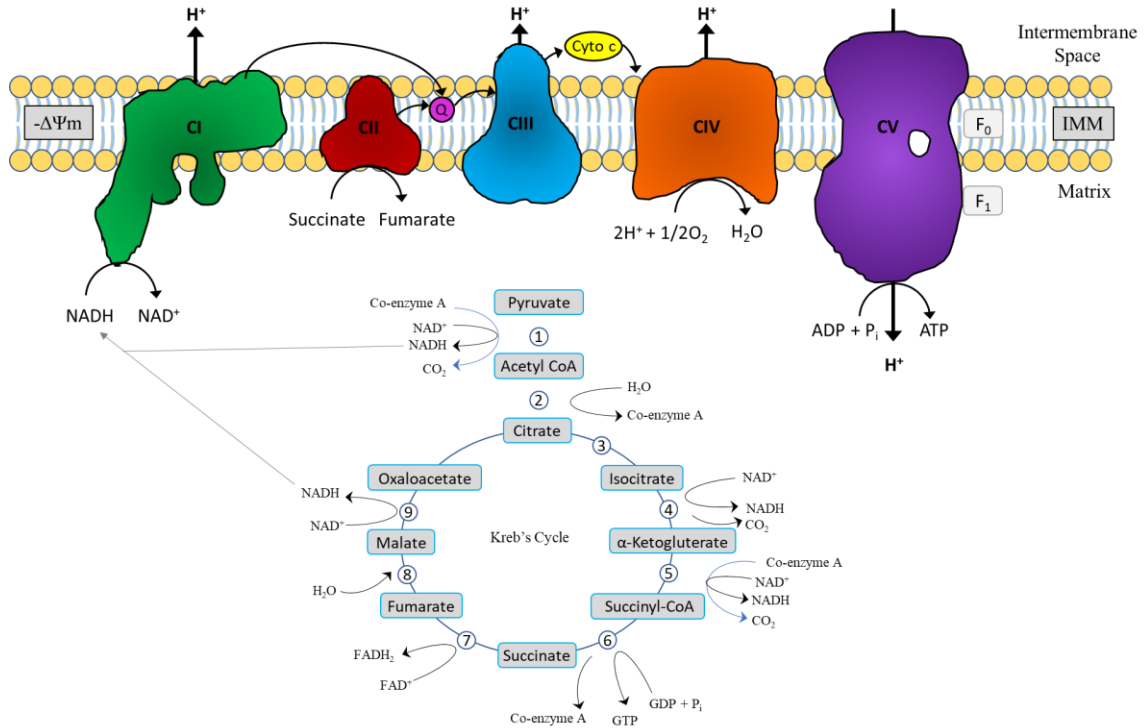
Figure 3. Bioenergetics of the ETC and the Kreb's Cycle.

The Kreb's cycle and the ETC occur in the mitochondrial matrix and on the IMM, respectively. Electron carriers, NADH and FADH2, produced during glycolysis and the Kreb's cycle pass their electrons to the ETC ending with ATP production. The encircled numbers refer to enzymes catalyzing the various reactions in the Kreb's cycle: 1. Pyruvate dehydrogenase; 2. Citrate synthase; 3. Aconitase; 4. Isocitrate dehydrogenase; 5. α-Ketogluterase dehydrogenase; 6. Succinyl CoA dehydrogenase; 7. Succinate dehydrogenase; 8. Fumarase; 9. Malate dehydrogenase.

1.2.3 Mitochondrial proton leak

The mechanisms of proton leak have been described in two excellent reviews (Jastroch et al. 2010; Divakaruni and Brand 2011)[77,78]. Briefly, ATP synthesis is not perfectly coupled to oxygen consumption because protons can return to the matrix through the mitochondrial inner membrane independently of ATP synthase. This is referred to as proton leak and it plays a role in accounting for differences in basal metabolic rate. Mitochondrial proton leak is the sum of basal leak which is unregulated and inducible leak which is regulated by IMM proteins. Basal leak is

mediated by mitochondrial anion carrier proteins, adenine nucleotide translocase (ANT) and the interface it forms with the lipid bilayer. It is characteristic of all mitochondria and contributes significantly to basal metabolic rate. ANT mediated basal leak is present in tissues with high OXPHOS rates and via mild uncoupling, confers protection against excessive ROS production without severe reductions in ATP synthesis. Furthermore, the uncoupling function of ANT can be activated by fatty acids and reactive alkenals, like hydroxynonenal (HNE). Inducible proton leak is regulated by ANT and uncoupling proteins (UCPs), but it can also be activated by fatty acids, superoxide, or peroxidation products. Thus, incompletely coupled OXPHOS will allow for adjustments to cellular respiration following mild uncoupling[77,78].

1.2.4 Oxidative stress

1.2.4.1 Mitochondrial ROS

Mitochondrial ROS production, accounting for approximately 2-3% of total oxygen consumed by mitochondria under normal physiological conditions[79], has long been discussed as an unwanted by-product of aerobic respiration. Under normal physiological conditions, ROS is metabolized efficiently for the cellular benefits of staving off infections through antioxidant mechanisms; however, this balance can be disrupted under pathological conditions, i.e. when ROS production exceeds the ability of defense antioxidants to clear them[79], thus leading to oxidative stress and cellular destruction[80]. Leakage of electrons during OXPHOS leads to premature one-electron reduction of O_2 at complexes I, II and III to form the superoxide anion radical (O_2^-), a ROS that is subsequently converted to hydrogen peroxide (H_2O_2) by superoxide dismutase (SOD)[81].

1.2.4.2 Antioxidant defenses

Given the destructive effects of ROS on cellular macromolecules, several cellular systems are in place to scavenge ROS. Mammalian cells possess a variety of ROS defense mechanisms including enzymatic antioxidants (SOD, catalase, glutathione peroxidase) and non-enzymatic antioxidants (e.g. vitamins C and E) whose role is protection against oxidative stress and re-establishing cellular homeostasis[82,83]. Antioxidant enzymes protect cells against oxidation by removing free radicals from cells to maintain the redox balance[83,84]. The three principal antioxidant enzyme systems that exist in cells include superoxide dismutase, catalase and the glutathione system.

1.2.4.3 Superoxide dismutase

SOD exists as the cells initial defense against superoxide radicals. The superoxide radical (O_2^-) or singlet oxygen radical ($^1O_2$) generated in tissues via metabolic processes or reactions in cells is dismutated into H_2O_2 and molecular oxygen (O_2) by SOD. There are three SOD isoforms of the enzyme present in mammals, and as metalloenzymes are differentiated by their transition metal cofactors, required in the active site for the enzyme to be catalytically active[85]. Copper zinc SOD (CuZnSOD; SOD1) is located mostly in the cytosol, manganese SOD (MnSOD; SOD2) is found in the mitochondrial matrix and iron SOD (FeSOD; SOD3) is primarily localized to the extracellular space; all three metalloenzymes are found in peroxisomes[85,86].

1.2.4.4 Catalase

Catalase is an antioxidant enzyme responsible for catalyzing the breakdown of H_2O_2 generated by SODs into water and molecular oxygen. Catalases are highly efficient enzymes, as

each catalase molecule can decompose millions of H_2O_2 molecules per second (kcat=10^6-10^7 M/s)[85]. When a cell experiences oxidative stress, catalase enzymes are activated because increased ROS are dismutated to H_2O_2, which can form the toxic hydroxyl radical in the presence of iron if not quickly eliminated by catalase[82,87]. Catalases are ubiquitously present and exist in a variety of locations in a cell but is primarily localized to the peroxisomes of mammalian cells, which is strategic because many H_2O_2 producing enzymes are located here. Catalase activity increases with increasing concentration of H_2O_2, and requires two H_2O_2 molecules to bind to its active site for enzyme activity: $2H_2O_2 \approx 2H_2O + O_2$, effectively completing the detoxification process initiated by SODs[85].

1.2.4.5 The glutathione system

The glutathione enzymes are an additional source of antioxidants for the cell, and primarily located in the cytosol and mitochondrial matrix. Glutathione is a powerful antioxidant which can be replenished by N-acetyl cysteine (NAC), a supplement form and precursor of L-cysteine that boosts the biosynthesis of glutathione and is widely used in vivo and in vitro[88]. Glutathione peroxidase catalyzes the reduction of H_2O_2 to water (and lipid peroxidases to their corresponding alcohol), using the reduced form of glutathione (GSH) as the electron donor, forming GSSG, the oxidized form. GSH can also directly react with free radicals as an antioxidant via donating a hydrogen atom[83,85,87–89].

1.2.4.6 Non-enzymatic antioxidants

Non-enzymatic antioxidants are found intracellularly and contribute to maintaining the redox balance. Many of these non-enzymatic antioxidants are naturally occurring compounds that

can be acquired from a variety of foods. The most common antioxidants include glutathione, vitamins A, C & E, carotenoids[82], and lipoic acid[88].

1.2.4.7 Heat shock proteins and their response to stress

Heat shock proteins (HSPs), also referred to as stress proteins, have known functions in the cellular response to stress. They are a family of proteins produced by cells upon exposure to stressful conditions like heat, cold, various environmental stressors (e.g. exercise, infection) and exposure to toxins (e.g. various drugs)[90]. HSPs participate in cytoprotective activities, often as chaperones, with roles ranging from polypeptide folding, assembling, and translocation of organelles across membranes, to facilitating repairs, and the degradation of irreparable peptides[80]. HSPs have been reported to work together with antioxidant systems to neutralize the cellular effects of ROS[80]. Using vascular smooth muscle cells from male Sprague-Dawley rats, Madamanchi et al (2001) demonstrate that in vitro exposure to 200 μM H_2O_2 for 24 hours increased the protein expression of HSP70 by 6-fold relative to unstimulated cells[91]. This finding suggests that HSP70, and possibly other HSPs, may play a key role in the adaptive response to oxidative stress.

1.2.5 Placental mitochondria in normal and pathological pregnancy

The placenta primarily uses OXPHOS for energy production, a process during which ROS is formed as a normal part of biology; when excessive, ROS can lead to cellular dysfunction and lead to oxidative stress. Pregnancy itself is characterised by increased oxidative stress primarily due to the placenta's significant mitochondrial mass which increases as gestation progresses. This oxidative stress is often magnified in placental pathologies[72,92,93]; and mitochondrial dysfunction is associated with a plethora of disorders including gestational complications[93]. The next sections will

serve to present evidence that placental mitochondria are crucial in the maintenance of a healthy pregnancy, and when dysfunctional, become implicated in the pathogenesis of pregnancy-related conditions.

1.2.6 Placental mitochondrial content

Changes to mitochondrial content, morphology, and ETC function are associated with placental pathologies such as PE and IUGR[92,93]. Mitochondrial content was reported as variably increased or decreased in the same gestational pathology (i.e. PE or IUGR) by different studies. Using placentae from term caesarean delivery, Lattuada et al (2008) report increased mitochondrial DNA in placentae from IUGR and IUGR+PE compromised pregnancies relative to placentae from uncomplicated pregnancies[94]. Conversely, Poidatz et al (2015) observed marked reductions in mitochondrial DNA in IUGR and IUGR+PE placentae when compared to control placentae[95]. In pathophysiological phenotypes, mitochondrial proliferation may occur as an adaptation in response to the perturbation of cellular bioenergetics. However, increased placental mitochondrial ROS can directly damage mitochondrial DNA, which effectively inhibits the adaptive biogenesis of the self-replicating mitochondria, reducing respiration[92]. Either increased or decreased mitochondrial biogenesis can occur to maintain normal fetal growth. The reported differences in mitochondrial responses within the same pathologies may be due to the severity and/or the timing of the disturbance and the subsequent ability of the placenta to adapt via altered mitochondrial content[92,93].

1.2.7 Cytotrophoblast vs syncytiotrophoblast mitochondria

Many placental investigations involve consideration of the whole tissue. However, mitochondria within different cell lineages will have distinct functions and are likely to respond differently to stimuli. In particular, mitochondria in two of the major placental cell types,

cytotrophoblasts and syncytiotrophoblast, exhibit vastly different structures and functions[96,97]. Using electron micrograph sections of placental tissue harvested from human term placentae, Matsubara et al (1997) reported mean mitochondrial diameter $\pm$ SD of 0.22 ± 0.06 and 0.43 ± 0.07 µm in syncytiotrophoblasts and cytotrophoblasts, respectively, and the average number $\pm$ SD of cristae counted on the electron micrograph was 3.1 ± 0.8 and 10.1 ± 3.1 per mitochondrion, respectively[98]. Similarly, using full term placentae from which cytotrophoblasts and syncytiotrophoblasts and their respective mitochondria were isolated, Castillo et al (2011) demonstrate that syncytiotrophoblasts contain smaller, irregularly shaped mitochondria with condensed matrices and vesicular cristae compared to those isolated from cytotrophoblasts[97]. In addition to the unorthodox cristae morphology, the syncytiotrophoblast mitochondria also possessed lower levels of complex V, the former being consistent with the latter; the integrity of complex V is documented as requisite for tubular cristae formation[97]. The literature suggests that it is typical to observe vesicular cristae in the mitochondria of steroidogenic tissues, such as Leydig cells of the testes[99,100] and syncytiotrophoblasts[97,101]. Indeed, syncytiotrophoblasts are steroidogenic whereas cytotrophoblasts do not posses this ability. Syncytiotrophoblast mitochondria contain cytochrome P450$_{scc}$ in the IMM which converts cholesterol to pregnenolone which is subsequently converted to progesterone by the 3-β-hydroxysteroid dehydrogenase also in the IMM[93,97]. The translocation of cholesterol to P450$_{scc}$ is the rate-limiting step in steroidogenesis, thus the greater surface to volume ratio afforded by the vesicular cristae may prove beneficial in this process as progesterone is required to keep the myometrium quiet to prevent miscarriage or preterm labour[92,97].

1.2.8 Mitochondrial ROS in placenta

The syncytiotrophoblast is in direct contact with maternal blood[102] and has been suggested to be the cell type most affected in IUGR and PE. Both PE and IUGR are associated with reduced or intermittent placental perfusion and increased oxidative stress[79,103]. The syncytiotrophoblast possess low levels of antioxidant enzymes[104], mitochondria with reduced coupling control of oxidative phosphorylation to ATP production, reduced membrane potential and increased H_2O_2 production when compared to the cytotrophoblasts[92]. The literature also supports a role for mitochondria as direct mediators in the differentiation of cytotrophoblasts into the syncytiotrophoblast.   In primary villous cytotrophoblasts, inhibition of the mitochondrial respiratory chain leads to a decrease in cell fusion and hormone production (hCG and leptin)[105]. Therefore, syncytiotrophoblast mitochondria may be more affected by hypoxia/reperfusion injuries. Importantly, the unique position of syncytium as the direct interface between maternal and fetal systems may cause it to be particularly sensitive to maternally derived perturbations.

1.2.9 Placental mitochondria and ETC disruption

In addition to energy metabolism, mitochondria maintain cellular homeostasis by interacting with ROS and responding appropriately to various stimuli.   In this context, the interaction of pharmacological agents with mitochondria represents an important aspect of molecular biology where enhancement of mitochondrial function may represent a critical component for addressing various disorders and diseases[106]. In mitochondria, there are several potential drug targets which may lead to toxicity. Some drugs (e.g. rotenone) are known inhibitors of the mitochondrial ETC, interfering with one or more of the complexes, subsequently leading to the production of free radicals[107,108]. Other drugs (e.g. non-steroidal anti-inflammatory drugs; NSAIDs) may lead to the uncoupling of OXPHOS[109].

Dysfunction of complex I is involved in many pathological processes and the literature is saturated with animal and in vitro models mimicking various diseases by compromising complex I via genetic disruption or by pharmacological means[101,105,106,110–113]. Importantly, complex I inhibition in human placental cells is demonstrated to mediate poor trophoblast outcomes.

1.2.9.1 Targeted disruption of complex I

A well-defined mechanism of action of the drugs targeting mitochondria is the inhibition of electron flow across the electron transport chain. Rotenone, a member of the rotenoid family and commonly used as an insecticide, is a semiquinone antagonist and potent inhibitor of complex I[76]. Rotenone inhibits the transfer of electrons from FeS centers in complex I to ubiquinone[87,114]. The primary consequences of such inhibition are impaired respiration, increased formation of ROS and damage to mitochondrial DNA[114]. Using breast cancer cell lines SKBR3 and 4T1, Ma et al (2013) demonstrated that 100 nM rotenone exposure induced significant ROS production and was attenuated via pre-treatment with NAC (an antioxidant pre-cursor to glutathione)[115]. Poidatz et al (2015) observed marked reductions in hCG production and attenuated transcription of *HERV-FRD* following 48 hours of 0.2 µM rotenone exposure in cytotrophoblasts isolated from first trimester placentae[105]. Additionally, while rotenone exposure prevented syncytialization as demonstrated by the strong E-cadherin (a cell membrane marker) staining at the cell boundaries, the unstimulated cells displayed morphological differentiation[105]. These findings demonstrate the necessity for unperturbed mitochondrial function as a mediator of trophoblast differentiation.

1.2.10   Are cannabinoids mitochondrial ETC inhibitors?

With increased legalization of cannabis use in recent years, researchers have been increasingly incentivized to investigate the biological effects of Δ9-tetrahydrocannabinol (THC), the main psychoactive constituent in cannabis. Recent evidence points to the presence of cannabinoid receptors, namely cannabinoid receptor 1 (CB1) on neuronal mitochondrial outer membranes and the activation of mitochondrial CB1 (mtCB1) influences aerobic respiration via inhibiting the mitochondrial cyclic adenosine monophosphate (cAMP)/protein kinase A (PKA)/complex 1 pathway[116–120]. The current literature provides rationale for both receptor- and non-receptor-mediated mechanisms of cannabinoid inhibitory action on mitochondrial respiration. Interestingly, similar mitochondrial localization of CB1 receptors has also been demonstrated in peripheral tissues, such as sperm cells and myocytes, where the proportion of mitochondrial CB1 appears to be higher than in the brain[121].

Pharmacological and genetic experiments showed that the effects of cannabinoids on mitochondrial respiration involve a specific cascade formed by different enzymatic proteins that ultimately negatively impact OXPHOS. Benard et al (2012) used signal transduction analyses to reveal reduced cAMP, subsequent inhibition of PKA, and complex I activities[117]. Soluble adenylyl cyclase (sAC), localized to the mitochondrial matrix, produces cAMP in the mitochondria of mammalian cells. Mitochondrial cAMP generated by sAC modulates the function of mitochondrial enzymes. Mitochondrial cAMP preserves complex I activity[122]. Inhibition of sAC increases the degradation of nuclear-encoded subunits of complex I[122]. Thus, if attenuated by upstream CB1 activation via endogenous or exogenous cannabinoids[117], complex I may be partially inhibited[117,118], and may serve as a signaling mechanism by which CB1 activation targets mitochondria.

1.3   CANNABIS

1.3.1 Overview

Cannabis, one of the worlds oldest plants with a history dating back over 12,000 years[123], contains over 500 different chemical compounds, >100 of which are phytocannabinoids (plant-derived cannabinoids) whose therapeutic effects and interplay have not yet been fully characterized[124]. The use of cannabis has been recorded going back over 3000 years for use as a medicinal agent, particularly its use as a surgical anesthetic[123,125]. Fundamental to understanding the effects of cannabis are discussions of how cannabis affects human biology. Cannabis has been reported to cause pathological and behavioural toxicity[126], particularly at vulnerable developmental life stages (i.e. pre-natal, adolescence).

Cannabis is derived from the plants *Cannabis sativa* or *Cannabis indica*. A third cannabis variety, *Cannabis ruderalis*, has been identified but has little psychotropic properties[127]. *Cannabis sativa* is dioecious[123,128], i.e. there are male and female plants in this species. The psychoactive constituents of the plant is largely derived from the flowering parts of the female plant; less is found in the leaves, and male plant and the stalks and seeds have virtually none[128]. In 1964, Mechoulam and his research team reported the main bioactive constituent in cannabis – delta-9 tetrahydrocannabinol (THC)[128], the most widely studied and psychogenic phytocannabinoid. Cannabis chemistry is far more complex than that of pure THC, thus various effects should be expected due to the presence of additional compounds. Indeed, the heating process that precedes smoking can produce an additional 2000+ compounds, including amino acids, sugars, terpenes, and simple fatty acids. As a complex mixture, these compounds contribute to the unique biological and toxicological properties of cannabis[126,129].

1.3.2 Trends in cannabis use

Cannabis is amongst the most widely used psychoactive drugs worldwide and it is a commonly used drug during pregnancy[130–132]. Based on current literature, approximately 2-20% of pregnant women report the use of cannabis at various stages throughout gestation[131,133]. The popular notion surrounding cannabis use is that it is a harmless pleasure[129,134], access to which should not be restricted or illegal[135], which is not the general opinion of regulatory agencies[136]. The prevalence data available for prenatal substance abuse is highly variable and thus difficult to firmly establish. The variations are likely due to factors such as varied sampling methods for the study cohort, whether self-report or biological sampling methods are used, and the methods utilized for drug detection and analysis[137]. Prenatal substance abuse continues to be a growing problem worldwide, which subsequently poses significant risks for the developing fetus[137]. Most drugs are known to cross the placenta and thus pose a threat to proper fetal development. The effects of nicotine and other components of cigarette smoke on the gestational outcomes have been studied since the 1960s; alcohol and opiate use since the 1970s; and various other illicit drugs since the 1980s[137]. A study conducted in Vancouver, Canada found that approximately 77% of cannabis use during pregnancy was for the purposes of combatting nausea[138]. In a US study, Brown et al (2017) report a 62% increase in past month cannabis use amongst pregnant women from 2002 to 2014 based on self-report, with the highest prevalence in women aged 18-25 years[139]. However, the effects on gestational development are largely unknown. Cannabis was legalized in Canada on October 17, 2018 and allows for the consumption of cannabis for medicinal and recreational purposes[140]. Legalization of this plant brings it into the realm of other recreational drugs such as alcohol and nicotine – the legal triad – the concern being that the legalization does not necessarily correlate to its safety[141].

Further to the above, there is an emergence of increasing use of cannabis extracts or concentrates, produced using a combination of crude plant materials and solvents. These products yield a substance that is far more potent than flower cannabis and is gaining popularity amongst chronic and novice cannabis users alike[135,142]. These extracts are often named based upon the product's consistency or appearance – e.g. shatter, honeycomb, crumble wax. Shatter is made by extracting and concentrating THC to create a highly potent product[142]. It is so named because it can break and shatter like glass. There are several methods used to extract shatter, i.e. a process that involves the use of solvents such as butane (hence the term "butane hash oil"; BHO) or CO_2 which is subsequently used in vapourizers[142]. These techniques are utilized so that the THC in parts of the plant that are not generally smoked can be salvaged in a desirable form and consumed. Shatter is then inhaled by balling up a portion of the cannabis extract, heating it in an administrative device, i.e. a vapourizer, then inhaling the vapour in one large dose. This behaviour is generally referred to as "dabbing"[142]. An internet-based study conducted by Daniulaityte et al (2017) reveals that >66% of the respondents (n = 673) reported use of cannabis concentrates, with approximately 13% of these respondents dabbing daily or almost daily[135]. As dabbing is gaining traction worldwide, the limited research surrounding this emerging trend is troubling[135,142]. As legislation continues to evolve, it becomes critical to comprehensively assess the potential risks to human health due to smoking or otherwise consuming cannabis and its derivatives.

1.3.3. THC

THC, the most abundant and (in)famous phytocannabinoid (plant-derived, exogenous cannabinoid), is a psychoactive compound extracted from the amber coloured resin of the cannabis plant. The chemical formula of THC is $C_{21}H_{30}O_2$ (Figure 4) with a molecular weight of 314.469 g/mol. THC has five major structural features: a lipophilic side chain at C-3, hydroxyl groups at

C-1 and C-11, and three rings: the aromatic A-ring, pyran B-ring, and cyclohexene C-ring. While a review of all the potential modifications is beyond the purpose of this chapter, the fundamental characteristics of each component are presented here. The side chain length is critical for retaining cannabinoid affinity and potency and requires a minimum of 3 carbon atoms, with the optimum being 5-8 carbons. Various chemical substitutions will profoundly affect its activity, e.g. an increase in the length will increase binding affinity and potency[143]. The hydroxyl group at C-1 and C-11 are important for its binding affinity at CB1 and CB2. Polar hydroxyl allows for the interaction with the hydrophobic region of the receptors; substitutions lead to marked reductions in the binding affinities, especially at CB1 receptors[143,144]. Various alterations of the tricyclic ABC rings will have mixed consequences regarding potency: inhibiting, potentiating, or leaving it unchanged[143]. Regarding nomenclature, THC has been described by two different atom-numbering systems: the dibenzopyran (Δ9) or the monoterpene (Δ1) system[126]. The unsaturated double bond in the cyclohexene ring is located between C-9 and C-10 in the dibenzopyran ring numbering system, which gives rise to the Δ9 in its current classification[145]. Upon ligand-receptor binding, the orientation of the bonds and the side chain determine how "high" one will get upon smoking or otherwise consuming cannabis[128].
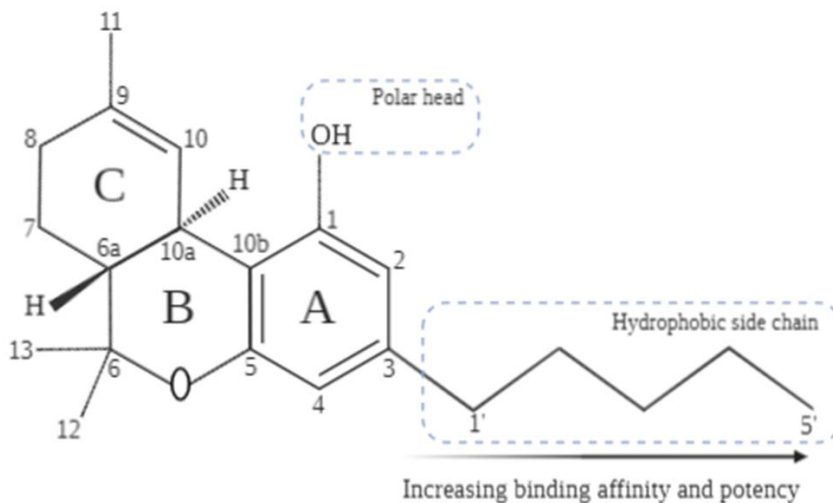
Figure 4. Structure of THC.
OSW created with BioRender.com.

THC produces feelings of euphoria, dysphoria, hypothermia, impaired memory and motor coordination[125], increased appetite, analgesia[146] and several other physiological effects[147]. Some of the other cannabis constituents, such as cannabidiol (CBD), also exhibit similar physiological effects such as antianxiety, anticonvulsive, anti-nausea, anti-inflammatory, and anti-proliferative properties, but without the associated "high"[125]. Clinically, THC (marketed as dronabinol and nabilone) is currently indicated for use as an anti-emetic for patients undergoing chemotherapy and as an appetite stimulant for HIV/AIDs patients[127]. While medicinal cannabis may prove beneficial for patients with certain conditions, its use comes with some challenges, including method of delivery (i.e. smoked, vapourized, oral, transdermal), variable physiological responses among patients, and the THC content[126,127].

1.3.4 Cannabis potency

Cannabis potency is defined by the concentration of THC. While other constituents do possess pharmacological properties, they do not contribute to the potency of cannabis and are not the subject of this dissertation. The potency of cannabis has markedly increased over the last few decades, as assessed by confiscated cannabis preparations[148–150]. For example, an analysis of over 35,000 confiscated samples in the USA over the course of 18 years revealed that the potency was less than 1.5% in 1980 and rose to approximately 4.5% in 1997[150]. A follow-up study, by the same lead author ElSohly et al (2016), was conducted between 1995 – 2014 on approximately 38,000 confiscated samples in the USA. Again, the authors report that the potency increased from approximately 4% in 1995 to approximately 12% in 2014. Importantly, the CBD content fell from approximately 0.28% in 2001 to less than 0.15% in 2014, thus shifting the ratio of THC:CBD from 14 times in 1995 to roughly 80 times in 2014[124]. Given the potential for increased THC content with hybrids, various subspecies of the plant and preparation methods[148], it is likely to result in increased use and increased potential for harm. This underscores an urgent need to assess the effects of prenatal cannabis exposure through an understanding of cannabis and THC pharmacology and physiology in the context of potential risks and benefits to maternal and prenatal health.

1.3.5 Pharmacokinetics of THC

The pharmacokinetic study of cannabinoids is challenging owing to several factors. The major difficulty is the low analyte concentrations and rapid and extensive metabolism. Moreover, the physicochemical characteristics (i.e. high lipid solubility) of cannabinoids restrict their separation from biological matrices and from each other and minimize drug recovery due to their adsorption into multiple body organs[126].

THC is present in cannabis as a mixture of mono-carboxylic acids, which gets rapidly and efficiently decarboxylated upon heating (i.e. for smoking or during cooking). It decomposes when exposed to air, heat or light[126,129] and readily binds to glass and plastic. Therefore, THC is typically stored in solubilizing agents within amber silicate glassware to minimize loss during pharmacological or in vitro studies[129], however, these agents (e.g. methanol, ethanol) carry their own pharmacological effects, and must be accounted for in study design.

1.3.5.1 Absorption

Cannabis is available mainly in the form of herbal plant material or dried resin[135]. Consumption of the raw cannabis plant is not likely to induce a state of intoxication since a carboxylic group is attached to the cannabinoids, rendering them inactive. The inactive acidic precursor of THC is known as tetrahydrocannabinolic acid (THC-A)[151]. Though THC-A is reported to have anti-inflammatory effects, it does not have psychoactive properties[151]. To achieve the characteristic "high", the inactive THC-A must be decarboxylated. This process is not mediated by enzymatic activity, but rather is achieved by the process of heating, such as that from smoking – the dominant route of administration (e.g. joint) or cooking (e.g. brownies, tea), thus forming the active THC[126,129]. In some instances, the process of heating can more than double the active THC concentration relative to the original starting plant material[128].

THC is rapidly absorbed after the inhalation of cannabis smoke (within minutes) and results in higher blood levels of cannabinoids and shorter duration of acute pharmacodynamic effects when compared to oral administration[152]. Generally, a maximum of 25-27% of the THC content in a joint is delivered to the systemic circulation. For example, between 2-44 µg of THC penetrates the brain after smoking a joint that contains 2-22 mg of THC (e.g. 1 g joint containing 0.2 – 2.2% THC, delivering between 0.2 and 4.4 mg of THC based on a smoked bioavailability of 10 to 25%)[152].

Rate of absorption depends on the inhalation technique and smoking frequency, resulting in highly variable bioavailabilities (10-35%). The absorption after oral administration is more erratic because of a variable degradation of the drug by stomach acids and the extensive liver first-pass metabolism and is lower than that following inhalation[153]. Once the active THC passes into the blood from the pulmonary or gastrointestinal systems, metabolism continues in the hepatocytes by a series of steps involving enzymatic activity.

1.3.5.2 Body fluids and tissue distribution

Because THC is lipophilic, it presents with low concentrations in body fluids[126]. In blood, due to the low partition coefficient of the cannabinoid into erythrocytes, about 10% of THC is distributed in erythrocytes and about 90% is distributed into the plasma. Greater than 95% of THC in plasma is bound to plasma lipoproteins which complicates the THC initial disposition[126,151]. THC moves rapidly from the blood into highly perfused tissues (e.g. lung, heart, brain, liver, placenta) after smoking and is readily metabolized by the liver; thus, its blood concentrations rapidly decline after smoking[126]. Owing to its lipophilicity, THC is readily taken up by adipose tissue, from which it is slowly released back into the circulation over time. This contributes to THC's long elimination half-life of approximately 4-5 days[152,154], the estimation of which can vary depending upon the pharmokinetic model employed[155]. The slow release of THC from body stores is the rate-limiting step in the its prolonged excretion and results in THC-COOH's flip-flop kinetics[126] (i.e. THC-COOH's distribution into blood from the slow THC release from tissues is slower than THC-COOH's elimination)[156,157].

In frequent smokers, THC's fat storage results in a large cannabinoid body burden; thus, cannabinoids can be stored in the body for an extended period of time during chronic, daily smokers' abstinence. Bergamaschi et al (2012) documented blood THC detection for up to 30 days,

11-OH-THC for up to 3 days, and THC-COOH for at least 33 days in chronic, daily smokers (mean ± SD of 10.2 ± 6.3 joints/day)[158]. Therefore, interpretation of a positive cannabinoid test can be challenging. Furthermore, a small number of studies have directly compared the cannabinoid disposition in occasional vs. frequent smokers. Work by Toennes et al (2008) demonstrated that although the highest concentration observed for THC (first sample collected at 5 min after smoking) and areas under the curves were significantly higher in frequent smokers (smoked ≥4 times per week) compared to occasional smokers (smoked ≤ 1 time per week), distribution and elimination patterns were comparable; however, blood THC, 11- OH-THC and THC-COOH was only monitored for 8 hours[155].

The relationships between THC content, dose administered, and resultant plasma levels have been investigated. The pharmacokinetics of THC in the body are regulated by its lipophilicity and its strong initial binding to carrier proteins (greater than 95%). Further, whole blood and plasma concentrations of THC are highly variable and, among other factors, is dependent upon the number, duration, and spacing of puffs, hold time, and inhalation volume, side stream smoke production, or even the expectation of drug reward (i.e. euphoria, analgesia)[126,159,160]. Schwope et al (2011) report peak median (range) THC levels in whole blood and plasma as approximately 50 (13-63) and 76 (18-110) µg/L, respectively, 15 minutes after smoking a 6.8% THC cannabis joint[159]. Using an automated procedure to sample blood during and immediately after smoking cessation, Huestis et al. (1992) reported a mean peak (range) plasma THC concentration of 162 (76–267) µg/L following administration of 3.55% (35mg) THC in cannabis joints. These THC levels rapidly increased and peaked prior to the end of smoking[161]. When smoking a joint, THC becomes detectable in plasma seconds after the first puff[160]. The automated procedure employed by Huestis et al (1992) allowed for the capture of true peak concentrations of THC which is reported to occur before the last puff following a number of puffs of a joint[159]. Although most cannabis users preferably smoke joints[162],

few studies have been conducted in humans that capture the portion of the population that opts to consume cannabis via oral preparations, i.e. edibles. Karschner et al (2012) administered oral THC (20-120 mg/day oral synthetic THC, Marinol®) for 8 days to chronic daily cannabis smokers while abstaining from smoked cannabis. THC quantified in whole blood peaked at median 6.4 ng/mL, 3 hours after the first oral dose of 20 mg. During multiple THC dosing, up to 120 mg/day, median whole blood peak concentration was 16.3 ng/mL at day 5, nearly 3-fold higher than following a single dose of 20 mg THC[162]. While these data advance our understanding of THC metabolism following smoked and orally consumed cannabis/THC in non-pregnant humans, what remains to be explored are the pharmacokinetics in pregnant women who opt to smoke or otherwise consume cannabis/THC.

In non-pregnant individuals, the distribution kinetics of THC has been described as having a rapid distribution phase and long terminal half-life largely driven by the extensive distribution of THC into adipose tissue. Though some studies have reported the presence of THC and its metabolites in meconium[163] and cord blood[164], there are few studies on the disposition of THC in humans during pregnancy. Based on the significant contribution of hepatic cytochrome P450 enzymes, such as CYP2C9 and CYP3A4, to THC metabolism[126] and their reported increase in expression during pregnancy[165], one may expect an increase in THC clearance during pregnancy. This may lead one to predict that maternal or fetal exposures to the metabolites of THC are also increased during pregnancy due to increased CYP activity, but it is not yet known how pregnancy may change the metabolite glucuronidation and clearance. Thus, additional research is warranted to investigate the elimination pathways of THC and its metabolites in pregnant women which will allow the determination of whether pregnancy-mediated changes in maternal THC disposition are of clinical significance[123].

1.3.5.2.1   THC concentration at the plasma membrane interface

Several studies have focussed on the effects of chronic cannabis exposure. Because THC has a half-life of up to 5 days, particularly in daily users, the daily consumption will result in tissue levels in the micromolar range rather than the nanomolar concentration needed to induce acute drug effects (i.e. intoxication, euphoria, analgesia)[166]. If cannabinoids have a toxic effect, it would be more pronounced due to their cumulative storage in cells. Indeed, the effects of different cannabinoids on several mammalian cell lines are exerted at micromolar concentrations[166]. If the aqueous concentration of THC is 0.1 µM (equivalent to 31.4 µg/L, a concentration found within the low-moderate end of the whole blood and plasma ranges reported by Schwope et al (2011) as described above) and the octanol:water coefficient (liposolubility) is 6000[126,167], the concentration at the plasma membranes may be 60 µM[166]. Therefore, the concentration of THC used throughout my dissertation, i.e. 20 µM, falls between that found in the plasma of recreational and chronic cannabis users.

1.3.5.3   Metabolism

Following consumption or inhalation of cannabis, various physiological processes alter the cannabinoids so that they can be detoxified and removed from the body. This section will focus on the psychoactive cannabinoid, THC. Briefly, THC is broken down by Phase I and Phase II metabolism. Phase I, occurring in the liver, involves the addition of an oxygen molecule by a group of enzymes called CYPs (specifically cytochrome P450s)[126,153]. Phase II, also occurring in the liver, involves the addition of a sugar-based molecule called glucuronide, a reaction catalyzed by a group of enzymes called uridine-diphosphate glucuronosyltransferases (UGTs) which catalyze the covalent addition of glucuronic acid to various lipophilic molecules. This is a key player in the

detoxification of endogenous and exogenous substances as they create substances that are more polar, thus facilitating urinary or biliary excretion[168].

1.3.5.3.1   Phase I – Oxidation

THC biotransformation takes place mainly in the liver and is catalysed by enzymes of the cytochrome P450 (CYP) complex. The CYP enzymes, (for example CYP2C9) function to add a molecule of oxygen and a molecule of hydrogen (hydroxylation) to carbon 11 of THC, producing an equipotent hydroxy (OH) form of THC, 11-OH-THC. This is an active metabolite of THC which does not naturally exist in the cannabis plant, with some sources citing that this may be more potent than THC[126]. Further oxidation occurs by the action of the same enzyme, producing a carboxylic acid form, THC-COOH. This metabolite is inactive, as it can no longer bind tightly to the cannabinoid receptors[126].

1.3.5.3.2   Phase II – Glucuronidation

Following oxidation, UGT enzymes will covalently attach a glucuronide molecule to THC-COOH at the level of the carboxyl group forming THC-COO-glu, effectively marking it for urinary excretion[168]. It is this metabolite that can be detected in the urine of a cannabis user. In fact, the metaboilites of cannabis can be detected in urine for up to 10 days in regular smokers, and up to 30 days in chronic heavy users[137].

1.3.5.4   Elimination of THC

Following the distribution phase, the rate-limiting step in the metabolism of THC is its redistribution from fat stores into blood[126]. Once metabolized and removed from circulation, the

elimination of unchanged THC from the body involves a complex process, one which is highly variable and can take several days or weeks[128,129]. This is attributable to the high lipid solubility of THC and some of its metabolites which exit circulation and enter fat stores[128] and highly vascularized organs[129]. The placenta, also a highly vascular organ[72] is therefore subject to THC accumulation. As THC and its metabolites are excreted by the body (approximately 1/3 in urine as conjugated acid metabolites, 2/3 in fecal matter as hydroxyl metabolites), the THC in adipose and highly vascular tissue will slowly be returned to the blood for elimination[128]. The absolute elimination time could require up to four weeks[158].

1.3.6 Pharmacodynamics of THC

1.3.6.1 The endocannabinoid system

Endocannabinoids are derived from the degradation of membrane phospholipids, i.e. arachidonic acid, and other poly-unsaturated fatty acids, which control basic physiological processes. Some of these processes include cell survival, apoptosis, neurotransmission, immune functions, metabolism and reproduction[169]. As such, they have gained recognition for their involvement in various aspects of human health and disease[1,125,170]. The ECS is essentially made up of the CB1 and CB2 receptors and their cognate ligands, N-arachidonoylethanolamine (AEA) commonly referred to as anandamide and 2-arachidonoyl glyceride (2-AG). While other endocannabinoids have been identified, research on their respective functions and biological relevance is limited[1], so the focus here is on AEA and 2-AG. Both AEA and 2-AG, representing the prototype members of endocannabinoids[169,171], and derived from the unsaturated fatty acid arachidonic acid[128], bind with different affinities to the canonical CB1 and CB2 receptors, which are two well-characterized 7-transmembrane G-protein coupled receptors (GPCRs). In addition to

these receptor targets, the ECS also consists of a variety of hydrolytic enzymes which readily inactivate AEA and 2-AG after their formation and release[128].

1.3.6.1.1   AEA synthesis

Anandamide was the first endogenous cannabinoid to be discovered. Its name was derived from the Sanskrit word "*ananda*" which means inner bliss[172], describing the euphoric effects of this ligand. It is produced by almost all cells of the body where it triggers signaling by engaging specific molecular targets. AEA acts as a partial agonist at CB1 and as a weak/partial agonist at CB2[172]. AEA activity is regulated via a multistep process and is synthesized on demand (i.e. in a stimulus-dependent manner)[173], largely triggered by cellular depolarization[174]. Briefly, the enzyme N-acyltransferase (NAT), whose activity is strongly stimulated by Ca^{2+}, catalyses the transfer of arachidonic acid from phosphatidylcholine to the head group of membrane-bound phosphatidylethanolamine, which leads to the formation of N-arachidonoyl-phosphatidylethanolamine (NAPE), the phospholipid precursor for AEA. The release of AEA from NAPE is catalysed by a Ca^{2+}-sensitive NAPE-selective phospholipase D (PLD) which is constitutively active[172,173]. Additional pathways have been characterized through which AEA is biosynthesized. In addition to the aforementioned transacylation-phosphodiesterase pathway (NAPE-PLD), these include the glycerophospho-N-acylethanolamine lipids (GP-NAEs) as important intermediates, and the phospho-N-arachidonoylethanolamine (pAEA) as a key intermediate in the synthesis of AEA[173]. Various factors may dictate which pathway is utilized for AEA synthesis; i.e. the phospholipid membrane composition at the site of synthesis, the tissue type, and possibly the presence or absence of pathology[173]. The existence of these and other pathways may also explain the recent finding that AEA tissue levels are unchanged in NAPE-PLD knockout mice when compared with wild-type mice[175].

1.3.6.1.2   2-AG synthesis

Tissue levels of 2-AG are significantly higher than that of AEA within the same tissue[172].
2-AG acts as a full agonist of cannabinoid receptors, and for this reason has been proposed as the
primary endogenous agonist of both CB1 and CB2[176]. The synthesis and release of 2-AG differs
from that of AEA, and like AEA, is stimulated by cellular depolarization[173,174]. 2-AG can be
synthesized in two steps. Phospholipase C (PLC) catalyzes the conversion of phosphatidylinositol
to 1-acyl-2-arachidonoylglycerol (diacylglycerol; DAG) with subsequent hydrolysis of DAG by a
diacylglycerol lipase (DAGL)[173]. Because 2-AG is a monoglyceride, its synthesis is closely
associated with the metabolism of triacylglycerol, mostly by the receptor-dependent activation of
phosphatidylinositol-specific PLC[125,173]. Inhibition of these enzymes led to a corresponding
decrease in 2-AG levels, thus confirming the importance of the PLC-DAGL pathway in 2-AG
biosynthesis[177]. Other pathways have been implicated in the production of 2-AG. One such
pathway has been proposed to lead to 2-AG synthesis which features a 2-arachidonoyl-
lysophosphatidylinositol (lyso-PI) intermediate[178]; however, its relevance is unclear[173]. Although
further research is required to further investigate the pathways involved in AEA and 2-AG
biosynthesis, these differences already suggest that with the use of specific inhibitors, one could
finely control endocannabinoid signaling[173]. Once AEA and 2-AG are produced, they target the
CB receptors in the same cell where they were formed, via diffusion within the plasmalemma, or
they can be released to the extracellular compartment where they reach distant targets via protein
carriers such as lipocalins or albumin and others[169].

1.3.6.1.3   Endocannabinoid transport and uptake

Endocannabinoids have the ability to activate plasma-membrane bound cannabinoid receptors, with additional targets found intracellularly, e.g. on the mitochondria[117,118,179]. It is poorly understood how AEA and particularly 2-AG transit the plasma membrane and how intracellular transport is regulated. Although endocannabinoids are lipophilic and thus can freely traverse cell membranes, research suggests the existence of other mechanisms facilitating endocannabinoid internalization[173]. Possible routes for AEA and 2-AG transmembrane transport are passive diffusion, endocytosis, transporter proteins, or a combination of these mechanisms. Various transport proteins exists to shuttle AEA and 2-AG into the cell, or transported to organellar targets[176,180,181]. Adiposomes have also been implicated in the cellular uptake of endocannabinoids[176]. Such transport proteins include lipocalins, albumins[169], fatty-acid-binding proteins (FABP)-5 and -7, albumin, HSP70 and the FAAH-like anandamide transporter protein (FLAT)[180]. Additionally, a putative endocannabinoid membrane transporter (EMT) has been suggested as a common carrier mechanism for AEA and 2-AG which is mechanistically distinct from other carrier proteins and degradative enzymes, which may further regulate cellular AEA and 2-AG trafficking and metabolism[176].

1.3.6.1.4   Endocannabinoid degradation

AEA and 2-AG are synthesized on demand and released in the extracellular environment, where they may agonize CB1 and CB2. However, their hydrolysis – a two-step process effectively and rapidly terminating endocannabinoid signaling – is an intracellular event[173]. Degradation involves cellular uptake and hydrolysis by two enzyme systems to ensure tight temporal and spatial control over their signaling function[173]. Endocannabinoid uptake is facilitated by lipid carriers as

discussed above. The potential coupling of endocannabinoid transport and degradation was once debatable. However, a recent report seems to confirm that transport and degradation are independent processes[182]. Briefly, the degradation of AEA and 2-AG is performed by two specific enzymes: the fatty acid amide hydrolase (FAAH) and the monoacylglyceride lipase (MAGL), respectively. FAAH is a widely distributed membrane-bound (particularly to that of the endoplasmic reticulum and nucleus) enzyme[169] that belongs to the serine hydrolase family and preferentially hydrolyzes AEA into ethanolamine and arachidonic acid. Although AEA and 2-AG are substrates for FAAH[183], the main enzyme responsible for the hydrolysis of 2-AG into arachidonic acid and glycerol is MAGL. This enzyme is also a serine hydrolase, a soluble enzyme with the catalytic sites facing intra- and extracellularly[176].

1.3.6.1.5 Canonical cannabinoid receptors

Two subtypes of CB receptors exist with different tissue distributions. CB1 is mainly expressed in the central nervous system, but also in peripheral tissues such as liver, adipocytes, skeletal muscle, and placenta. CB2 is primarily detected in cells of the immune system with distribution in neurons and other cells of the central nervous system[125,184,185]. As suggested by its name, CB1 was the first of the cannabinoid receptors to be discovered. In 1990, Matsuda et al (1990) cloned an orphan GPCR, known as SKR6, from a rat cerebral cortex cDNA library and demonstrated that this receptor is agonized by THC[186]. As this GPCR binds cannabis-derived compounds, it became established as the first cannabinoid receptor – CB1[171]. The second cannabinoid receptor, CB2, was discovered three years later in 1993 by Munro et al[187]. Using a myeloid cell line, HL60, the authors of this study identified novel GPCRs expressed in myeloid cells and found that a clone they isolated called CX5 shared high sequence homology with the previously discovered CB1. They subsequently demonstrated that this receptor was agonized by

cannabinoid compounds in cells transfected with the CX5 clone, conclusively demonstrating that this was a true cannabinoid receptor and suggested it be called CB2[171,187].

CB1 and CB2 have an overall sequence homology of 44%; this rises to approximately 70% homology in the transmembrane domain when considering residues important for ligand binding[125,171]. CB1 and CB2 are members of the largest family of membrane proteins, GPCRs. All GPCRs are characterized by the presence of seven transmembrane-spanning α-helical regions, an extracellular amino-terminal region, and an intracellular carboxy-terminal tail[171,188]. Ligand binding leads to a conformational change of the GPCR that results in the activation of receptor-associated heterotrimeric G proteins and consequent downstream signaling[188]. Heterotrimeric G proteins consist of three subunits, α, β, and γ. Ligand binding catalyzes the exchange of bound guanosine diphosphate (GDP) on the Gα subunit for guanosine triphosphate (GTP). The exchange in the guanine nucleotides leads to a reduction in the affinity of the Gα subunit for the Gβγ complex and functional dissociation of the heterotrimer[188]. The dissociated Gβγ complex can then transmit signals to effector proteins, such as enzymes, protein kinases and ion channels, causing rapid changes in the intracellular concentration of signaling molecules, like cAMP and cytosolic ions (i.e. Ca^{2+}), which affect a variety of cellular functions[188]. Furthermore, like most GPCRs, their activation leads to the recruitment of β-arrestin to the intracellular aspect of the receptor, which then mediates cannabinoid receptor desensitization or internalisation and removal from the cell surface[125,171].

1.3.6.2 Mechanism of action of THC

The mechanism of action of THC is well-established, while that of the other constituents of therapeutic interest, i.e. the bioactive metabolite of THC, 11-OH-THC, requires deeper exploration. Most of THC's effects are mediated by binding to the canonical cannabinoid receptors.

Most of the psychotropic effects of THC are attributed to CB1 receptor binding. This is mainly because CB1 receptors are abundantly expressed in the brain[143]. CB1 receptors are also present in the periphery and exert various physiological effects. CB2 receptors are primarily localized to immune cells (e.g. lymphocytes, spleen, thymus) but are also found within the central nervous system[143,189]. THC binding to CB1 or CB2 inhibits the conversion of adenylyl cyclase to cAMP, primarily via G_i-coupling proteins, subsequently inhibiting PKA. This results in suppression of the voltage gated Ca^{2+} channels and activation of the K^+ channels resulting in hyperpolarization. In addition to these well-established signaling events, cannabinoid receptors also modulate several pathways that are more directly involved in ROS production[118], mitochondrial function[118,190,191], the control of cell proliferation and survival, including cell cycle inhibition via induction of p27[kip1,192], impaired cellular differentiation[102], and extracellular signal-regulated kinase[191].

As discussed in section 1.2.10, it has been suggested that upon ligand-receptor binding, signal transduction leads to inhibition of sAC, suggesting signaling in the intermembrane space. THC then decreases PKA-dependent phosphorylation of complex I proteins, particularly NDUFS2, leading to reduced ATP production and availability[191,193] (Figure 5). Considering that constitutively active PKA as well as a mimetic for phosphorylated NDUFS2 rescue the effects of cannabinoids on mitochondrial respiration and block cannabinoid-induced amnesia in vivo[191], a direct link between mitochondrial CB1, neuronal bioenergetics, and higher brain functions emerges[193]. Furthermore, the effects of THC on glucose metabolism have also been described that may be a consequence of primary mitochondrial effects[194]. Because THC exposure has been linked to poor gestational outcomes, like IUGR, which are subsequently linked to metabolic abnormalities[101,195], there is good rationale to explore this in the context of gestational and long-term abnormalities, whose consequences may stem from primary mitochondrial perturbations (Figure 5).
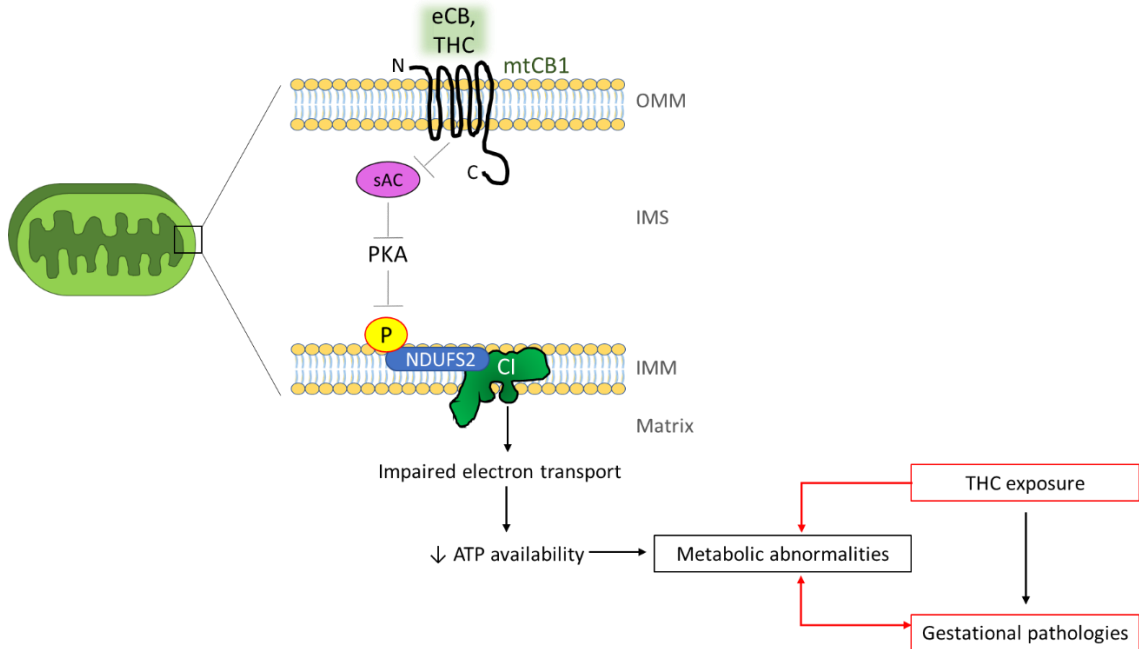
Figure 5. Schematic of the mechanisms of action of THC.
Once bound to its ligand, mitochondrial cannabinoid receptor 1 (mtCB1), prevents the release of soluble adenylyl cyclase (sAC) which inhibits protein kinase A (PKA). Subsequently, PKA-dependent phosphorylation of complex I proteins, namely NDUFS2, is prevented, thus inhibiting mitochondrial complex I function and reducing the availability of ATP. Disturbances to metabolic process occur upon reduced ATP production, which has been linked to THC exposure and gestational pathologies[191].

1.3.7 Pre-natal cannabis/THC exposure and birth outcomes: A focus on fetal growth restriction

While endocannabinoids are the natural ligands, exogenous forms (e.g. THC and synthetic derivatives), can disrupt the rhythm of this system, the relevance of which has been associated with pregnancy and its various outcomes[102,196]. It has been reported that approximately one-third of THC in the maternal circulation can cross the placenta[132] and enter fetal circulation[149]. In the developing fetal brain, CB1 receptor expression is detectable as early as 5-6 weeks post-conception[132]; most studies on the effects of cannabis exposure during the gestational period have focused on the

neurological deficits[197–200]. In addition to the reported variable effects in several areas of cognitive development[132,201,202], aberrant or excessive signaling associated with fetal exposure to cannabis or THC has been connected with IUGR[195], increased risk of infertility and miscarriage, preterm birth[203,204] (and subsequent need for placement into NICU[149]), exaggerated startle reflex and tremors in the neonate[205]. A recent study by Benevenuto et al (2017) using pregnant mice exposed only to filtered air (control animals) or to cannabis smoke by inhalation, demonstrated an embryotoxic and fetotoxic effect of cannabis exposure as evidenced by reduced weight of the pups[197]. As many cannabis users also smoke cigarettes and/or drink alcohol, teasing out the effects of cannabis exposure alone can prove difficult. The research conducted by Benevenuto et al allowed for the isolation of the effects of cannabis on its own, which eliminates the confounding effects of poly-drug use for ease of translatability to human clinical outcomes. Benevenuto et al conclude from their data that there is an association of moderate reductions in birth weight with cannabis exposure (at low doses)[197]. Lastly, Wasserman et al (2015) utilized a mouse model (5-11 PND[198]; equivalent to the third trimester of human fetal development[206]) to demonstrate that perturbation of the endocannabinoid system by THC exposure (5mg/kg/day intraperitoneally) stunted the growth of vertebral and long bones, an effect that was not seen with cannabinoid receptor deletion, and was largely mediated by CB1[198]. Taken together, cannabis or THC exposure during prenatal development is potentially harmful to the offspring of mothers who opt to use the drug during pregnancy.

1.3.8 THC and impaired placentation?

The negative prenatal effects and birth outcomes may stem from perturbations to placental form and function. The ECS and the signaling therein are emerging as key regulators of reproductive function, as evidenced by tight regulation of intrauterine ECS signaling[207,208],

preimplantation embryonic development, oviductal transport[209,210], implantation[211,212] and placentation[141,213,214]. Although THC readily crosses the placental barrier, its active metabolite, 11-OH-THC, does not[137]. While other drugs, like nicotine, are found in higher concentrations in the fetal compartment relative to maternal circulation, the placenta appears to limit fetal exposure to cannabis, as various animal models demonstrate lower fetal concentrations of THC[137]. The detrimental effects of whole cannabis or THC exposure on fetal development (i.e. various neurological deficits), therefore, may be attributed to complex drug-receptor interactions on the developing fetal structures, altered uterine blood flow[137] or placental development[62,195,215,216]. Indeed, Natale et al (2020) have recently demonstrated in rats that THC treatment led to symmetrical fetal growth restriction, in part, due to placental insufficiency as evidenced by reduced blood vessel surface area available for nutrient exchange[195]. Similarly, using a mouse model, Chang et al (2017) demonstrated that THC exposure caused intrauterine growth restriction.[216] This was attributed to impaired placental development due to increased diameters of trophoblastic septa in labyrinth zones which increased the diffusion distance for nutrients between maternal and fetal blood supplies[216]. Considering the increased popularity of cannabis use during pregnancy, along with the increasing potency of THC in cannabis preparations, it is critical to understand the molecular impacts of THC exposure on the development of the feto-placental unit. These themes will be elaborated upon in the appended chapters.

2.   CHAPTER 2

2.1   RATIONALE FOR THE PRESENT STUDY

While maternal and fetal outcomes in response to cannabis and THC exposure are being elucidated, what is lacking is an understanding of the effects of THC on establishing the materno-fetal interface. The placenta, mediating all the physiological exchanges between the mother and her baby, has not been well characterized with respect to the effects of THC on placental morphology and function. Restricted fetal growth, the most common finding that is associated with in utero cannabis exposure, is associated with placental pathology, stemming from altered trophoblast invasion and syncytialization.

The current legislation on cannabis in Canada allows the consumption of cannabis for medicinal and recreational purposes. Legalization of this plant brings it into the realm of other recreational drugs such as alcohol and nicotine, the concern being that the legalization is not equivalent to its safe use[217]. Given the potential for increased THC content with hybrids and various subspecies of the plant, and the use of cannabis concentrates, it is likely to result in increased use and increased potential for harm.

The literature suggests that CB1 receptor signaling, primarily studied within neurobiology, can regulate mitochondrial physiology in non-neuronal tissue[117]. The placenta, for instance, is a highly metabolically active organ that is rich in mitochondria[73], which has been shown to express CB1[117,141]; thus disturbances to ECS signaling can disrupt the ability of mitochondria to regulate the energy demands of the trophoblasts[1,117,193]. Though located on the mitochondria, what remains to be elucidated is the way in which THC affects placental physiology, via the mitochondria, the signals from which may negatively impact fetal development.

2.2   OVERALL HYPOTHESIS

An understanding of the relationship between mitochondria and placental development is crucial as several pharmaceutical and environmental chemicals along with dietary factors have been shown to affect mitochondria; thus, may affect the development and function of the materno-fetal interface. Importantly, THC has been shown to induce mitochondrial dysfunction and increase cellular ROS levels. I therefore *hypothesize* that the introduction of exogenous cannabinoid THC will negatively impact trophoblast development and because placental cells have high energetic demands, these changes may act in part, via mechanisms that involve the mitochondria.

2.3   STUDY AIMS

The general aim of my study is to investigate the influence of mitochondrial dysfunction, and that elicited by THC exposure, on trophoblast physiology.

2.4   STUDY OBJECTIVES

1) To determine if direct pharmacological disruption of mitochondria will result in trophoblast abnormalities in vitro. (Presented in Chapter 3 and Appendix A)

2) To determine if THC can alter the process of invasion and syncytialization in trophoblasts along with its effect on growth factor secretion/expression in vitro. (Presented in Chapters 4, 5 and Appendix B)

3) To investigate the in vitro effects of THC exposure on placental mitochondrial dynamics and function in the context of invasion, syncytialization and hormone secretion. (Presented in Chapters 4, 5 and Appendix B)

3.   CHAPTER 3

REACTIVE OXYGEN SPECIES FROM MITOCHONDRIA IMPACTS TROPHOBLAST FUSION AND THE PRODUCTION OF ENDOCRINE HORMONES BY SYNCYTIOTROPHOBLASTS.

Authors: Walker OS, Ragos R, Wong MK, Adam M, Cheung A, Raha S.

Department of Pediatrics

McMaster University

Hamilton, ON, L8S 4L8

Author contributions:

Conceptualization: OSW, MKW, SR

Data curation: OSW, RR, MKW

Formal analysis: OSW

Funding acquisition: SR

Methodology: OSW, RR, MKW, MA, AC

Project administration: SR

Supervision: MKW, SR

Writing – original draft: OSW

Writing – review & editing: OSW, AC, SR

ABSTRACT

The placenta, a tissue that is metabolically active and rich in mitochondria, forms a critical interface between the mother and developing fetus. Oxidative stress within this tissue, derived from the dysregulation of reactive oxygen species (ROS), has been linked to a number of adverse fetal outcomes. While such outcomes have been associated with mitochondrial dysfunction, the causal role of mitochondrial dysfunction and mitochondrially generated ROS in altering the process of placentation remains unclear. In this study, mitochondrial complex I activity was attenuated using 10 nM rotenone to induce cellular oxidative stress by increasing mitochondrial ROS production in the BeWo choriocarcinoma cell line. Increased mitochondrial ROS resulted in a significant decrease in the transcripts which encode for proteins associated with fusion (GCM1, ERVW-1, and ERVFRD-1) resulting in a 5-fold decrease in the percentage of BeWo fusion. This outcome was associated with increased indicators of mitochondrial fragmentation, as determined by decreased expression of MFN2 and OPA1 along with an increase in a marker of mitochondrial fission (DRP1). Importantly, increased mitochondrial ROS also resulted in a 5.0-fold reduction of human placental lactogen (PL) and a 4.4-fold reduction of insulin like growth factor 2 (IGF2) transcripts; hormones which play an important role in regulating fetal growth. The pre-treatment of rotenone-exposed cells with 5 mM N-acetyl cysteine (NAC) resulted in the prevention of these ROS mediated changes in BeWo function and supports a central role for mitochondrial ROS signaling in the maintenance and function of the materno-fetal interface.

INTRODUCTION

Throughout gestation, the placenta supports the nourishment, growth, and development of the fetus by providing immunological protection and the secretion of various hormones and growth factors necessary for embryonic and fetal survival [1]. The establishment of this critical materno-fetal exchange interface results from the terminal differentiation and fusion of mononucleated villous cytotrophoblasts (CTs) into the multinucleated syncytiotrophoblasts (ST) [1, 2]. Essential to this process is the mitochondrion, an organelle that regulates energy production and serves as the primary source of reactive oxygen species (ROS) [3, 4]. While ROS is an important cellular signal, increased exposure can result in significant damage to mitochondrial function and contribute to overall placental dysfunction [2]. Altered mitochondrial function in the placenta has been associated with various pathological conditions [5] such as intrauterine growth restriction (IUGR). This condition is commonly caused by uteroplacental insufficiency, which in part, may stem from deficiencies in the CT/ST differentiation pathways [6]. Other pregnancy complications, such as preeclampsia (PE) or even pregnancy failure, can stem from perturbations to this differentiation pathway [7]. Perturbed syncytialization will limit the transplacental delivery of critical substrates such as oxygen, glucose and amino acids to the fetus, as well as the removal of fetal waste products. Thus, minor defects in placentation can have profound effects on pregnancy outcome [8]. Importantly, these conditions are often associated with increased oxidative stress [9, 10] in the placenta and result in altered fetal growth. Additional support for the integral role of mitochondrial function in placentation is provided by the observations of Chen and Chan (2010) which demonstrate that mutations in placental mitochondrial fusion genes lead to embryonic lethality [11]. Taken together, the rapid growth and development of the placenta during the early stages of pregnancy makes it susceptible to oxidative stress/damage; a period of vulnerability which is thought to last through to the end of the second trimester [12]. During this period, insults which

alter mitochondrial function can potentiate the level of placental oxidative stress and increase the risk of adverse pregnancy outcomes. Mechanistically, the altered intrauterine environment that ensues may affect fetal development by modifying gene expression and the functioning of trophoblasts. Alterations to mitochondrial function can have deleterious effects, particularly in cells that have a high metabolic demand, such as placental trophoblast cells [12]. Trophoblasts have a high demand for ATP [2] which allows for active transport of substrates across the materno-fetal interface and for continued proliferation of the cytotrophoblasts throughout gestation [1].

Mitochondria are dynamic organelles which are involved in a variety of cellular processes including OXPHOS, apoptosis, and cellular stress responses [3]. They participate in these processes and regulate cellular function through calcium signaling, ROS generation and altered mitochondrial morphology resulting from changes to the fission and fusion dynamics. While complex I and III are generally thought of as the primary sources for free radical generation [3], recent evidence suggests that complex II may also contribute to the pool of mitochondrially generated ROS [13]. Rotenone, the most potent member of the rotenoids, enhances ROS formation during forward electron transfer from FeS centres to ubiquinone leading to superoxide production from mitochondrial respiratory chain complex I and can result in increased oxidative stress to cellular components [3]. Therefore, rotenone [3] is a valuable tool to mimic complex 1-associated disorders and initiate mitochondrial production of ROS in a targeted fashion.

Using an in vitro model of syncytialization, we hypothesize that mitochondrially-generated ROS, induced by pharmacological inhibition of complex I in placental BeWo cells, leads to reduced BeWo syncytialization, and altered secretory profile of the trophoblast cells. We employed an antioxidant precursor, N-acetyl cysteine (NAC), to assess the role of ROS in mediating many of the adverse effects of excess ROS production in BeWo cells.

MATERIALS AND METHODS

Cell culture

The work in this manuscript was conducted in accordance with McMaster University Biosafety Utilization Protocols (BUP-023) and with the approval of the McMaster University Biosafety committee. BeWo cells (ATCC® CCL-98) were grown and maintained in Ham's F-12K medium supplemented with 10% FBS, 1% penicillin/streptomycin, and 1% L-glutamine, maintained in a humidified atmosphere of 5% CO_2 at 37°C. For experimental analysis, cells were seeded at 10,000 cells/cm^2 (approximately 70% confluence). 24 hrs later, cells were treated with epidermal growth factor (EGF; 50ng/mL) to facilitate monolayer formation via its ability to induce proliferation [14, 15]. Following 48 hrs of EGF treatment, the media was supplemented with forskolin (FSK; 50μM) to promote fusion [16, 17], and EGF. The BeWo cells were permitted to differentiate for 48 hrs and then harvested for the analysis outlined below. Rotenone treatment was carried out by exposing BeWo cells to 10 nM rotenone at the same time at FSK/EGF supplementation; in total rotenone treatment lasted for 48 hrs in all cases. The effects of NAC pretreatment on rotenone-mediated ROS generation were investigated by supplementing the media with 5 mM NAC at the same time as EGF addition, 24 hrs following seeding of the cells. Following 48hrs, the media was then supplemented with rotenone, EGF and FSK at the concentrations outlined above. Following 48 hrs of treatment, cells were harvested for immunofluorescence, RNA analysis and Western blot analysis.

MTS assay (3-(4,5-dimethylthiazol-2-yl)-5-(3-carboxymethoxyphenyl)-2-(4-sulfophenyl)-2H-tetrazolium)

In order to determine concentrations of rotenone that would inhibit complex 1 function without causing overwhelming toxicity, BeWo cells were subcultured into a 96-well plate at a density of 1 x 10^5 cells/cm^2 in 100 µL of media. Once a confluency of 70-80% was reached, cells were treated with various concentrations of rotenone. Control wells containing media without cells were allocated to determine background absorbance. Following 48 hours of rotenone exposure, the cells were treated with 20 µL of CellTiter 96® AQ$_{ueous}$ Non-Radioactive Cell Proliferation Assay (Promega, G5421) for 2 hours at 37°C in a humidified, 5% CO_2 atmosphere. The absorbance was immediately recorded at 490nm using a 96-well plate reader (Miltiskan® Spectrum spectrophotometer; Thermo Scientific, Canada) as per the manufacturer's instructions. The average 490nm absorbance value from the "no cell" control wells were subtracted from all other absorbance values to yield the corrected absorbance. Further experiments with rotenone were carried out by using the concentration that gave half of the maximal response.

Lactate Dehydrogenase (LDH) Assay

As a measure of cell death, plasma membrane integrity was quantified using a LDH assay. Lactate dehydrogenase (LDH) release into culture supernatants was detected spectrophotometrically at 490nm and 680nm, using the Pierce LDH Cytotoxicity Assay Kit (Cat. No. #88953), according to the manufacturer's recommended protocol. The results are presented as fold increase in the absorbance measured (normalized to untreated cells).

DCFDA assay (2',7'-dichlorofluorescin diacetate)

BeWo cells were seeded in a black, clear bottom 96-well microplate at a cell density of approximately 3000 cells per well and supplemented with EGF (50 ng/mL), FSK (50 µM), rotenone (10 nM), and/or NAC (5 mM). The protocol was carried out as per the manufacturer's instructions (Abcam DCFDA Cellular ROS Detection Assay Kit, ab113851). Using 1X supplemented buffer as the diluent, cells were treated with initial drugs as listed above in a total of 100 µL total volume per well. Tert-Butyl Hydrogen Peroxide (TBHP) solution (100 µM) in 1X supplemented buffer was used as the positive control. After an incubation time of 4 hours, cells were analyzed on a fluorescent plate reader (BioTek Synergy 4) at excitation and emission wavelengths of 485 and 535, respectively. Data were standardized as a percent of control after background (blank wells with media only) subtraction, followed by normalization to total protein content (BCA).

Total protein extraction

Total protein was isolated following cell lysis using ice-cold radioimmunoprecipitation assay (RIPA) buffer supplemented with protease and phosphatase inhibitor tablets (1 tablet each per 10 mL of RIPA). Cells were further homogenized by sonication for 7-10 pulses at 7 Hz. Samples were centrifuged at 10 000 xg for 5 minutes at 4°C to pellet the cell debris. The supernatant containing total protein was transferred to a fresh tube and placed on ice for immediate BCA analysis or stored at -80°C for later use.

BCA assay

Protein concentration was determined by using the bicinchoninic assay (BCA; ThermoFisher, Canada) with bovine serum albumin (BSA; 0-2000 µg/mL) as a concentration standard according to manufacturers instructions. Total protein concentration was measured with a 96-well plate reader (Miltiskan® Spectrum spectrophotometer; Thermo Scientific, Canada) at 562nm.

SDS-PAGE and western blotting

20 µg of total protein was separated on a 10% polyacrylamide gel (unless otherwise stated) and transferred to PVDF membranes. Following the transfer, the membranes were rinsed with tris-buffered saline with tween (TBS-T; TBS with 0.1% Tween) and stained with 1X AMIDO to confirm the efficiency of the transfer. The membranes were then rinsed with water and immersed in an aqueous solution of 0.1 M NaOH for 10-30 seconds, followed by a rinse with water.

PVDF membranes were blocked in 5% skim milk in TBS-T at room temperature for 2 hours. Primary antibodies of interest were then diluted in 5% milk in TBS-T and the membranes were incubated overnight at 4°C. The membranes were washed three times, five minutes each in TBS-T before incubation in secondary horseradish peroxidase-linked donkey anti-rabbit or sheep anti-mouse antibody (1:5000 dilution, GE Healthcare UK) for 1 hour at room temperature. After washing in TBS-T, immunoreactive bands were visualized using an enzyme-linked chemiluminescence detection reagent (Pierce) and visualized using Image Reader LAS-3000IR (Fujifilm). The intensity of the bands were quantified using ImageJ. The ImageJ values generated for the proteins of interest were normalized to GAPDH and/or beta actin on the same membrane.

Immunofluorescence

BeWo cells were seeded on coverslips and incubated with the corresponding treatments. Cells were washed with DPBS and fixed with 2% paraformaldehyde (PFA) for 10 minutes at room temperature. After fixation, they were washed twice with PBS-T (PBS and 0.01% Tween 20) at room temperature. 10% goat serum with 1% BSA, diluted in PBS-T, was used to block the samples for 2 hours at room temperature. Cells were washed twice with PBS-T. The primary antibody against E-cadherin EP700Y (Abcam) was diluted (1:500) in PBS-T with 0.1% BSA. The primary antibody solution was incubated overnight at 4°C. Cells were washed twice with PBS-T. A goat anti-rabbit antibody conjugated to AlexaFluor 488 (Abcam) was diluted in PBS-T with 0.1% BSA to a 1:100 dilution. Cells were incubated with the secondary antibody solution for 2 hours at room temperature in the dark. After washing twice with PBS-T, cells were incubated with a DAPI solution (1.5 ug/mL, diluted in PBS-T and 0.1% BSA, Santa Cruz) for 5 minutes in the dark. Cells were washed twice with PBS-T and mounted onto microscope slides with Fluoromount™ (Diagnostic Biosystems Inc., USA). Coverslips were imaged at 200X magnification with a Nikon Eclipse Ti-E (Nikon Instruments Inc., USA). Five non-overlapping fields of view were captured per sample. Total fusion percentage was calculated as follows: (total number of nuclei in fused cells/total number of nuclei) *100%. Fused cells were counted as cells that had more than one nucleus per continuous membrane as visualized by E-cadherin staining.

RNA extraction and RT-PCR

Cells grown/treated on 12-well plates were lysed with 500 µL of ice-cold TRIzol™ reagent (Thermo Fisher Scientific, Canada) and homogenized by trituration and left to incubate at room temperature for 5 minutes. After 5 minutes, RNA was either immediately isolated or stored at -80°C. RNA was isolated using the Direct-zol™ RNA kit (Zymo Research, USA) as per the

manufacturer's instructions. 500 ng of the resulting RNA was converted to cDNA with the High-Capacity cDNA Reverse Transcription Kit (Applied Biosystems™, Canada) as per the manufacturer's instructions. RT-PCR was performed (CFX384 Touch™ Real-Time PCR Detection System, Bio-Rad, Canada) by adding 7 µL of primer mix (5 µL SYBR Green, 1.5 µL primer (2.5 µM of forward and reverse primers), 0.5 µL ddH$_2$O) and 3 µL of 1:10 diluted cDNA. All genes and their respective primer sequences are listed in Table 1. Fold change mRNA expression was quantified using ΔΔCt analysis, normalized to housekeeping gene (18S) then expressed as the relative fold change to the vehicle control sample expression.

Statistical analyses

Data are presented as the mean ± S.E.M. of three independent experiments. For comparisons between treatment groups, one-way ANOVA or two-way ANOVA followed by Bonferroni's post hoc test was performed using the GraphPad Prism software version 6.0. Differences were considered significant at $P < 0.05$.

RESULTS

Inhibition of complex I results in increased ROS formation, concomitant with the induction of cellular stress responses and upregulation of antioxidant defences

We first sought to determine the concentration of rotenone which would allow for complex I inhibition without severely compromising cell viability using an MTS assay (Fig. S1, panels A and B). An IC$_{50}$ value of 10 nM was determined, in the MTS assay, for undifferentiated and

differentiated BeWo cells. We also carried out an LDH assay (Fig. S1, panels C and D) at these same concentrations. Cell death at 10 nM was not significantly different from untreated cells, but did increase significantly following treatment with 100 nM rotenone. Since inhibition of complex I is known to increase oxidative stress [3], we performed a ROS assay to determine intracellular ROS levels. ROS levels were increased by 1.5-fold in the ST (differentiated BeWo cells) population (P < 0.05), while the levels remained relatively unchanged across the CT (undifferentiated BeWo) cells (Fig.1). We next assessed whether there was a change in oxidative damage by quantifying levels of 4-hydroxynonenal (4-HNE); a well-established marker of oxidative lipid damage [18]. In response to increased levels of ROS demonstrated in Fig. 1, rotenone treatment of BeWo cells resulted in increased levels of 4-HNE in both the CT (10.1-fold) and ST cells (4.8-fold) (Fig. 2; P < 0.01). Importantly, pre-treatment with NAC conferred protection against increased intracellular ROS levels (Fig. 1) and prevented an increase in 4-HNE production in the ST population (Fig. 2).

Oxidative damage to cells can result in one of two opposing responses: apoptosis to remove damaged cells, or a stress response as an attempt to prevent damage and facilitate recovery [19]. Since complex I inhibition did not result in significant cell death (MTS and LDH assay in Fig. S1), we decided to examine the induction of stress responses in the BeWo cells. We examined protein biomarkers associated with management of cellular stress such as heat shock proteins 60 and 70 (HSP60, HSP70) and antioxidant enzymes manganese superoxide dismutase (MnSOD) and copper zinc superoxide dismutase (CuZnSOD) (Fig. 3). In all cases, exposure to 10 nM rotenone for 48 hrs increased the expression of HSP60, HSP70, MnSOD or CuZnSOD (Fig. 3. Panels B-E, respectively). In both the CT and ST trophoblasts, rotenone exposure resulted in induced stress responses and increased the relative levels of MnSOD and CuZnSOD (Fig. 3) protein expression. The CT and ST cells showed a significant increase in the expression of HSP60 (Fig. 3A, B) and

HSP70 (Fig. 3A, C) protein ($P < 0.01$ for CT, $P < 0.0001$ for ST). Furthermore, there was a significant upregulation of MnSOD ($P < 0.001$ for CT; $P < 0.0001$ for ST) and CuZnSOD ($P < 0.01$ for CT; $P < 0.0001$ for ST) in response to the rotenone-induced ROS production in both the CT and ST populations (Fig. 3A, D, E). These rotenone-mediated changes were all normalized in the presence of 5mM NAC. Furthermore, the changes in the expression of the mRNA's encoding these proteins (Fig. S2) also paralleled what is observed in the Western blots shown in Figure 3.

Mitochondrial function is important for trophoblast differentiation/syncytialization

In response to rotenone exposure, CT and ST cells showed a 2.1- and 2.0-fold reduction, respectively, in transcript levels of *ERVW-1* (Fig. 4B; $P < 0.05$). However, only ST cells demonstrated a 1.9-, 4.8-, 3.8-, and 5.9-fold reduction in *GCM1* (Fig. 4A; $P < 0.01$), *ERVFRD-1*, *CG*α and *CG*β transcript levels (Fig. 4C-E; $P < 0.0001$, $P < 0.05$, $P < 0.0001$) respectively. Upon examination of total hCG protein expression (Fig. 4F), similar trends followed, with rotenone treatment reducing the expression of hCG in the ST cells by 12.3-fold ($P < 0.001$). While NAC pretreatment mitigated the rotenone-mediated decreases in *GCM1*, *ERW-1*, *ERVFRD-1*, *CG*α and *CG*β transcripts (Fig. 4, panels A-E), it potentiated the level of hCG protein when compared to ST cells not exposed to rotenone (Fig. 4F; $P < 0.05$).

Mitochondrial ROS production disrupts basal mitochondrial fission/fusion and reduces trophoblast fusion

Both CT and ST cells exhibited increased levels of *DRP1* transcript levels (Fig. 5A; $P < 0.05$), by 2.5- and 6.1-fold, respectively in response to rotenone treatment. Concomitantly, there

was a 2-fold decrease in *MFN2* and *OPA1* transcript levels (Fig. 5C and 5D; $P < 0.05$, $P < 0.01$) respectively. No change was observed in *MFN1* transcript level (Fig. 5B). There were no statistically significant changes in the mitochondrial morphology proteins OPA1, MFN2, nor DRP1 (Fig. 6A-C, respectively) in the CT population of BeWo cells. However, upon rotenone treatment, the levels of OPA1 and MFN2 protein expressions were markedly reduced ($P < 0.0001$, $P < 0.05$, respectively) along with a 26.5-fold increase in DRP1 expression (Fig. 6) in the ST cells. Importantly, pretreatment of rotenone-exposed cells with NAC resulted in transcript (Fig. 5C, 5D) and protein (Fig.s. 6A, 6B, 6D) levels of OPA1 and MFN2 that were similar to that observed in the vehicle treated cells. Increases in *DRP1* transcript were partially protected against in response to NAC pre-treatment (Fig. 5A; $P < 0.05$), however, this effect was not evident at the level of protein expression (Fig. 6D).

Rotenone treatment of BeWo cells resulted in a reduction in cellular fusion (Fig. 7), as evidenced by greater disruption in the continuity of the cell boundaries stained by E-cadherin (green) and the increase in the number of boundaries containing single nuclei, stained by DAPI (blue) (Fig. 7B for CTs and Fig. 7F for STs). Importantly, pre-treatment with NAC, in the presence of rotenone, allowed the BeWo cells to differentiate and fuse into multinucleated cells (Fig. 7H, 7I) to the same extent as the vehicle treated cells.

Predictors of fetal growth are altered in response to mitochondrial dysfunction in placental cells

Insulin-like growth factor 2 (IGF-2) [20] and human placental lactogen (hPL) [21] are known to play a role in determining placental nutrient supply and subsequent fetal growth [20]. We quantified the expression of the genes encoding hPL and IGF2 in differentiated and undifferentiated BeWo cells treated with (i) rotenone (ii) NAC (iii) both rotenone and NAC. *hPL*

and *IGF-2* expression were not affected in CT cells treated with rotenone (Fig. 8A, 8B). Interestingly, NAC treatment produced a 2.5-fold increase in *IGF2* in the CT population (Fig. 8B, $P < 0.0001$). Rotenone treatment of ST cells reduced the level of *PL* by 5.0-fold (Fig. 8A) and IGF2 by 4.4 fold (Fig. 8B) ($P < 0.0001$), an effect which was fully and partially protected against by NAC pre-treatment regarding the expression of PL and IGF2, respectively.

DISCUSSION

Fetal growth depends on placental function. Once established, the human placenta mediates all of the physiological exchanges between the mother and her fetus [12]. As an active endocrine organ, it is rich in mitochondria [12, 22], which are required to support the metabolic demands of protein and steroid hormone production. Previous work has demonstrated that mitochondria undergo morphological and functional changes upon fusion of the placental trophoblast cells [23–25]. When compared to mitochondria of the cytotrophoblast population, syncytiotrophoblast mitochondria are smaller, contain vesicular cristae rather than lamellar cristae, and accumulate P450$_{SCC}$, which is a mitochondrial enzyme responsible for catalyzing the first step in progesterone production [23]. These structural differences may result in differential changes to mitochondrial signaling, which may be implicated in altered trophoblast fusion and differentiation programs. Indeed, altered mitochondrial function has been associated with placental pathologies that also demonstrate impaired trophoblast fusion [25–27]. Placentae from PE pregnancies display ultrastructural changes that affect the flow of electrons through the mitochondrial electron transport chain, potentiating excessive ROS production or oxidative stress [26], whereas placentae from IUGR pregnancies demonstrate altered mitochondrial biogenesis [27]. Although the mitochondria are differentially altered in placentae of PE and IUGR pregnancies, both disrupt normal

mitochondrial signaling possibly governing placental development. Despite the evidence of mitochondrial dysfunction observed in placental pathologies in the published literature, the exact mechanisms of how it may impair placental development remain elusive. We suggest that alterations to the mitochondria may disrupt the mitochondrial ROS signaling implicated in trophoblast fusion and differentiation processes, ultimately leading to unfavourable clinical manifestations. To demonstrate a link between mitochondrial function and trophoblast fusion, Poidatz et al. (2015) administered mitochondrial inhibitors to induce mitochondrial dysfunction in primary cytotrophoblasts in vitro [2]. Upon administration, cells demonstrated decreased syncytin mRNA expression and endocrine secretion, which suggest that trophoblast fusion requires fully functional respiratory chain activity [2]. However, the mechanisms by which impaired mitochondrial signaling inhibits trophoblast fusion and differentiation remains to be elucidated. This study investigated how mitochondrially produced ROS, by pharmacologically inhibiting complex I with rotenone, may be implicated in the impaired fusion process [28].

Oxidative stress is largely implicated in reproductive failures, including but not limited to infertility, miscarriage, endometriosis, pre-term labour, and PE [29]. Furthermore, excess ROS can trigger pathological events in the placenta, embryo, and fetus [30]. Defense mechanisms against free radical production increases as pregnancy progresses [12]. The initial response to oxidative stress is to upregulate defense systems such as HSPs [19] and antioxidant enzymes [12]. HSPs are classically thought of as chaperones that prevent misfolding of proteins in response to various stressors, and to facilitate their refolding and renaturation [19]. In response to harmful stimuli, HSPs are capable of modulating pro-apoptotic signaling pathways to promote survival of the cell [19]. Antioxidant enzymes, in particular the superoxide dismutases, have been shown to increase as gestation progresses, as evidenced from placental preparations at early, midgestation and at term [12], along with free radical scavengers such as glutathione; a response that is likely due to

increased O^{2-} as pregnancy progresses [12]. Several studies have generated ROS using partial inhibition of complex 1 [2, 31–33]. In our study, though BeWo cells were subjected to mitochondrial dysfunction via rotenone-induced complex I inhibition, the CT cells displayed no significant change in relative ROS levels, while the ST cells exposed to rotenone showed a significant increase in relative ROS levels. This could be explained by our observation that the antioxidant enzymes MnSOD and CuZnSOD were equally upregulated in both the CT and ST cells in response to partial mitochondrial inhibition at complex I by rotenone, while the stress response was significantly greater in the ST population, as evidenced by the greater expression of HSPs in the ST cells. This may carry the implication that the ST cells are more sensitive to changes in their oxidative status, as terminal differentiation into STs involves structural and functional changes to the mitochondria [23, 24]. Indeed, it is reported that placental STs are very sensitive to oxidative stress, in part because they form the lining the placenta and must react to the dynamic changes in maternal blood oxygen concentrations [34]. Contributory to this observation may be the finding that ST cells contain fewer antioxidant enzymes relative to other placental cells, for reasons that have yet to be elucidated [34]. Moreover, research has demonstrated that these two trophoblast subpopulations display different nuclear [35] and mitochondrial [2] morphologies, which may further underscore their differing functions and sensitivities to oxidative perturbations.

Mitochondria are dynamic organelles that continually undergo fusion and fission thus having variable morphological features which are intimately associated with adaptive and functional alterations. Mitochondria participate in key cellular functions and thus affect the processes of most major chronic diseases, aging, and oxidative tissue injury [3]. In this study, the effect of rotenone treatment on differentiating BeWo cells and the associated fusion/fission events was explored in the context of trophoblastic syncytialization. We examined the expression of the mitochondrial pro-fusion markers MFN1, MFN2 and OPA1, along with the pro-fission marker

DRP1. Localized to the outer mitochondrial membrane (OMM), MFN1 and MFN2 have been identified as critical for the fusion of the OMM, while OPA1, is localized to and mediates the fusion of the inner mitochondrial membrane (IMM) [36]. Inhibition of fusion in mammalian cells has been associated with loss of mitochondrial respiratory function [37]. Indeed, upon rotenone treatment of BeWo cells, we demonstrate a marked reduction in the expression of MFN2 and OPA1, which is indicative of increased mitochondrial fission. Interestingly, we observed no change in the expression of *MFN1* transcript in response to rotenone treatment of BeWo cells. Although both MFN1 and MFN2 are required for the maintenance of normal mitochondrial morphology, it may be that MFN2 plays a more direct role in maintaining the OMM. Indeed, Chen et al (2003) have demonstrated that cellular overexpression of one mitofusin while the other is made experimentally deficient is sufficient to restore mitochondrial morphology by promoting fusion [38]. Although the MFN complexes are involved in mitochondrial fusion, they may also serve distinct functions [38]. Largely localized in the cytosol is the opposing dynamin related protein DRP1 which, upon mitochondrial recruitment, promotes OMM and IMM constriction during the process of mitochondrial fission [36, 39]. While some DRP is localized to the mitochondria, likely marking sites of future fission [36], ROS may induce acute recruitment of DRP1 to the mitochondria to orchestrate the process of fragmentation, an effect which was protected against in the ST cells by pre-treatment with NAC.

NAC is known as a ROS scavenger and is used in various clinical applications [40]. In this study, we utilized NAC, an acetylated form of L-cysteine and a substrate for glutathione synthesis, to protect human placental trophoblast cells from excessive ROS-induced damage in an in vitro setting. It serves as a powerful antioxidant and has proven useful in diseases which are subject to excessive free radical production (reviewed in Mokhtari et al) [40]. Importantly, there are no known detrimental effects of NAC on maternal or fetal metabolism [40]. In this study, we pre-treated

BeWo cells with NAC, then selectively reduced electron transport at complex I to determine if we could protect the trophoblast cells from exposure to excessive free radical formation. Our observations demonstrate that perturbing mitochondrial function by interfering with electron trafficking is a detriment to the process of syncytialization. Importantly, the fusogenic potential of the trophoblast cells were preserved upon pretreatment with NAC, protecting the cells from the damaging effects of increased mitochondrial ROS. Interestingly, the CT cells showed a 2.5-fold increase in *IGF2* transcript upon NAC treatment. This may be explained, in part, by the insulin sensitizing effect of NAC [40]. Since IGFs promote growth [1], it is logical that they are nutritionally regulated, with their concentrations serving as an indicator of the availability of substrates from the maternal diet, the availability of which will be limited with placental insufficiency. The greatest inference derived from our study is that of the negative effect of mitochondrial dysfunction and increased ROS production on the expression profile of transcripts and proteins which are implicated in the promotion of normal fetal growth. Various hormones are secreted by placental trophoblasts which are crucial for maintaining the viability of the fetus. Some of these hormones have been specifically linked to fetal growth, as they affect aspects of maternal and fetal metabolism [41]. Two key predictors assessed in our study were the transcript levels of *IGF2* and *hPL*.

Insulin-like growth factor (IGF) has a fundamental role in the control of placental and fetal growth. IGF not only stimulates production of glucose and amino acids, but it also facilitates trophoblast proliferation and differentiation [42], thus promoting proper endocrine function. Increasing throughout gestation, progesterone inhibits insulin-like growth factor binding protein-1 (IGFBP-1), thus allowing for an increase in the bioavailability of IGFs to the growing embryo/fetus [43]. Rotenone treatment of BeWo cells resulted in a marked reduction in *IGF2* transcript levels. This suggests the increased trophoblastic oxidative stress may, through the dysregulation of IGF2,

may contribute to reduced fetal growth. Mechanistically, an increase in IGF is required to stimulate transplacental passage of nutrients, particularly in the third trimester [42]. Furthermore, the action of IGFs are, at least in part, modulated by hPL, which is secreted by the ST cells [16]. Acting with placental growth hormone, hPL is involved in mediating maternal and fetal amino acid, carbohydrate and lipid metabolism [44]. Though able to stimulate the increase in the bioavailability of IGFs, it is not fully known how hPL exerts its somatogenic effects on the fetus [44]. In our hands, increased mitochondrial ROS production, significantly suppressed two key predictors of fetal growth (*IGF2* and *hPL*), effects which were protected against by pretreatment with an antioxidant.

Functionally, rotenone treatment during the BeWo syncytialization process resulted in impaired cell fusion, reduced *GCM1*, *ERVW-1*, and *ERVFRD-1* transcript expression, along with reduced β-hCG secretion. Importantly, our findings reveal the effect of NAC pretreatment protects trophoblasts from the effects of excessive mitochondrial ROS and restored the expression of fusogenic genes and proteins. Other intracellular signaling pathways, such as ER stress and immune signalling, may also contribute to mediating the fusogenic pathways of trophoblast cells as they are known to impact mitochondrial function [45–48].

One important limitation when examining the dynamic trophoblast fusion process is that there is always a mix of differentiating cytotrophoblasts and syncytiotrophoblasts [49]. Therefore, our genomic data reflects changes in both populations and does not detract from our conclusion that mitochondrially produced free radicals significantly attenuates the fusion process.

Taken together, our work demonstrates the importance of mitochondrial health in trophoblast fusion. Thus, pathologies or drugs that involve the mitochondria as a target for their mechanism of action may also put pregnancies at risk for developing placental pathologies. Since ROS signaling is an important part of pregnancy, understanding its regulation and its relationship

to fetal growth and development will provide important insights into how placental oxidative stress impacts post-natal health of the fetus.

REFERENCES

1.   Gude NM, Roberts CT, Kalionis B, King RG. Growth and function of the normal human placenta. Thromb Res. 2004;114(5):397–407.

2.   Poidatz D, Dos Santos E, Gronier H, Vialard F, Maury B, De Mazancourt P, et al. Trophoblast syncytialisation necessitates mitochondrial function through estrogen-related receptor-γ activation. Mol Hum Reprod. 2015;21(2):206–16.

3.   Lenaz G, Genova ML. Structure and organization of mitochondrial respiratory complexes: A new understanding of an old subject. Antioxid Redox Signal. 2010;12(8):961–1008.

4.   Al-Hasan YM, Evans LC, Pinkas GA, Dabkowski ER, Stanley WC, Thompson LP. Chronic hypoxia impairs cytochrome oxidase activity via oxidative stress in selected fetal guinea pig organs. Reprod Sci. 2013;20(3):299–307.

5.   Babbar, M., Sheikh MS. Metabolic stress and disorders related to alterations in mitochondrial fission or fusion. Mol Cell Pharmacol. 2014;5(3):109–33.

6.   Knöfler M, Vasicek R, Schreiber M. Key regulatory transcription factors involved in placental trophoblast development - A review. Placenta. 2001;22:S83–92.

7.   Gupta SK, Malhotra SS, Malik A, Verma S, Chaudhary P. Cell signaling pathways involved during invasion and syncytialization of trophoblast cells. Am J Reprod Immunol. 2015;75(3):361–71.

8.   Carey EAK, Albers RE, Doliboa SR, Hughes M, Wyatt CN, Natale DRC, et al. AMPK knockdown in placental trophoblast cells results in altered morphology and function. Stem Cells Dev. 2014;23(23):2921–30.

9.   Wu F, Tian F-J, Lin Y. Oxidative stress in placenta: Health and diseases. Biomed Res Int. 2015;2015:1–15.

10.   Holland O, Nitert MD, Gallo LA, Vejzovic M, Fisher JJ, Perkins A V. Review: Placental mitochondrial function and structure in gestational disorders. Placenta. 2017;54(2017):2–9.

11.   Chen H, Chan DC. Physiological functions of mitochondrial fusion. Ann NY Acad Sci. 2010;1201:21–5.

12.   Casanueva E, Viteri FE. Iron and oxidative stress in pregnancy. J Nutr. 2003;133:1700–8.

13.   Boulton S, Birch-Machin M. Impact of hyperpigmentation on superoxide flux and melanoma cell metabolism at mitochondrial complex II. FASEB J. 2015;29(1):346–53.

14.   Crowe A, Keelan J. Development of a model for functional studies of ABCG2 (breast cancer resistance protein) efflux employing a standard BeWo clone (B24). Assay Drug Dev Technol. 2012;10:476–84.

15.   Morrish D, Bhardwaj D, Dabbagh L, Marusyk H, Siy O. Epidermal growth factor induces differentiation and secretion of human chorionic gonadotropin and placental lactogen in normal human placenta. J Clin Endocrinol Metab. 1987;65:1282–90.

16.   Orendi K, Gauster M, Moser G, Meiri H, Huppertz B. The choriocarcinoma cell line BeWo: Syncytial fusion and expression of syncytium-specific proteins. Reproduction. 2010;140:759–66.

17.   Wice B, Menton D, Geuze H, Schwartz AL. Modulators of cyclic AMP metabolism induce syncytiotrophoblast formation in vitro. Exp Cell Res. 1990;186:306–16.

18.   Dalleau S, Baradat M, Guéraud F, Huc L. Cell death and diseases related to oxidative stress: 4-hydroxynonenal (HNE) in the balance. Cell Death Differ. 2013;20:1615–30.

19.   Beere HM. "The stress of dying": the role of heat shock proteins in the regulation of apoptosis. J Cell Sci. 2004;117:2641–51.

20.   Melmed S. Endocrinology of fetal development. In: Melmed, S., Polonsky, K.S., Larsen, P.R., Kronenberg HM, editor. Williams Textbook of Endocrinology. 13th ed. Elsevier Health Sciences; 2016. p. 877–8.

21.   Handwerger, S., Freemark M. The roles of placental growth hormone and placental lactogen in the regulation of human fetal growth and development. J Pediatr Endocrinol Metab. 2000;13(4):343–56.

22.   Raha S, Taylor VH, Holloway AC. Effect of atypical antipsychotics on fetal growth: Is the placenta involved? J Pregnancy. 2012;2012:1–9.

23.   Martinez F, Kiriakidou M, Strauss JF. Structural and functional changes in mitochondria associated with trophoblast differentiation: Methods to isolate enriched preparations of syncytiotrophoblast mitochondria. Endocrinology. 1997;138(5):2172–83.

24.   De Los Rios Castillo D, Zarco-Zavala M, Olvera-Sanchez S, Pardo JP, Juarez O, Martinez F, et al. Atypical cristae morphology of human syncytiotrophoblast mitochondria: Role for complex V. J Biol Chem. 2011;286(27):23911–9.

25.   Matsubara S, Minakami H, Sato I, Saito T. Decrease in cytochrome c oxidase activity detected cytochemically in the placental trophoblast of patients with pre-eclampsia. Placenta. 1997;18(4):255–9.

26.   Muralimanoharan S, Maloyan A, Mele J, Guo C, Myatt LG, Myatt L. MIR-210 modulates mitochondrial respiration in placenta with preeclampsia. Placenta. 2012;33(10):816–23.

27.   Poidatz D, Dos Santos E, Duval F, Moindjie H, Serazin V, Vialard F, et al. Involvement of estrogen-related receptor-γ and mitochondrial content in intrauterine growth restriction and preeclampsia. Fertil Steril. 2015;104(2):483–90.

28.   Raha S, Robinson BH. Mitochondria, oxygen free radicals, disease and ageing. Trends Biochem Sci. 2000;25(10):502–8.

29.   Agarwal A, Gupta S, Sharma RK. Role of oxidative stress in female reproduction. Reprod Biol Endocrinol. 2005;3(28).

30.   Thompson LP, Al-Hasan Y. Impact of oxidative stress in fetal programming. J Pregnancy. 2012;2012.

31.   Fato R, Bergamini C, Bortolus M, Maniero AL, Leoni S, Ohnishi T, et al. Differential effects of mitochondrial complex I inhibitors on production of reactive oxygen species. Biochim Biophys Acta. 2009;1787(5):384–92.

32.   Kushnareva Y, Murphy AN, Andreyev A. Complex I-mediated reactive oxygen species generation: Modulation by cytochrome c and NAD(P) T oxidation-reduction state. Biochem J. 2002;368:545–53.

33.   Li N, Ragheb K, Lawler G, Sturgis J, Rajwa B, Andres Melendez J, et al. Mitochondrial complex I inhibitor rotenone induces apoptosis through enhancing mitochondrial reactive oxygen species production. J Biol Chem. 2002;278:8516–25.

34.   Jauniaux E, Burton GJ. Oxygen delivery at the deciduoplacental interface. In: Pijnenborg R, Brosens I, Romero R, editors. Placental Bed Disorders. Cambridge: Cambridge University Press; 2010. p. 63–74.

35.   Fogarty NME, Burton GJ, Ferguson-Smith AC. Different epigenetic states define syncytiotrophoblast and cytotrophoblast nuclei in the trophoblast of the human placenta. Placenta. 2015;36(8):796–802.

36.   Chan DC. Mitochondria: Dynamic organelles in disease, aging, and development. Cell. 2006;125:1242–52.

37.   Cassidy-Stone A, Chipuk JE, Ingerman E, Song C, Yoo C, Kuwana T, et al. Chemical inhibition of the mitochondrial division dynamin reveals its role in bax/bak-dependent mitochondrial outer membrane permeabilization. Dev Cell. 2008;14:193–204.

38.   Chen H, Detmer SA, Ewald AJ, Griffin EE, Fraser SE, Chan DC. Mitofusins Mfn1 and Mfn2 coordinately regulate mitochondrial fusion and are essential for embryonic development. J Cell Biol. 2003;160(2):189–200.

39.   van der Bliek AM, Shen Q, Kawajiri S. Mechanisms of mitochondrial fission and fusion. Cold Spring Harb Perspect Biol. 2013;5.

40.   Mokhtari V, Afsharian P, Shahhoseini M. A review on various uses of N-acetyl cysteine. Cell J. 2017;19(1):11–7.

41.   Ferretti C, Bruni L, Dangles-Marie V, Pecking AP, Bellet D. Molecular circuits shared by placental and cancer cells, and their implications in the proliferative, invasive and migratory capacities of trophoblasts. Hum Reprod Update. 2007;13(2):121–41.

42.   Kurjak A. Hormonal regulation of fetal growth. In: Chervenak FA, editor. Textbook of perinatal medicine: 2 volume set. 3rd ed. Jp Medical Publishers; 2015. p. 1033–6.

43.   Davies S, Richardson MC, Anthony FW, Mukhtar D, Cameron IT. Progesterone inhibits insulin-like growth factor binding protein-1 (IGFBP-1) production by explants of the Fallopian tube. Mol Hum Reprod. 2004;10(12):935–9.

44.   Anthony R V, Pratt SL, Liang R, Holland MD. Placental-fetal hormonal interactions: Impact on fetal growth. J Anim Sci. 1995;73:1861–71.

45.   Collett GP, Redman CW, Sargent IL, Vatish M. Endoplasmic reticulum stress stimulates the release of extracellular vesicles carrying danger-associated molecular pattern (DAMP) molecules. Oncotarget. 2018;9(6):6707–17.

46.   Marchi S, Patergnani S, Pinton P. The endoplasmic reticulum-mitochondria connection: One touch, multiple functions. Biochim Biophys Acta. 2013;1837:461–9.

47.   Weinberg SE, Sena LA, Chandel NS. Mitochondria in the regulation of innate and adaptive immunity. Immunity. 2015;42(3):406–17.

48.   Burton G, Yung H, Murray A. Mitochondrial-Endoplasmic reticulum interactions in the trophoblast: Stress and senescence. Placenta. 2017;52:146–55.

49.   Gauster M, Huppertz B. Fusion of cytothrophoblast with syncytiotrophoblast in the human placenta: Factors involved in syncytialization. J Reproduktionsmed Endokrinol. 2008;5:76–82.

TABLE AND FIGURES

Gene	Forward (5'→3')	Reverse (5' → 3')
18S	CACGCCACAAGATCCCA	AAGTGACGCAGCCCTCTATG
CGα	GCAGGATTGCCCAGAATGC	TCTTGGACCTTAGTGGAGTGG
CGβ	ACCCCTTGACCTGTGAT	CTTTATTGTGGGAGGATCGG
CuZnSOD	AAAGATGGTGTGGCCGATGT	CAAGCCAAACGACTTCCAGC
DRP1	AAACTTCGGAGCTATGCGGT	AGGTTCGCCCAAAAGTCTCA
GCM1	CCTCTGAAGCTCATCCCTTGC	ATCATGCTCTCCCTTTGACTGG
ERVW-1	GTTAATGACATCAAAGGCACCC	CCCCATCTCAACAGGAAAACC
ERVFRD-1	GCCTACCGCCATCCTGATTT	GCTGTCCCTGGTGTTTCAGT
HSP60	GAAGGCATGAAGTTTGATCG	TTCAAGAGCAGGTACAATGG
HSP70	GGAGTTCAAGAGAAAACACAAG	AAGTCGATGCCCTCAAAC
IGF2	GCCAATGGGGAAGTCGATGCTGG	GAGGCTGCAGGATGGTGGCG
MFN1	TTGGAGCGGAGACTTAGCAT	GCCTTCTTAGCCAGCACAAAG
MFN2	CACAAGGTGAGTGAGCGTCT	ACCAGGAAGCTGGTACAACG
MnSOD	GCTCCGGTTTTGGGGTATCT	GATCTGCGCGTTGATGTGAG
OPA1	GCTCTGCATACATCTGAAGAACA	AGAGGCTGGACAAAAGACGTT
PL	GCCATTGACACCTACCAG	GATTTCTGTTGCGTTTCCTC

Table 1. Primer sequences of human genes analyzed via RT-PCR
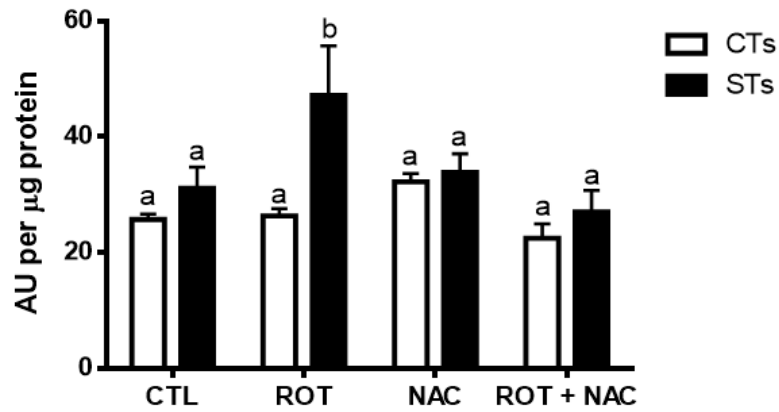
Figure 1. Rotenone induces intracellular ROS production in syncytiotrophoblasts.

A DCFDA assay was performed to determine intracellular ROS levels following rotenone and/or NAC exposure. Tert-Butyl Hydrogen Peroxide (TBHP) solution (100 µM) was used as the positive control (not shown). Significance was determined by a two-way ANOVA, followed by a Bonferroni post hoc test. Results were normalized to the protein content of cell lysates via the BCA assay, as described by Masaki et al (2009), which enables the standardization of ROS production as a function of cell number (protein level). The data represents the mean ± SEM (n = 3). Bars with different letters differ significantly at $P < 0.05$. CTL = control, ROT = rotenone, NAC = N-acetyl cysteine, CT = cytotrophoblasts, ST - syncytiotrophoblasts. AU = arbitrary units.
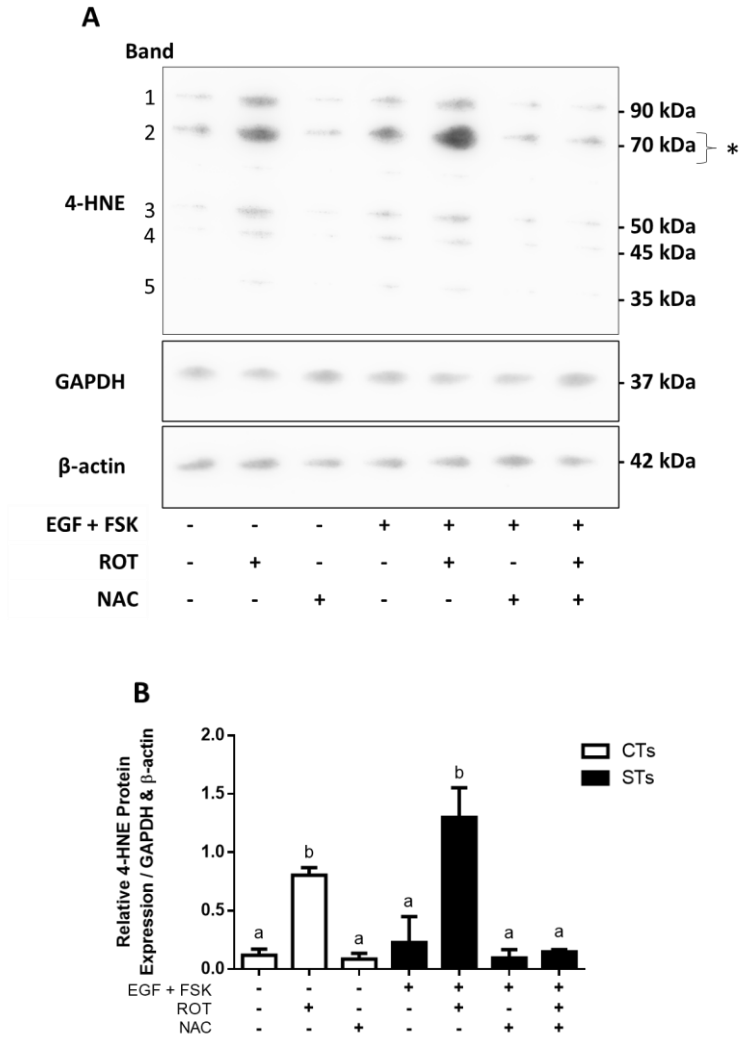
Figure 2. Rotenone-induced mitochondrial complex I inhibition promotes lipid peroxidation in BeWo trophoblast cells.
Panel A: Five major protein bands with molecular weights of approximately 90, 70, 50, 45, and 35 kDa showed immunoreactivity for 4-HNE modifications in control and treated trophoblast cells from whole cell lysates. Panel B: Quantification of the density of the five major protein bands for each treatment group are shown, normalized to GAPDH and β-actin. The asterisk (*) indicates a ~70 kDa band of proteins which show greater sensitivity to oxidative damage. Significant differences were determined by a one-way ANOVA followed by a Bonferroni post hoc test. Results are mean ± SEM (n = 3). Bars with different letters differ significantly at P < 0.01 (B). EGF = epidermal growth factor, FSK = forskolin, ROT = rotenone, NAC = N-acetyl cysteine.
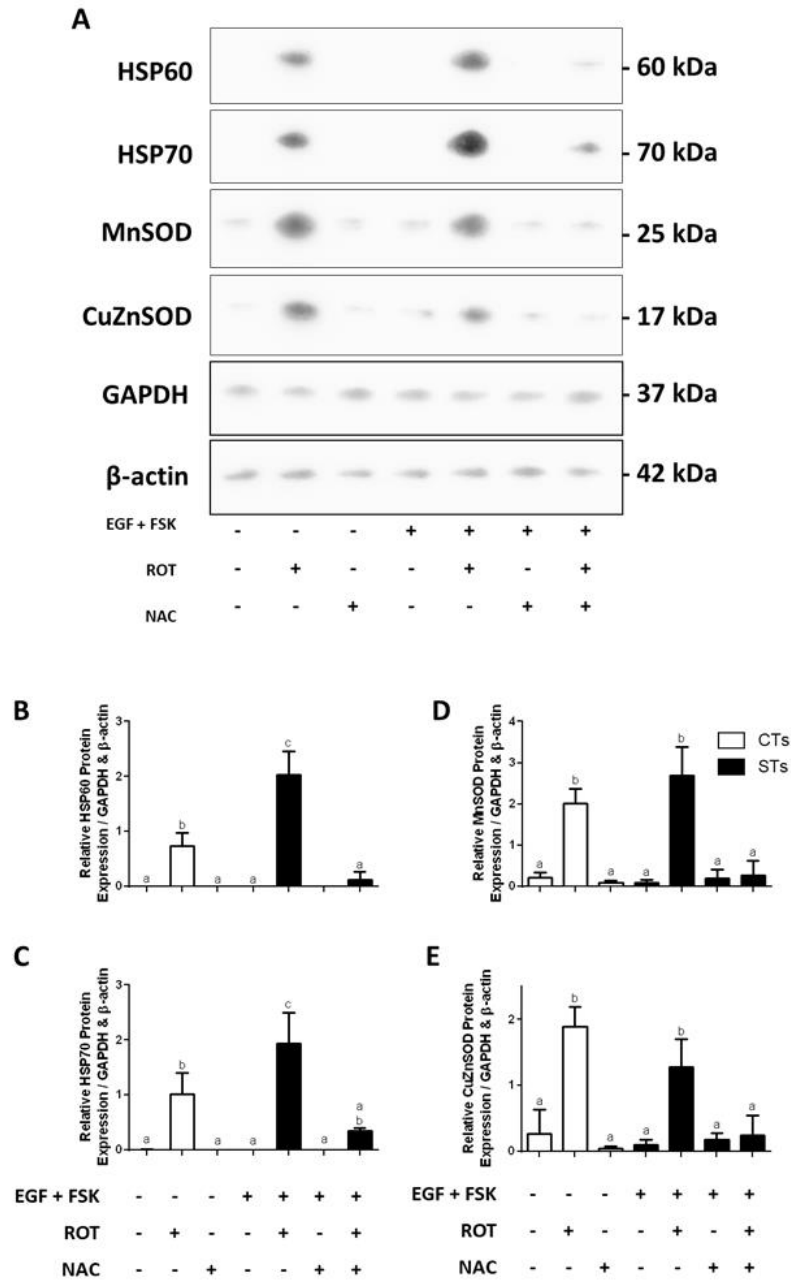
Figure 3. Rotenone treatment of BeWo cells results in the induction of cellular stress response proteins and antioxidant defense enzymes.
Panel A: Western blot analyses of HSP60, HSP70, MNSOD, and CuZnSOD from whole cell lysates from BeWo trophoblast cells. Panels B-E: Summary histograms representing the densitometric measurements of Western blots of HSP60, HSP70, MnSOD, and CuZnSOD protein expressions. Data are presented as mean ± SEM, n = 3. Bars with different letters differ significantly at $P < 0.05$ (B, C), $P < 0.001$ (D), $P < 0.01$ (E).
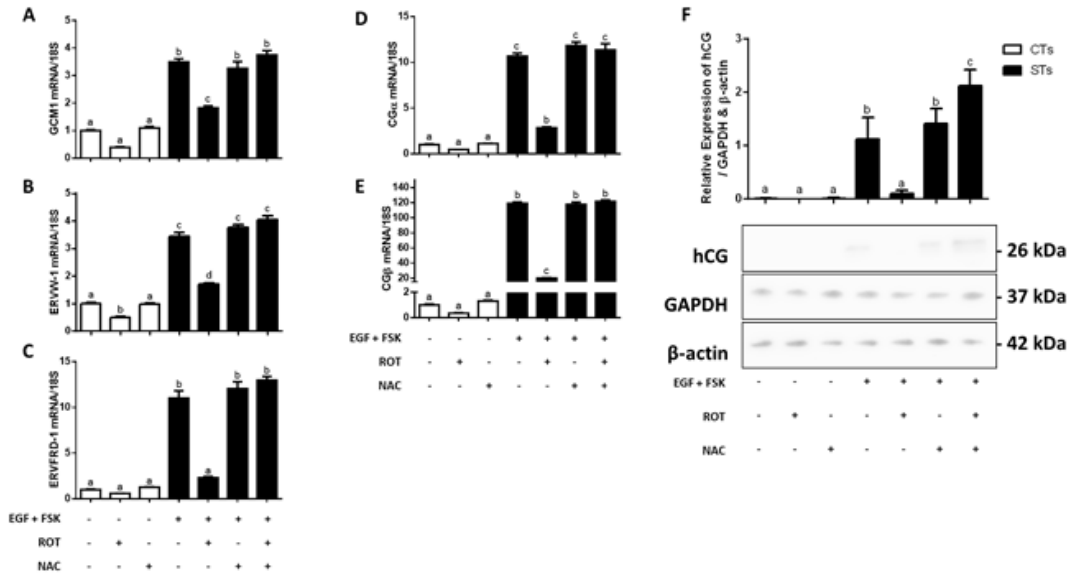
Figure 4. Transcriptional and translational markers of syncytialization and biochemical differentiation are significantly decreased by rotenone. Differentiated BeWo (+FSK, +EGF) or undifferentiated BeWo cells were treated with rotenone, NAC or in combination. The following concentrations were used and administered to cells as described in Methods: DMSO (0.01%) vehicle control, FSK (50 µM), EGF (50 ng/mL), NAC (5 mM) and rotenone (10 nM). Total RNA was isolated from the cells and analyzed by RT-PCR (500 ng) with 18S used as the housekeeping gene. Summary histograms of relative *GCM1* (A), *ERVW-1* (B), *ERVFRD-1* (C), *CGα* (D), and *CG*β (E) mRNA expression in each treatment group normalized to 18S, then compared to the gene in the vehicle control. Gene fold changes are indicated in the histograms. (F) Quantification of total hCG protein expression from whole cell lysates and a representative Western blot are shown, with GAPDH and β-actin used as the loading controls. Significant differences were determined by a one-way ANOVA, followed by a Bonferroni post hoc test. Data are presented as means ± SEM (n = 3). Bars with different letters differ significantly at $P < 0.01$ (A), $P < 0.05$ (B, D), $P < 0.0001$ (C, E), $P < 0.001$ (F).
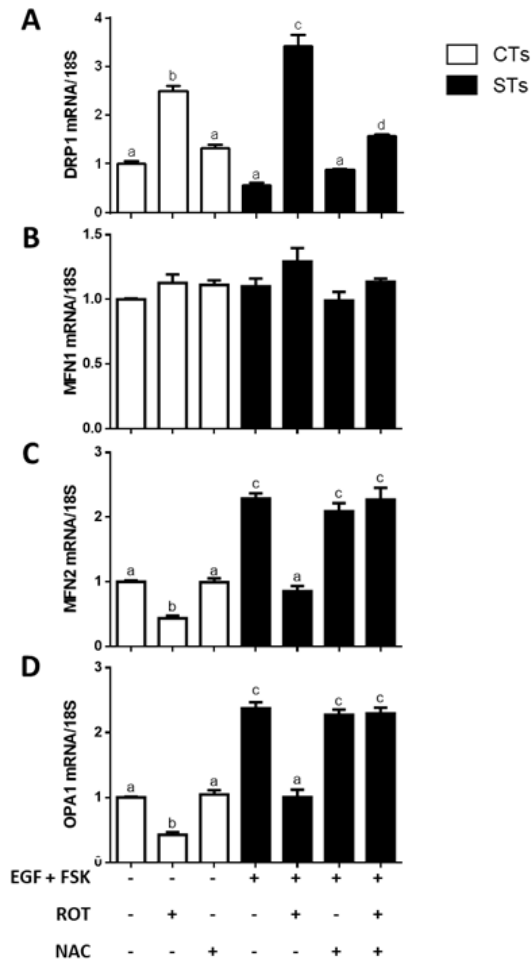
Figure 5. Rotenone treatment of BeWo cells results in altered mRNA expression of the indicators of mitochondrial fission and fusion.
Total RNA was isolated from the cells and analyzed by RT-PCR (1 µg) with 18S used as the housekeeping gene. Summary histograms of relative *DRP1* (A), *MFN1* (B), *MFN2* (C), and *OPA1* (D) mRNA expression in each treatment group normalized to 18S, then compared to the gene in the vehicle control group. Significant differences were determined by a one-way ANOVA, followed by a Bonferroni post hoc test. Data are presented as means ± SEM (n = 3). Bars with different letters differ significantly at $P < 0.05$ (A, C), $P = 0.0515$ (ns) (B), $P < 0.01$ (D).
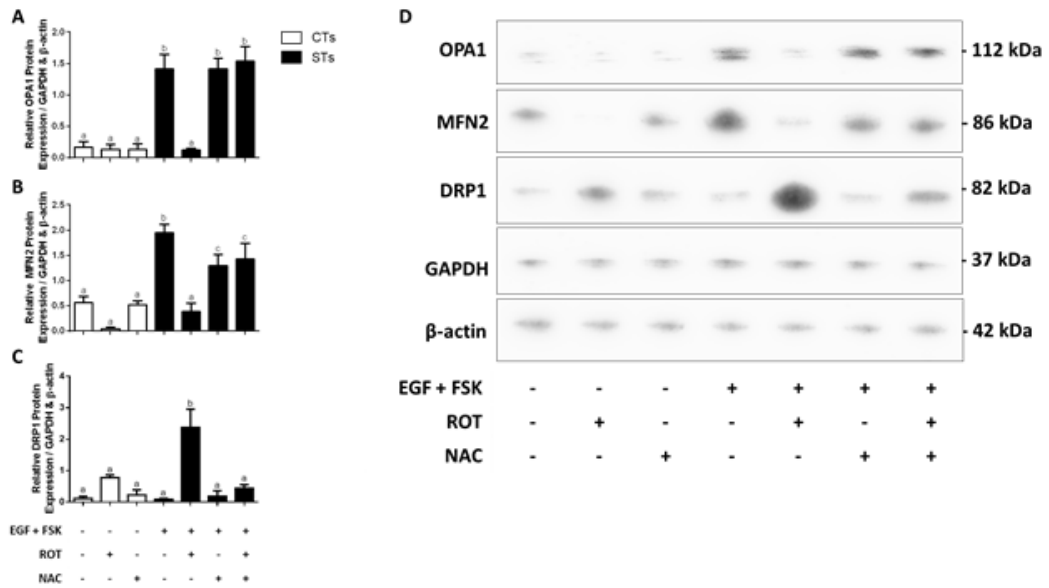
Figure 6. Rotenone treatment alters the expression of proteins responsible for mitochondrial morphology.

Total protein was isolated from BeWo cells and analyzed by Western blot (20µg) with GAPDH and β-actin used as loading controls. Summary histograms of relative OPA1 (A), MFN2 (B), and DRP1 (C) of relative band density in each treatment group normalized to total GAPDH and β-actin. Significant differences were determined by a one-way ANOVA, followed by a Bonferroni post hoc test. Data are presented as means ± SEM (n = 3). Bars with different letters differ significantly at $P < 0.0001$ (A, C), $P < 0.05$ (B).
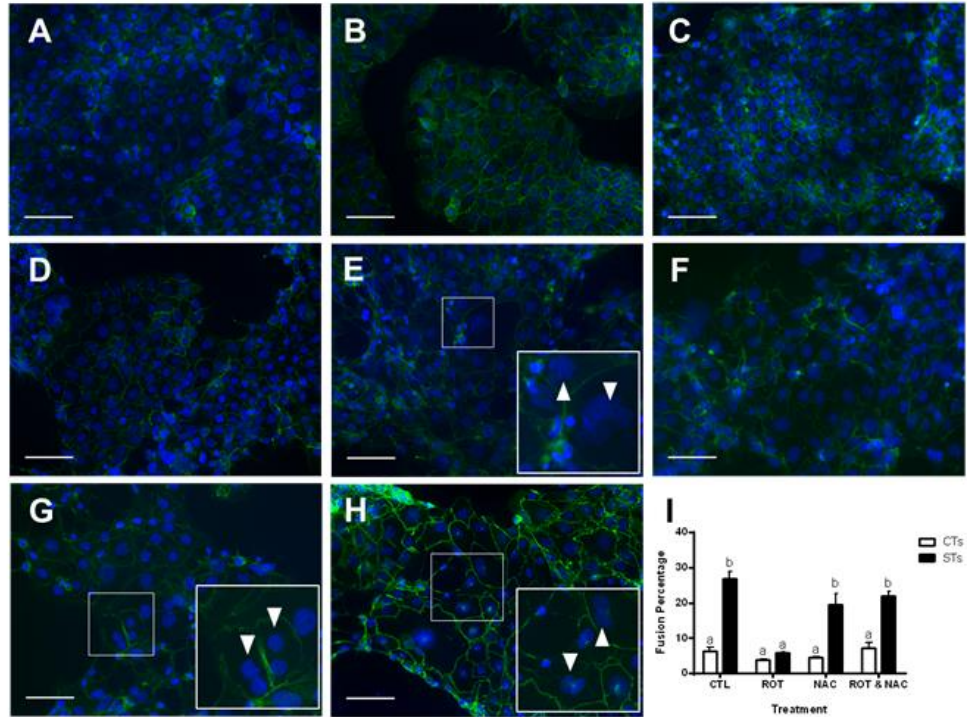
Figure 7. Rotenone treatment of BeWo prevents cellular fusion.
BeWo cells showing immunofluorescent staining (A-H) for E-cadherin distribution at the cell membrane using FITC-conjugated secondary antibody (green) and counterstained with 4', 6-diamidino-2-phenylindole (DAPI) identifying the nuclei (blue). Representative fluorescent microscopy images (20X) are shown (A-H), selected from five random, non-overlapping regions per treatment group (n=3); scale bars indicate 100 µm. A= CT CTL, B= CT ROT, C= CT NAC, D= CT ROT + NAC, E= ST CTL, F= ST ROT, G= ST NAC, H= ST ROT + NAC. Insets represent close up magnifications of E-cadherin localization with depiction of multinucleated syncytiotrophoblasts (arrowheads). Cell counts were performed by two researchers, the average of which were calculated to determine the fusion percentage across all groups (I). Significant differences were determined by a two-way ANOVA, followed by a Bonferroni post hoc test. Data are presented as means ± SEM (n = 3). Bars with different letters differ significantly at P < 0.001 (I).
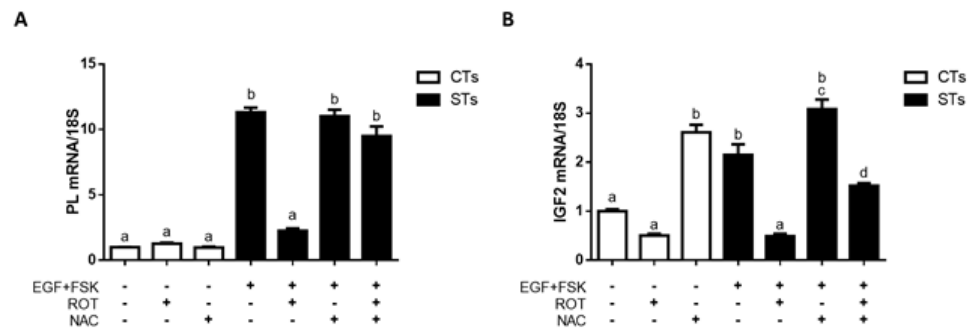
Figure 8. Predictors of fetal growth are impacted by rotenone treatment of BeWo cells.

Panel A: *hPL* transcript. Panel B: *IGF2* transcript. Data are presented as mean ± SEM, n = 3. Significant differences were determined by a one-way ANOVA, followed by a Bonferroni post hoc test. Bars with different letters differ significantly at $P < 0.0001$ (A), $P < 0.01$ (B).

SUPPORTING INFORMATION
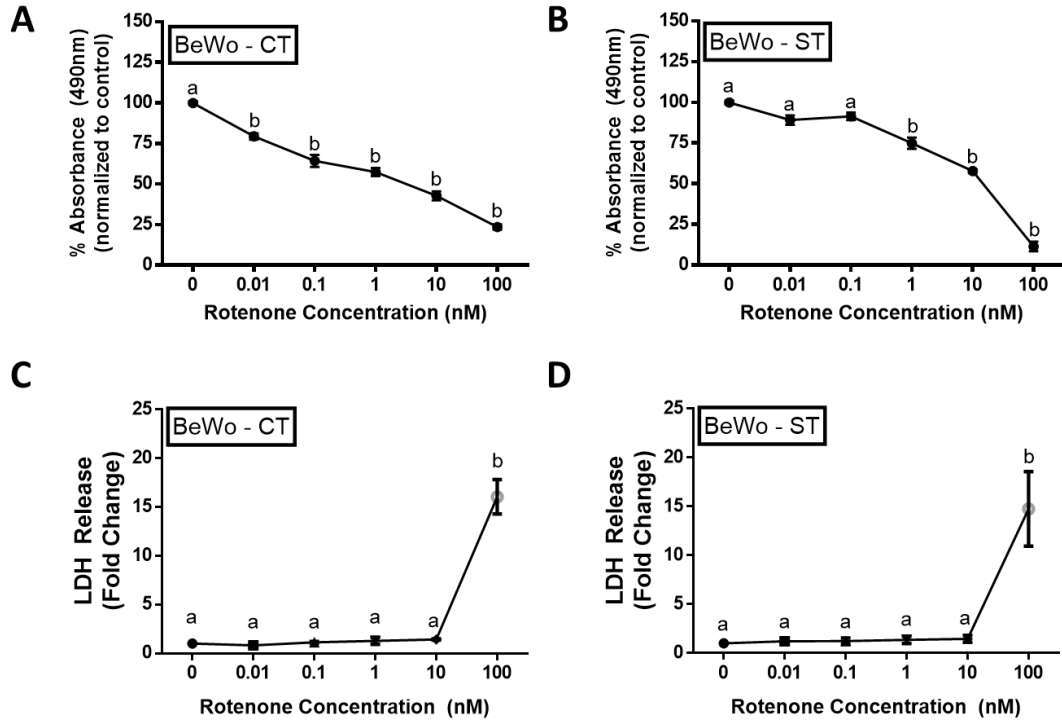
Figure S1.   10 nM rotenone negatively impacts proliferation of undifferentiated (CT) and differentiated (ST) BeWo cells without induction of cell membrane damage (A - D).
The cells were treated with rotenone as indicated. MTS data in panels A, B. LDH data in panels C, D. Each data point represents the mean ± S.E.M. of 3 replicates. Significant differences were determined by a one-way ANOVA followed by a Bonferroni post hoc test. Points with different letters differ significantly at P < 0.0001 (A-C) P < 0.001 (D) from control. Further experiments with rotenone were carried out by using the concentration that gave half of the maximum response, i.e. the point at which MTS values were reduced by 50%, thus successfully inhibiting RCC1 without causing overwhelming toxicity to the cells (C, D).
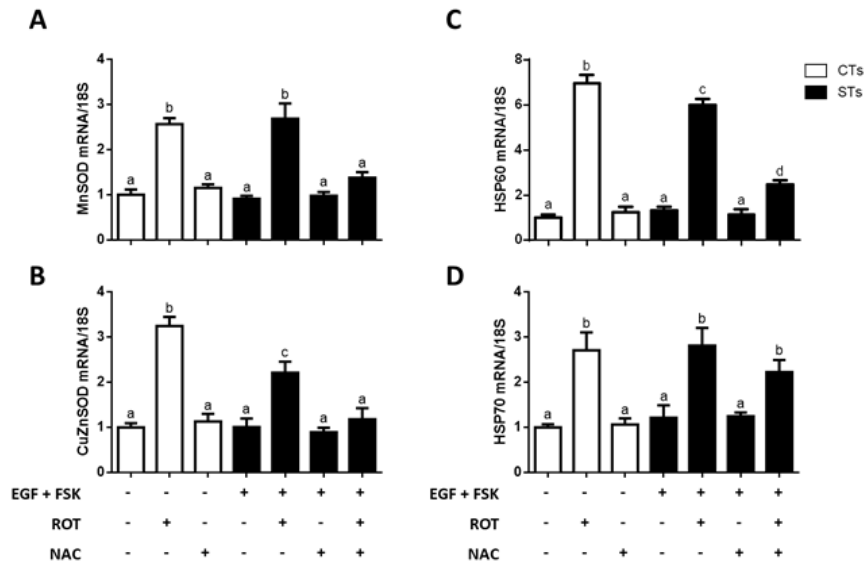
Figure S2. Altered transcript expression of HSP60, HSP70, MnSOD and CuZnSOD in rotenone treated BeWo cells.
Total RNA was isolated from the cells and analyzed by RT-PCR (1 µg) with 18S used as the housekeeping gene. (A - D) Summary histograms of relative *MnSOD* (A), *CuZnSOD* (B), *HSP60* (C), and *HSP70* (D) mRNA expression in each treatment group normalized to 18S, then compared to the gene in the vehicle control group. Significant differences were determined by a one-way ANOVA, followed by a Bonferroni post hoc test. Data are presented as mean ± SEM, n = 3. Bars with different letters differ significantly at $P < 0.0001$ (A), $P < 0.001$ (B), $P < 0.01$ (C), $P < 0.05$ (D).

4.   CHAPTER 4

DELTA-9-TETRAHYDROCANNABINOL DISRUPTS MITOCHONDRIAL FUNCTION AND INHIBITS SYNCYTIALIZATION IN HUMAN PLACENTAL BEWO CELLS.

Authors: Walker OS, Ragos R, Gurm H, Lapierre M, May LL, Raha S

Department of Pediatrics

McMaster University

Hamilton, ON, L8S 4L8

OSW and SR designed the project. OSW, RR, HG, and ML performed the experiments. LLM performed the mitochondrial respiration assays. The manuscript was written by OSW and SR with editing by all authors.

ABSTRACT

The psychoactive component in cannabis, delta-9-tetrahydrocannabinol, can restrict fetal growth and development. Delta-9-tetrahydrocannabinol has been shown to negatively impact cellular proliferation and target organelles like the mitochondria resulting in reduced cellular respiration. In the placenta, mitochondrial dysfunction leading to oxidative stress prevents proper placental development and function. A key element of placental development is the proliferation and fusion of cytotrophoblasts to form the syncytium that comprises the materno-fetal interface. The impact of delta-9-tetrahydrocannabinol on this process is not well understood. To elucidate the nature of the mitochondrial dysfunction and its consequences on trophoblast fusion, we treated undifferentiated and differentiated BeWo human trophoblast cells, with 20 µM delta-9-tetrahydrocannabinol for 48 hours. At this concentration, delta-9-tetrahydrocannabinol on BeWo cells reduced the expression of markers involved in syncytialization and mitochondrial dynamics, but had no effect on cell viability. Delta-9-tetrahydrocannabinol significantly attenuated the process of syncytialization and induced oxidative stress responses in BeWo cells. Importantly, delta-9-tetrahydrocannabinol also caused a reduction in the secretion of human chorionic gonadotropin and the production of human placental lactogen and insulin growth factor 2, three hormones known to be important in facilitating fetal growth. Furthermore, we also demonstrate that delta-9-tetrahydrocannabinol attenuated mitochondrial respiration, depleted adenosine triphosphate and reduced mitochondrial membrane potential. These changes were also associated with an increase in cellular reactive oxygen species, and the expression of stress responsive chaperones, HSP60 and HSP70. These findings have important implications for understanding the role of delta-9-tetrahydrocannabinol-induced mitochondrial injury and the role this might play in compromising human pregnancies.

INTRODUCTION

Cannabis is a commonly used recreational drug amongst pregnant women (Wu et al. 2011; Alpár et al. 2016), and its legalization in many states as well as Canada may lead to the perception that it does not contribute to adverse pregnancy outcomes and is safe to use. Data collected from 2002 to 2014 in the U.S. show that 7.5% of pregnant women between 18 and 25 years of age smoke or otherwise consume cannabis, while the rate of use across all pregnant women is approximately 4% (Brown et al. 2017). The therapeutic benefits of cannabis use, including its anti-emetic and analgesic effects (Chakravarti et al. 2014; Parker et al. 2014; Webb and Webb 2014) make it an attractive drug of choice for pregnant women to manage the related symptoms of pregnancy, particularly because these women may view cannabis as natural product. Although there are presently no reported teratogenic effects in rodent or human studies, cannabis use has been implicated in neurodevelopmental disorders in the offspring (Vela et al. 1998; de Salas-Quiroga et al. 2015; Grant et al. 2018). The main psychoactive constituent, delta-9-tetrahydrocannabinol (THC), is lipophilic and it has been reported that approximately one-third of THC in the maternal circulation can cross the placenta (Wu et al. 2011) and/or 1) directly act on its molecular targets in the fetus, 2) act within the decidua/placenta, with the potential to attenuate placental secretions/signaling to the fetus or uteroplacental blood flow, and lastly 3) exert negative effects on maternal physiology which may, by secondary means, influence the fetus, such as increased secretion of stress-related hormones (Ross et al. 2015). Cannabinoids, including THC, largely exert their biological effects via the activation of G protein-coupled cannabinoid receptors – CB1 and CB2; an integral part of the endocannabinoid system (Habayeb et al. 2008; Bénard et al. 2012; Costa 2016a). CB1 and CB2 are expressed in several organs and tissues and participate in multiple physiological events (Howlett et al. 2002). Both of these receptors have also been identified on term placentae and in the BeWo choriocarcinoma cell line (Costa 2016a). Cannabinoid receptors

have also been localized on the mitochondria (Bénard et al. 2012), which are found in abundance in placentae (Casanueva and Viteri 2003), a highly metabolically active organ (Mandò et al. 2014). While mitochondrial dysfunction is known to be linked to poor placental development (Maloyan et al. 2012; Mandò et al. 2014; Poidatz et al. 2015a), whether such associations exist for cannabis use during pregnancy is not well defined. Restricted fetal growth, the most common finding that is associated with in utero cannabis exposure (Costa 2016a), may be associated with placental pathology stemming from impaired trophoblast function. We, along with others, have recently demonstrated that compromised placental development can be correlated to reduced fetal growth (Hayes et al. 2012; Benevenuto et al. 2017; Deyssenroth et al. 2017; Natale et al. 2020).

Two lineages of trophoblasts are primarily involved in the formation of the materno-fetal interface: cytotrophoblasts and syncytiotrophoblasts. Cytotrophoblasts exist in close proximity to the syncytiotrophoblasts and can fuse to give rise to multinucleated syncytium which forms the materno-fetal interface. The syncytium is found in direct contact with maternal blood, thus it mediates the exchange of oxygen, nutrients, gasses and waste products, and is primarily responsible for the endocrine functions of the placenta, secreting hormones such as human chorionic gonadotropin (hCG), human placental lactogen (hPL) and progesterone (Gude et al. 2004). The biochemical and morphological differentiation of cytotrophoblasts into syncytiotrophoblasts is critical for proper placental development, and consequently, for a healthy pregnancy (Gupta et al. 2015). For example, THC has been shown to attenuate glucose (Araújo et al. 2008) and folic acid (Keating et al. 2009) uptake by the syncytial barrier as well as inhibit the proliferation of BeWo cells (Khare et al. 2006) and impair the differentiation from cytotrophoblasts to syncytiotrophoblasts (Costa et al. 2015) in human trophoblasts. In vivo, treatment of mice with THC during pregnancy resulted in reduced number of pups and lower maternal and placental weights (Chang et al. 2017).

While it has been demonstrated that THC impairs mitochondrial function in neuronal systems (Athanasiou et al. 2007; Wolff et al. 2015), the consequences of THC on trophoblast mitochondrial dynamics, respiration and associated stress responses have not been fully explored. Given that mitochondrial dysfunction, oxidative stress and poor trophoblast outcomes (Walker et al. 2020) and, THC exposure during pregnancy leading to poor placentation and restricted intrauterine growth (Natale et al. 2020) has been demonstrated in rats, we hypothesize that THC may directly increase oxidative stress and reduce ATP generation, and alter trophoblast gene expression resulting in attenuated syncytialization. We report that exposure of human derived BeWo cells to concentrations of THC found in frequent users (Cherlet and Scott 2002; Khare et al. 2006) results in reduced mitochondrial membrane potential, reduced mitochondrial respiration, and increased cellular reactive oxygen production. Functionally, these changes were concomitant with reduced BeWo cell syncytialization and transcription of important fetal growth hormones.

MATERIALS AND METHODS

Cell culture

All cell culture experiments were carried out under McMaster University Biohazard Utilization Protocol BUP023. BeWo cells (ATCC® CCL-98) were routinely grown and maintained in Hams F-12K medium supplemented with 10% FBS, 1% penicillin/streptomycin, and 1% L-glutamine, maintained in a humidified atmosphere of 5% CO_2 at 37°C. Undifferentiated BeWo cells were treated with 20 μM THC (Sigma, Cat. No. T4764) for 48 hours. To induce syncytialization, BeWo cells were treated with epidermal growth factor (EGF; 50ng/mL) (Johnstone et al. 2005) for 48 hours to facilitate monolayer formation and subsequently differentiated using forskolin (FSK; 50μM) (Orendi et al. 2010), along with the replenishment of

EGF, to promote fusion for an additional 48 hours. The media was supplemented with 20 µM THC concomitant with the addition of FSK.

Assessment of cellular viability

The reduction of 3-(4,5-dimethylthiazol-2-yl)-5-(3-carboxymethoxyphenyl)-2-(4-sulfophenyl)-2H-tetrazolium (MTS assay) to a formazan salt was used as a measure of cell viability. BeWo cells were subcultured into a 96-well plate at a density of $1x10^4$ cells/well. Control wells containing media without cells were allocated to determine background absorbance. Cells were treated with THC for 48 hours. BeWo cells were treated with 20 µL of CellTiter 96® AQ$_{ueous}$ Non-Radioactive Cell Proliferation Assay (Promega Corp., Cat. No. G5421) for 2 hours at 37°C in a humidified, 5% CO_2 atmosphere. The absorbance was immediately recorded at 490nm using a 96-well plate reader (Miltiskan® Spectrum spectrophotometer; Thermo Scientific, Canada). The results are presented as percent of the MTS absorbance obtained in untreated cells (100%).

Assessment of plasma membrane integrity

As a measure of plasma membrane integrity, lactate dehydrogenase (LDH) release into culture supernatants was detected spectrophotometrically at 490nm and 680nm, using the Pierce LDH Cytotoxicity Assay Kit (Cat. No. 88953), according to the manufacturer's recommended protocol. The results are presented as fold increase in the absorbance measured (normalized to untreated cells).

Immunofluorescence

BeWo cells were seeded on coverslips ($1x10^5$ cells/cm^2) and treated with THC or vehicle. Cells were immunostained according to previously established procedures (Wong et al. 2018). Briefly, the primary antibody against E-cadherin (Abcam, UK) was diluted (1:500) in phosphate buffered saline with tween (PBS-T) with 0.1% bovine serum albumin (BSA) and incubated with the fixed cells overnight at 4°C. Cells were washed twice with PBS-T. A goat anti-rabbit antibody conjugated to AlexaFluor 488 was diluted (1:100) in PBS-T with 0.1% BSA. Cells were incubated with the secondary antibody solution for 2 hours at room temperature in the dark. After washing twice with PBS-T, cells were incubated with 4', 6-diamidino-2-phenylindole (DAPI, 1.5 µg/mL, diluted in PBS-T and 0.1% BSA) for 5 minutes in the dark. Cells were washed twice with PBS-T and mounted onto microscope slides with Fluoromount™ (Diagnostic Biosystems Inc., USA). Coverslips were imaged with a Nikon Eclipse Ti-E (Nikon Instruments Inc., USA). Five fields of view were captured per sample. An average fusion percentage from the various fields of view was calculated and was used to quantify cell fusion. Total cell fusion percentage was calculated ((total number of nuclei in fused cells/total number of nuclei) x 100%). Fused cells were counted as cells that had two or more nuclei per continuous membrane as visualized by E-cadherin staining. Counts were performed by two individuals blinded to the treatment groups.

Enzyme-Linked Immunosorbent Assay (ELISA)

BeWo cells were seeded ($1x10^5$ cells/cm^2) on 96-well plates and treated with corresponding culture conditions. Supernatants were collected and the levels of secreted hCGβ protein were analyzed by ELISA as previously described by our lab (Wong et al. 2018). The concentration of hCGβ was normalized to total cell lysate in each well.

DCFDA assay (2',7'-dichlorofluorescin diacetate)

BeWo cells were seeded in a black, clear bottom 96-well microplate at a cell density of $3x10^4$ cells/well; differentiated and treated with THC as described above. ROS was detected using the Abcam DCFDA Cellular ROS Detection Assay Kit (Cat. No. ab113851) as per the manufacturer's recommended protocol. The resulting fluorescent signal was quantified (BioTek Synergy 4) at excitation and emission wavelengths of 485 and 535nm, respectively. Data were standardized as a percent of control after background (blank wells with media only) subtraction, followed by normalization to total protein content via the bicinchoninic assay (BCA) (Masaki et al. 2009) which enables the standardization of ROS production as a function of cell number.

BCA assay

Protein concentration was determined by using the BCA (ThermoFisher Scientific, Cat. No. 23252) with BSA (0-2000 µg/mL) as a concentration standard. Total protein concentration was measured by quantifying the absorbance at 562nm using a multi-well plate reader (Miltiskan® Spectrum spectrophotometer; Thermo Scientific, Canada).

RNA extraction and RT-PCR

Cells grown on 12-well plates were lysed with 500 µL of ice-cold TRIzol™ reagent (Thermo Fisher Scientific, Canada). Total RNA isolation and quantification of gene expression (RT-PCR) was performed as previously described by our research group (Wong et al. 2018). All genes and their respective primer sequences are listed in Table 1. Fold change mRNA expression was quantified using the double delta Ct (ΔΔCt) analysis, normalized to housekeeping gene, 18S, then expressed as the relative fold change to the vehicle control sample expression.

Mitochondrial respiration assay

The mitochondrial oxygen consumption rate (OCR) was measured at 37°C in an XFe24 Extracellular Flux Analyzer (Agilent, Santa Clara, CA, USA). In brief, BeWo cells were plated at a density of 5×10^4 cells/well in 250 µL culture media, in 24-well microtiter plates. Syncytiotrophoblasts were differentiated and treated with THC as described above. After 48 hours, culture media was removed and replaced with XF base medium (Seahorse Bioscience, Cat. No. 102365-100) supplemented with 100 mM sodium pyruvate (ThermoFisher Scientific, Cat. No. 11360-070), 200 mM L-glutamine (ThermoFisher Scientific, Cat. No. 25030081), 5 mL of 45% glucose solution (Millipore-Sigma, Cat. No. G8769), warmed to 37°C (pH 7.4). The assay medium was pre-equilibrated at 37°C for 1 hour. OCR was detected under basal conditions followed by the sequential injection of oligomycin (ATP-synthase inhibitor), carbonyl cyanide-4-(trifluoromethoxy)phenylhydrazone (FCCP; mitochondrial respiration uncoupler), and rotenone combined with antimycin (electron transport blockers). These agents were injected through ports of the Seahorse Flux Pak cartridges to reach final concentrations of 1, 2 and 0.5 µM, respectively. The OCR value measured after oligomycin treatment represents the amount of oxygen consumption linked to ATP production, and that after FCCP injection denotes the maximal mitochondrial respiratory capacity of the cells. The final injection of rotenone and antimycin inhibits the flux of electrons through complex I and III, respectively, and thus no oxygen is further consumed at complex V. The OCR reading after this treatment is primarily non-mitochondrial. OCR measurements were obtained using the Seahorse XFe24 Analyzer and the OCR values were normalized to the amount of protein content from each well. The detection of OCR was performed with 4 biological replicates per experiment, for each treatment condition, and repeated 3 more times.

Mitochondrial membrane potential

THC-stimulated changes in the mitochondrial membrane potential ($\Delta\Psi$m) were assessed using the fluorescent reagent tetraethylbenzimidazolylcarbocyanine iodide (JC-1) with the JC-1-Mitochondrial Membrane Potential Assay kit (Abcam, Cat. No. ab113850) following the manufacturer's protocol. BeWo cells were seeded at a density of 5×10^4 cells/well and allowed to adhere overnight in a black, clear-bottom 96 well plate. Cells were treated with 20 µM THC for 48 hours. Following treatment, cells were washed once with 1X dilution buffer and then incubated with 20 µM JC-1 dye in 1X dilution buffer for 10 minutes at 37°C, protected from light. JC-1 dye was then removed, cells were washed once with 1X dilution buffer, 100 µL of fresh 1X dilution buffer was added to each well. The red fluorescence in excitation (535 nm)/emission (590 nm) and green fluorescence excitation/emission (475 nm/530 nm) was measured using a Spark multimode microplate reader (Tecan Group Ltd.). Background fluorescence was subtracted from the fluorescence of treated cells, then the ratio of red (polarized) fluorescence divided by that of green (depolarized) fluorescence was obtained.

CB1 and CB2 receptor antagonist treatments

To attenuate the effects of THC at the canonical cannabinoid receptors CB1 and CB2, BeWo cells were preincubated with selective CB1 antagonist AM281(1 µM) (Lan et al. 1999; Ford et al. 2002) and selective CB2 antagonist AM630 (1 µM) (Pertwee et al. 1995, 2010; Ford et al. 2002) for 30 minutes before the administration of THC (20 µM). This concentration of AM281 was previously shown to completely block the loss in mitochondrial membrane polarity in BeWo cells induced by WINN-55,212, a synthetic cannabinoid, whereas AM630 attenuated this effect (Almada et al. 2017). Further, this concentration of AM630 was previously demonstrated to reverse the THC-induced inhibition of hCG secretion in BeWo cells (Costa et al. 2015).

Statistical analyses

All experiments were performed in biological triplicates (unless otherwise stated). Comparisons between two groups were performed using Student's t-test. One or two-way analysis of variance (ANOVA) and Bonferroni post hoc tests were used to compare data sets with more than two groups. Data are reported as means ± SEM. P < 0.05 was considered significant. The experimental parameters were analyzed using XFe Wave software V2.6.1 and Excel (for OCR measurements) and GraphPad Prism software V6.0.

RESULTS

THC reduces proliferation as assessed by MTS assay and inhibits syncytialization in trophoblast cells

The MTS assay was used to quantify change in the number of cells and the LDH assay was used to determine cytotoxicity in response to THC treatment. Syncytiotrophoblasts treated for 48 hours with a range of THC concentrations (Fig. S1 B) demonstrated decreased proliferation between 20 and 30 µM (Fig. S1 B, P < 0.01). Proliferation of the cytotrophoblast population was not significantly affected by the range of THC used in our study (Fig. S1 A). The LDH assay demonstrated that no cell death was evident over the concentration range of THC tested in either cellular subpopulation (Fig. S1 C, D).

To obtain cytotrophoblast and syncytiotrophoblast populations, BeWo cells were cultured in the absence of (cytotrophoblast), or presence of EGF+FSK (syncytiotrophoblast), to induce differentiation. We evaluated the impact of THC on the cytotrophoblast population as well as on the fusion of cytotrophoblasts to form a syncytium. At the transcript and protein levels, various markers of syncytialization and biochemical differentiation were significantly reduced in response

to THC treatment (Figs. 1 and 2). As expected, the indices for the above processes did not change significantly within the cytotrophoblast population. In the syncytiotrophoblast population, we observed a marked increase in the expression of transcripts associated BeWo fusion in comparison to undifferentiated cells. This increase was reduced by 4-7 fold for glial cell missing 1 (*GCM1*, Fig. 1A, P < 0.05), endogenous retrovirus group W member 1 (*ERVW-1*, Fig. 1B, P < 0.01), and a more than 10-fold reduction for endogenous retrovirus group FRD member 1 (*ERVFRD-1*, Fig. 1C, P < 0.001) following THC exposure. We also observed more than a 50-fold reduction in the transcripts for human chorionic gonadotropin α and β (*CG*A and *CG*B, Fig. 2A, B, P < 0.01); this corresponded to a 2-fold reduction (Fig. 2C, P < 0.0001) in the release of hCG β over the concentration range of THC tested. To compliment these findings, we assessed cellular fusion using immunofluorescent staining. The presence of two or more nuclei within a cell boundary, stained using E-cadherin, was defined as syncytialization. Treatment with THC over a 48-hour time course increased the number of nuclei surrounded by E-cadherin positive boundaries. This translates to a decrease in fusion percentage (total number of nuclei in fused cells/total number of nuclei) x 100%) (Fig. 3, histogram in panel F).

PL and IGF2 are markedly reduced following THC treatment

Following 48 hours of THC treatment, the expression of *PL* and insulin-like growth factor 2 (*IGF2*) transcripts were reduced by 5- (Fig. 4A, P < 0.0001) and 2.5-fold (Fig. 4B, P < 0.01), respectively.

THC affects markers of mitochondrial fragmentation in trophoblast cells

To explore the mechanisms by which THC could influence mitochondrial fragmentation, we examined the transcript abundance of some key factors that regulate mitochondrial morphology/dynamics in differentiated BeWo cells. We analyzed the change in the expression of the mitochondrial fission mediator dynamin-related protein 1 (*DRP1*), and fusion mediators mitofusin 1 and 2 (*MFN1*, *MFN2*) and optic atrophy 1 (*OPA1*). BeWo cells treated for 48 hours with THC exhibited a significant reduction in the expression of the fusion effectors (Fig. 5A, $P < 0.01$, 5B, C, $P < 0.001$). This was concomitant with a 100% increase in the expression of *DRP1*, the fission effector (Fig. 5D, $P < 0.001$).

Intracellular stress responses and defenses are increased upon THC treatment in BeWo cells, concomitant with an increase in oxidative stress

THC exposure resulted in a 2-fold increase in intracellular reactive oxygen species (ROS) generation (Fig. 6E, $P < 0.05$). Increased levels of intracellular ROS have been shown to induce the transactivation of heat shock factor-1 (HSF1) (Lee et al. 2015), the principle transcription factor of heat shock protein 60 and 70 (HSP60 (Ciocca et al. 2013) and HSP70 (Ciocca et al. 2013; Lee et al. 2015)). Following 48 hours of THC treatment in BeWo cells, we observed a 5- and 2.5-fold upregulation of *HSP60* and *HSP70* transcripts, respectively (Fig. 6A, B, $P < 0.0001$). Furthermore, transcript levels of manganese superoxide dismutase (*SOD2*; the mitochondrial isoform) and copper zinc superoxide dismutase (*SOD1*; the cytosolic isoform) (Fig. 6C, $P < 0.0001$, D, $P < 0.001$); two enzymes routinely associated with the regulation of cellular oxidative stress (Thompson and Al-Hasan 2012) were also upregulated in response to THC exposure.

CB1 or CB2 receptor antagonists attenuated THC-induced inhibition of BeWo cell syncytialization and mitochondrial fusion

To determine whether THC mediated the observed impairments to BeWo cell fusion or mitochondrial fusion through CB1 and/or -CB2, BeWo cells were pre-treated with AM281 (CB1 antagonist, 1 µM) and AM630 (CB2 antagonist, 1 µM) for 30 minutes followed by treatment with THC at 20 µM for 48 hours. THC significantly reduced all the transcriptional markers of syncytial formation (*ERVW-1*, *ERVFRD-1*, *CGA* and *CGB*, Fig. 6A-D) and mitochondrial fusion (*MFN1*. *MFN2*, *OPA1*, Fig. 6E-G) while concomitantly increasing the transcriptional expression of *DRP1* (Fig. 6H), a marker of mitochondrial fission. CB1 antagonism, completely abolished the effects on *ERVW-1*, *ERVFRD-1*, *CGA* and *CGB*. However, the effects on *MFN2*, *OPA1* and *DRP1* (Fig. 6F-H) expression were only partially attenuated. The THC-induced reduction on *CGA* and *CGB* transcripts were completely blocked in the presence of the CB2 antagonist (Fig. 6C-D) while the remaining transcripts remained unchanged.

THC alters mitochondrial membrane potential

We used JC-1, a selective $\Delta\Psi$m dye, to explore the role of mitochondrial dysfunction in THC-induced responses. Because JC-1 fluorescence shifts from red to green with membrane depolarization, changes in $\Delta\Psi$m were quantified by changes in the JC-1 red/green fluorescence intensity ratio. Treatment with 20 µM THC for 48 hours significantly decreased the JC-1 red/green fluorescence intensity ratio by 44.1% in syncytiotrophoblasts, compared to untreated controls (Fig. 7F, $P < 0.001$, respectively).

THC reduces oxygen consumption rate and ATP production in differentiated BeWo cells

To further investigate the changes in mitochondrial function that occurred in BeWo cells in response to THC, a Cell Mito Stress assay kit was used to detect the OCR. Trophoblast cells were treated with 20 µM THC for 48 hours before exposure to 1 µM oligomycin, 2 µM FCCP and 0.5 µM rotenone and antimycin. As demonstrated in Figure 8A, THC reduced OCR in BeWo cells, suggesting that THC attenuates mitochondrial respiration. When compared to untreated cells, THC did not significantly affect basal respiration in syncytiotrophoblasts (Fig. 8B). In syncytiotrophoblasts, THC significantly reduced non-mitochondrial respiration by 69.8% (Fig. 8E, $P < 0.0001$) and ATP production by 43.2% (Fig. 8F, $P < 0.01$), while markedly increasing proton leak by 122.2% (Fig. 8C, $P < 0.05$). Interestingly, maximal respiration was significantly increased by 87.5% ($P < 0.01$) in the syncytiotrophoblasts upon THC treatment (Fig. 8D).

DISCUSSION

The placenta is an autonomous and transient organ that is critical for the maintenance of pregnancy and materno-fetal exchanges. Aberrant formation and function of the placenta is associated with pregnancy disorders such as preeclampsia and intrauterine growth restriction (Gupta et al. 2015). The syncytium is critical in forming the materno-fetal interface. In vivo, formation of the syncytium is dependent upon the differentiation and fusion of the underlying stem cells, the cytotrophoblasts. Cytotrophoblast differentiation is characterized by biochemical and morphological changes, including upregulation and expression of hPL, hCGβ, and production of estrogen and progesterone (Wice et al. 1990; Gude et al. 2004; Gupta et al. 2015). As the placenta is an organ with high endocrine activity, hormone production and release are vital aspects of a

placental/trophoblast model. hCG is a secreted peptide hormone that mediates important physiological events such as progesterone production (Weedon-Fekjær and Taskén 2012), placental vascularization (Cole 2010), immune protection for mother and fetus (Wan et al. 2007), fetal organogenesis (Cole 2010), and promotes the continuous differentiation of cytotrophoblasts to syncytiotrophoblasts throughout gestation (Shi et al. 1992; Pidoux et al. 2007; Cole 2010).

To evaluate whether THC treatment impacted these critical trophoblast functions, we used the BeWo cells as a model to study proliferation, differentiation, and syncytialization, as they are the only cell line which can be induced to differentiate and syncytialize in a protein kinase A (PKA)-dependent process (Knerr et al. 2005); emulating what is observed in trophoblasts in vivo, in humans (Knerr et al. 2005; Pidoux 2015). While there are acknowledged differences between isolated human primary trophoblast cells and cultured trophoblast cell lines, the use of established cell lines have been advocated for by many researchers (Bode et al. 2008; Orendi et al. 2010; Rothbauer et al. 2017) and reviewed by Sullivan 2004 (Sullivan 2004).

In the present study, we assessed the effect of THC exposure on the process of BeWo fusion by quantifying 1) markers of syncytialization and indicators of trophoblast fusion; 2) hCG secretion; and 3) the observation of multinucleated syncytia via immunofluorescent staining. We demonstrate that exposure of BeWo cells to THC results in a significant reduction in CG gene transcription mediated by both CB1 and CB2 and attenuated the release of hCGβ from the STs. Furthermore, THC exposure also resulted in reductions in the transcriptional markers of syncytialization largely mediated via CB1 binding, and a reduction in the percentage of fused trophoblasts. Aberrant syncytialization has been implicated in preeclampsia (Roland et al. 2016), and several reports have indicated that the master players in syncytialization, including GCM1 and the syncytins (Vargas et al. 2009), are also downregulated in preeclampsia (Langbein et al. 2008; Orendi et al. 2010; Roland

et al. 2016). In this way, THC may interfere with the mechanisms involved in trophoblast fusion, and thus, be implicated in poor pregnancy outcomes.

One of the primary functions of the human placenta is to produce hormones and other mediators which are critical for pregnancy success. These include hPL and IGFs, molecules which are implicated in fetal growth and development (Mcintyre et al. 2000; Constância et al. 2002; Forbes et al. 2008). Treatment of trophoblasts with THC for 48 hours led to reduced transcriptional expression of both markers, which further suggests perturbed syncytial function. Various studies demonstrate that infants that are born small for their gestational age (SGA) were exposed to decreased levels of hPL and IGFs when compared to infants of normal pregnancies (Mirlesse et al. 1993; Mcintyre et al. 2000; Koutsaki et al. 2011). These growth factors were measured in maternal serum, plasma and term placental tissue, respectively. hPL is a polypeptide hormone mainly secreted by syncytiotrophoblasts and its overall function is that of regulation of fetal and maternal lipid and carbohydrate metabolism (Costa 2016b). Furthermore, hPL and IGFs are also potent stimulators of tissue growth and regulate the metabolic status of both mother and fetus (Forbes et al. 2008). IGF1 and IGF2 are expressed by fetal tissues and placenta; however, reduced fetal growth in mice lacking the placental specific transcript of IGF2 (Constância et al. 2002) is associated with reduced placental mass (Sibley et al. 2004).

Birth weight is indicative of future risk of metabolic disorders including obesity, diabetes and cardiovascular disease (Freemark 2010). Healthy fetal growth and weight gain is dependent upon maternal metabolism, and placental development and function (Anthony et al. 1995; Freemark 2010). The possibility that THC mediated changes in the placenta can restrict fetal growth is supported by the recent finding of Natale et al. (2020). Using a rat model of pregnancy, Natale et al. (2020) reported symmetrical fetal growth restriction following in utero exposure to THC (Natale et al. 2020). Furthermore, this group also demonstrated an increase in the labyrinth region of the

placenta, leading to an overall greater mass for placentae from dams exposed to THC. Changes in placental vascularization, resulting from the development of narrower vascular networks, has also been observed in women who smoked cannabis without the confounding co-exposure of alcohol or tobacco (Chang et al. 2018). Thus, the effect of THC on the reduced expression of hPL and IGF2 in our in vitro system may contribute to the better understanding of mechanisms linking exposure of the syncytium to THC and outcomes reported in SGA fetuses.

Oxidative stress and mitochondrial dysfunction in the placenta have been previously associated with SGA offspring (Mandò et al. 2014). In fact, the regulation of oxidative stress is a critical parameter for normal progression of pregnancy (Holland et al. 2017) and excessive placental oxidative stress is characteristic of several gestational disorders, such as intrauterine growth restriction and preeclampsia (Holland et al. 2017). Mitochondria are known to contribute to placental oxidative stress (Myatt and Cui 2004) and have also been shown to be negatively impacted by THC (Costa et al. 2015). Recent work by Lojpur et al. (2019) suggested that 15-30 µM THC triggered reduced mitochondrial oxidative phosphorylation and increased endoplasmic reticulum (ER) stress in unfused BeWo cytotrophoblasts. However, mitochondrial function and signals play a wide range of roles in the placenta including the regulation of syncytialization (Maloyan et al. 2012). To advance the understanding of how THC may reduce mitochondrial function and increase syncytiotrophoblast stress, we investigated the consequences of THC exposure on syncytiotrophoblast mitochondrial respiratory function, dynamics, antioxidant enzyme expression as well as cellular ROS production and markers of cellular stress.

The MTS and LDH assays measure different aspects of cellular function. The MTS assay quantifies mitochondrial metabolic activity and indirectly reflects cellular proliferation. Conversion of MTS to its purple formazan precipitate is mediated by mitochondrial dehydrogenases. This precipitate, measured spectrophotometrically upon solubilization, is directly

proportional to the number of viable cells (Rai et al. 2018), while the LDH assay allows for the assessment of plasma membrane integrity (Moghimi et al. 2005). We demonstrate that at 20 µM THC, mitochondrial metabolic activity was impaired while leaving the plasma membrane unperturbed. Furthermore, we show that THC, partly mediated via canonical CB1, also perturbs mitochondrial dynamics in trophoblasts as indicated by the increase in the markers of fission, DRP1, and the decrease in the markers of fusion, MFNs and OPA1. Interestingly, antagonism of CB2 did not normalize the THC-mediated reduction of MFN2, OPA1 and DRP1. A healthy mitochondrial reticulum is fundamental for ATP synthesis, regulation of apoptosis, calcium signaling and ROS production (Poidatz et al. 2015b). Healthy mitochondrial reticulum is also an important indicator of overall cellular health and changes in its morphology is indicative of cellular stress (Eisner et al. 2018; Zemirli et al. 2018). We therefore assessed common indicators of oxidative and cellular stress. We observed elevated levels of cellular ROS, increased expression of *HSP60* and *HSP70* as well as *SOD1* and *SOD2*. Normally, ROS generation by the mitochondria is tightly controlled by SOD2 in mitochondria and SOD1 in the cytosol (Wang and Walsh 1998). In our study, the BeWo cells demonstrate the capacity to compensate for the THC-induced increase in ROS generation by increasing the synthesis of *SOD2* and *SOD1* transcripts. Because intracellular ROS may indirectly regulate DRP1 in physiological and pathological processes (Gan et al. 2014; Guo et al. 2014), our results raise the question whether increased DRP1 expression leads to trophoblast dysfunction driven by oxidative stress in our in vitro model.

Decreased mitochondrial membrane potential, a signal characteristic of dysfunctional mitochondria, can trigger mitophagy or mitochondrial recycling (Twig et al. 2008; Twig and Shirihai 2011). This process represents the targeted degradation of mitochondria and a mechanism by which a cell can maintain a healthy mitochondrial pool. Fission precedes mitophagy as this ensures that defective mitochondria are small enough to be engulfed by autophagosomes for

subsequent breakdown in the autolysosome (Osellame et al. 2012). A number of factors can contribute to mitochondrial stress and mitophagy, such as increased ROS, and loss of mitochondrial membrane potential (Twig et al. 2008). We also demonstrate that similar markers of mitochondrial stress are triggered by THC treatment of BeWo cells and associated with markers of mitophagy. While mitochondria are replenished via division of the existing mitochondrial pool, deficits in this process may shift the equilibrium to a state where the cell contains defective mitochondria, perpetuating insufficient respiratory activity and oxidative stress/damage (Twig et al. 2008; Osellame et al. 2012). Twig et al. demonstrated that mitochondria undergoing fission are more likely to undergo mitophagy and that this pool of mitochondria has a significantly lower mitochondrial membrane potential than the cellular pool of mitochondria that is fusion-competent (Twig et al. 2008).

Critical for the maintenance of the mitochondrial membrane potential is the transfer of electrons through the ETC which results in the phosphorylation of ADP to form ATP via complex V – ATP synthase. Measurements of mitochondrial OCR in syncytiotrophoblasts allowed for direct quantification of the effect of THC on various aspects of the electron transport chain function. While we did not observe significant differences in basal respiration, ATP production was significantly reduced in THC treated cells. Interestingly, both the proton leak and maximal respiration demonstrated an increase following exposure to THC. Elevated proton leak may be a sign of mitochondrial inner membrane damage (Eisner et al. 2018) and may be connected to the decrease in membrane potential observed in THC treated cells. Further, the reduced non-mitochondrial oxygen consumption observed in this study can be attributed to non-mitochondrial processes, such as enzymatic activity of oxygenases (Brand and Nicholls 2011; Manfredi et al. 2019). Regarded as an indicator of bioenergetic health, non-mitochondrial OCR varies (Wagner et al. 2011) and may decrease in the presence of stressors (Decleer et al. 2018) like ROS. It is well

established that mitochondria are a target for the deleterious effects of reactive oxygen intermediate. Indeed, our group have demonstrated that 10 nM rotenone over 48 hours attenuated complex I activity in BeWo cells and led to increased ROS production concomitant with perturbed syncytialization (Walker et al. 2020).

Maximal respiratory rate is determined by several factors, including the functional capacity of the electron transport chain. The improved maximal respiration in the syncytiotrophoblasts concomitant with increased proton leak and decreased ATP production may be suggestive of a compensatory mechanism to preserve maximum oxygen consumption in the syncytiotrophoblasts. In fact, due to various perturbations, several mitochondrial compensatory responses have been reported in the literature ((Haylett et al. 2016; Ireland et al. 2018; Manfredi et al. 2019) and references therein). These compensatory changes, along with the increase in SOD1 and SOD2 reported herein, may impart a protective effect on the placenta and the developing fetus in response to additional stressors, such as maternal obesity or preeclampsia. Lojpur et al. (2019) demonstrated that treatment of undifferentiated BeWo cells for 24 hours with 15µM THC resulted in reduced state 3 respiration and this was associated with reduced expression of mitochondrial electron transport chain proteins. Lojpur et al. (2019) observed a reduction in basal respiration upon 24 hours of 15 µM THC exposure in undifferentiated BeWo cells (Lojpur et al. 2019), while we report no significant change in basal respiration in the differentiated BeWo cells. It may be important to consider that there have been reports of ultrastructural differences in the cristae structure of mitochondria from cytotrophoblasts and syncytiotrophoblasts (Martinez et al. 1997; Castillo et al. 2011). Syncytial mitochondria are thought to have lower ATP capacity and have smaller cristae structure to more effectively facilitate steroidogenesis (Castillo et al. 2011).

Mitochondrial dysfunction and the resulting oxidative stress are often associated with endoplasmic reticulum stress (Burton et al. 2017). While we did not evaluate ER stress, it has been

recently shown that in CTs, THC-mediated reduction in mitochondrial function was associated with ER stress (Lojpur et al. 2019). There are numerous reports (Muralimanoharan et al. 2012; Shi et al. 2013; Mizuuchi et al. 2016; Lojpur et al. 2019; Natale et al. 2020; Walker et al. 2020) that have associated mitochondrial dysfunction and/or ER stress to adverse trophoblast function and birth outcomes. While we did not evaluate ER stress, it has been recently shown that in cytotrophoblasts, THC-mediated reduction in mitochondrial function, as assessed by reduced OCR and impaired expression of ETC proteins, was associated with ER stress (Lojpur et al. 2019). Indeed, OXPHOS is, in part, regulated by crosstalk with intracellular calcium, such that efflux of calcium from the ER into the mitochondrial matrix signals an increase in energy demands. When mitochondrial calcium influx is excessive and prolonged, particularly when concomitant with oxidative stress, this may lead to various pathological changes, such as the release of apoptotic proteins from the matrix. Mitochondrial health is intimately linked to cellular viability and, when impaired, becomes associated with various disease states (Osellame et al. 2012).

Taken together, our findings demonstrate that THC attenuates the process of syncytialization and reduces the expression of hPL and IGF2, two important growth hormones connected to pregnancy success. Given the association between THC and reduced fetal growth, it is important to more clearly understand the mechanisms that underpin this association. Our report demonstrates that the observed mitochondrial dysfunction in syncytialized trophoblasts also contributes to increases in the markers of oxidative stress and changes to the dynamics of the mitochondrial reticulum. While it is important to verify these observations in primary trophoblasts, our data advance our understanding of the adverse effects of THC on the materno-fetal interface.

REFERENCES

Almada M, Costa L, Fonseca BM, Amaral C, Teixeira N, Correia-da-Silva G. The synthetic cannabinoid WIN-55,212 induced-apoptosis in cytotrophoblasts cells by a mechanism dependent on CB1 receptor. Toxicology 2017;385:67–73.

Alpár A, Di Marzo V, Harkany T. At the tip of an iceberg: Prenatal marijuana and its possible relation to neuropsychiatric outcome in the offspring. Biol Psychiatry 2016;79:e33–45.

Anthony R V, Pratt SL, Liang R, Holland MD. Placental-fetal hormonal interactions: Impact on fetal growth. J Anim Sci 1995;73:1861–71.

Araújo J, Gonçalves P, Martel F. Modulation of glucose uptake in a human choriocarcinoma cell line (BeWo) by dietary bioactive compounds and drugs of abuse. J Biochem 2008;144:177–86.

Athanasiou A, Clarke AB, Turner AE, Kumaran NM, Vakilpour S, Smith PA, Bagiokou D, Bradshaw TD, Westwell AD, Fang L, et al. Cannabinoid receptor agonists are mitochondrial inhibitors: A unified hypothesis of how cannabinoids modulate mitochondrial function and induce cell death. Biochem Biophys Res Commun 2007;364:131–7.

Bénard G, Massa F, Puente N, Lourenço J, Bellocchio L, Soria-Gómez E, Matias I, Delamarre A, Metna-Laurent M, Cannich A, et al. Mitochondrial CB1 receptors regulate neuronal energy metabolism. Nat Neurosci 2012;15:558–64.

Benevenuto SG, Domenico MD, Martins MAG, Costa NS, de Souza ARL, Costa JL, Tavares MFM, Dolhnikoff M, Veras MM. Recreational use of marijuana during pregnancy and negative gestational and fetal outcomes: An experimental study in mice. Toxicology 2017;376:94–101.

Bode CJ, Jin H, Rytting E, Silverstein PS, Young AM, Audus KL. In vitro models for studying trophoblast transcellular transport. Methods Mol Med 2008;122:225–39.

Brand MD, Nicholls DG. Assessing mitochondrial dysfunction in cells. Biochem J 2011;435:297–312.

Brown Q, Sarvet A, Schmulewitz D, Martins S, Wall M, Hasin D. Trends in marijuana use among pregnant and nonpregnant reproductive-aged women, 2002-2014. JAMA 2017;317.

Burton G, Yung H, Murray A. Mitochondrial-Endoplasmic reticulum interactions in the trophoblast: Stress and senescence. Placenta 2017;52:146–55.

Casanueva E, Viteri FE. Iron and oxidative stress in pregnancy. J Nutr 2003;133:1700–8.

Castillo DDLR, Zarco-Zavala M, Olvera-Sanchez S, Pardo JP, Juarez O, Martinez F, Mendoza-Hernandez G, Flores-Herrera O. Atypical cristae morphology of human syncytiotrophoblast mitochondria. J Biol Chem 2011;286:23911–9.

Chakravarti B, Ravi J, Ganju RK. Cannabinoids as therapeutic agents in cancer: Current status and future implications. Oncotarget 2014;5:5852–72.

Chang X, Bian Y, He Q, Yao J, Zhu J, Wu J, Wang K, Duan T. Suppression of STAT3 signaling by Δ9-tetrahydrocannabinol (THC) induces trophoblast dysfunction. Cell Physiol Biochem 2017;42:537–50.

Chang X, Li H, Li Y, He Q, Yao J, Duan T, Wang K. RhoA/MLC signaling pathway is involved in Δ9-tetrahydrocannabinol-impaired placental angiogenesis. Toxicol Lett 2018;285:148–55.

Cherlet T, Scott JE. Tetrahydrocannabinol (THC) alters synthesis and release of surfactant-related material in isolated fetal rabbit type II cells. Drug Chem Toxicol 2002;25:171–90.

Ciocca DR, Arrigo, Patrick A, Calderwood SK. Heat shock proteins and heat shock factor 1 in carcinogenesis and tumor development: An update. Arch Toxicol 2013;87:19–48.

Cole LA. Hyperglycosylated hCG, a review. Placenta 2010;31:653–64.

Constância M, Hemberger M, Hughes J, Dean W, Ferguson-Smith A, Fundele R, Stewart F, Kelsey G, Fowdenk A, Sibley C, et al. Placental-specific IGF-II is a major modulator of placental and fetal growth. Nature 2002;417:945–8.

Costa MA. The endocannabinoid system: A novel player in human placentation. Reprod Toxicol 2016a;61:58–67.

Costa MA. The endocrine function of human placenta: An overview. Reprod Biomed Online 2016b;32:14–43.

Costa MA, Fonseca BM, Marques F, Teixeira NA, Correia-da-Silva G. The psychoactive compound of Cannabis sativa, Δ9-tetrahydrocannabinol (THC) inhibits the human trophoblast cell turnover. Toxicology 2015;334:94–103.

Decleer M, Jovanovic J, Vakula A, Udovicki B, Agoua R, Madder A, De Saeger S, Rajkovic A. Oxygen consumption rate analysis of mitochondrial dysfunction caused by Bacillus cerus cereulide in Caco-2 and HepG2 cells. Toxins (Basel) 2018;10.

Deyssenroth MA, Li Q, Lacasaña M, Nomura Y, Marsit C, Chen J. Expression of placental regulatory genes is associated with fetal growth. J Perinat Med 2017;45:887–93.

Eisner V, Picard M, Hajnóczky G. Mitochondrial dynamics in adaptive and maladaptive cellular stress responses. Nat Cell Biol 2018;20:755–65.

Forbes K, Westwood M, Baker PN, Aplin JD. Insulin-like growth factor I and II regulate the life cycle of trophoblast in the developing human placenta. Am J Physiol Cell Physiol 2008;294:1313–22.

Ford WR, Honan SA, White R, Hiley CR. Evidence of a novel site mediating anandamide-induced negative inotropic and coronary vasodilatator responses in rat isolated hearts. Br J Pharmacol 2002;135:1191–8.

Freemark R. Placental hormones and the control of fetal growth. J Clin Endocrinol Metab 2010;95:2054–7.

Gan X, Huang S, Wu L, Wang Y, Hu G, Li G, Zhang H, Yu H, Swerdlow RH, Chen JX, et al. Inhibition of ERK-DLP1 signaling and mitochondrial division alleviates mitochondrial dysfunction in Alzheimer's disease cybrid cell. Biochim Biophys Acta 2014;1842:220–31.

Grant KS, Petroff R, Isoherranen N, Stella N, Burbacher TM. Cannabis use during pregnancy: Pharmacokinetics and effects on child development. Pharmacol Ther 2018;182:133–51.

Gude NM, Roberts CT, Kalionis B, King RG. Growth and function of the normal human placenta. Thromb Res 2004;114:397–407.

Guo X, Sesaki H, Qi X. Drp1 stabilizes p53 on the mitochondria to trigger necrosis under oxidative stress conditions in vitro and in vivo. Biochem J 2014;461:137–46.

Gupta SK, Malhotra SS, Malik A, Verma S, Chaudhary P. Cell signaling pathways involved during invasion and syncytialization of trophoblast cells. Am J Reprod Immunol 2015;75:361–71.

Habayeb OMH, Taylor AH, Bell SC, Taylor DJ, Konje JC. Expression of the endocannabinoid system in human first trimester placenta and its role in trophoblast proliferation. Endocrinology 2008;149:5052–60.

Hayes EK, Lechowicz A, Petrik JJ, Storozhuk Y, Paez-Parent S, Dai Q, Samjoo IA, Mansell M, Gruslin A, Holloway AC, et al. Adverse fetal and neonatal outcomes associated with a life-long high fat diet: Role of altered development of the placental vasculature. PLoS One 2012;7:e33370.

Haylett W, Swart C, Van Der Westhuizen F, Van Dyk H, Van Der Merwe L, Van Der Merwe C, Loos B, Carr J, Kinnear C, Bardien S. Altered mitochondrial respiration and other features of mitochondrial function in parkin-mutant fibroblasts from Parkinson's Disease patients. Park Dis 2016;2016.

Holland O, Nitert MD, Gallo LA, Vejzovic M, Fisher JJ, Perkins A V. Review: Placental mitochondrial function and structure in gestational disorders. Placenta 2017;54:2–9.

Howlett AC, Barth F, Bonner TI, Cabral G, Casellas P, Devane WA, Felder CC, Herkenham M, Mackie K, Martin BR, et al. International union of pharmacology. XXVII. Classification of cannabinoid receptors. Pharmacol Rev 2002;54:161–202.

Ireland KE, Maloyan A, Myatt L. Melatonin improves mitochondrial respiration in syncytiotrophoblasts from placentas of obese women. Reprod Sci 2018;25:120–30.

Johnstone ED, Sibley CP, Lowen B, Guilbert LJ. Epidermal growth factor stimulation of trophoblast differentiation requires MAPK11/14 (p38 MAP Kinase) activation. Biol Reprod 2005;73:1282–8.

Keating E, Gonçalves P, Campos I, Costa F, Martel F. Folic acid uptake by the human syncytiotrophoblast: Interference by pharmacotherapy, drugs of abuse and pathological conditions. Reprod Toxicol 2009;28:511–20.

Khare M, Taylor AH, Konje JC, Bell SC. Delta 9-Tetrahydrocannabinol inhibits cytotrophoblast cell proliferation and modulates gene transcription. Mol Hum Reprod 2006;12:321–33.

Knerr I, Schubert SW, Wich C, Amann K, Aigner T, Vogler T, Jung R, Rg J, Tsch D, Rascher W, et al. Stimulation of GCMa and syncytin via cAMP mediated PKA signaling in human trophoblastic cells under normoxic and hypoxic conditions. FEBS Lett 2005;579:3991–8.

Koutsaki M, Sifakis S, Zaravinos A, Koutroulakis D, Koukoura O, Spandidos DA. Decreased placental expression of hPGH, IGF-I and IGFBP-1 in pregnancies complicated by fetal growth restriction. Growth Horm IGF Res 2011;21:31–6.

Lan R, Gatley J, Lu Q, Fan P, Fernando SR, Volkow ND, Pertwee R, Makriyannis A. Design and synthesis of the CB1 selective cannabinoid antagonist AM281: A potential human SPECT ligand. AAPS PharmSci 1999;1.

Langbein M, Strick R, Strissel PL, Vogt N, Parsch H, Beckmann MW, Schild RL. Impaired cytotrophoblast cell–cell fusion is associated with reduced syncytin and increased apoptosis in patients with placental dysfunction. Mol Reprod Dev 2008;75:175–83.

Lee J-H, Lee Y-K, Lim JJ, Byun H-O, Park I, Kim G-H, Xu WG, Wang H-J, Yoon G. Mitochondrial respiratory dysfunction induces claudin-1 expression via reactive oxygen species-mediated heat shock factor 1 activation, leading to hepatoma cell invasiveness. J Biol Chem 2015;290:21421–31.

Lojpur T, Easton Z, Raez-Villanueva S, Laviolette S, Holloway AC, Hardy DB. Δ9-Tetrahydrocannabinol leads to endoplasmic reticulum stress and mitochondrial dysfunction in human BeWo trophoblasts. Reprod Toxicol 2019;87:21–31.

Maloyan A, Mele J, Muralimanohara B, Myatt L. Measurement of mitochondrial respiration in trophoblast culture. Placenta 2012;33:456–8.

Mandò C, Palma C De, Stampalija T, Anelli GM, Figus M, Novielli C, Parisi F, Clementi E, Ferrazzi E, Cetin I. Placental mitochondrial content and function in intrauterine growth restriction and preeclampsia. Am J Physiol Endocrinol Metab 2014;306:404–13.

Manfredi LH, Ang J, Peker N, Dagda RK, Mcfarlane C. G protein-coupled receptor kinase 2 regulates mitochondrial bioenergetics and impairs myostatin-mediated autophagy in muscle cells. Am J Physiol Cell Physiol 2019;317:674–86.

Martinez F, Kiriakidou M, Stauss JF. Structural and functional changes in mitochondria associated with trophoblast differentiation: Methods to isolate enriched preparations of syncytiotrophoblast mitochondria. Endocrinology 1997;138:2172–83.

Masaki H, Izutsu Y, Yahagi S, Okano Y. Reactive oxygen species in HaCaT keratinocytes after UVB irradiation are triggered by intracellular Ca2+ levels. J Investig Dermatology Symp Proc 2009;14:50–2.

Mcintyre HD, Serek R, Crane DI, Veveris-Lowe T, Parry A, Johnson S, Leung KC, Ho KKY, Bougoussa M, Hennen G, et al. Placental growth hormone (GH), GH-binding protein, and insulin-like growth factor axis in normal, growth-retarded, and diabetic pregnancies: Correlations with fetal growth. J Clin Endocrinol Metab 2000;85:1143–50.

Mirlesse V, Frankenne F, Alsat E, Poncelet M, Hennen G, Evain-Brion D. Placental growth hormone levels in normal pregnancy and in pregnancies with intrauterine growth retardation. Int Pediatr Res Found Inc 1993;34:439–42.

Mizuuchi M, Cindrova-Davies T, Olovsson M, Stephen Charnock-Jones D, Burton GJ, Wa Yung H. Placental endoplasmic reticulum stress negatively regulates transcription of placental growth factor via ATF4 and ATF6β: Implications for the pathophysiology of human pregnancy complications. J Pathol J Pathol 2016;238:550–61.

Moghimi SM, Symonds P, Murray JC, Hunter AC, Debska G, Szewczyk A. A two-stage poly(ethylenimine)-mediated cytotoxicity: Implications for gene transfer/therapy. Mol Ther 2005;11:990–5.

Muralimanoharan S, Maloyan A, Mele J, Guo C, Myatt LG, Myatt L. MIR-210 modulates mitochondrial respiration in placenta with preeclampsia. Placenta 2012;33:816–23.

Myatt L, Cui X. Oxidative stress in the placenta. Histochem Cell Biol 2004;122:369–82.

Natale B V, Gustin KN, Lee K, Holloway AC, Laviolette SR, Natale DRC, Hardy DB. Δ9-tetrahydrocannabinol exposure during rat pregnancy leads to symmetrical fetal growth restriction and labyrinth-specific vascular defects in the placenta. Sci Rep 2020;10.

Orendi K, Gauster M, Moser G, Meiri H, Huppertz B. The choriocarcinoma cell line BeWo: Syncytial fusion and expression of syncytium-specific proteins. Reproduction 2010;140:759–66.

Osellame LD, Blacker TS, Duchen MR. Cellular and molecular mechanisms of mitochondrial function. Best Pract Res Clin Endocrinol Metab 2012;26:711–23.

Parker LA, Rock EM, Limebeer CL. Regulation of nausea and vomiting by cannabinoids and the endocannabinoid system. Eur J Pharmacol 2014;722:134–46.

Pertwee R, Griffin G, Fernando S, Li X, Hill A, Makriyannis A. AM630, a competitive cannabinoid receptor antagonist. Life Sci 1995;56:1949–55.

Pertwee RG, Howlett AC, Abood ME, Alexander SPH, Marzo V Di, Elphick MR, Greasley PJ, Hansen HS, Kunos G, Mackie K, et al. International union of basic and clinical pharmacology. LXXIX. Cannabinoid receptors and their ligands: Beyond CB1 and CB2. Pharmacol Rev 2010;62:588–631.

Pidoux G. Spatiotemporal regulation of cAMP signaling controls the human trophoblast fusion. Front Pharmacol 2015;6:1–14.

Pidoux G, Gerbaud P, Tsatsaris V, Marpeau O, Ferreira F, Meduri G, Guibourdenche J, Badet J, Evain-Brion D, Frendo J-L. Biochemical characterization and modulation of LH/CG-receptor during human trophoblast differentiation. J Cell Physiol 2007;212:26–35.

Poidatz D, Dos Santos E, Gronier H, Vialard F, Maury B, De Mazancourt P, Dieudonné M-N. Trophoblast syncytialisation necessitates mitochondrial function through estrogen-related receptor-γ activation. Mol Hum Reprod 2015a;21:206–16.

Poidatz D, Dos Santos E, Loı H, Gronier S, Vialard F, Maury B, De Mazancourt P, Dieudonné M-N. Trophoblast syncytialisation necessitates mitochondrial function through estrogen-related receptor-γ activation. Mol Hum Reprod 2015b;21:206–16.

Rai Y, Pathak R, Kumari N, Sah DK, Pandey S, Kalra N, Soni R, Dwarakanath BS, Bhatt AN. Mitochondrial biogenesis and metabolic hyperactivation limits the application of MTT assay in the estimation of radiation induced growth inhibition. Sci Rep 2018;8.

Roland CS, Hu J, Ren CE, Chen H, Li J, Varvoutis MS, Leaphart LW, Byck DB, Zhu X, Jiang SW. Morphological changes of placental syncytium and their implications for the pathogenesis of preeclampsia. Cell Mol Life Sci 2016;73:365–76.

Ross EJ, Graham DL, Money KM, Stanwood GD. Developmental consequences of fetal exposure to drugs: What we know and what we still must learn. Neuropsychopharmacology 2015;40:61–87.

Rothbauer M, Patel N, Gondola H, Siwetz M, Huppertz B, Ertl P. A comparative study of five physiological key parameters between four different human trophoblast-derived cell lines. Sci Rep 2017;7:1–11.

de Salas-Quiroga A, Díaz-Alonso J, García-Rincón D, Remmers F, Vega D, Gómez-Cañas M, Lutz B, Guzmán M, Galve-Roperh I. Prenatal exposure to cannabinoids evokes long-lasting functional alterations by targeting CB 1 receptors on developing cortical neurons. Proc Natl Acad Sci 2015;112:13693–8.

Shi QJ, Lei ZM, Rao C V, Lin J. Novel role of human chorionic gonadotropin in differentiation of human cytotrophoblasts. Endocrinology 1992;132:1387–95.

Shi Z, Long W, Zhao C, Guo X, Shen R, Ding H. Comparative proteomics analysis suggests that placental mitochondria are involved in the development of pre-eclampsia. PLoS One 2013;8, DOI: 10.1371/journal.pone.0064351.

Sibley CP, Coan PM, Ferguson-Smith AC, Dean W, Hughes J, Smith P, Reik W, Burton GJ, Fowden AL, Constâ M, et al. Placental-specific insulin-like growth factor 2 (Igf2) regulates the diffusional exchange characteristics of the mouse placenta. PNAS 2004;101:8204–8.

Sullivan M. Endocrine cell lines from the placenta. Mol Cell Endocrinol 2004;228:103–19.

Thompson LP, Al-Hasan Y. Impact of oxidative stress in fetal programming. J Pregnancy 2012;2012.

Twig G, Elorza A, Molina AJ, Mohamed H, Wikstrom JD, Walzer G, Stiles L, Haigh SE, Katz S, Las G, et al. Fission and selective fusion govern mitochondrial segregation and elimination by autophagy. EMBO J 2008;27:433–46.

Twig G, Shirihai OS. The interplay between mitochondrial dynamics and mitophagy. Antioxid Redox Signal 2011;14:1939–51.

Vargas A, Moreau J, Landry S, Lebellego F, Toufaily C, Rassart É, Lafond J, Barbeau B. Syncytin-2 plays an important role in the fusion of human trophoblast cells. J Mol Biol 2009;392:301–18.

Vela G, Martín S, García-Gil L, Crespo JA, Ruiz-Gayo M, Fernández-Ruiz JJ, García-Lecumberri C, Pélaprat D, Fuentes JA, Ramos JA, et al. Maternal exposure to delta9-tetrahydrocannabinol facilitates morphine self-administration behavior and changes regional binding to central mu opioid receptors in adult offspring female rats. Brain Res 1998;807:101–9.

Wagner B, Venkataraman S, Buettner G. The rate of oxygen utilization by cells. Free Radic Biol Med 2011;51:700–12.

Walker OS, Ragos R, Wong MK, Adam M, Cheung A, Raha S. Reactive oxygen species from mitochondria impacts trophoblast fusion and the production of endocrine hormones by syncytiotrophoblasts. PLoS One 2020;15:e0229332.

Wan H, Versnel MA, Yee Cheung W, Leenen PJM, Khan NA, Benner R, Kiekens RCM. Chorionic gonadotropin can enhance innate immunity by stimulating macrophage function. J Leukoc Biol 2007;82:926–33.

Wang Y, Walsh SW. Placental mitochondria as a source of oxidative stress in pre-eclampsia. Placenta 1998;19:581–6.

Webb CW, Webb SM. Therapeutic benefits of cannabis: A patient survey. Hawai'i J Med Public Heal 2014;73:109–11.

Weedon-Fekjær MS, Taskén K. Review: Spatiotemporal dynamics of hCG/cAMP signaling and regulation of placental function. Placenta 2012;26:S87–91.

Wice B, Menton D, Geuze H, Schwartz AL. Modulators of cyclic AMP metabolism induce syncytiotrophoblast formation in vitro. Exp Cell Res 1990;186:306–16.

Wolff V, Schlagowski AI, Rouyer O, Charles AL, Singh F, Auger C, Schini-Kerth V, Marescaux C, Raul JS, Zoll J, et al. Tetrahydrocannabinol induces brain mitochondrial respiratory chain dysfunction and increases oxidative stress: A potential mechanism involved in cannabis-related stroke. Biomed Res Int 2015;2015.

Wong MK, Shawky SA, Aryasomayajula A, Green MA, Ewart T, Selvaganapathy PR, Raha S. Extracellular matrix surface regulates self-assembly of three-dimensional placental trophoblast spheroids. PLoS One 2018;13:e0199632.

Wu CS, Jew CP, Lu HC. Lasting impacts of prenatal cannabis exposure and the role of endogenous cannabinoids in the developing brain. Future Neurol 2011;6:459–80.

Zemirli N, Morel E, Molino D. Mitochondrial dynamics in basal and stressful conditions. Int J Mol Sci 2018;19.

TABLE AND FIGURES

Gene	Forward (5'→3')	Reverse (5' → 3')
18S	CACGCCACAAGATCCCA	AAGTGACGCAGCCCTCTATG
CGA	GCAGGATTGCCCAGAATGC	TCTTGGACCTTAGTGGAGTGG
CGB	ACCCCTTGACCTGTGAT	CTTTATTGTGGGAGGATCGG
DRP1	AAACTTCGGAGCTATGCGGT	AGGTTCGCCCAAAAGTCTCA
ERVFRD-1	GCCTACCGCCATCCTGATTT	GCTGTCCCTGGTGTTTCAGT
ERVW-1	GTTAATGACATCAAAGGCACCC	CCCCATCTCAACAGGAAAACC
GCM1	CCTCTGAAGCTCATCCCTTGC	ATCATGCTCTCCCTTTGACTGG
HSP60	GAAGGCATGAAGTTTGATCG	TTCAAGAGCAGGTACAATGG
HSP70	GGAGTTCAAGAGAAAACACAAG	AAGTCGATGCCCTCAAAC
IGF2	GCCAATGGGGAAGTCGATGCTGG	GAGGCTGCAGGATGGTGGCG
MFN1	TTGGAGCGGAGACTTAGCAT	GCCTTCTTAGCCAGCACAAAG
MFN2	CACAAGGTGAGTGAGCGTCT	ACCAGGAAGCTGGTACAACG
OPA1	GCTCTGCATACATCTGAAGAACA	AGAGGCTGGACAAAAGACGTT
PL	GCCATTGACACCTACCAG	GATTTCTGTTGCGTTTCCTC
SOD1	AAAGATGGTGTGGCCGATGT	CAAGCCAAACGACTTCCAGC
SOD2	GCTCCGGTTTTGGGGTATCT	GATCTGCGCGTTGATGTGAG

Table 1. Primer sequences of human genes analyzed via RT-PCR
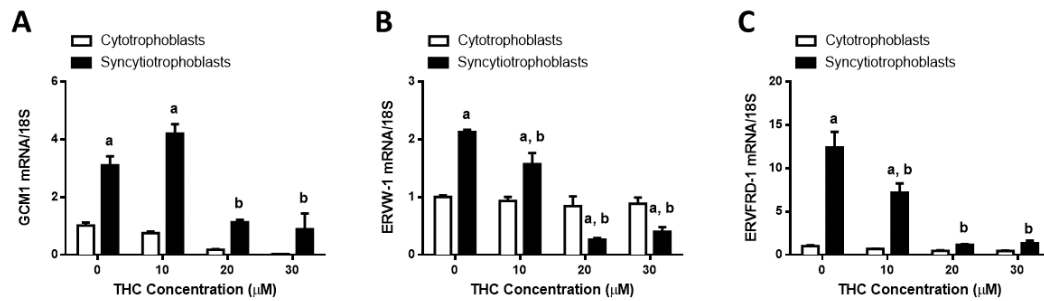
Figure 1. Transcriptional markers of syncytialization and biochemical differentiation are significantly suppressed by THC.
Summary histograms of relative GCM1 (A), ERVW-1 (B), and ERVFRD-1 (C) transcript expression in each treatment group normalized to 18S, then compared to the gene in the vehicle control. Significant differences were determined by a two-way ANOVA, followed by a Bonferroni post hoc test. Data are presented as means ± SEM (n = 3). Different letters denote significant differences compared to the cytotrophoblast (a) or syncytiotrophoblasts (b) vehicle controls. $P < 0.05$ (A); $P < 0.01$ (B); $P < 0.001$ (C).
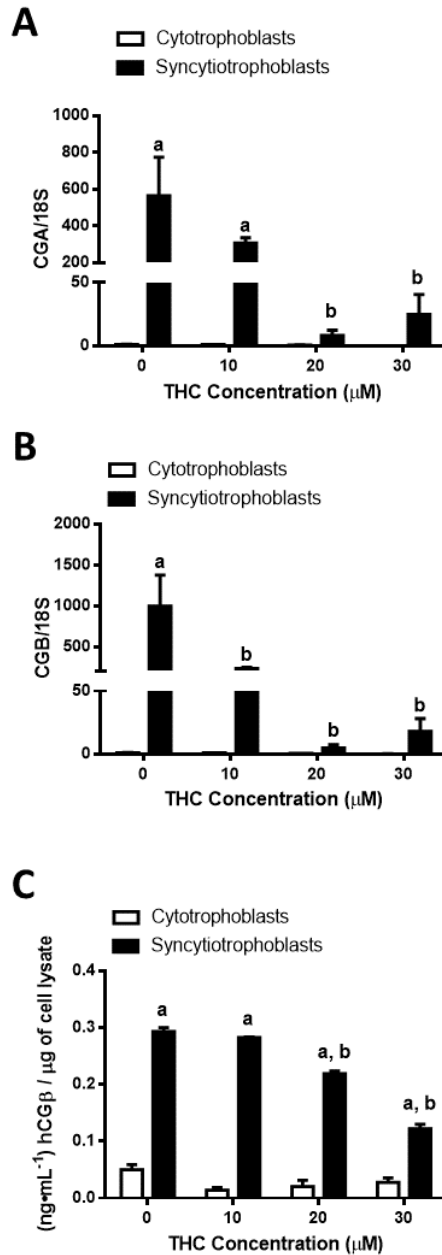
Figure 2. mRNA expression of CG subunits and secretion of hCGβ is significantly decreased by THC exposure.
Summary histograms of relative CGA (A) and CGB (B) are shown. (C) Media was collected 48 hours after the administration of THC. The concentration of hCGβ was normalized to total cell lysate in each well. Significant differences were determined by a two-way ANOVA, followed by a Bonferroni post hoc test. Data are presented as means ± SEM (n = 3). Different letters denote significant differences compared to the cytotrophoblast (a) or syncytiotrophoblast (b) vehicle controls. P < 0.01 (A, B); P < 0.0001 (C).
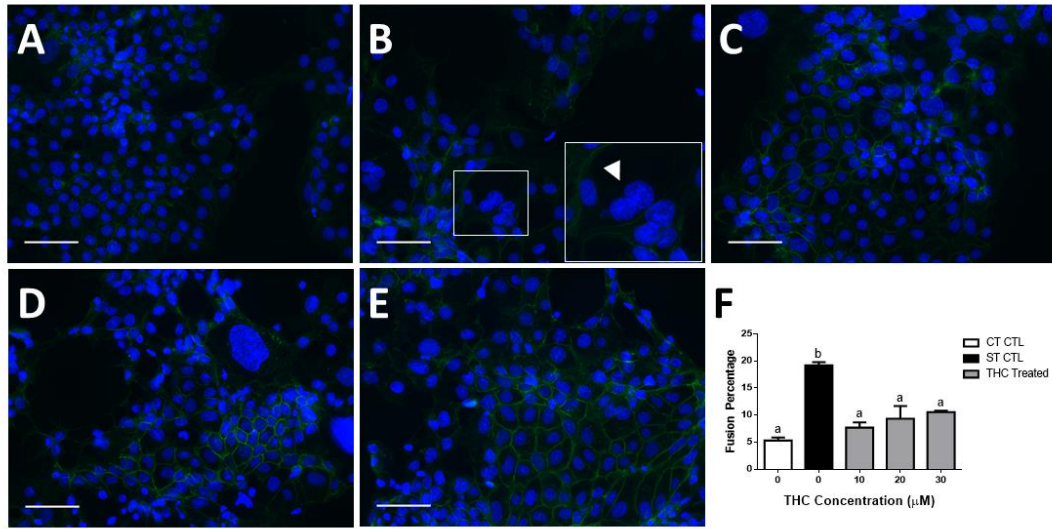
Figure 3. BeWo cell fusion is reduced following exposure to THC.

BeWo cells showing immunofluorescent staining (A-D) for E-cadherin distribution at the cell membrane using FITC-conjugated secondary antibody (green) and counterstained with DAPI identifying the nuclei (blue). Representative fluorescent microscopy images (magnification 200x) are shown (A-E), selected from five random, non-overlapping regions per treatment group (n=3); scale bars indicate 100 µm. A = CT Control; B = ST Control (EGF, FSK); C = 10 µM THC, EGF, FSK; D = 20 µM THC, EGF, FSK; E = 30 µM THC, EGF, FSK. Insets represent close-up magnifications of E-cadherin localization with an example of multinucleated syncytiotrophoblasts (arrowhead in panel B). Cell counts were performed by two researchers and the average was used to determine the fusion percentage across all groups (F). Significant differences were determined by a one-way ANOVA, followed by a Bonferroni post hoc test. Data are presented as means ± SEM (n = 3). Different letters denote significant differences among control and treated groups at P < 0.01.
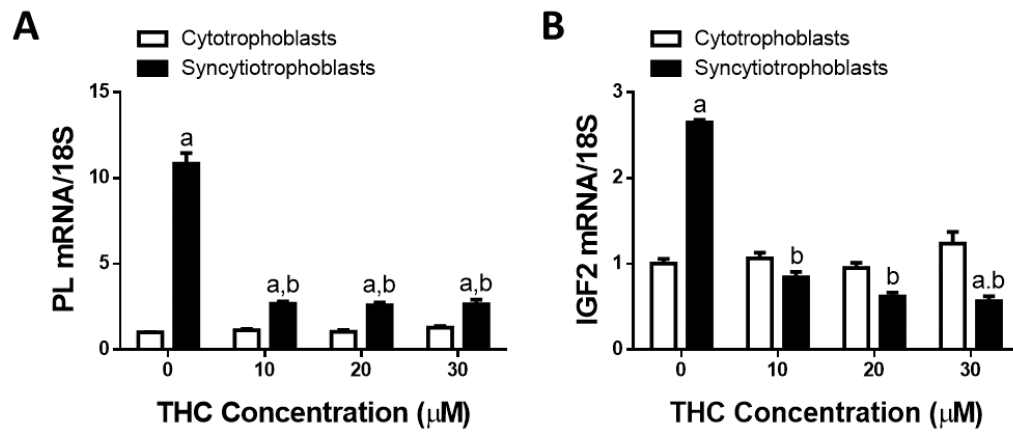
Figure 4. Expression of IGF2 and PL in differentiated BeWo cells is reduced following THC treatment.

Panel A: PL transcript. Panel B: IGF2 transcript. Data are presented as mean ± SEM, n = 3. Different letters denote significant differences compared to the cytotrophoblast (a) or syncytiotrophoblast (b) vehicle controls. $P < 0.0001$ (A); $P < 0.01$ (B).
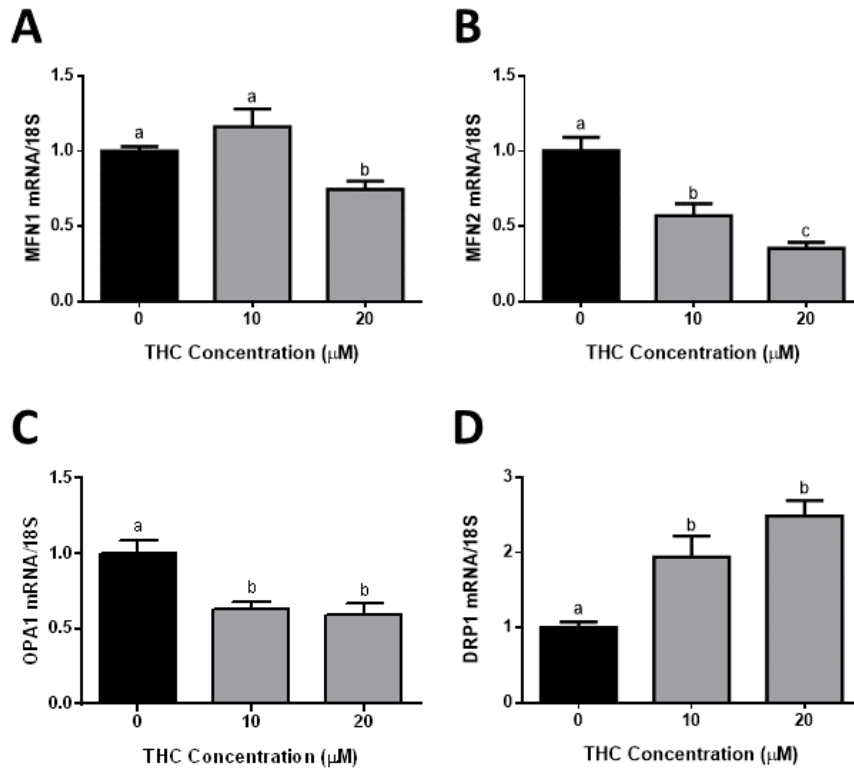
Figure 5. Mitochondrial fusion and fission transcripts in differentiated BeWo cells are altered following exposure to THC.
Summary histograms are shown of relative MFN1 (A), MFN2 (B) OPA1 (C) and DRP1 (D) transcript expression in each treatment group were normalized to 18S, then compared to the gene in the vehicle control group. Significant differences were determined by a one-way ANOVA, followed by a Bonferroni post hoc test. Data are presented as means ± SEM (n = 3). Different letters denote significant differences among control and treated groups at $P < 0.01$ (A); $P < 0.001$ (B-D).
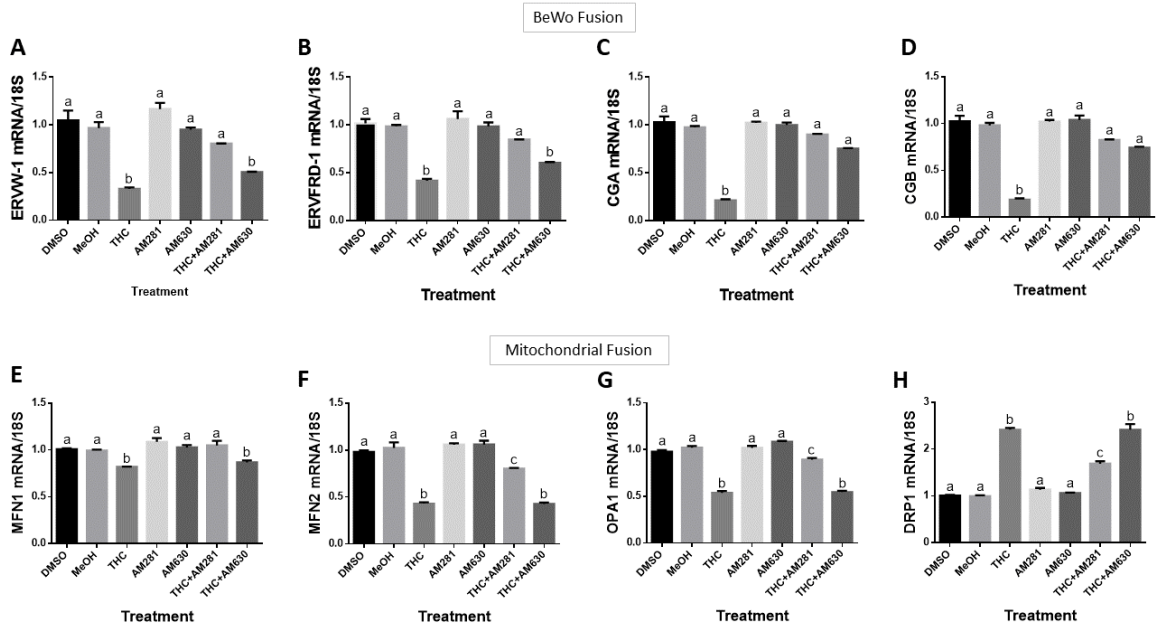
Figure 6. THC-CB receptor binding reduces markers of syncytialization and mitochondrial fusion.
Summary histograms are shown of relative ERVW-1 (A), ERVFRD-1 (B), CGA (C), CGB (D), MFN1 (E), MFN2 (F), OPA1 (G) and DRP1 (H) transcript expression in each treatment group as indicated. Significant differences were determined by a one-way ANOVA, followed by a Bonferroni post hoc test. Data are presented as means ± SEM (n = 3). Different letters denote significant differences among vehicle control (1% v/v) and treated groups at P < 0.0001 (A-H). THC, 20 µM; AM281, 1 µM; AM630, 1 µM.
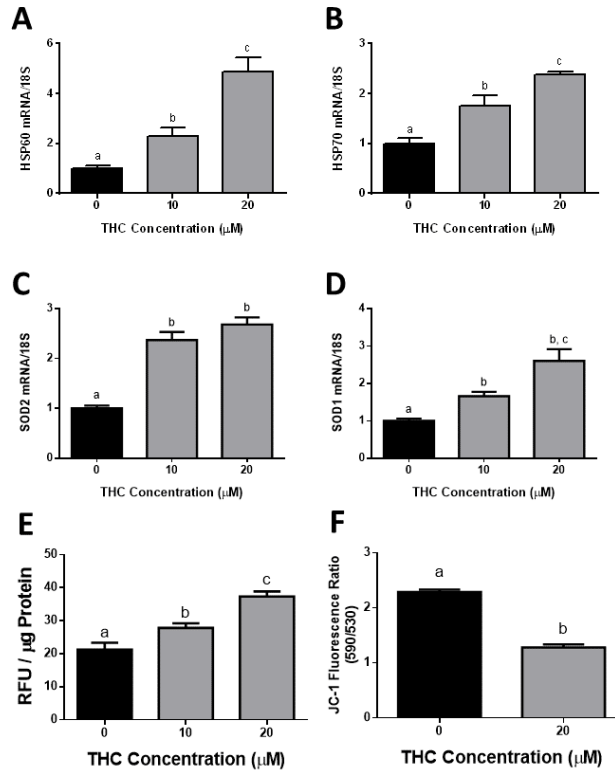
Figure 7. Stress responses, intracellular defenses, ROS production and mitochondrial membrane potential are altered in ST cells upon THC treatment.

Summary histograms are shown of relative HSP60 (A), HSP70 (B) SOD2 (C) and SOD1 (D) transcript expression. Each treatment group was normalized to 18S, then compared to the gene in the vehicle control group. (E) DCFDA assays were performed to determine intracellular ROS levels following THC treatment. Tert-Butyl Hydrogen Peroxide (TBHP) solution (100 μM) was used as the positive control. Results were normalized to the protein content of cell lysates. Significant differences were determined by a one-way ANOVA, followed by a Bonferroni post hoc test. Data are presented as means ± SEM (n = 3). Different letters denote significant differences among control and treated groups at P < 0.0001 (A-C); P < 0.001 (D); P < 0.05 (E). RFU = relative fluorescence units. (F) Mitochondrial depolarization in response to THC exposure. A Student's t-test indicates significance (P < 0.001) between vehicle treated and THC-treated samples.
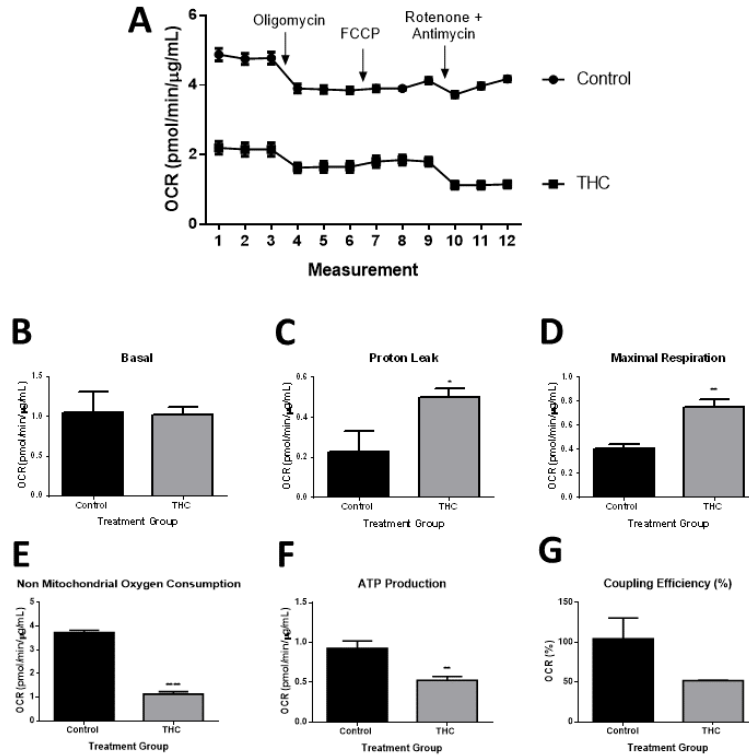
Figure 8. Mitochondrial function in ST cells is impaired following 20μM THC treatment.

OCR was detected under basal conditions followed by the sequential injection of oligomycin (ATP-synthase inhibitor), carbonyl cyanide-4-(trifluoromethoxy)phenylhydrazone (FCCP; mitochondrial respiration uncoupler), and rotenone combined with antimycin (electron transport blockers). These agents were injected through ports of the Seahorse Flux Pak cartridges to reach final concentrations of 1, 2 and 0.5 μM, respectively. The OCR value measured after oligomycin represents the amount of oxygen consumption linked to ATP production, and that after FCCP injection denotes the maximal mitochondrial respiratory capacity of the cells. The final injection of rotenone/antimycin inhibits the flux of electrons through complex I & III, and thus no oxygen is further consumed at complex V. The OCR reading after this treatment is primarily nonmitochondrial and is due to cytosolic oxidase enzymes. OCR measurements were obtained using the Seahorse XFe24 Analyzer and the OCR values were normalized to the amount of protein content from each well using the BCA assay (μg/mL). The detection of OCR was performed with 4 biological replicates per experiment, for each treatment condition, and repeated 3 more times. (see Supplemental Fig. 2 for experiments 2-4). Group mean and SEM (A-G) are displayed. Arrows indicate addition of the respective compounds. Significance was assessed by Student's t-test (*$P < 0.05$, **$P < 0.01$, ****$P < 0.0001$). A. Representative oxygen consumption rate (OCR) tracing, B. Basal respiration, C. Proton leak, D. Maximal respiration, E. Non-mitochondrial oxygen consumption, F. ATP production, and G. Coupling efficiency (%).

SUPPLEMENTARY FIGURES
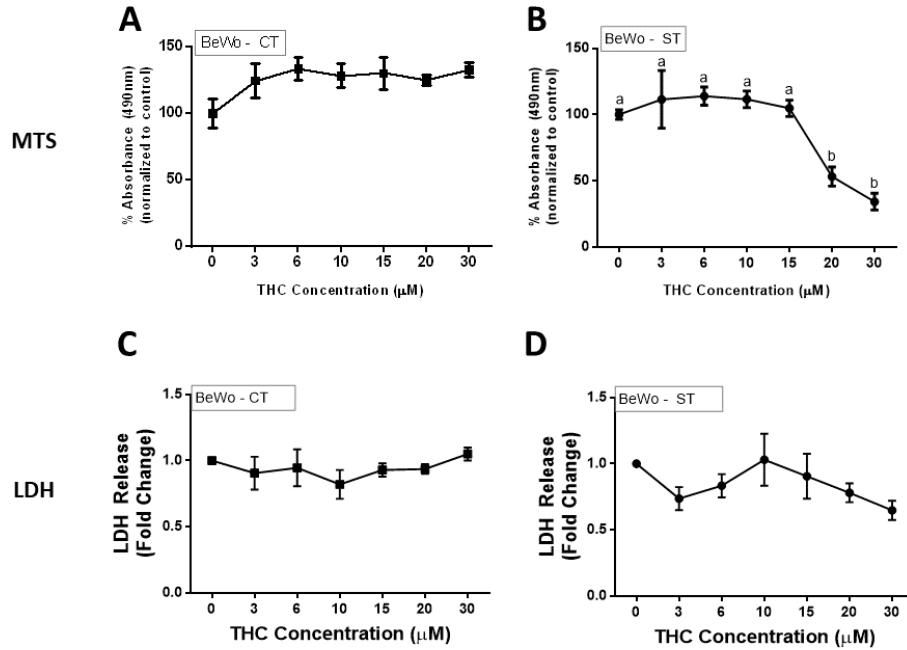
Supplemental Figure 1.   THC negatively impacts proliferation of differentiated placental trophoblast cells without induction of cell membrane damage.
(A – D) BeWo cells were treated without or with FSK and EGF to establish the CT and ST populations, respectively, with DMSO and methanol used as vehicle controls. The cells were treated with THC as indicated. Each data point represents the mean ± SEM. of 3 replicates measured at 490nm. Significant differences were determined by a one-way ANOVA followed by a Bonferroni post hoc test. $P < 0.01$ (B).
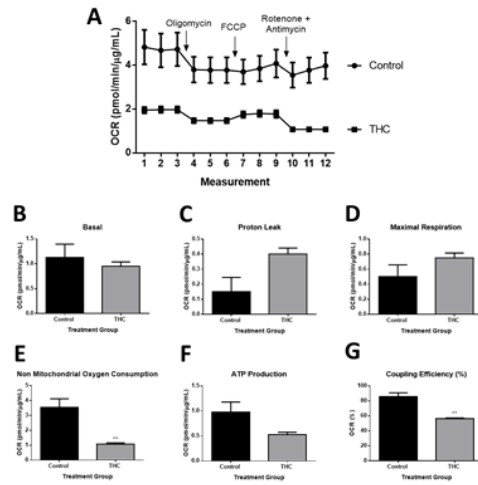
Supplementary Figure 2, OCR, Run #2
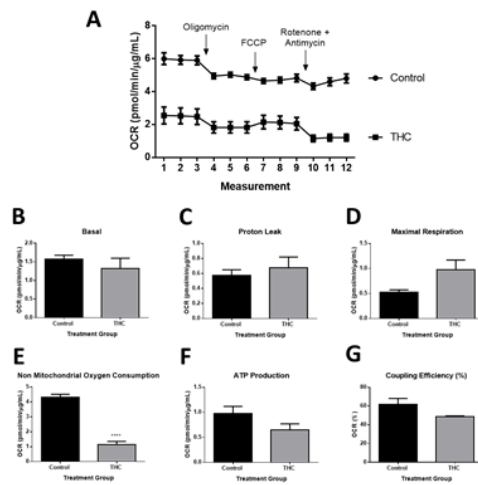
Supplementary Figure 2, OCR, Run #3
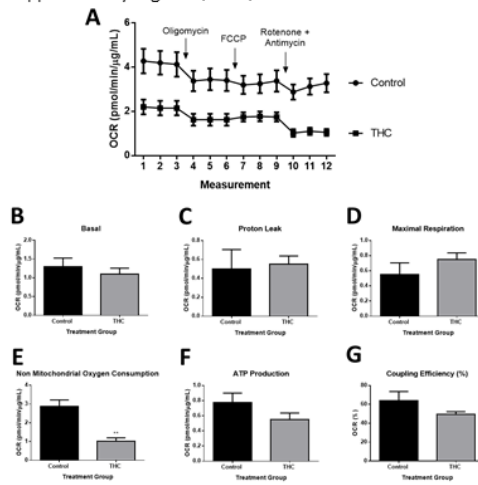
Supplementary Figure 2, OCR, Run #4

Supplemental Figure 2 (experiments 2-4). Mitochondrial function in ST cells is impaired following treatment with 20µM THC.

OCR was detected under basal conditions followed by the sequential injection of oligomycin (ATP-synthase inhibitor), carbonyl cyanide-4-(trifluoromethoxy)phenylhydrazone (FCCP; mitochondrial respiration uncoupler), and rotenone combined with antimycin (electron transport blockers). These agents were injected through ports of the Seahorse Flux Pak cartridges to reach final concentrations of 1, 2 and 0.5 µM, respectively. The OCR value measured after oligomycin represents the amount of oxygen consumption linked to ATP production, and that after FCCP injection denotes the maximal mitochondrial respiratory capacity of the cells. The final injection of rotenone/antimycin inhibits the flux of electrons through complex I & III, and thus no oxygen is further consumed at complex V. The OCR reading after this treatment is primarily nonmitochondrial and is due to cytosolic oxidase enzymes. OCR measurements were obtained using the Seahorse XFe24 Analyzer and the OCR values were normalized to the amount of protein content from each well using the BCA assay (µg/mL). The detection of OCR was performed with 4 biological replicates per experiment, for each treatment condition, and repeated 3 more times. Group mean and SEM (A-G) are displayed. Arrows indicate addition of the respective compounds. Significance was assessed by Student's t-test (**$P < 0.01$, ****$P < 0.0001$). A. Representative oxygen consumption rate (OCR) tracing. B. Basal respiration, C. Proton leak, D. Maximal respiration, E. Non-mitochondrial oxygen consumption, F. ATP production, G. Coupling efficiency (%).

5.   CHAPTER 5

DELTA-9-TETRAHYDROCANNABINOL INHIBITS INVASION OF HTR8/SVNEO HUMAN EXTRAVILLOUS TROPHOBLAST CELLS AND NEGATIVELY IMPACTS MITOCHONDRIAL FUNCTION.

This paper has been submitted to Scientific Reports (under review).

Authors: Walker OS, Gurm H, Sharma R, Verma N, May LL, Raha S.

Department of Medical Sciences

McMaster University

Hamilton, ON, L8S 4L8

OSW and SR designed the project. OSW, HG, RS and NV performed the experiments. LLM performed the mitochondrial respiration assays. The manuscript was written by OSW and SR with editing by all authors.

ABSTRACT

Prenatal cannabis use is a significant problem and poses important health risks for the developing fetus. The molecular mechanisms underlying these changes are not fully elucidated but are thought to be attributed to delta-9-tetrahydrocannabinol (THC), the main bioactive constituent of cannabis. It has been reported that THC may target the mitochondria in several tissue types, including placental tissue and trophoblast cell lines, and alter their function. In the present study, in response to 48-hour THC treatment of the human extravillous trophoblast cell line HTR8/SVneo, we demonstrate that cell proliferation and invasion are significantly reduced. We further demonstrate THC-treatment elevated levels of cellular reactive oxygen species and markers of lipid damage. This was accompanied by evidence of increased mitochondrial fission. We also observed increased expression of cellular stress markers, HSP70 and HSP60, following exposure to THC. These effects were coincident with reduced mitochondrial respiratory function and a decrease in mitochondrial membrane potential. Taken together, our results suggest that THC can induce mitochondrial dysfunction and reduce trophoblast invasion; outcomes that have been previously linked to poor placentation. We also demonstrate that these changes in HTR8/SVneo biology may be variably mediated by cannabinoid receptors CB1 and CB2.

INTRODUCTION

The active components of *Cannabis sativa* have been used for centuries for both recreational and medicinal purposes [1, 2], and the clinical use of cannabis-based medicines is increasing worldwide [3]. Delta-9-tetrahydrocannabinol (THC) is the primary constituent of cannabis with pharmacological and toxicological effects [2] mediated by the canonical G-protein coupled cannabinoid receptors CB1 and CB2 found in the central nervous system (CB1) and various peripheral tissues (CB1 and CB2) [4], including the placenta [5, 6]. Cannabis is commonly used amongst pregnant women [7–9], purportedly due to the view that it is a natural product with therapeutic benefits, particularly its antiemetic and analgesic effects [10, 11]. Though it was a very small study, a survey of pregnant women conducted in Vancouver, Canada revealed that 77% of respondents used cannabis to manage nausea [12]. This study demonstrates the propensity of women in certain demographics to use cannabis, but larger studies suggest numbers range from 2-20% [13, 14]. Although the pathophysiology is not fully understood, poor pregnancy outcomes are associated with maternal cannabis/THC use. Maternal circulating THC crosses the placenta to impact placental and fetal development [8]. While there are presently no reported teratogenic effects, cannabis has been heavily implicated in neurodevelopmental disorders in the offspring [15–17], intrauterine growth restriction [18, 19], and preterm birth [19–21]. Though the pathogenesis of the above have yet to be fully elucidated, they are thought to stem from trophoblast abnormalities [22-26].

Trophoblasts are the main cell type of the placenta. Normal placentation requires invasion of extravillous trophoblasts (EVTs) into the maternal decidua and approximately the inner third of the myometrium [27]. This invasive process is tightly controlled both spatially (restricted to the decidua, inner third of the myometrium and the spiral arteries) and, temporally (primarily in the first trimester) by several interactions between the invading trophoblasts, the decidua, and the

maternal vasculature and immune system [27] (for review, see [28]). To facilitate invasion, trophoblasts secrete proteases, such as matrix metalloproteinases (MMPs), whose in vivo activity is regulated by their tissue inhibitors of MMPs (TIMPs) [27]. The balance between MMPs and TIMPs is critical for embryonic implantation, and when disturbed, can lead to various pregnancy complications, like PE [28].

Oxidative stress occurring locally at the materno-fetal interface can lead to impaired trophoblast function, preventing physiological remodelling of the uterine spiral arteries, ultimately leading to shallow placental implantation; characteristic of PE [29]. Furthermore, placental oxidative stress is also linked to mitochondrial dysfunction [30,31]. Adequate mitochondrial function is essential in pregnancy because it sustains the increased metabolic activity of the placenta throughout gestation [31]. Mitochondrial dysfunction represents a critical physiological factor for fetal programming in cases of placental insufficiency [31]. In mouse embryos, mitochondrial dysfunction affects subsequent placentation and fetal growth [32]. Additionally, maternal undernutrition in rats induces impaired placental mitochondrial function and results in fetal and placental growth restriction [33]. Recently, associations between mitochondrial dysfunction and THC exposure have been suggested [33]. THC treatment in human lung cancer cells (H460) was shown to reduce mitochondrial complex I and complex II-III activities, reduce mitochondrial membrane potential, and induce oxidative stress and apoptosis [34].

THC is thought to alter mitochondrial function in brain, muscle [35–37], thymus, spleen [38], and placental tissue [19,22]. The high energetic demands of a tissue like the placenta make it susceptible to agents that might attenuate mitochondrial function. In the process of electron transport to generate ATP, mitochondria can be a major source of reactive oxygen species (ROS). These ROS species also serve as important signaling molecules and can trigger cellular dysfunction or cell death by damaging proteins, lipids, and mitochondrial DNA. Therefore, it is important for

the mitochondria to have mechanisms to ensure the maintenance of healthy mitochondria [39]. Quality control can occur by fission and fusion to allow segregation of damaged mitochondria, mitophagy to remove damaged mitochondria, and cell death if the damage is too severe [39]. Decreased inner mitochondrial membrane potential, which is approximately -120 mV [40], is an important trigger for mitochondrial fission. Indeed, we have shown that targeted perturbation of mitochondria resulted in reduced syncytiotrophoblast function and increased ROS production [41]. Based on the role of mitochondria in energy transduction, it is not surprising that any perturbations in mitochondrial energy production, or propagation would result in the development of placental pathology or susceptibility to placental damage [30,31,39].

We hypothesized that exposure to 20 µM THC, within the range of concentrations measured in the serum of cannabis users [25,42], for 48 hours would lead to an inhibitory effect on the invasive capability of trophoblast cells. Using a first-trimester immortalized trophoblast cell line, HTR8/SVneo, a well accepted model of extravillous trophoblasts [43–45], our study objective was to evaluate the effect of THC exposure on cell viability, MMP and TIMP expression, transwell invasion, alongside the assessment of mitochondrial function.

RESULTS

20 µM THC inhibits proliferative activity of HTR8/SVneo cells without damage to the plasma membrane

Fig. S1 demonstrates that HTR8/SVneo proliferation, over 48 hrs, was reduced following exposure to THC concentrations $\geq$ 15 µM (MTS assay, $P < 0.05$), with a 50% reduction evident at 20 µM ($P < 0.0001$). Plasma membrane damage became evident only at 30 µM THC (increased

LDH release into media, P < 0.05) when compared to unstimulated cells. We utilized 20 µM THC for treatments in subsequent studies.

THC markedly reduced the invasive capacity of trophoblasts

The effect of THC on HTR8/SVneo invasion was determined using Matrigel®-coated transwell inserts. The number of invasive HTR8/SVneo cells was profoundly reduced upon exposure to THC, as shown in Fig. 1 (P < 0.0001). We evaluated HTR8/SVneo invasion at 10 µM and 20 µM THC treatment. These two concentrations are well within physiological levels but had quite different effects on cell proliferation (Fig. S1A). We observed almost a 90% reduction in cell invasion using both concentrations of THC (P < 0.0001).

THC exposure negatively alters MMP and TIMP transcript and protein expression

Changes in transcript and protein expressions of MMP2, MMP9, TIMP1 and TIMP2 were assessed following 48-hours of THC exposure. The THC-stimulated cells showed a 2-fold reduction in *MMP2* (P < 0.0001) and *MMP9* (P < 0.01) transcripts concomitant with a 2.5- and 4.5-fold increase in *TIMP1* (P < 0.01) and *TIMP2* (P < 0.0001), respectively, when compared to unstimulated cells (Fig. 2). Similarly, we demonstrate a marked reduction in MMP2 and MMP9 (P < 0.01, P < 0.05, respectively, Fig. 3A, B) protein expression along with significantly increased protein expression of the inhibitors TIMP1 and TIMP2 (P < 0.01, P < 0.0001, respectively; Fig. 3C, D).

Mitochondrial fission and fusion transcripts are significantly altered in response to THC

To investigate the effects of THC on altering markers that govern mitochondrial dynamics, we treated HTR8/SVneo cells for 48 hours with 20 µM THC and assessed the transcript expression of key fission and fusion markers. In response to THC treatment, we demonstrate an approximately 50% reduction in *MFN1*, *MFN2*, and *OPA1* transcript expression, while *DRP1* transcript expression increased over 2-fold, relative to untreated control cells (Fig. 4, P < 0.0001, P < 0.01, P < 0.01, P < 0.001, respectively).

Involvement of cannabinoid receptors in anti-invasive actions of THC

We evaluated whether the canonical cannabinoid receptors are involved in THC-mediated reduction in HTR8/SVneo cell invasion using CB1 (AM281, 1 µM) and CB2 (AM630, 1 µM) antagonists. The reductions in *MMP2* transcripts that were observed with THC treatment were completely blocked by CB2 antagonism (P < 0.0001) while remaining unchanged in response to antagonizing CB1 (Fig. 5A). THC-induced suppression of *MMP9* transcripts was partially blocked following both CB1 and CB2 antagonism (Fig. 5B, P < 0.0001). At the same concentration of both CB1 and CB2 antagonists, the THC-induced transcription of *TIMP1* and *TIMP2* were partially blocked (Fig. 5C, D, P < 0.0001).

Effects of CB1 and CB2 receptor antagonism on THC-mediated mitochondrial perturbation

HTR8/SVneo cells were treated with CB1 and CB2 antagonists to determine which receptors mediated the transcriptional changes in mitochondrial fission and fusion markers. THC-

141

stimulated reductions in *MFN1*, *MFN2* and *OPA1* and the THC-stimulated increase in *DRP1* was completely blocked by CB1 antagonism ($P < 0.0001$). CB2 antagonism had no effect on these transcriptional markers (Fig. 5E-H).

THC increases transcriptional markers of stress responses, ROS production and 4-HNE adducts in HTR8/SVneo cells without changing the intracellular defenses

We further investigated whether oxidative stress is induced in trophoblast cells following THC treatment. THC exposure stimulated ROS production, as detected by DCF fluorescence (Fig. 6E). Treatment of HTR8/SVneo cells with 20 µM THC for 48 hours significantly increased DCF fluorescence by 60%, compared with that of unstimulated control cells ($P < 0.001$).

Since THC increased ROS production in HTR8/SVneo cells, we investigated the effects of THC on intracellular stress responses and free radical defenses. THC treatment resulted in significant increases in heat shock protein (*HSP*) 60 and 70 (Fig. 6A, $P < 0.001$; B, $P < 0.05$) along with the detection of increased 4-HNE protein adduct levels (Fig. 6G, H, $P < 0.05$). While increased markers of cellular stress and oxidative damage were observed, there was no evidence of an increase in the level of mRNA encoding the antioxidant enzymes manganese superoxide dismutase and copper zinc superoxide dismutase (*SOD2* and *SOD1*) (Fig. 6C, D).

OXPHOS proteins are decreased without changing CS expression following THC exposure

Given our observed indicators of mitochondrial dysfunction, we next investigated whether THC decreased the expression of the proteins which comprise the electron transport chain. THC

reduced the levels of mitochondrial OXPHOS protein subunits of the respiratory chain following 48 hours of exposure (Fig. 7). Specifically, electron transport chain (ETC) complex protein subunits NADH dehydrogenase (ubiquinone) 1 beta sub complex 8 (NDUFB8; complex I, $P < 0.01$), succinate dehydrogenase complex, subunit B (SDHB; complex II, $P < 0.05$), and cytochrome c oxidase subunit 2 (COXII; complex IV, $P < 0.01$) were significantly reduced. Ubiquinol-cytochrome c reductase core protein II (UQCR2; complex III) and ATP synthase 5A (ATP 5A, Complex V) were not significantly changed in response to 20 µM THC relative to untreated controls. The citrate synthase protein level, a proxy for mitochondrial mass [44], was not significantly altered relative to untreated controls following 48 hrs of THC treatment (Fig. 7A, G).

THC causes mitochondrial membrane depolarization in HTR8/SVneo cells

Treatment with 20 µM THC for 48 hours significantly decreased the JC-1 red/green fluorescence intensity ratio by 50.8% in HTR8/SVneo cells compared to untreated controls (Fig. 6F, $P < 0.001$).

THC reduces electron transport chain function in HTR8/SVneo cells

Since mitochondrial function is directly linked to mitochondrial polarization state [45], we investigated the changes in mitochondrial aerobic metabolism that occurred in HTR8/SVneo cells in response to THC. A Cell Mito Stress assay kit was used to detect the OCR. HTR8/SVneo cells were treated with 20 µM THC for 48 hours before exposure to 1 µM oligomycin, 2 µM FCCP and 0.5 µM rotenone and antimycin. As demonstrated in Figure 8A, THC reduced OCR in HTR8/SVneo cells. THC did not significantly change basal respiration (Fig. 8B). THC

significantly reduced maximal respiration (Fig. 8D, 47.6%, $P < 0.05$), non-mitochondrial oxygen consumption (Fig. 8E, 33.3%, $P < 0.01$), ATP production (Fig. 8F, 66.7%, $P < 0.001$) and spare respiratory capacity (Fig. 8G, 38.5%, $P < 0.001$), while significantly increasing proton leak (Fig. 8C, 71.4%, $P < 0.05$) when compared to the untreated cells.

DISCUSSION

THC impacts a number of physiological processes [2,48]. Here, we provide insight into the effects of THC on impairing human trophoblast invasion, a critical step in the placentation process. Several studies employing THC in the µM range (up to 30 µM), representative of moderate to heavy cannabis consumption [49], have shown that THC inhibits cytotrophoblasts proliferation and transcription of genes encoding proteins involved in processes such as, apoptosis and ion exchange [25], trophoblast migration and invasion [50], as well as angiogenesis in the placentae of cannabis users [51]. Importantly, we have previously shown that THC impairs cytotrophoblast fusion into syncytia, hormonal secretion, and mitochondrial function, i.e. reduced ATP production and increased ROS production [26].

Our present work demonstrates that THC reduced the ability of HTR8/SVneo cells to proliferate and invade due to changes in the transcript levels of genes that play important roles in this process. In addition, THC-induced ROS production was accompanied by disruption of mitochondrial dynamics in HTR8/SVneo cells. Mitochondrial morphology is determined by a dynamic equilibrium between organelle fusion and fission [52]. Perturbation of mitochondrial dynamics, as demonstrated by alterations in the transcriptional markers used in this study, has been linked to altered trophoblast function [26,30,41]. Importantly, increases in mitochondrial fission have been associated with poor gestational outcomes [31]. Our previous study using human

placental BeWo cells [26] demonstrated that THC treatment increased markers of mitochondrial fission and negatively impacted the secretion of hormones critical for fetal growth.

The reduction in the invasive capacity of HTR8/SVneo trophoblast cells can be attributed, in part, to the observed reduction in the transcription and protein expression of MMPs. In support of this, THC and endogenous cannabinoids have been shown to interact with cancer cells to negatively impact growth and proliferation [53–59]. Like tumour cells, invasiveness is a feature of trophoblasts. However, unlike tumour invasion, trophoblast invasion is a strictly controlled physiological event [27,60]. Excessive trophoblast invasion may result in placenta accrete [61,62], while insufficient invasion of the trophoblast may result in PE [63]. Trophoblast invasion into the decidual spiral arteries is crucial for normal placental development and pregnancy success. Impaired spiral artery remodelling, which has been associated with attenuated trophoblast invasion [28,64] can lead to a failure to accommodate high capacity blood flow; an outcome that has been associated with a host of pregnancy-related pathologies [27].

The observed attenuation of invasion can be a consequence of reduced MMP activity. While we did not quantify metalloproteinase activity, we do demonstrate that THC-mediated a significant reduction in transcription of the genes encoding MMP2 and MMP9 as well as their protein expression levels. The gelatinase MMPs (MMP2 and MMP9), are secreted as proenzymes that are subsequently activated by proteolytic processing [63] and permit digestion of the extracellular matrix (ECM) and surrounding tissue [27] in order to facilitate trophoblastic decidual invasion [28]. In breast cancer and glioma cells, using in vitro and in vivo methods, treatment with THC resulted in reductions in MMP2 expression and activity [58,59]. Furthermore, a direct link between cannabinoid receptor activation and MMP expression has been identified by Adhikary et al (2012). Using selective CB receptor agonists GP1a or O-1996, these researchers identified that CB2 receptor signaling reduced migration of bone marrow-derived dendritic cells in both in vitro

and in vivo (murine) models, primarily by inhibiting expression of MMP9 [65]. In addition, Blázquez et al (2008) demonstrated reduced MMP2 transcript levels in glioma cells in response to 24h THC exposure, which was completely reversed by CB2 antagonism, but not by CB1 antagonism [59]; a finding that is reflected in our observations. Moreover, Ramer and Hinz (2008) used human cervical cancer cells (HeLa) to assess invasiveness following treatment with an endogenous cannabinoid (anandamide) analog R(+)-methanandamide (MA) and THC with or without CB1 and CB2 receptor antagonists. The authors report that both MA and THC reduce invasiveness of the HeLa cells concomitant with increased expression of TIMP1 transcript and protein, all of which were suppressed upon pre-treatment with CB1 and CB2 receptor antagonism [66]. Similarly, we also observed increased gene and protein expression of TIMP1 and TIMP2, proteins which are known to attenuate MMP2 and MMP9 proteolytic activity [63,66]. Taken together, our results suggest that the THC-mediated reduction in invasive activity of trophoblasts may be due to reduced MMP function.

Following 48-hour exposure to THC, we sought to determine mitochondrial respiration measurements in HTR8/SVneo cells. An increase in proton leak and a decrease in mitochondrial respiration, as we have demonstrated in HTR8/SVneo cells, are indicative of mitochondrial dysfunction [67]. Mitochondrial oxygen consumption was increased by uncoupling the mitochondria via the addition of FCCP. This resulted in an increase in the maximal respiratory response. Following the delivery of rotenone and antimycin, inhibiting the mitochondrial ETC, we observed the loss of the enhanced OCR, thus confirming the portion of the profile that was linked with mitochondria-specific respiration. While the bulk of oxygen is consumed by mitochondria, enzymatic reactions and oxygenases outside of mitochondria will also contribute to the total cellular oxygen consumption [68]. We conclude that overall cellular metabolism is decreased as both mitochondrial and non-mitochondrial oxygen consumption are reduced in response to THC.

Further, FCCP-induced maximal respiration allows the determination of spare respiratory capacity (%), defined as the difference between maximum (uncoupled) OCR and basal OCR [67], which is reduced in the HTR8/SVneo cells exposed to THC. Spare respiratory capacity can be used as a surrogate readout for the ability of the mitochondria to increase oxygen consumption in response to an increased demand for ATP. Supporting our evidence, a recent study by Lojpur et al, using the BeWo choriocarcinoma cell line, demonstrated that 24-hour treatment with 15 µM THC negatively impacted mitochondrial respiration as assessed via OCR, in part due to reduced expression of proteins associated with the mitochondrial respiratory chain complexes [22]. Our observations also suggest that THC treatment reduces expression of subunit proteins associated with complexes I, II and III. Other studies have also demonstrated that THC disrupted mitochondrial function in other cell types, although this was observed with concentrations of THC that were greater than that used in our work (up to 120 µM and approximately 50µM, respectively) [69,70].

Monitoring mitochondrial membrane potential in parallel with respiration, both of which were reduced following 48-hour THC exposure, allowed for a more powerful and informative measure of mitochondrial dysfunction [68]. Decreased mitochondrial membrane potential (decreased JC-1 fluorescence ratio) is linked to increased mitochondrial recycling [71]. Additionally, increased ROS production has also been associated greater mitochondrial fission and formation of smaller, more punctate mitochondria [72]. These smaller structures, independent of the reticulum-like structure that is associated with healthy cellular function, are thought to have altered cristae structure and be characterized by less efficient ETC activity [73]. In support of this, we observed increased expression of transcripts indicative increased mitochondrial fragmentation (DRP1) and decreased expression of genes encoding proteins involved in promoting mitochondrial fusion. Importantly, while we demonstrate increased mitochondrial fission, the overall

mitochondrial mass may not be changing, as indicated by the lack of change in the steady state levels of CS in our system. It is possible that a pool of more fragmented mitochondria are contributing to less efficient ATP production, as indicated by reduced expression of OXPHOS enzymes, and reduced ATP production and OCR. Furthermore, this pool of mitochondria may be an important source of oxidative stress and contribute to increased lipid peroxidation in trophoblast cells [74].

Oxidative stress, described as ROS production which exceeds the ability of antioxidant defenses to scavenge them, is an important contributing factor in the pathophysiology of complicated pregnancies [75,76]. Thus, oxidative stress can result from increased ROS production and/or defects in antioxidant defense systems [76]. Oxidative damage occurs from the interaction of free radicals with DNA and intracellular macromolecules such as proteins and membrane lipids, including lipid peroxidation, subsequently leading to cellular dysfunction [77]. Although a physiological balance between ROS and antioxidant defense systems is maintained in uncomplicated pregnancies, an imbalance may increase oxidative stress [76]. Indeed, in response to THC exposure, HTR8/SVneo cells demonstrate a significant increase in intracellular stress responses (HSP60 and HSP70 transcripts), concomitant with an increase in oxidative stress. However, antioxidant defenses (SOD1 and SOD2) remained unchanged relative to control. The overall lack of change in the expression of SODs may contribute to the significant increase in ROS in our study, thus precipitating significant oxidative stress. Indeed, Akhigbe and Id (2020) treated male rabbits with codeine (4mg/kg and 10 mg/kg, for 6 weeks) and assessed testicular antioxidant enzyme activities and demonstrated marked increases in oxidative stress without the concomitant increase in SOD activity [77]. Downstream of the induction of oxidative stress is the initiation of peroxidation and subsequent lipid dysfunction [78]. Physiological levels of ROS are normally managed by the activation of SOD enzymes as well as the ensuing damage elicited by lipid

peroxidation [78]. However, when protective systems are overwhelmed by oxidative stress, this may lead to various pathological changes [77–79]. Indeed, following THC treatment, HTR8/SVneo cells demonstrate marked increases in ROS production and the expression of the lipid aldehyde, 4-HNE, which is a marker of lipid peroxidation. We demonstrate that exposure of these trophoblasts to 20 µM THC for 48 hours overwhelmed the inherent defense systems, as SOD enzyme expressions were not changed.

Considering that metabolic impairment has been linked to the pathophysiology of several placental disorders [30,31], we speculate that THC-induced decreases in mitochondrial respiratory chain functioning and increased mitochondrial fission mediated by CB1 could be an important mechanism of action of THC. Interestingly, inhibition of CB2 receptor did not significantly impact the effects of THC on the markers of mitochondrial fragmentation. We have made similar observations in syncytialized BeWo cells treated with THC [26]. Drawing from the "double-hit" hypothesis [80] in the context of trophoblast physiology, THC users may have compromised mitochondrial function such that they will less effectively handle the impact of a subsequent stressor on the mitochondrial reticulum (such as poor maternal nutritional status) [80].

Conclusion

Our results suggest a potential cascade of molecular changes that occur in the placenta upon exposure to THC. We have demonstrated that THC impairs trophoblast invasion by reducing MMP expression and increasing TIMP expression, mediated in part by the canonical CB receptors. We further demonstrate that THC adversely affects the function of human trophoblasts by altering mitochondria-dependent pathways leading to increased organellar fission, reduced OCR, and aberrant ROS production. Furthermore, recently published data from our group demonstrates that THC reduces the molecular signals for BeWo syncytialization and the expression of growth factors important for fetal growth41. Taken together, these observations suggest that this cannabinoid

alters the process of placentation through its influence, in part, on trophoblasts function. Recent work from Natale et al (2020) also demonstrate the THC can alter angiogenesis in placenta and reduce birth weight in the offspring of rat dams injected with THC during pregnancy [23]. Importantly, our work also suggests that mitochondria, via the CB1 receptor, may have a role in mediating the effects of THC. Our work contributes to the understanding of the cellular mechanisms underpinning the adverse pregnancy outcomes associated with cannabis use during gestation.

METHODS

Cell culture

All cell culture experiments were carried out under McMaster University Biohazard Utilization Protocol BUP023. HTR8/SVneo cells (a kind gift from Dr. Peeyush K. Lala, Professor in the Department of Oncology at Western University, London, ON, Canada) were grown and maintained in RPMI-1640 medium (Lonza, 12-115F, Walkersville, MD, USA) supplemented with 5% FBS, 1% penicillin/streptomycin, and 1% L-glutamine, maintained in a humidified atmosphere of 5% CO_2 at 37°C.

Cell viability assays

Cell viability assays were conducted as previously described by our group [41]. Briefly, HTR8/SVneo cells were seeded into a 96-well plate at a density of 10,000 cells/well. Control wells containing media without cells were allocated to determine background absorbance. Cells were treated with THC (Sigma, Cat. No. T4764) or vehicle (methanol; MeOH) for 48 hours.

For the MTS Assay, the cells were treated with 20 µL of CellTiter 96® AQueous Non-Radioactive Cell Proliferation Assay (Promega Corp., Cat. No. G5421) for 2 hours at 37°C in a humidified, 5% CO_2 atmosphere. The absorbance was recorded at 490nm using a 96-well plate reader (Miltiskan® Spectrum spectrophotometer; Thermo Scientific, Canada). The results are normalized to the untreated cells and plotted as a percent of control.

As a measure of plasma membrane integrity, lactate dehydrogenase (LDH) release into culture supernatants was detected spectrophotometrically at 490nm and 680nm, using the Pierce LDH Cytotoxicity Assay Kit (Cat. No. 88953), according to the manufacturer's recommended protocol. The results are presented as fold increase in the absorbance measured normalized to untreated cells.

DCFDA (2',7'-dichlorofluorescin diacetate) assay

HTR8/SVneo cells were seeded in a black, clear bottom 96-well microplate at a cell density of 30,000 cells/well. The cells were treated with 100 µL of media supplemented with THC or vehicle. The cells were assayed using the Abcam DCFDA Cellular ROS Detection Assay Kit (Abcam Cat. No. ab113851) according to the manufacturers recommended protocol. Cells were analyzed on a fluorescent plate reader (BioTek Synergy 4) read in endpoint mode at excitation and emission wavelengths of 485 and 535nm, respectively. Data were standardized as a percent of control after background (blank wells with media only) subtraction, followed by normalization to total protein content (BCA) [81].

Transwell invasion assay

Transwell invasion assays were carried out as per manufacturers instructions (Corning). Briefly, Matrigel® invasion assays were carried out at 37°C for 48 hours using 24-well transwell

inserts with 8.0μm pores (Corning Cat. No. 353097) coated with 0.3mg/mL of GFR Matrigel (Corning, Cat. No. 354230). In the apical chambers, 50,000 cells were seeded on top of the Matrigel® and supplemented with 500μL of serum-free RPMI-1640 containing vehicle or THC (10μM or 20μM), while 750μL media with chemoattractant (5% FBS) supplemented with vehicle or THC was placed into the basal chambers. Following 48 hrs, non-invading cells and Matrigel® were gently removed from the apical side of the membrane using a cotton swab moistened with cold phosphate buffered saline (PBS). Cells that migrated and invaded through the membrane were fixed in ice-cold 100% MeOH for 5 minutes at -20°C and incubated with 4', 6-diamidino-2-phenylindole (DAPI, 1.5 µg/mL, diluted in PBS with Tween and 0.1% bovine serum albumin (BSA)) for 5 minutes at room temperature and visualized at 200X magnification with a Nikon Eclipse Ti-E (Nikon Instruments Inc., USA). Five non-overlapping fields of view were captured per sample. The number of cells that traversed the Matrigel® and membrane were counted by two individuals who were blinded to the treatment groups using ImageJ software (National Institutes of Health, Bethesda, MD, USA). The mean number of cells were determined, and the percent invasion was expressed as the mean number of invaded cells exposed to the drug relative to untreated cells.

RNA extraction and RT-PCR

HTR8/SVneo cells grown on 12-well plates were lysed with 500 µL of ice-cold TRIzol™ reagent (Thermo Fisher Scientific, Canada). Total RNA isolation and quantification of gene expression (RT-PCR) was performed as previously described by our research team [82]. All genes and their respective primer sequences are listed in Table 1. Fold change transcript expression was quantified using the double delta Ct (ΔΔCt) analysis, normalized to housekeeping gene, 18S, then expressed as the relative fold change to the vehicle control sample expression.

BCA assay

Protein concentration was determined by using the bicinchoninic assay (BCA; ThermoFisher, Canada) with BSA (0-2000 µg/mL) as a concentration standard. Total protein concentration was measured with a 96-well plate reader (Miltiskan® Spectrum spectrophotometer; Thermo Scientific, Canada) set at A562nm.

SDS-PAGE and western blotting

HTR8/SVneo cells were lysed in radioimmunoprecipitation assay (RIPA) lysis buffer containing protease inhibitor cocktails (Roche Diagnostics, Cat. No. 04693159001). Samples were loaded for gel electrophoresis at 20 µg/sample and all gels (12%) were imaged using the stain-free application on the ChemiDocTM (Bio-Rad) imager immediately after the protein separation and prior to western blotting. Protein gels were blotted using the Trans-Blot Turbo transfer apparatus PVDF Midi transfer packs (Bio-Rad). Antibody conditions are listed in Table 2. Immunoreactive bands were visualized using Clarity MaxTM Western ECL Substrate (Bio-Rad) and visualized using ChemiDocTM Imaging System (BioRad, V2.3.0.07). The intensities of the bands were quantified using Image LabTM (BioRad, V6.0.1). The Image LabTM values generated for the proteins of interest were normalized to total protein on the same stain-free membrane. Full blots available in the Supplementary Information files.

CB1 and CB2 antagonism

To address the role of the canonical cannabinoid receptors, CB1 and CB2, in mediating the effects of THC, selective antagonists AM281 and AM630 [83], respectively, were used at a final concentration of 1 µM each [84]. These receptor antagonists were used at a concentration of 1 µM,

which is within the range of concentrations that have been reported to inhibit cellular responses to activation of the canonical receptors [84, 85].

HTR8/SVneo cells were pre-incubated with the antagonists for 30 minutes [84], followed by treatment with 20 µM THC for 48 hours.

Mitochondrial respiration assay

Cellular energetics were measured using an XFe24 Extracellular Flux Analyzer (Agilent, Santa Clara, CA, USA) as previously described by our group [26]. The mitochondrial oxygen consumption rate (OCR) was measured at 37°C in an XFe24 Extracellular Flux Analyzer (Agilent, Santa Clara, CA, USA). Crucial for this assay, cell density was optimized. HTR8/SVneo cells were plated at a density of 60,000 cells/well in 250 µL culture media, in 24-well microtiter plates and allowed to adhere overnight. The day before running the XF Assay, the Seahorse XF Sensor Cartridge was hydrated by adding 1 mL of sterilized double distilled water to each well of the XF Utility Plate. The hydrated cartridge was kept in a non-CO_2 37°C incubator overnight to remove CO_2 that would otherwise interfere with measurements that are pH sensitive. HTR8/SVneo cells were exposed to THC for 48 hours. On the day of the XF Assay, culture media was aspirated and replaced with XF base medium (Seahorse Bioscience, Cat. No. 102365-100) supplemented with 100 mM sodium pyruvate (ThermoFisher Scientific, Cat. No. 11360-070), 200 mM L-glutamine (ThermoFisher Scientific, Cat. No. 25030081), 5 mL of 45% glucose solution (Millipore-Sigma, Cat. No. G8769), warmed to 37°C (adjusted to pH 7.4). The assay medium was pre-equilibrated at 37°C for 1 hour. OCR was detected under basal conditions followed by the sequential injections of oligomycin (ATP-synthase inhibitor), carbonyl cyanide-4-(trifluoromethoxy)phenylhydrazone (FCCP; mitochondrial respiration uncoupler), and rotenone combined with antimycin (electron transport blockers). These agents were injected through ports of the Seahorse Flux Pak cartridges

to reach final concentrations of 1, 2 and 0.5 µM, respectively. The OCR value measured after oligomycin treatment indicates the amount of oxygen consumption linked to ATP production, and that after FCCP injection represents the maximal mitochondrial respiratory capacity of the cells. The final injection of rotenone and antimycin inhibits the flux of electrons through complex I and III, respectively, and thus no oxygen is further consumed at complex V. The OCR reading after this treatment is primarily non-mitochondrial. OCR measurements were obtained using the Seahorse XFe24 Analyzer and the OCR values were normalized to the amount of protein content from each well. The detection of OCR was performed with 4 biological replicates per experiment, for each treatment condition, and repeated 3 more times.

Mitochondrial membrane potential

THC-stimulated changes in the mitochondrial membrane potential ($\Delta\Psi$m) were assessed using the fluorescent reagent tetraethylbenzimidazolylcarbocyanine iodide (JC-1) with the JC-1-Mitochondrial Membrane Potential Assay kit (Abcam, Cat. No. ab113850) following the manufacturer's protocol. HTR8/SVneo cells were seeded at a density of 50,000 cells/well and allowed to adhere overnight in a black, clear-bottom 96 well plate. Cells were treated with 20 µM THC for 48 hours. Following treatment, cells were washed once with 1X dilution buffer and then incubated with 20 µM JC-1 dye in 1X dilution buffer for 10 minutes at 37°C, protected from light. JC-1 dye was then removed, cells were washed once with 1X dilution buffer, 100 µL of fresh 1X dilution buffer was added to each well. The red fluorescence in excitation (535 nm)/emission (590 nm) and green fluorescence excitation/emission (475 nm/530 nm) was measured using a Spark multimode microplate reader (Tecan Group Ltd.). Background fluorescence was subtracted from the fluorescence of treated cells, then the ratio of red (polarized) fluorescence divided by that of green (depolarized) fluorescence was obtained.

Statistical analyses

All experiments were performed in biological triplicates or quadruplets. Comparisons between vehicle control and THC-treated cells were performed using Student's t-test. One-way analysis of variance (ANOVA) and Bonferroni post hoc tests were used to compare data sets with more than two groups. Data are reported as means $\pm$ SEM. Differences were considered significant at $P < 0.05$. The experimental parameters were analyzed using XFe Wave software V2.6.1 and Excel (for OCR measurements) and GraphPad Prism software V6.0.

REFERENCES

1.   Parker, L. A., Rock, E. M. & Limebeer, C. L. Regulation of nausea and vomiting by cannabinoids and the endocannabinoid system. Eur. J. Pharmacol. 722, 134–146 (2014).

2.   Sharma, P., Murthy, P. & Bharath, M. M. S. Chemistry, metabolism, and toxicology of cannabis: Clinical implications. Iran. J. Psychiatry 7, 149–156 (2012).

3.   Pacher, P., Batkai, S. & Kunos, G. The endocannabinoid system as an emerging target of pharmacotherapy. Pharmacol Rev 58, 389–462 (2006).

4.   Pertwee, R. G. Pharmacology of cannabinoid CB1 and CB2 receptors. Pharmacol. Ther. 74, 129–180 (1997).

5.   Habayeb, O. M. H., Taylor, A. H., Bell, S. C., Taylor, D. J. & Konje, J. C. Expression of the endocannabinoid system in human first trimester placenta and its role in trophoblast proliferation. Endocrinology 149, 5052–5060 (2008).

6.   Trabucco, E. et al. Endocannabinoid system in first trimester placenta: Low FAAH and high CB1 expression characterize spontaneous miscarriage. Placenta 30, 516–522 (2009).

7.   Alpár, A., Di Marzo, V. & Harkany, T. At the tip of an iceberg: Prenatal marijuana and its possible relation to neuropsychiatric outcome in the offspring. Biol. Psychiatry 79, e33–e45 (2016).

8.   Wu, C. S., Jew, C. P. & Lu, H. C. Lasting impacts of prenatal cannabis exposure and the role of endogenous cannabinoids in the developing brain. Future Neurol. 6, 459–480 (2011).

9.   Campolongo, P., Trezza, V., Ratano, P., Palmery, M. & Cuomo, V. Developmental consequences of perinatal cannabis exposure: Behavioral and neuroendocrine effects in adult rodents. Psychopharmacology (Berl). 214, 5–15 (2011).

10.   Marijuana and medicine: Assessing the science base. (National Academy of Sciences, 1999).

11.   Roberson, E. K., Patrick, W. K. & Hurwitz, E. L. Marijuana use and maternal experiences of severe nausea during pregnancy in Hawai'i. Hawai'i J. Med. Public Heal. 73, 283–7 (2014).

12.   Westfall, R. E., Janssen, P. A., Lucas, P. & Capler, R. Survey of medicinal cannabis use among childbearing women: Patterns of its use in pregnancy and retroactive self-assessment of its efficacy against 'morning sickness'. Complement. Ther. Clin. Pract. 12, 27–33 (2006).

13.   Corsi, D. J., Hsu, H., Weiss, D., Fell, D. B. & Walker, M. Trends and correlates of cannabis use in pregnancy: A population-based study in Ontario, Canada from 2012 to 2017. Can. J. Public Heal. 110, 76–84 (2019).

14.   Ko, J. Y., Farr, S. L., Tong, V. T., Creanga, A. A. & Callaghan, W. M. Prevalence and patterns of marijuana use among pregnant and nonpregnant women of reproductive age. Am. J. Obstet. Gynecol. 213, e1-10 (2015).

15.   de Salas-Quiroga, A. et al. Prenatal exposure to cannabinoids evokes long-lasting functional alterations by targeting CB 1 receptors on developing cortical neurons. Proc. Natl. Acad. Sci. 112, 13693–13698 (2015).

16.   Grant, K. S., Petroff, R., Isoherranen, N., Stella, N. & Burbacher, T. M. Cannabis use during pregnancy: Pharmacokinetics and effects on child development. Pharmacol. Ther. 182, 133–151 (2018).

17.   Vela, G. et al. Maternal exposure to delta9-tetrahydrocannabinol facilitates morphine self-administration behavior and changes regional binding to central mu opioid receptors in adult offspring female rats. Brain Res. 807, 101–109 (1998).

18.   Hingson, R. et al. Effects of maternal drinking and marijuana use on fetal growth and development. Pediatrics 70, 539–546 (1982).

19.   Costa, M. A., Fonseca, B. M., Marques, F., Teixeira, N. A. & Correia-da-Silva, G. The psychoactive compound of Cannabis sativa, Δ9-tetrahydrocannabinol (THC) inhibits the human trophoblast cell turnover. Toxicology 334, 94–103 (2015).

20.   Leemaqz, S. Y. et al. Maternal marijuana use has independent effects on risk for spontaneous preterm birth but not other common late pregnancy complications. Reprod. Toxicol. 62, 77–86 (2016).

21.   Benevenuto, S. G. et al. Recreational use of marijuana during pregnancy and negative gestational and fetal outcomes: An experimental study in mice. Toxicology 376, 94–101 (2017).

22.   Lojpur, T. et al. Δ9-Tetrahydrocannabinol leads to endoplasmic reticulum stress and mitochondrial dysfunction in human BeWo trophoblasts. Reprod. Toxicol. 87, 21–31 (2019).

23.   Natale, B. V et al. Δ9-tetrahydrocannabinol exposure during rat pregnancy leads to symmetrical fetal growth restriction and labyrinth-specific vascular defects in the placenta. Sci. Rep. 10, (2020).

24.   Almada, M. et al. Synthetic cannabinoids JWH-018, JWH-122, UR-144 and the phytocannabinoid THC activate apoptosis in placental cells. Toxicol. Lett. (2020). doi:10.1016/j.toxlet.2019.11.004

25.   Khare, M., Taylor, A. H., Konje, J. C. & Bell, S. C. Delta 9-Tetrahydrocannabinol inhibits cytotrophoblast cell proliferation and modulates gene transcription. Mol. Hum. Reprod. 12, 321–333 (2006).

26.   Walker, O. et al. Delta-9-tetrahydrocannabinol disrupts mitochondrial function and attenuates syncytialization in human placental BeWo cells. Physiol. Rep. In Press, (2020).

27.   Fitzgerald, J. S., Poehlmann, T. G., Schleussner, E. & Markert, U. R. Trophoblast invasion: The role of intracellular cytokine signalling via signal transducer and activator of transcription 3 (STAT3). Hum. Reprod. Update 14, 335–344 (2008).

28.   Gupta, S. K., Malhotra, S. S., Malik, A., Verma, S. & Chaudhary, P. Cell signaling pathways involved during invasion and syncytialization of trophoblast cells. Am J Reprod Immunol 75, 361–371 (2015).

29.   Takagi, Y. et al. Levels of oxidative stress and redox-related molecules in the placenta in preeclampsia and fetal growth restriction. Virchows Arch. 444, 49–55 (2004).

30.   Holland, O. et al. Review: Placental mitochondrial function and structure in gestational disorders. Placenta 54, 2–9 (2017).

31.   Mandò, C. et al. Placental mitochondrial content and function in intrauterine growth restriction and preeclampsia. Am J Physiol Endocrinol Metab 306, 404–413 (2014).

32.   Wakefield, S. L., Lane, M. & Mitchell, M. Impaired mitochondrial function in the preimplantation embryo perturbs fetal and placental development in the mouse. Biol. Reprod. 84, 572–580 (2011).

33.   Mayeur, S. et al. Maternal calorie restriction modulates placental mitochondrial biogenesis and bioenergetic efficiency: Putative involvement in fetoplacental growth defects in rats. Am J Physiol Endocrinol Metab 304, 14–22 (2013).

34.   Athanasiou, A. et al. Cannabinoid receptor agonists are mitochondrial inhibitors: A unified hypothesis of how cannabinoids modulate mitochondrial function and induce cell death. Biochem. Biophys. Res. Commun. 364, 131–137 (2007).

35.   Campbell, V. A. Tetrahydrocannabinol-induced apoptosis of cultured cortical neurones is associated with cytochrome c release and caspase-3 activation. Neuropharmacology 40, 702–709 (2001).

36.   Chiu, P., Karler, R., Craven, C., Olsen, D. & Turkanis, S. The influence of delta9-tetrahydrocannabinol, cannabinol and cannabidiol on tissue oxygen consumption. Res Commun Chem Pathol Pharmacol 12, 267–286 (1975).

37.   Singh, N., Hroudová, J. & Fišar, Z. Cannabinoid-induced changes in the activity of electron transport chain complexes of brain mitochondria. J. Mol. Neurosci. 56, 926–931 (2015).

38.   McKallip, R. J., Lombard, C., Martin, B. R., Nagarkatti, M. & Nagarkatti, P. S. Delta(9)-tetrahydrocannabinol-induced apoptosis in the thymus and spleen as a mechanism of immunosuppression in vitro and in vivo. J. Pharmacol. Exp. Ther. 302, 451–465 (2002).

39.   Youle, R. J. & Van Der Bliek, A. M. Mitochondrial fission, fusion, and stress. Science. 337, 1062–1065 (2012).

40.   Liesa, M. & Shirihai, O. S. Mitochondrial dynamics in the regulation of nutrient utilization and energy expenditure. Cell Metab. 17, 491–506 (2013).

41.   Walker, O. S. et al. Reactive oxygen species from mitochondria impacts trophoblast fusion and the production of endocrine hormones by syncytiotrophoblasts. PLoS One 15, e0229332 (2020).

42.   Cherlet, T. & Scott, J. E. Tetrahydrocannabinol (THC) alters synthesis and release of surfactant-related material in isolated fetal rabbit type II cells. Drug Chem. Toxicol. 25, 171–190 (2002).

43.   Noorali, S. et al. Role of HERV-W syncytin-1 in placentation and maintenance of human pregnancy. Appl. Immunohistochem. Mol. Morphol. 17, 319–328 (2009).

44.   Sullivan, M. Endocrine cell lines from the placenta. Mol. Cell. Endocrinol. 228, 103–119 (2004).

45.   Hannan, N. J., Paiva, P., Dimitriadis, E. & Salamonsen, L. A. Models for study of human embryo implantation: Choice of cell lines? Biol. Reprod. 82, 235–245 (2010).

46.   Scaini, G. et al. Evaluation of Krebs cycle enzymes in the brain of rats after chronic administration of antidepressants. Brain Res. Bull. 82, 224–227 (2010).

47.   Zorova, L. D. et al. Mitochondrial membrane potential. Anal. Biochem. 552, 50–59 (2018).

48.   Maccarrone, M. Endocannabinoids: Friends and foes of reproduction. Prog. Lipid Res. 48, 344–354 (2009).

49.   Nahas, G., Paton, W. & Harvey, D. The Reims Symposium. in Marihuana and Medicine (eds. Nahas, G., Sutin, K., Harvey, D. & Agurell, S.) 13–19 (Humana Press, 1999).

50.   Chang, X. et al. Suppression of STAT3 signaling by Δ9-tetrahydrocannabinol (THC) induces trophoblast dysfunction. Cell. Physiol. Biochem. 42, 537–550 (2017).

51.   Chang, X. et al. RhoA/MLC signaling pathway is involved in Δ9-tetrahydrocannabinol-impaired placental angiogenesis. Toxicol. Lett. 285, 148–155 (2018).

52.   Chen, H. et al. Mitofusins Mfn1 and Mfn2 coordinately regulate mitochondrial fusion and are essential for embryonic development. J. Cell Biol. 160, 189–200 (2003).

53.   Chakravarti, B., Ravi, J. & Ganju, R. K. Cannabinoids as therapeutic agents in cancer: Current status and future implications. Oncotarget 5, 5852–72 (2014).

54.   Śledziński, P., Nowak, A., Zeyland, J. & Słomski, R. Endocannabinoid system and anticancer properties of cannabinoids. Folia Biol. Oecologica 12, 11–25 (2016).

55.   Hermanson, D.J., Marnett, L. J. Cannabinoids, Endocannabinoids and Cancer. Cancer Metastasis Rev 30, 599–612 (2011).

56.   Wang, D. et al. Loss of cannabinoid receptor 1 accelerates intestinal tumor growth. Cancer Res. 68, 6468–6476 (2008).

57.   Nithipatikom, K. et al. 2-Arachidonoylglycerol: A novel inhibitor of androgen-independent prostate cancer cell invasion. Cancer Res. 64, 8826–8830 (2004).

58.   Caffarel, M. M. et al. Cannabinoids reduce ErbB2-driven breast cancer progression through Akt inhibition. Mol. Cancer 9, (2010).

59.   Blázquez, C. et al. Cannabinoids inhibit glioma cell invasion by down-regulating matrix metalloproteinase-2 expression. Cancer Res 68, 1945–52 (2008).

60.   Ferretti, C., Bruni, L., Dangles-Marie, V., Pecking, A. P. & Bellet, D. Molecular circuits shared by placental and cancer cells, and their implications in the proliferative, invasive and migratory capacities of trophoblasts. Hum. Reprod. Update 13, 121–141 (2007).

61.   Gaynor, L. M. & Colucci, F. Uterine natural killer cells: Functional distinctions and influence on pregnancy in humans and mice. Front. Immunol 8, 467 (2017).

62.   Acar, N., Ustunel, I. & Demir, R. Uterine natural killer (uNK) cells and their missions during pregnancy: A review. Acta Histochem. 113, 82–91 (2011).

63.   Sosa, S. E. Y. et al. New insights into the role of matrix metalloproteinases in preeclampsia. Int. J. Mol. Sci. 18, 1–10 (2017).

64.   Hayes, E. K. et al. Trophoblast invasion and blood vessel remodeling are altered in a rat model of lifelong maternal obesity. Reprod. Sci. 21, 648–657 (2014).

65.   Adhikary, S., Kocieda, V., Yen, J., Tuma, R. & Ganea, D. Signaling through cannabinoid receptor 2 suppresses murine dendritic cell migration by inhibiting matrix metalloproteinase 9 expression. Blood 120, 3741–3749 (2012).

66.   Ramer, R. & Hinz, B. Inhibition of cancer cell invasion by cannabinoids via increased expression of tissue inhibitor of matrix metalloproteinases-1. J Natl Cancer Inst 100, 59–69 (2008).

67.   Yépez, V. A. et al. OCR-Stats: Robust estimation and statistical testing of mitochondrial respiration activities using Seahorse XF Analyzer. PLoS One 13, 1–18 (2018).

68.   Brand, M. D. & Nicholls, D. G. Assessing mitochondrial dysfunction in cells. Biochem. J 435, 297–312 (2011).

69.   Badawy, D. et al. Cannabinoids inhibit the respiration of human sperm. Fertil. Steril. 91, 2471–2476 (2009).

70.   Sarafian, T. A., Kouyoumjian, S., Khoshaghideh, F., Tashkin, D. P. & Roth, M. D. Delta-9-tetrahydrocannabinol disrupts mitochondrial function and cell energetics. Am. J. Physiol. Lung Cell Mol. Physiol. 284, L298–L306 (2003).

71.   Tait, S. W. & Green, D. R. Mitochondria and cell signalling. J. Cell Sci. 125, 807–815 (2012).

72.   Cymerys, J., Chodkowski, M., Słońska, A., Krzyżowska, M. & Bańbura, M. W. Disturbances of mitochondrial dynamics in cultured neurons infected with human herpesvirus type 1 and type 2. J. Neurovirol. 25, 765–782 (2019).

73.   Buck, M. D. et al. Mitochondrial dynamics controls T cell fate through metabolic programming. Cell 166, 63–76 (2016).

74.   Wang, Y. & Walsh, S. W. Placental mitochondria as a source of oxidative stress in pre-eclampsia. Placenta 19, 581–586 (1998).

75.   Casanueva, E. & Viteri, F. E. Iron and oxidative stress in pregnancy. J. Nutr 133, 1700–1708 (2003).

76.   Myatt, L. & Cui, X. Oxidative stress in the placenta. Histochem. Cell Biol. 122, 369–382 (2004).

77.   Akhigbe, R. & Id, A. A. Testicular toxicity following chronic codeine administration is via oxidative DNA damage and up-regulation of NO/TNF-α and caspase 3 activities. PLoS One 15, e0224052 (2020).

78.   Mihalas, B. P., De Iuliis, G. N., Redgrove, K. A., McLaughlin, E. A. & Nixon, B. The lipid peroxidation product 4-hydroxynonenal contributes to oxidative stress-mediated deterioration of the ageing oocyte. Sci. Rep. 7, (2017).

79.   Breitzig, M., Bhimineni, C., Lockey, R. & Kolliputi, N. 4-Hydroxy-2-nonenal: A critical target in oxidative stress? Am. J. Physiol. - Cell Physiol. 311, C537–C543 (2016).

80.   Richardson, K. A., Hester, A. K. & McLemore, G. L. Prenatal cannabis exposure - The "first hit" to the endocannabinoid system. Neurotoxicol. Teratol. 58, 5–14 (2016).

81.   Masaki, H., Izutsu, Y., Yahagi, S. & Okano, Y. Reactive oxygen species in HaCaT keratinocytes after UVB irradiation are triggered by intracellular Ca2+ levels. J. Investig. Dermatology Symp. Proc. 14, 50–52 (2009).

82.   Wong, M. K. et al. Extracellular matrix surface regulates self-assembly of three-dimensional placental trophoblast spheroids. PLoS One 13, e0199632 (2018).

83.   Pertwee, R. G. et al. International union of basic and clinical pharmacology. LXXIX. Cannabinoid receptors and their ligands: Beyond CB1 and CB2. Pharmacol. Rev. 62, 588–631 (2010).

84.   Almada, M. et al. The synthetic cannabinoid WIN-55,212 induced-apoptosis in cytotrophoblasts cells by a mechanism dependent on CB1 receptor. Toxicology 385, 67–73 (2017).

85.   Jacobsson, S., Wallin, T. & Fowler, C. Inhibition of rat C6 glioma cell proliferation by endogenous and synthetic cannabinoids. Relative involvement of cannabinoid and vanilloid receptors. J. Pharmacol. Exp. Ther. 299, 951–959 (2001).

TABLES AND FIGURES

Gene	Forward	Reverse	GenBank
18S	CACGCCACAAGATCCCA	AAGTGACGCAGCCCTCTATG	NR_003286.2
DRP1	AAACTTCGGAGCTATGCGGT	AGGTTCGCCCAAAAGTCTCA	NM_012062.5
HSP60	GAAGGCATGAAGTTTGATCG	TTCAAGAGCAGGTACAATGG	NM_002156.5
HSP70	GGAGTTCAAGAGAAAACACAAG	AAGTCGATGCCCTCAAAC	NM_005345.6
MFN1	TTGGAGCGGAGACTTAGCAT	GCCTTCTTAGCCAGCACAAAG	NM_033540.3
MFN2	CACAAGGTGAGTGAGCGTCT	ACCAGGAAGCTGGTACAACG	NM_014874.4
MMP2	TCTCCTGACATTGACCTTGGC	CAAGGTGCTGGCTGAGTAGATC	NM_004530.5
MMP9	CCGGCATTCAGGGAGACGCC	TTGAACCACGACGCCCTTGC	NM_004994.2
OPA1	GCTCTGCATACATCTGAAGAACA	AGAGGCTGGACAAAAGACGTT	NM_130831.3
SOD1	AAAGATGGTGTGGCCGATGT	CAAGCCAAACGACTTCCAGC	NM_000454.5
SOD2	GCTCCGGTTTTGGGGTATCT	GATCTGCGCGTTGATGTGAG	NM_001024465.3
TIMP1	GGGCTTCACCAAGACCTACA	TGCAGGGGATGGATAAACAG	NM_003254.2
TIMP2	GAAGAGCCTGAACCACAGGT	GGGGGAGGAGATGTAGCA	NM_003255.4

Table 1. Primer sequences of human genes analyzed via RT-PCR

Antibody	Manufacturer	Catalogue Number	Host Organism	Blocking Medium (in TBST)	Dilution	Antibody Dilutant (in TBST)	RRID
4-HNE	Abcam	ab48506	Mouse	5% BSA	1:2000	3% BSA	AB_867452
CS	A kind gift from Dr. B.H Robinson, Hospital for Sick Children, Toronto ON.	N/A	Rabbit	5% BSA	1:10,000	3% BSA	N/A
MMP-2	Abcam	ab51125	Rabbit	5% milk	1:1000	5% milk	AB_881239
MMP-9	GeneTex	GTX61537	Rabbit	5% milk	1:1000	5% milk	AB_10619391
OXPHOS	MitoSciences/ Abcam	MS601-360	Mouse	5% BSA	1:1000	5% BSA	AB_1619331
TIMP-1	GeneTex	GTX112096	Rabbit	5% milk	1:1000	5% milk	AB_11174643
TIMP-2	GeneTex	GTX21828	Mouse	5% milk	1:1000	5% milk	AB_372322

Table 2. Antibodies used for western blot
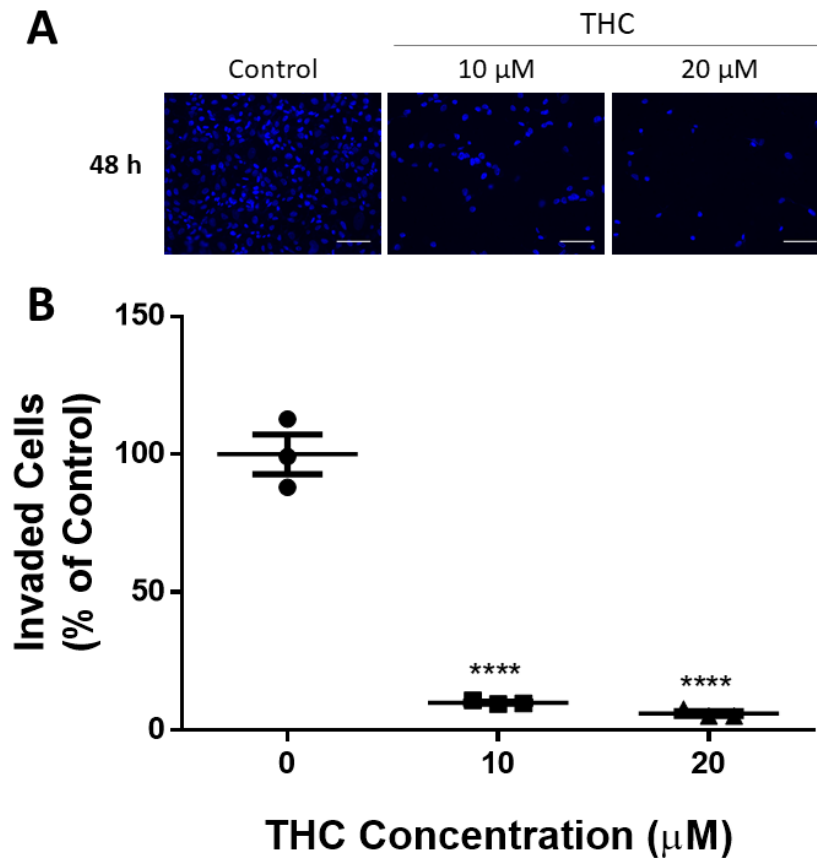
Figure 1. THC reduces HTR8/SVneo cell invasion.
HTR8/SVneo cells were added to Matrigel®-coated insert wells. The inserts were incubated for 48 hours as described in Methods. (A) Representative immunofluorescent images of invaded HTR8/SVneo cells are shown, with the nuclei staining blue, magnification 200x and scale bar indicates 100µm. (B) A summary histogram reporting the percentage of invaded cells relative to the vehicle control group (methanol), each data point is shown, the horizontal lines represent the means and the error bars represent SEM (n = 3). Significant differences were determined by a one-way ANOVA, followed by a Bonferroni post hoc test. **** $P < 0.0001$ (B).
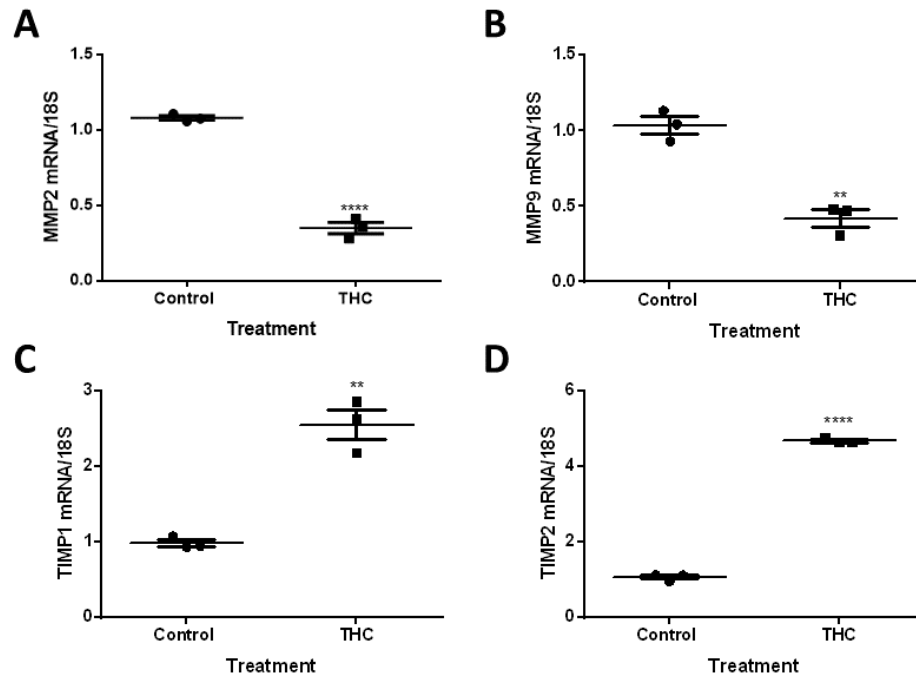
Figure 2. THC alters the mRNA expression of degradative enzymes and their inhibitors.

HTR8/SVneo cells were treated as indicated for 48 hours. Summary histograms of relative MMP2 (A), MMP9 (B), TIMP1 (C), and TIMP2 (D) transcript expression in each treatment group normalized to 18S, then compared to the gene in the vehicle control. Each data point represents the mean ± SEM of 3 biological replicates. Significant differences were determined by Student's t-test. **** $P < 0.0001$ (A, D); ** $P < 0.01$ (B, C).
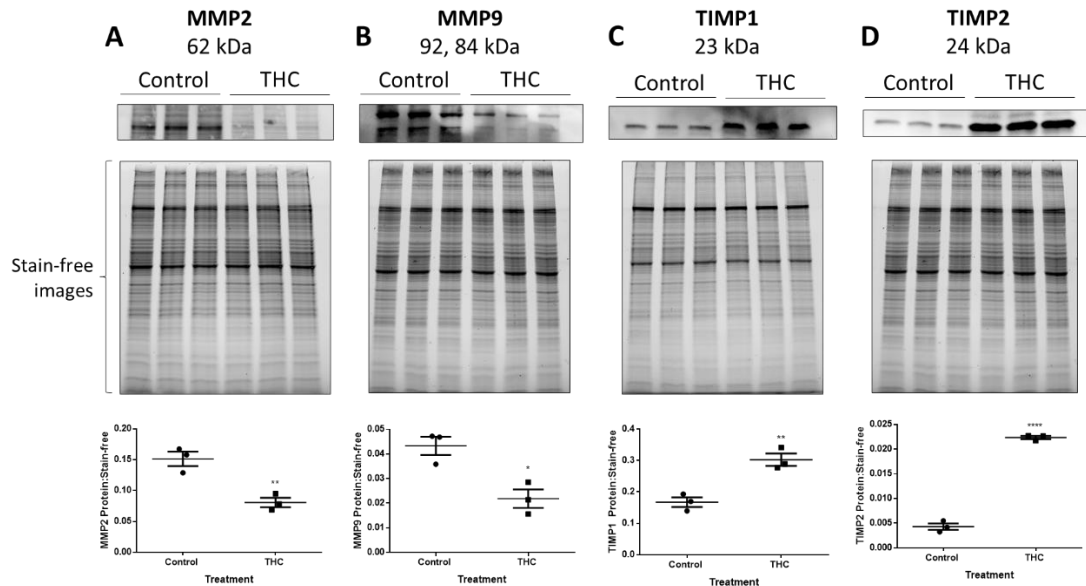
Figure 3. THC alters the expression of MMP and TIMP proteins in HTR8/SVneo cells.

(A-D) Total protein was isolated from HTR8/SVneo cells and analyzed by Western blot (20µg). Summary histograms of active MMP2 **(A)**, pro-MMP9 and active MMP9 **(B)**, TIMP1 **(C)**, and TIMP2 **(D)** of relative band density in each treatment group normalized to stain-free image are shown below the Western blot images. Significant differences were determined by Student's t-test. The individual points represent the ratios of proteins (n = 3), the horizontal lines represent the means and the error bars represent SEM. ** P < 0.01 (A, C), * P < 0.05 (B), **** P < 0.0001 (D).
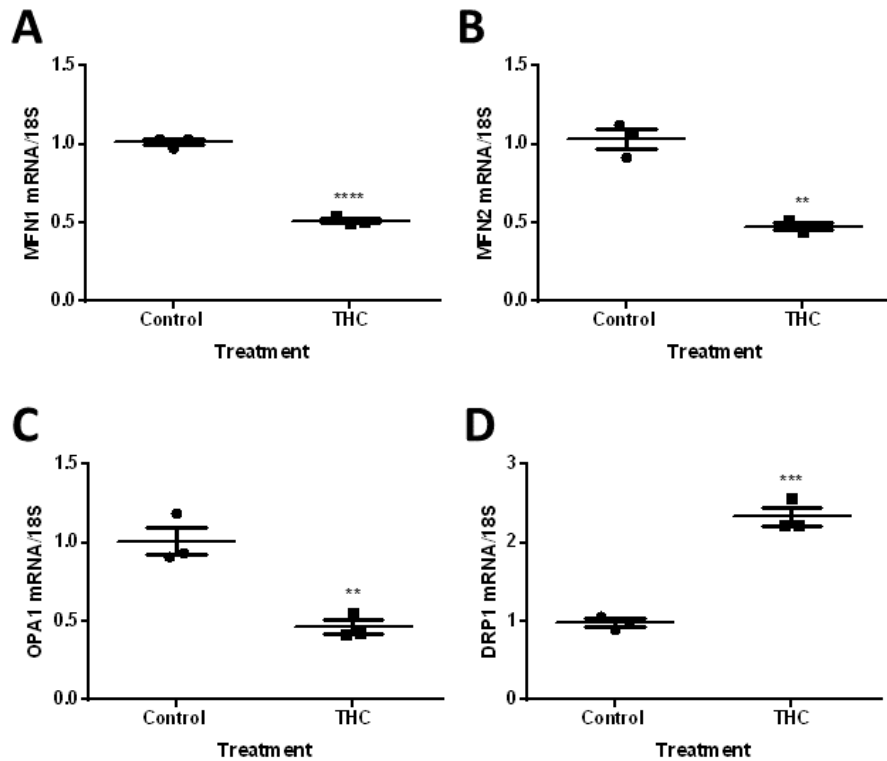
Figure 4. Mitochondrial fusion and fission transcripts are altered in response to 20 μM THC in HTR8/SVneo cells.
Summary histograms are shown of relative MFN1 (A), MFN2 (B) OPA1 (C) and DRP1 (D) transcript expression in each treatment group which were normalized to 18S, then compared to the gene in the vehicle control group. Significant differences were determined by Student's t-test. Individual data points are presented, the mean represented by the horizontal lines ± SEM (n = 3). **** $P < 0.0001$ (A), ** $P < 0.01$ (B, C), *** $P < 0.001$ (D).
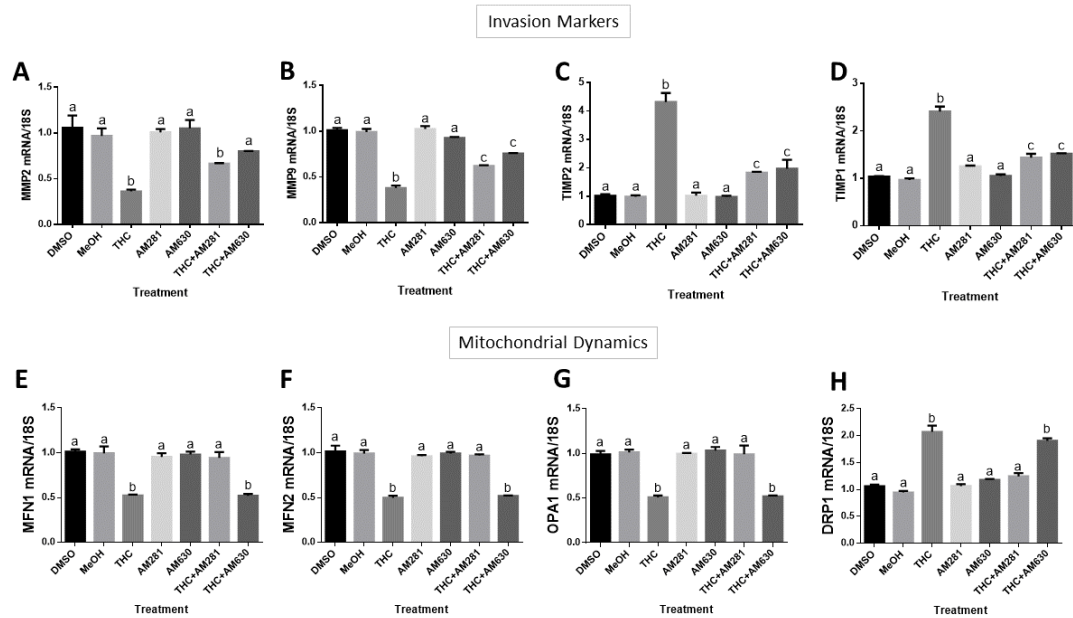
Figure 5. CBR-THC binding reduces invasive potential and disturbs mitochondrial dynamics in HTR8/SVneo cells.

HTR8/SVneo cells were treated for 48 hours as indicated, with DMSO and methanol (MeOH) used as vehicle controls. Summary histograms of relative MMP2 (A), MMP9 (B), TIMP2 (C), TIMP1 (D) MFN1 (E), MFN2 (F), OPA1 (G) and DRP1 (H) transcript expression in each treatment group normalized to 18S, then compared to the gene in the vehicle controls. Significant differences were determined by a one-way ANOVA, followed by a Bonferroni post hoc test. Data are presented as means ± SEM (n = 3). Different letters denote significant differences compared to vehicle controls (A-H, P< 0.0001). THC: 20 uM; AM281: 1µM; AM630: 1µM.
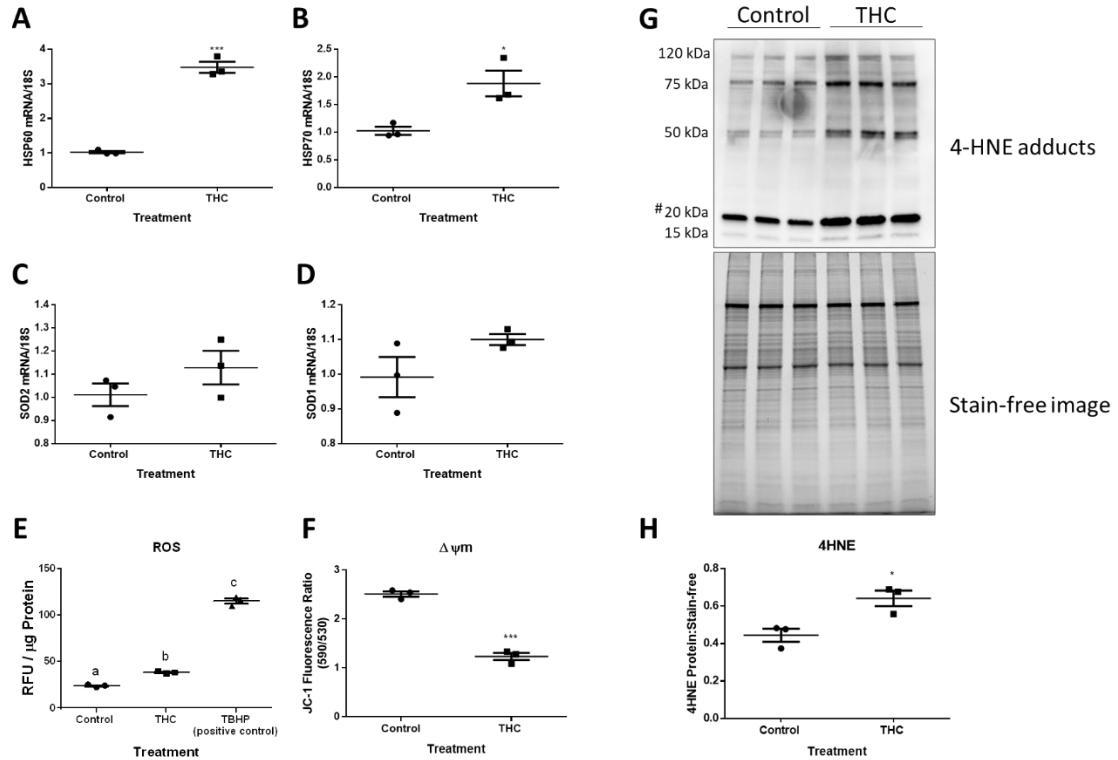
Figure 6. THC increases transcriptional markers of stress responses, ROS production and lipid peroxidation in HTR8/SVneo cells without changing the expression of superoxide dismutases.

Summary histograms are shown of relative HSP60 (A), HSP70 (B), SOD2 (C), and SOD1 (D) transcript expression in each treatment group which were normalized to 18S, then compared to the gene in the vehicle control group. (E) DCFDA assays were performed to determine intracellular ROS levels following THC treatment. Tert-Butyl Hydrogen Peroxide (TBHP) solution (100 µM) was used as the positive control. Results were normalized to the protein content of cell lysates via the BCA assay, which enables the standardization of ROS production as a function of cell number (protein level). (F) THC decreased JC-1 fluorescence ratio. (G) A western blot showing four major protein bands with molecular weights of approximately 120, 75, 50, 20 and 15 kDa showed immunoreactivity for 4-HNE modifications in control and treated trophoblast cells from whole cell lysates (20 µg). (H) Quantification of the density of the four major protein bands in the 4-HNE blot for each treatment group are shown as a ratio normalized to stain-free image. The hashtag (#) indicates a ~20 kDa band of proteins which show greater sensitivity to oxidative damage. The individual points represent measurements (n = 3), the horizontal lines represent the means and the error bars represent SEM. Significant differences were determined by Student's t-test. *** $P < 0.001$ (A, E), * $P < 0.05$ (B, H), $P = $ ns (C, D), $P < 0.001$ (F). RFU = relative fluorescence units.
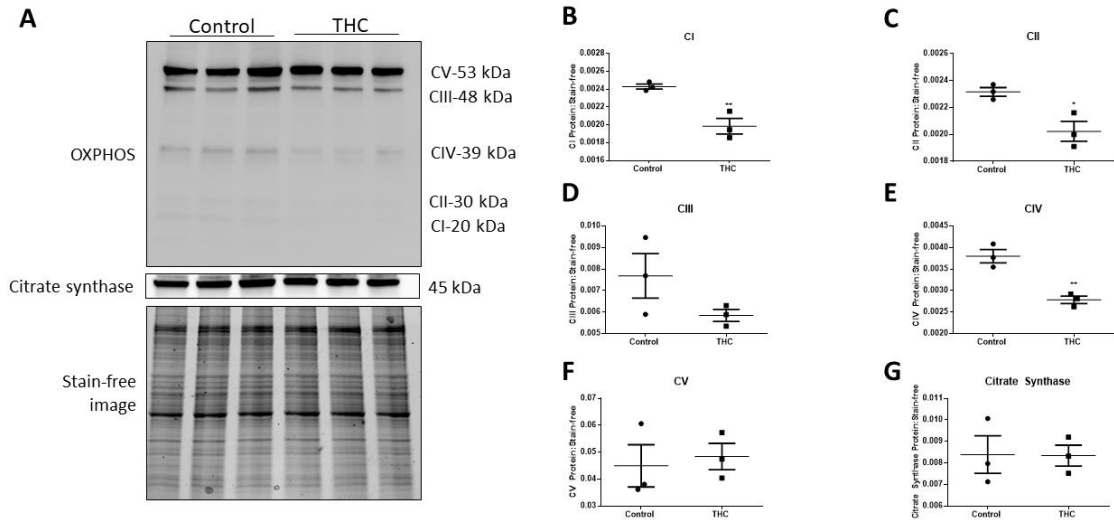
Figure 7. THC reduces levels of mitochondrial complex proteins without altering citrate synthase protein expression.

(A) Western blot images of mitochondrial OXPHOS respiratory complex protein levels, citrate synthase and stain-free image in control and THC treated conditions. A cocktail antibody comprising the following subunits of respiratory complex proteins was used: NADH dehydrogenase (ubiquinone) 1 beta subcomplex 8 (NDUFB8; complex I), succinate dehydrogenase complex, subunit B (SDHB; complex II), ubiquinol-cytochrome c reductase core protein II (UQCR2; complex III), cytochrome c oxidase subunit 2 (COXII; complex IV) and ATP synthase 5A (ATP 5A, Complex V). Quantification of the levels of each of the above-mentioned subunits and CS expression are shown, respectively (B-G). The individual points represent the ratios of proteins normalized to stain-free image (n = 3), the horizontal lines represent the means and the error bars represent SEM. Significant differences were determined by Student's t-test. **$P < 0.01$ (B, E); *$P < 0.05$ (C); P = ns (D, F, G).
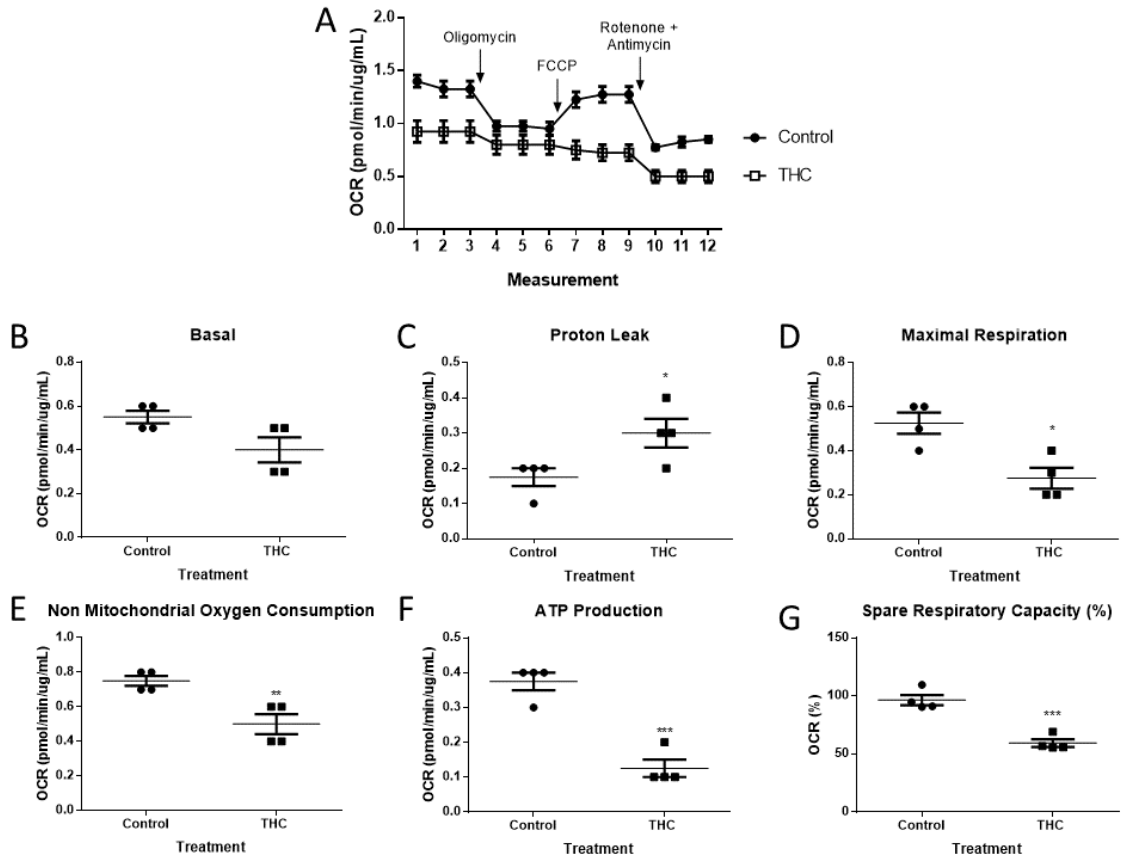
Figure 8. Mitochondrial respiration indices are impaired in HTR8/SVneo cells upon exposure to THC.
(A) Representative OCR tracing. (B-G) Mitochondrial parameters as indicated. The detection of OCR was performed with 4 biological replicates per experiment, for each treatment condition, and repeated 3 more times (see Supplemental Fig. 5.2 for experiments 2-4). Individual data(B-G), group mean and SEM (A-G) are shown. Significance was assessed by Student's t-test (*P < 0.05, **P < 0.01, ***P < 0.001).

SUPPLEMENTARY FIGURES
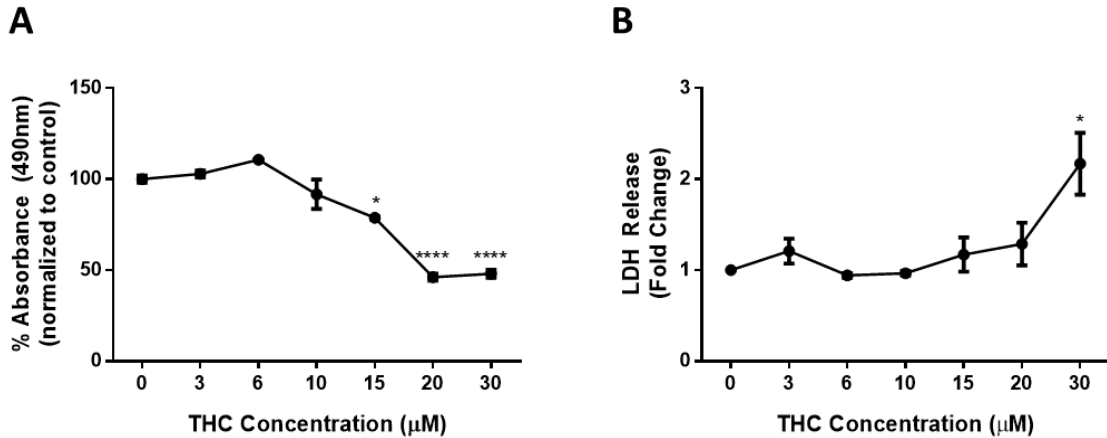
Figure S1. THC negatively impacts HTR8/SVneo cells viability and plasma membrane integrity.
HTR8/SVneo cells were treated with THC as indicated for 48 hours and subjected to MTS (A) and LDH (B) assays. Each data point represents the mean ± SEM of 3 biological replicates measured at 490nm (MTS) or 490nm and 680nm (LDH). Significant differences were determined by a one-way ANOVA followed by a Bonferroni post hoc test. *P < 0.05; ****P < 0.0001, relative to control.
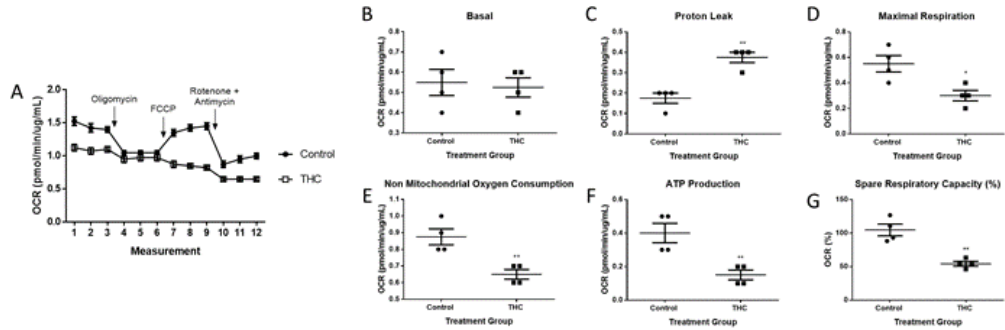
Supplemental Figure 2, OCR, run #2
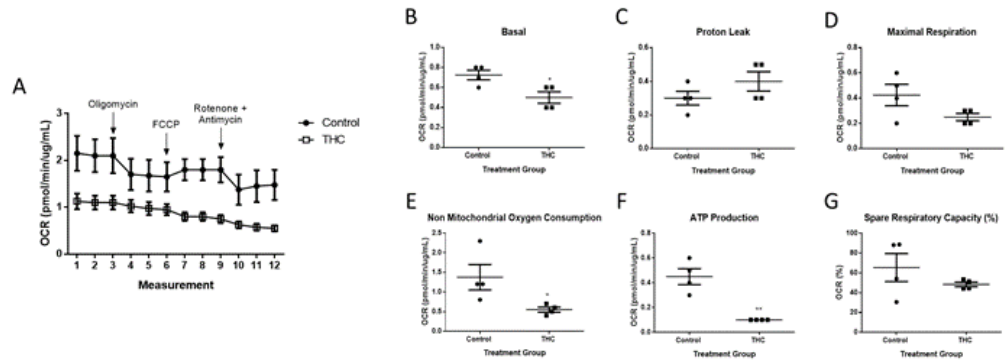
Supplemental Figure 2, OCR, run #3
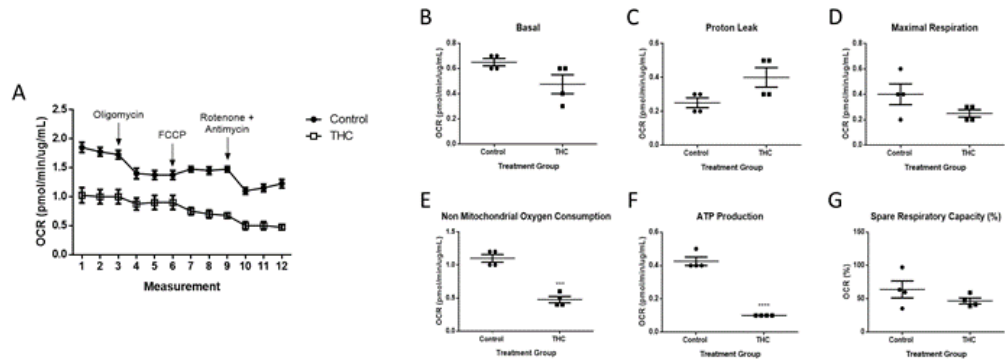
Supplemental Figure 2, OCR, run #4

Figure S2.   Mitochondrial respiration indices are impaired in HTR8/SVneo cells upon exposure to THC (experiments 2-4).
(A) Representative mitochondrial profile. (B-G) Mitochondrial parameters as indicated. The detection of OCR was performed with 4 biological replicates per experiment, for each treatment condition, and repeated 3 more times. Individual data (B-G), group mean and SEM (A-G) are shown. Significance was assessed by Student's t-test (*P < 0.05, **P < 0.01, ***P < 0.001).

CHAPTER 6: CONCLUSION & DISCUSSION

6.1 CONCLUSION

The objective of the current dissertation was to investigate the potential negative impact of mitochondrial dysfunction in regulating human trophoblast invasion and syncytialization, as well as the role of THC in mediating these processes. Our results provide insight into the cellular and molecular events regulated by THC in trophoblast cells and is summarized in Figure 1 below.

As described in **Chapter 3**, the effects of rotenone, a mitochondrial complex I inhibitor, on human trophoblast fusion was studied using the choriocarcinoma cell line, BeWo. The link between oxidative stress in the placenta and altered fetal growth is well established. While the role of the mitochondria in this process has been implied by a number of researchers, the connection between mitochondrial signals and the specific fetal growth signals, which might be impacted, has yet to be established. This chapter links mitochondrial signals, such as reactive oxygen species, to changes in endocrine signals which are important for fetal growth. The data shows that elevated ROS signals caused by perturbation of the electron transport chain influence the ability of the cultured trophoblasts to form a syncytial barrier, an important step in the development of a functional materno-fetal interface. Furthermore, mitochondrial complex I inhibition contributed to the reductions in hCG, hPL and IGF2. Importantly, these effects were negated by pre-treatment with an antioxidant, NAC. Taken together, these data serve to more concretely establish the role of the mitochondria in contributing to placental function and fetal outcomes, particularly via mitochondrial ROS signals. Importantly, this chapter provides a mechanistic link for publications that suggest placental oxidative stress can lead to changes in fetal growth and development[46,101,218–220], as this may be mediated by impaired release of placental endocrine factors such as hPL and IGF2.

Because direct mitochondrial inhibition led to impaired BeWo cell differentiation, ROS production and decreased hormonal transcription, in **Chapter 4** we opted to test the applicability of the aforementioned outcomes using THC, which is also reported to act as a complex I inhibitor. Recent reports have suggested that THC attenuates mitochondrial function in undifferentiated BeWo cells and can also impact the differentiation of trophoblasts. However, the data from this chapter advances these findings in three important, and novel, aspects. We demonstrate that THC treatment of BeWo cells not only attenuates syncytialization but also reduces the production of three hormonal transcripts, hCG, hPL and IGF2, important for promoting fetal growth. The data shows that THC not only reduces mitochondrial ATP production in the syncytiotrophoblast but also increases cellular ROS levels. Further, the increase in the expression of markers for mitochondrial fragmentation, which is correlated to the decreased mitochondrial membrane potential, is also demonstrated. These findings also associate well with the demonstration that cellular chaperones such as HSP60 and HSP70 are increased, supporting the conclusion that exposure to THC increased levels of cellular stress. Importantly we show that these effects are mediated, in part, via CB1 agonism. Taken together, these results help to advance the understanding of the impact of THC on trophoblast mitochondrial and cellular physiology. The trophoblast functional outcomes, such as reduced hPL and IGF2 production, correlate with observations in human and animal models which suggests that exposure to cannabis or THC during pregnancy leads to fetal growth restriction.

Having established the negative impact of THC in a syncytialization model of placentation, **Chapter 5**, was an investigation of THC and its impact on an equally vital process underlying placental formation – invasion – using a human EVT model, HTR8/SVneo. We demonstrate that markers of cellular invasion were altered such that invasiveness of the HTR8/SVneo cells were significantly reduced. Critically, THC treatment impaired transwell invasion via reduced MMP and increased TIMP transcripts and proteins. Additionally, we demonstrate that mitochondrial function

was markedly disturbed following THC exposure. For example, indices for mitochondrial fusion and fission were perturbed in favour of the latter, and ATP production was impaired. These findings provide important insights into the molecular mechanisms underlying the anti-invasive effects of THC on human EVTs and enhance our understanding of placentation in the context of drug exposure.

The THC-induced mitochondrial responses between the HTR8/SVneo and BeWo cells were quite different with respect to the mRNA expression of SOD enzymes – i.e. no change vs. a 2.5-fold increase, respectively. The SOD activity levels were not assessed in this thesis. If the oxidative stress is manageable or short-lasting, SOD expression/activity increases, as shown in the BeWo response to THC herein. Conversely, when oxidative stress persists or becomes exaggerated, SOD becomes overwhelmed and results in a decline in SOD expression or activity relative to control conditions or no change[221] as reflected by the significant increase in ROS in the HTR8/SVneo cells following exposure to THC. Differential expression of antioxidant response genes may, in part, be the cause of this discrepancy between the HTR8/SVneo and BeWo cells, notably so in pregnancies complicated by pre-eclampsia and IUGR[222,223]. HTR8/SVneo and BeWo cells have a different epigenetic profile than primary extravillous trophoblasts which may be associated with altered gene expression and response to pharmacological perturbations[224]. Indeed, while cell lines are associated with a gain of methylation, the level of DNA methylation in HTR8/SVneo cells is reportedly higher than that of tumour-derived cell lines, i.e. BeWo[224]. This may make the HTR8/SVneo cells more sensitive to pharmacological stressors compared to BeWo cells. HTR8/SVneo and BeWo cells represent distinct trophoblast differentiation pathways which may bear an impact on this outcome. The HTR8/SVneo cells represent invasive extravillous trophoblasts as they detach from the chorionic villi and invade the decidua. BeWo cells retain the characteristics of villous syncytiotrophoblasts, i.e. fusion and hormone secretion. Based on these

characteristics, any perturbation to the EVTs may contribute to unsuccessful implantation of the blastocyst, while disturbances to villous trophoblasts function may impair the continuous syncytialization that occurs throughout gestation and negatively impact hormone secretion. Whether these points are facts or artifacts of cell derivation will require further investigation in the context of trophoblast physiology.

In **Appendix A**, the response to rotenone in HTR8/SVneo cells were characterized. Using an in vitro model of invasion, we tested the hypothesis that mitochondrial dysfunction induced by pharmacological inhibition of mitochondrial complex I in human placental HTR8/SVneo cells leads to a negative cascade of events: increased ROS production, reduced proliferative capacity of HTR8/SVneo cells, and reduced evidence of invasion. Upon complex I inhibition with 0.1 nM rotenone for 48 hours, HTR8/SVneo cells had reduced proliferative capacity (Figure A1); poorly invaded Matrigel-coated inserts (Figure A2) due to significantly reduced MMP-2 and MMP-9 transcript expression concomitant with a marked increase in TIMP-1 and TIMP-2 transcript expression (Figure A3). These changes were coincident with significant reductions in mitochondrial fusion mediators MFN1, MFN2 and OPA1 and an increase in DRP1, indicative of mitochondrial fission (Figure A4). Lastly, ROS production was significantly increased along with cellular indicators of stress (HSP60 and HSP70), albeit without changes to the transcriptional expression of antioxidant defense enzymes SOD1 and SOD2 (Figure A5). Thus, the rotenone response is similar to that of THC in our model of trophoblast invasion.

Mitochondrial respiration indices in response to THC exposure in undifferentiated BeWo cells are presented in **Appendix B**, most of which are impaired (Figure B1; $P < 0.01$). Also, cannabinoid receptor expression is discussed here. The literature reports the presence of CB1 and CB2 on first trimester trophoblasts[216], undifferentiated BeWo cells[216] and in the syncytial layer of primary trophoblast cells[141,216]. We have confirmed the presence of CB1 and CB2 via western

blotting on HTR8/SVneo and both undifferentiated and differentiated BeWo cells (Figure B2). Although protein expression did not display significant differences in undifferentiated or differentiated BeWo cells following THC treatment, this may indicate that changes in the receptor expression are not requisite for BeWo cells to have a response upon THC binding. Curiously, in HTR8/SVneo cells, the receptor expression of CB1 did not change with THC treatment, while CB2 expression was significantly ($P < 0.05$) reduced following THC exposure. Our antagonist data on select transcriptional markers of invasion, syncytialization and mitochondrial dynamics (Chapter 4 and 5) show that the effects of THC were completely or partially reversed when pre-treated with the receptor antagonists. From this, we can conclude that the effect of THC in our system is partially dependent upon THC-CB1 and THC-CB2 agonism, whether receptor expression is changed following THC exposure.

In summary, these results describe he negative impact of THC during the processes of invasion and syncytialization concomitant with disruptions to mitochondrial morphology and function. Mitochondria respond to a range of stimuli[65] and are the primary source of energy production for placental growth, transport, hormone production and synthesis[92,101]. Many pregnancy pathologies are the result of altered placental oxygen supply, which is likely due to altered mitochondrial structure and function, thus making mitochondria etiologically relevant in the context of placental disorders. Importantly, these mechanisms are partly mediated via THC binding at the canonical cannabinoid receptors, which may disturb ECS homeostasis during gestation. The results of this study will prove significant as it will ***deepen our mechanistic understanding*** of human pregnancies compromised by poor placentation due to THC-mediated perturbances to mitochondrial function.
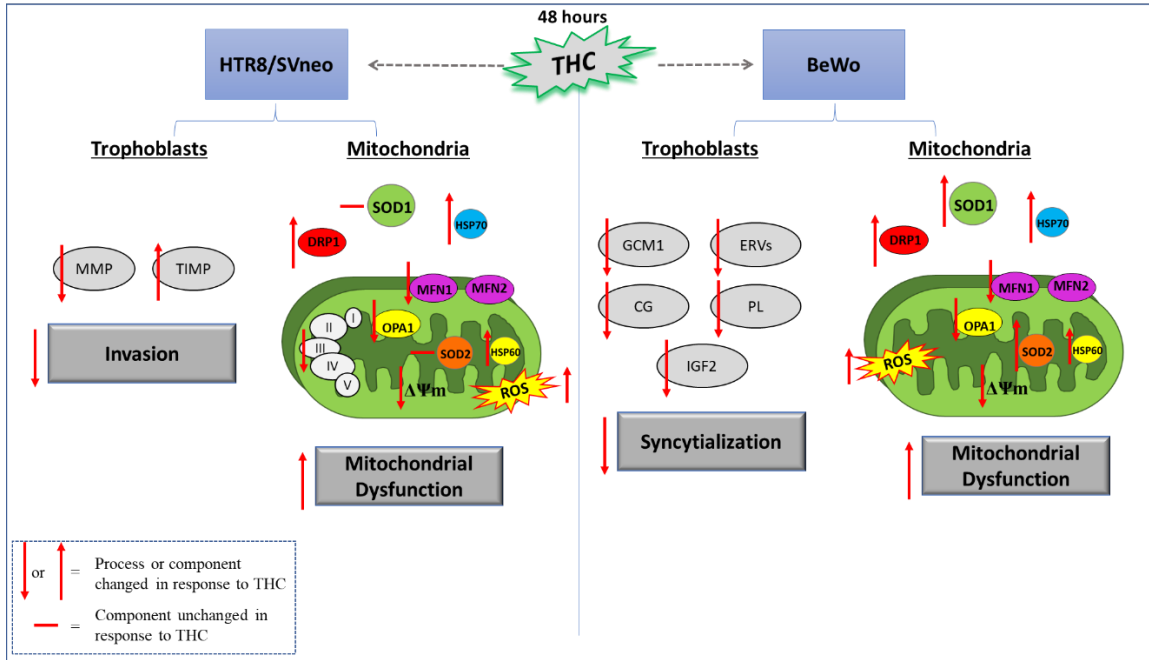
Figure 1. Summary of overall study findings.

6.2   OVERALL DISCUSSION OF THIS STUDY

The articles presented within this compilation thesis have illuminated a collection of scientific questions. This section of my dissertation is guided by some of these key questions.

6.2.1 Do THC and a known complex I inhibitor act in a similar manner?

There are shared and divergent molecular mechanisms between rotenone and THC that may explain the coincident regulation of mitochondrial function in trophoblast cells. Complex I inhibitors (i.e. rotenone) and some small molecules (e.g. metformin[225]) are chemically neutral, aromatic and highly lipophilic molecules that are reported to differentially inhibit complex I[226]. Specifically, rotenone is an irreversible inhibitor of complex I, its accumulation is not dependent on the presence of specific transporters on the plasma membrane thus it readily accumulates

intracellularly, and it stimulates ROS production. The flavin site within complex I produces ROS and it is reported that rotenone inhibits complex I downstream of the flavin site, stimulating ROS generation. Conversely, metformin binds upstream of the flavin site and does not produce ROS[227]. However, some small molecules produce mitochondrial depolarization, reduce ATP production, and increase ROS production, much like what was demonstrated in our studies with THC.

Like rotenone, THC is uncharged, aromatic and highly hydrophobic; compounds with this phenotype are known to interfere with mitochondrial electron transport[228]. One might speculate that THC serves as an example of such a small molecule capable of complex I inhibition. Indeed, the literature reports THC as a putative complex I inhibitor[118]. Unlike rotenone, THC requires the presence of specific plasma membrane transporters to gain access to the cell. However, like rotenone[226], THC impairs the bioavailability of NADH[228], which consequently decreases electron acceptors leading to electron leakage and ROS production[229]. Whether THC has a specific binding site to that of complex I or whether the reported inhibition is via various intermediate means, i.e. via mitochondrial CB1 agonism, remains to be fully examined.

6.2.2 If an aspect of mitochondrial function is blocked with specific inhibitors, will the magnitude of THC-induced deficits be the same?

If a specific mitochondrial process is blocked, i.e. fission, one may expect that the THC-induced deficits may be lessened. Importantly, this will demonstrate a direct effect on mitochondria following THC exposure. Fission is selected here as an example because markers of this process were markedly increased in both HTR8/SVneo and BeWo cells following THC exposure. Using mitochondrial division inhibitor 1 (mdivi-1), a selective inhibitor of DRP1, one can effectively suppress mitochondrial fission[230]. Pre-treatment with mdivi-1 followed by THC exposure, may partially alleviate mitochondrial dysfunction relative to cells treated with THC alone. In addition,

one may expect that mitochondrial density, morphology and respiration may be positively altered in response to mdivi-1 treatment because inhibition of mitochondrial fission may mitigate further mitochondrial dysfunction, i.e. maintenance of the membrane potential and respiration[230]. However, while mdivi-1 may confer protective effects on mitochondrial morphology, the impact on other mitochondrial processes will need to be examined in this context to fully appreciate the relevance of THC-induced effects, as there may be alternative and independent signaling means by which THC can perturb mitochondrial function in trophoblast cells.

6.2.3 Might inhibition or siRNA knockdown of antioxidant systems exaggerate THC-induced ROS levels and further reduce invasion and/or syncytialization?

The data suggests that mitochondria may have a role in the process of THC signaling in trophoblasts based on the cannabinoid receptors impacting some of these functions, including fragmentation. Our recent publication on the effects of rotenone-mediated complex I inhibition in BeWo cells demonstrated that mitigation of reactive oxygen species using NAC, a known cellular antioxidant, led to the improvement of BeWo cell fusion. Furthermore, based on the existing literature, we expect that siRNA-mediated knockdown of antioxidant systems (example SOD2) will allow for the generation of ROS given that SODs confer protection against oxidative stress[84]. Thus, I expect that under this experimental protocol, THC-induced ROS levels would be exaggerated, leading to further reductions in BeWo cell fusion. However, the impact of this intervention may be less clear in the HTR8/SVneo cells, as *SOD1* and *SOD2* transcripts remained unchanged in response to THC exposure.

6.2.4 How might the constituents of whole cannabis affect the outcome measures in this in vitro system? Where does my data sit in this context?

It is my hypothesis that the application of whole cannabis rather than purified THC will alter the outcome measures such that the outcome measures will be dampened but the directionality of the changes will remain the same, in effect taming THC but not reversing its impact. THC is a dominant constituent in cannabis preparations, being the cannabinoid on which potency is based, having diverse therapeutic and detrimental effects. Importantly, its concentration in modern cannabis preparations is significantly higher than that from decades ago, which led to a shift in its ratio relative to the other constituents. The several compounds in cannabis span many chemical classes including phytocannabinoids, nitrogenous compounds, amino acids, fatty acids, terpenes, and vitamins[126,129]. Little is known about the pharmacological actions of the other constituents in cannabis. However, very few in vitro and in vivo studies report that some of the components (i.e. terpenes) may have a variety of actions (e.g. antioxidant, anti-inflammatory, antinociceptive[231]). The "entourage effect" proposes that terpenes may, to an extent, modify or potentiate the physiological effects of cannabinoids[232]. There is no consensus, however, on the mechanisms that may govern these actions[231].

While there is value both experimentally and therapeutically to studying the effects of whole cannabis on our experimental outcomes, it is advantageous to study the constituents individually because it allows one to tease out the potential therapeutic effects (symptom relief) or negative consequences (pathology). In this dissertation, the effect of THC isolated from full spectrum cannabis allowed us to determine the specific negative molecular events initiated by THC in the setting of trophoblast physiology.

6.2.5 Why is exposure to THC relevant given that most people use cannabis?

Because the potency of cannabis is attributed to the concentration of THC, the adverse effects following acute or long-term use are in direct relation to the THC content[233]. Despite the psychoactive effects of THC, it is showing stronger correlation with therapeutic relief rather than relying on the more socially acceptable symptomatic relief achieved using CBD[234]. Further, cannabis extracts containing high THC concentrations are now amongst the most commonly used drugs[142]. While smoking cannabis is currently the most popular and fastest way for THC to enter the systemic circulation, carcinogens are released, and it destroys some of the medical compounds[134]. Vapourizing, particularly high THC products like shatter, uses lower temperatures to heat and vapourize the cannabinoid preparation and like smoking, this method allows THC to quickly enter the circulation[134,142]. Moreover, since vapourizing THC concentrates using e-cigarette type devices is more discreet than smoking a joint, more pregnant women may opt for this method of achieving relief of pregnancy-related symptoms[134,135].

6.3 LIMITATIONS OF THIS STUDY

There are clear ethical restrictions regarding the experimental use of human models to study placentation in response to THC (or cannabis) exposure. Further, and importantly, it is not possible to obtain placentae from all stages of gestation, so we are limited to terminations and term placentae which provides fewer opportunities to perform mechanistic studies. Therefore, acceptable surrogates involve the use of various cell lines. BeWo cells, derived from metastatic gestational carcinoma cultured numerous times within the hamster cheek pouch, are widely used to study syncytialization, but may retain some of the characteristics of their malignant origins[2]. However,

they can remain in vitro as cytotrophoblasts in a monolayer, or they can be induced to differentiate and fuse under the influence of FSK which increases intracellular cAMP[235]. HTR8/SVneo cells are an immortalized cell line, derived by transfection with Simian virus-40 containing the T-antigen (SV40Tag), which retains all of the EVT cell markers[9]. Given that cellular properties can change with repeated cell passaging[236], one may wish to consider, as I have, using cells with low passage numbers (i.e. ≤10). This may reduce the degree of genetic deviation from the parent cells and thus may facilitate better reproducibility across experimental replicates.

The experiments presented in this dissertation were performed in vitro, therefore, they do not perfectly reflect the in vivo situation. In vivo, trophoblast cells interact with numerous cell types, including cells of the decidua and immune cells, and are subjected to endocrine hormonal influences from the maternal circulation. In vitro, the cells were cultured in monolayers submerged in culture media only, removing the influence of in vivo variables. However, this is advantageous as it permitted the isolation of the specific influence of THC on molecular outcomes in the two in vitro systems employed in this study by means of excluding the complexities and variables of the in vivo situation. Subsequent and confirmatory studies using trophoblasts harvested from human first trimester and term placentae, explants, specific co-culture systems and in vivo rodent/non-human primate models may prove to be more relevant to the mechanisms that underpin the in vivo events that lead to normal and pathological placentation.

6.4   FUTURE DIRECTIONS

The data herein contributes to increase our understanding of the cellular and molecular mechanisms that underpin THC exposure on human trophoblast cells during the processes of invasion and syncytialization. However, more detailed, and comprehensive studies using

appropriate study models (e.g. placental explants, animal models) are required to better advance our knowledge about human placentation. Future directions ought to consider the following:

1. Trophoblast cells interact with decidualized endometrial stromal cells and immune cells which secrete a variety of growth factors (e.g. EGF, VEGF) in vivo. Studies using first trimester, term placentae and decidual explants in an in vitro co-culture system could provide more information regarding the coordinated outcome of growth factor regulation and THC exposure.

2. The molecular mechanisms underlying trophoblast cell invasion involve the regulated expression of cell-cell adhesion molecules by cadherins, the specific degradation/activation of ECM components by MMPs, but also the regulated expression of cell-adhesion molecules by integrins. Thus, the possible roles of integrins in activin-induced trophoblast invasion and vascular differentiation are unknown, particularly in response to THC treatment.

3. The question of whether inhibition or siRNA knockdown of antioxidant systems (e.g. SODs) will exaggerate THC-induced ROS formation and further reduce invasion and/or syncytialization remains to be addressed.

4. The intermediate signaling mechanisms employed by CB receptors to target the mitochondria require further investigation to strengthen the argument for this hypothesis, particularly in placental cells. The signal transduction pathway may involve elements of the JAK-STAT signaling pathway; thus, the investigation may begin by exploring the various components of the JAK-STAT pathway.

5. Confirmatory studies performed in primary human first and term placental cells to further verify the results we obtained in the HTR8/SVneo and BeWo cell lines. Generally speaking, there are more similarities than differences between primary trophoblasts and cell lines[237]. Although cell lines are more resilient than cultures of primary trophoblasts isolated and purified from first or term placentae, namely longer lifespan in vitro[238], there is some value in using primary cells. Primary

trophoblast cells have the advantage of representing normal, untransformed cells. Further, they have the capacity to spontaneously fuse and form syncytia[33].

6. To really strengthen the argument that mitochondria are critical and indeed mediating THC-induced negative outcomes in trophoblast physiology, it may prove useful to utilize a cellular or a mouse model wherein mitochondrial CB1 is knocked out, followed by exposure to THC. It will allow for the assessment of mitochondrial morphology and function, i.e. parameters like fusion and respiration, to see if they remain largely intact in cells and animals which received the knockout. In addition, this will allow one to separate the extent to which THC is acting via complex I vs. mitochondrial CB1. Alternatively, as described in this dissertation, THC-induced complex I inhibition may be mediated first via mitochondrial CB1 agonism.

These routes of investigation will be exciting to explore.

6.5 SIGNIFICANCE TO PUBLIC HEALTH AND TRANSLATIONAL POTENTIAL

Part of the growing concern is that THC concentrations are very likely to be higher now than what was smoked 70 years ago, i.e. "it's not your mama's weed!" Therefore, cannabis and its preparations may be capable of more strongly perturbing the endogenous cannabinoid system and altering placental structure/function, with subsequent negative fetal outcomes.

Throughout pregnancy, frequent contact is made with healthcare providers – i.e. General Practitioner, OB/GYN, Midwife – who play crucial roles in providing patient education regarding the risks associated with cannabis use during pregnancy and are well-positioned to advise against its use during pregnancy. The results from this dissertation will contribute to the foundation of

knowledge surrounding cannabis use in pregnancy, particularly exposure to its main bioactive constituent THC, such that it can inform policy makers, healthcare providers, patients and the general public about the importance of understanding the effects of cannabis use, particularly in this vulnerable population.

REFERENCES

1. Walker, O. S., Holloway, A. C. & Raha, S. The role of the endocannabinoid system in female reproductive tissues. *J. Ovarian Res.* **12**, (2019).

2. Turco, M. Y. & Moffett, A. Development of the human placenta. *Development* **146**, (2019).

3. Moffett, A. & Colucci, F. Uterine NK cells: Active regulators at the maternal-fetal interface. *J. Clin. Invest.* **124**, 1872–1879 (2014).

4. Gude, N. M., Roberts, C. T., Kalionis, B. & King, R. G. Growth and function of the normal human placenta. *Thromb. Res.* **114**, 397–407 (2004).

5. Zhu, J.-Y., Pang, Z.-J. & Yu, Y.-H. Regulation of trophoblast invasion: The role of matrix metalloproteinases. *Rev. Obstet. Gynecol.* **5**, e137-43 (2012).

6. Gupta, S. K., Malhotra, S. S., Malik, A., Verma, S. & Chaudhary, P. Cell signaling pathways involved during invasion and syncytialization of trophoblast cells. *Am J Reprod Immunol* **75**, 361–371 (2015).

7. Plaks, V. *et al.* Matrix metalloproteinase-9 deficiency phenocopies features of preeclampsia and intrauterine growth restriction. *Proc. Natl. Acad. Sci. U. S. A.* **110**, 11109–11114 (2013).

8. Fitzgerald, J. S., Poehlmann, T. G., Schleussner, E. & Markert, U. R. Trophoblast invasion: The role of intracellular cytokine signalling via signal transducer and activator of transcription 3 (STAT3). *Hum. Reprod. Update* **14**, 335–344 (2008).

9. Lala, P. K., Lee, B. P., Xu, G. & Chakraborty, C. Human placental trophoblast as an in vitro model for tumor progression. *J. Physiol. Pharmacol* **80**, 142–149 (2002).

10. Ferretti, C., Bruni, L., Dangles-Marie, V., Pecking, A. P. & Bellet, D. Molecular circuits shared by placental and cancer cells, and their implications in the proliferative, invasive

and migratory capacities of trophoblasts. *Hum. Reprod. Update* **13**, 121–141 (2007).

11. Lash, G. E. *et al.* Interaction between uterine natural killer cells and extravillous trophoblast cells: effect on cytokine and angiogenic growth factor production. *Hum. Reprod.* **26**, 2289–2295 (2011).

12. Sosa, S. E. Y. *et al.* New insights into the role of matrix metalloproteinases in preeclampsia. *Int. J. Mol. Sci.* **18**, 1–10 (2017).

13. Staun-Ram, E., Goldman, S., Gabarin, D. & Shalev, E. Expression and importance of matrix metalloproteinase 2 and 9 (MMP-2 and -9) in human trophoblast invasion. *Reprod. Biol. Endocrinol.* **2**, 59 (2004).

14. Wu, D. *et al.* CXCR2 is decreased in preeclamptic placentas and promotes human trophoblast invasion through the Akt signaling pathway. *Placenta* **43**, 17–25 (2016).

15. Xu, P. *et al.* Effects of matrix proteins on the expression of matrix metalloproteinase-2, -9, and -14 and tissue inhibitors of metalloproteinases in human cytotrophoblast cells during the first trimester. *Biol. Reprod.* **65**, 240–246 (2001).

16. Lash, G. E. *et al.* Inhibition of trophoblast cell invasion by TGFB1, 2, and 3 is associated with a decrease in active proteases. *Biol. Reprod.* **73**, 374–381 (2005).

17. Strongin, A. Y. Proteolytic and non-proteolytic roles of membrane type-1 matrix metalloproteinase in malignancy. *Biochim. Biophys. Acta* **2010**, 133–141 (2009).

18. Rivera, S., Khrestchatisky, M., Kaczmarek, L., Rosenberg, G. A. & Jaworski, D. M. Metzincin proteases and their inhibitors: Foes or friends in nervous system physiology? *J. Neurosci.* **30**, 15337–15357 (2010).

19. Butler, G. S., Tam, E. M. & Overall, C. M. The canonical Methionine 392 of matrix metalloproteinase 2 (gelatinase A) is not required for catalytic efficiency or structural integrity PROBING THE ROLE OF THE METHIONINE-TURN IN THE METZINCIN

METALLOPROTEASE SUPERFAMILY. *J. Biol. Chem.* **279**, 15615–15620 (2004).

20. Iyer, S., Wei, S., Brew, K. & Acharya, K. R. Crystal structure of the catalytic domain of matrix metalloproteinase-1 in complex with the inhibitory domain of tissue inhibitor of metalloproteinase-1. *J. Biol. Chem.* **282**, 364–371 (2007).

21. Ukaji, T., Sasazawa, Y., Umezawa, K. & Simizu, S. Involvement of conserved tryptophan residues for secretion of TIMP-2. *Oncol. Lett.* **7**, 631–634 (2014).

22. Ramer, R. & Hinz, B. Inhibition of cancer cell invasion by cannabinoids via increased expression of tissue inhibitor of matrix metalloproteinases-1. *J Natl Cancer Inst* **100**, 59–69 (2008).

23. Nissi, R. *et al.* Circulating matrix metalloproteinase MMP-9 and MMP-2/TIMP-2 complex are associated with spontaneous early pregnancy failure. *Reprod. Biol. Endocrinol.* **11**, 2 (2013).

24. Zhu, J. Y., Zhong, M., Pang, Z. J. & Yu, Y. H. Dysregulated expression of matrix metalloproteinases and their inhibitors may participate in the pathogenesis of pre-eclampsia and fetal growth restriction. *Early Hum. Dev.* **90**, 657–664 (2014).

25. Shokry, M., Omran, O. M., Hassan, H. I., Elsedfy, G. O. & Hussein, M. R. A. Expression of matrix metalloproteinases 2 and 9 in human trophoblasts of normal and preeclamptic placentas: Preliminary findings. *Exp. Mol. Pathol.* **87**, 219–225 (2009).

26. Sun, J. Matrix metalloproteinases and tissue inhibitor of metalloproteinases are essential for the inflammatory response in cancer cells. *J. Signal Transduct.* **2010**, (2010).

27. Richards, C. D. *et al.* Regulation of tissue inhibitor of metalloproteinase-1 in fibroblasts and acute phase proteins in hepatocytes in vitro by mouse oncostatin M, cardiotrophin-1, and IL-6. *J. Immunol.* **159**, 2431–2437 (1997).

28. Korzus, E., Nagase, H., Rydell, R. & Travis, J. The mitogen-activated protein kinase and

JAK-STAT signaling pathways are required for an oncostatin M-responsive element-mediated activation of matrix metalloproteinase 1 gene expression. *J. Biol. Chem.* **272**, 1188–1196 (1997).

29.   Dechow, T. N. *et al.* Requirement of matrix metalloproteinase-9 for the transformation of human mammary epithelial cells by Stat3-C. *Proc. Natl. Acad. Sci. U. S. A.* **101**, 10602–10607 (2004).

30.   Gerbaud, P. & Pidoux, G. Review: An overview of molecular events occurring in human trophoblast fusion. *Placenta* **29**, S35–S42 (2014).

31.   Larsson, L.-I., Bjerregaard, B. & Talts, J. F. Cell fusions in mammals. *Histochem Cell Biol* **129**, 551–561 (2008).

32.   Blond, J.-L. *et al.* An envelope glycoprotein of the human endogenous retrovirus HERV-W is expressed in the human placenta and fuses cells expressing the type D mammalian retrovirus receptor. *J. Virol.* **74**, 3321–3329 (2000).

33.   Frendo, J., Olivier, D., Blond, J., Bouton, O. & Vidaud, M. Direct involvement of HERV-W Env glycoprotein in human trophoblast cell fusion and differentiation. *Mol. Cell. Biol.* **23**, 3566–3574 (2003).

34.   Noorali, S. *et al.* Role of HERV-W syncytin-1 in placentation and maintenance of human pregnancy. *Appl. Immunohistochem. Mol. Morphol.* **17**, 319–328 (2009).

35.   Ruebner, M. *et al.* Impaired cell fusion and differentiation in placentae from patients with intrauterine growth restriction correlate with reduced levels of HERV envelope genes. *J. Mol. Med.* **88**, 1143–1156 (2010).

36.   Knerr, I. *et al.* Endogenous retroviral syncytin: Compilation of experimental research on syncytin and its possible role in normal and disturbed human placentogenesis. *Mol. Hum. Reprod.* **10**, 581–588 (2004).

37.   Lavialle, C. *et al.* Paleovirology of ' syncytins ', retroviral env genes exapted for a role in placentation. *Philos. Trans. R. Soc. Lond. B. Biol. Sci.* **368:201205**, (2013).

38.   Mi, S. *et al.* Syncytin is a captive retroviral envelope protein involved in human placental morphogenesis. *Nature* **403**, 785–789 (2000).

39.   Muroi, Y. *et al.* CD9 regulates transcription factor GCM1 and ERVWE1 expression through the cAMP/protein kinase A signaling pathway. *Reproduction* **138**, 945–951 (2009).

40.   Leduc, K. *et al.* Leukemia inhibitory factor regulates differentiation of trophoblastlike BeWo cells through the activation of JAK/STAT and MAPK3/1 MAP kinase-signaling pathways. *Biol. Reprod.* **86**, 1–10 (2012).

41.   Pidoux, G. Spatiotemporal regulation of cAMP signaling controls the human trophoblast fusion. *Front. Pharmacol.* **6**, 1–14 (2015).

42.   Huang, Q. *et al.* Syncytin-1 modulates placental trophoblast cell proliferation by promoting G1/S transition. *Cell. Signal.* **25**, 1027–1035 (2013).

43.   Tolosa, J. M. *et al.* The endogenous retroviral envelope protein syncytin-1 inhibits LPS/PHA-stimulated cytokine responses in human blood and is sorted into placental exosomes. *Placenta* **33**, 933–941 (2012).

44.   Vargas, A. *et al.* Syncytin proteins incorporated in placenta exosomes are important for cell uptake and show variation in abundance in serum exosomes from patients with preeclampsia. *FASEB J.* **28**, 3703–3719 (2014).

45.   Muralimanoharan, S. *et al.* MIR-210 modulates mitochondrial respiration in placenta with preeclampsia. *Placenta* **33**, 816–823 (2012).

46.   Takagi, Y. *et al.* Levels of oxidative stress and redox-related molecules in the placenta in preeclampsia and fetal growth restriction. *Virchows Arch.* **444**, 49–55 (2004).

47.   Vargas, A. *et al.* Reduced expression of both syncytin 1 and syncytin 2 correlates with severity of preeclampsia. *Reprod. Sci.* **18**, 1085–1091 (2011).

48.   Chiang, M.-H. *et al.* Mechanism of hypoxia-induced GCM1 degradation: Implications for the pathogenesis of preeclampsia. *J. Biol. Chem.* **284**, 17411–9 (2009).

49.   Langbein, M. *et al.* Impaired cytotrophoblast cell–cell fusion is associated with reduced syncytin and increased apoptosis in patients with placental dysfunction. *Mol. Reprod. Dev.* **75**, 175–183 (2008).

50.   Biswas, S., Ghosh, S. K. & Chhabra, S. Surface area of chorionic villi of placentas: An index of intrauterine growth restriction of fetuses. *J. Obstet. Gynaecol. Res.* **34**, 487–493 (2008).

51.   Costa, M. A. The endocrine function of human placenta: An overview. *Reprod. Biomed. Online* **32**, 14–43 (2016).

52.   Anthony, R. V, Pratt, S. L., Liang, R. & Holland, M. D. Placental-fetal hormonal interactions: Impact on fetal growth. *J Anim Sci* **73**, 1861–1871 (1995).

53.   Shah, J. & Baxi, B. Identification of biomarkers for prediction of preterm delivery. *J. Med. Soc.* **30**, 3–14 (2016).

54.   Jansson, T. Placenta plays a critical role in maternal–fetal resource allocation. *Proc. Natl. Acad. Sci.* **113**, 11066–11068 (2016).

55.   Cole, L. A. Hyperglycosylated hCG, a review. *Placenta* **31**, 653–664 (2010).

56.   Freemark, R. Placental hormones and the control of fetal growth. *J Clin Endocrinol Metab* **95**, 2054–2057 (2010).

57.   Halasz, M. & Szekeres-Bartho, J. The role of progesterone in implantation and trophoblast invasion. *J. Reprod. Immunol.* **97**, 43–50 (2013).

58.   Laškarin, G. *et al.* Progesterone induced blocking factor (PIBF) mediates progesterone

induced suppression of decidual lymphocyte cytotoxicity. *Am. J. Reprod. Immunol.* **48**, 201–209 (2002).

59.   Mirlesse, V. *et al.* Placental growth hormone levels in normal pregnancy and in pregnancies with intrauterine growth retardation. *Int. Pediatr. Res. Found. Inc* **34**, 439–442 (1993).

60.   Hamilton, G. S., Lysiak, J. J., Han, V. K. M. & Lala, P. K. Autocrine-paracrine regulation of human trophoblast invasiveness by insulin-like growth factor (IGF)-II and IGF-binding protein (IGFBP)-1. *Exp. Cell Res.* **244**, 147–156 (1998).

61.   Wagner, P. K., Otomo, A. & Christians, J. K. Regulation of pregnancy-associated plasma protein A2 (PAPPA2) in a human placental trophoblast cell line (BeWo). *Reprod. Biol. Endocrinol.* **9**, 1–7 (2011).

62.   Costa, M. A. The endocannabinoid system: A novel player in human placentation. *Reprod. Toxicol.* **61**, 58–67 (2016).

63.   Benaitreau, D. *et al.* Adiponectin promotes syncytialisation of BeWo cell line and primary trophoblast cells. *Reprod. Biol. Endocrinol.* **8**, 128 (2010).

64.   Chan, D. C. Mitochondria: Dynamic organelles in disease, aging, and development. *Cell* **125**, 1242–1252 (2006).

65.   Osellame, L. D., Blacker, T. S. & Duchen, M. R. Cellular and molecular mechanisms of mitochondrial function. *Best Pract. Res. Clin. Endocrinol. Metab.* **26**, 711–723 (2012).

66.   McBride, H. M., Neuspiel, M. & Wasiak, S. Mitochondria: More Than Just a Powerhouse. *Curr. Biol.* **16**, R551–R560 (2006).

67.   Kühlbrandt, W. Structure and function of mitochondrial membrane protein complexes. *BMC Biol.* **13**, (2015).

68.   Youle, R. J. & Van Der Bliek, A. M. Mitochondrial fission, fusion, and stress. *Science.*

337, 1062–1065 (2012).

69. van der Bliek, A. M., Shen, Q. & Kawajiri, S. Mechanisms of mitochondrial fission and fusion. *Cold Spring Harb. Perspect. Biol.* **5**, (2013).

70. Eisner, V., Picard, M. & Hajnóczky, G. Mitochondrial dynamics in adaptive and maladaptive cellular stress responses. *Nat Cell Biol* **20**, 755–765 (2018).

71. Yu, S. B. & Pekkurnaz, G. Mechanisms orchestrating mitochondrial dynamics for energy homeostasis. *J. Mol. Biol.* **430**, 3922–3941 (2018).

72. Casanueva, E. & Viteri, F. E. Iron and oxidative stress in pregnancy. *J. Nutr* **133**, 1700–1708 (2003).

73. Raha, S., Taylor, V. H. & Holloway, A. C. Effect of atypical antipsychotics on fetal growth: Is the placenta involved? *J. Pregnancy* **2012**, 1–9 (2012).

74. Twig, G. *et al.* Fission and selective fusion govern mitochondrial segregation and elimination by autophagy. *EMBO J.* **27**, 433–446 (2008).

75. Zorova, L. D. *et al.* Mitochondrial membrane potential. *Anal. Biochem.* **552**, 50–59 (2018).

76. Lenaz, G. & Genova, M. L. Structure and organization of mitochondrial respiratory complexes: A new understanding of an old subject. *Antioxid. Redox Signal.* **12**, 961–1008 (2010).

77. Jastroch, M., Divakaruni, A. S., Mookerjee, S., Treberg, J. R. & Brand, M. D. Mitochondrial proton and electron leaks. *Essays Biochem.* **47**, 53–67 (2010).

78. Divakaruni, A. S. & Brand, M. D. The regulation and physiology of mitochondrial proton leak. *Physiology* **26**, 192–205 (2011).

79. Myatt, L. & Cui, X. Oxidative stress in the placenta. *Histochem. Cell Biol.* **122**, 369–382 (2004).

80. Chukwudi Ikwegbue, P., Masamba, P., Oyinloye, B. E. & Kappo, A. P. Roles of Heat

Shock Proteins in Apoptosis, Oxidative Stress, Human Inflammatory Diseases, and Cancer. *Pharmaceuticals* **11**, (2017).

81.   Wagner, B., Venkataraman, S. & Buettner, G. The rate of oxygen utilization by cells. *Free Radic Biol Med* **51**, 700–712 (2011).

82.   Finkel, T. & Holbrook, N. J. Oxidants, oxidative stress and the biology of ageing. *Nature* **408**, 239–247 (2000).

83.   Poston, L. *et al.* Role of oxidative stress and antioxidant supplementation in pregnancy disorders. *Am. J. Clin. Nutr.* **94**, 1980S-1985S (2011).

84.   Ishihara, Y., Takemoto, T., Itoh, K., Ishida, A. & Yamazaki, T. Dual role of superoxide dismutase 2 induced in activated microglia OXIDATIVE STRESS TOLERANCE AND CONVERGENCE OF INFLAMMATORY RESPONSES. *J. Biol. Chem.* **290**, 22805–22817 (2015).

85.   Ighodaro, O. M. & Akinloye, O. A. First line defence antioxidants-superoxide dismutase (SOD), catalase (CAT) and glutathione peroxidase (GPX): Their fundamental role in the entire antioxidant defence grid. *Alexandria J. Med.* **54**, 287–293 (2018).

86.   Lobo, V., Patil, A., Phatak, A. & Chandra, N. Free radicals, antioxidants and functional foods: Impact on human health. *Pharmacognosy Reviews* **4**, 118–126 (2010).

87.   Raha, S. & Robinson, B. H. Mitochondria, oxygen free radicals, disease and ageing. *Trends Biochem. Sci.* **25**, 502–508 (2000).

88.   Mokhtari, V., Afsharian, P. & Shahhoseini, M. A review on various uses of N-acetyl cysteine. *Cell J.* **19**, 11–17 (2017).

89.   Wu, F., Tian, F.-J. & Lin, Y. Oxidative stress in placenta: Health and diseases. *Biomed Res. Int.* **2015**, 1–15 (2015).

90.   Beere, H. M. 'The stress of dying': The role of heat shock proteins in the regulation of

apoptosis. *J. Cell Sci.* **117**, 2641–2651 (2004).

91. Madamanchi, N. R., Li, S., Patterson, C. & Runge, M. S. Reactive oxygen species regulate heat-shock protein 70 via the JAK/STAT pathway. *Arter. Thromb Vasc Biol* **21**, 321–326 (2001).

92. Holland, O. *et al.* Review: Placental mitochondrial function and structure in gestational disorders. *Placenta* **54**, 2–9 (2017).

93. Fisher, J. J., Bartho, L. A., Perkins, A. V. & Holland, O. J. Placental mitochondria and reactive oxygen species in the physiology and pathophysiology of pregnancy. *Clin. Exp. Pharmacol. Physiol.* **47**, 176–184 (2020).

94. Lattuada, D. *et al.* Higher mitochondrial DNA content in human IUGR placenta. *Placenta* **29**, 1029–1033 (2008).

95. Poidatz, D. *et al.* Involvement of estrogen-related receptor-γ and mitochondrial content in intrauterine growth restriction and preeclampsia. *Fertil. Steril.* **104**, 483–490 (2015).

96. Martinez, F., Kiriakidou, M. & Strauss, J. F. Structural and functional changes in mitochondria associated with trophoblast differentiation: Methods to isolate enriched preparations of syncytiotrophoblast mitochondria. *Endocrinology* **138**, 2172–2183 (1997).

97. De Los Rios Castillo, D. *et al.* Atypical cristae morphology of human syncytiotrophoblast mitochondria: Role for complex V. *J. Biol. Chem.* **286**, 23911–23919 (2011).

98. Matsubara, S., Minakami, H., Sato, I. & Saito, T. Decrease in cytochrome c oxidase activity detected cytochemically in the placental trophoblast of patients with pre-eclampsia. *Placenta* **18**, 255–259 (1997).

99. Park, S. J. *et al.* HCG-induced endoplasmic reticulum stress triggers apoptosis and reduces steroidogenic enzyme expression through activating transcription factor 6 in Leydig cells of the testis. *J. Mol. Endocrinol.* **50**, 151–166 (2013).

100. Issop, L. *et al.* Mitochondria-Associated membrane formation in hormone-stimulated Leydig cell steroidogenesis: Role of ATAD3. *Endocrinology* **156**, 334–345 (2015).

101. Mandò, C. *et al.* Placental mitochondrial content and function in intrauterine growth restriction and preeclampsia. *Am J Physiol Endocrinol Metab* **306**, 404–413 (2014).

102. Costa, M. A., Fonseca, B. M., Marques, F., Teixeira, N. A. & Correia-da-Silva, G. The psychoactive compound of Cannabis sativa, Δ9-tetrahydrocannabinol (THC) inhibits the human trophoblast cell turnover. *Toxicology* **334**, 94–103 (2015).

103. Shibata, E. *et al.* Enhancement of mitochondrial oxidative stress and up-regulation of antioxidant protein peroxiredoxin III/SP-22 in the mitochondria of human pre-eclamptic placentae. *Placenta* **24**, 698–705 (2003).

104. Jauniaux, E. & Burton, G. J. Oxygen delivery at the deciduoplacental interface. in *Placental Bed Disorders* (eds. Pijnenborg, R., Brosens, I. & Romero, R.) 63–74 (Cambridge University Press, 2010). doi:10.1017/CBO9780511750847.009

105. Poidatz, D. *et al.* Trophoblast syncytialisation necessitates mitochondrial function through estrogen-related receptor-γ activation. *Mol. Hum. Reprod.* **21**, 206–216 (2015).

106. Hroudová, J. & Fišar, Z. In vitro inhibition of mitochondrial respiratory rate by antidepressants. *Toxicol. Lett.* **213**, 345–352 (2012).

107. Fato, R. *et al.* Differential effects of mitochondrial complex I inhibitors on production of reactive oxygen species. *Biochim Biophys Acta* **1787**, 384–392 (2009).

108. Li, N. *et al.* Mitochondrial complex I inhibitor rotenone induces apoptosis through enhancing mitochondrial reactive oxygen species production. *J. Biol. Chem.* **278**, 8516–8525 (2002).

109. Somasundaram, S. *et al.* Mitochondrial damage: A possible mechanism of the 'topical' phase of NSAID induced injury to the rat intestine. *Gut* **41**, 344–353 (1997).

110. Ireland, K. E., Maloyan, A. & Myatt, L. Melatonin improves mitochondrial respiration in syncytiotrophoblasts from placentas of obese women. *Reprod. Sci.* **25**, 120–130 (2018).

111. Melmed, S. Endocrinology of fetal development. in *Williams Textbook of Endocrinology* (ed. Melmed, S., Polonsky, K.S., Larsen, P.R., Kronenberg, H. M.) 877–878 (Elsevier Health Sciences, 2016).

112. Haylett, W. *et al.* Altered mitochondrial respiration and other features of mitochondrial function in parkin-mutant fibroblasts from Parkinson's Disease patients. *Park. Dis.* **2016**, (2016).

113. Dimauro, S. & Schon, E. A. Mitochondrial Respiratory-Chain Diseases. *New Engl J Med* **348**, 2656–68 (2003).

114. Olszewska, A. & Szewczyk, A. Mitochondria as a pharmacological target: Magnum overview. *IUBMB Life* **65**, 273–281 (2013).

115. Ma, J. *et al.* Mitochondrial dysfunction promotes breast cancer cell migration and invasion through HIF1a accumulation via increased production of reactive oxygen species. *PLoS One* **8**, e69485 (2013).

116. Hebert-Chatelain, E. *et al.* Cannabinoid control of brain bioenergetics: Exploring the subcellular localization of the CB1 receptor. *Mol. Metab.* **3**, 495–504 (2014).

117. Bénard, G. *et al.* Mitochondrial CB1 receptors regulate neuronal energy metabolism. *Nat. Neurosci.* **15**, 558–564 (2012).

118. Athanasiou, A. *et al.* Cannabinoid receptor agonists are mitochondrial inhibitors: A unified hypothesis of how cannabinoids modulate mitochondrial function and induce cell death. *Biochem. Biophys. Res. Commun.* **364**, 131–137 (2007).

119. Fišar, Z., Singh, N. & Hroudová, J. Cannabinoid-induced changes in respiration of brain mitochondria. *Toxicol. Lett.* **11**, 4 (2014).

120. Singh, N., Hroudová, J. & Fišar, Z. Cannabinoid-induced changes in the activity of electron transport chain complexes of brain mitochondria. *J. Mol. Neurosci.* **56**, 926–931 (2015).

121. Busquets-Garcia, A., Bains, J. & Marsicano, G. CB 1 Receptor Signaling in the Brain: Extracting Specificity from Ubiquity. *Neuropsychopharmacology* **43**, 4–20 (2018).

122. De Rasmo, D. *et al.* Intramitochondrial adenylyl cyclase controls the turnover of nuclear-encoded subunits and activity of mammalian complex I of the respiratory chain. *Biochim. Biophys. Acta* **2015**, 183–191 (2014).

123. Grant, K. S., Petroff, R., Isoherranen, N., Stella, N. & Burbacher, T. M. Cannabis use during pregnancy: Pharmacokinetics and effects on child development. *Pharmacol. Ther.* **182**, 133–151 (2018).

124. ElSohly, M. A. *et al.* Changes in cannabis potency over the last two decades (1995-2014) - Analysis of current data in the united states. *Biol. Psychiatry* **79**, 613–619 (2016).

125. Pacher, P., Batkai, S. & Kunos, G. The endocannabinoid system as an emerging target of pharmacotherapy. *Pharmacol Rev* **58**, 389–462 (2006).

126. Huestis, M. A. Human cannabinoid pharmacokinetics. *Chem. Biodivers.* **4**, 1770–1804 (2007).

127. Borgelt, L. M., Franson, K. L., Nussbaum, A. M., Wang, G. S. The pharmacologic and clinical effects of medical cannabis. *Pharmacotherapy* **33**, 195–209 (2013).

128. Iversen, L. L. *The Science of Marijuana*. (Oxford University Press, Inc., 2000).

129. Sharma, P., Murthy, P. & Bharath, M. M. S. Chemistry, metabolism, and toxicology of cannabis: Clinical implications. *Iran. J. Psychiatry* **7**, 149–156 (2012).

130. Brown, H. & Graves, C. Smoking and Marijuana Use in Pregnancy. *Clin. Obstet. Gynecol.* **56**, 107–113 (2010).

131. Corsi, D. J., Hsu, H., Weiss, D., Fell, D. B. & Walker, M. Trends and correlates of cannabis use in pregnancy: A population-based study in Ontario, Canada from 2012 to 2017. *Can. J. Public Heal.* **110**, 76–84 (2019).

132. Wu, C. S., Jew, C. P. & Lu, H. C. Lasting impacts of prenatal cannabis exposure and the role of endogenous cannabinoids in the developing brain. *Future Neurol.* **6**, 459–480 (2011).

133. Ko, J. Y., Farr, S. L., Tong, V. T., Creanga, A. A. & Callaghan, W. M. Prevalence and patterns of marijuana use among pregnant and nonpregnant women of reproductive age. *Am. J. Obstet. Gynecol.* **213**, e1-10 (2015).

134. Thompson, R., DeJong, K., Lo, J. & Gynecol Surv, O. Marijuana use in pregnancy: A review. *Obs. Gynecol Surv* **74**, 415–428 (2019).

135. Daniulaityte, R. *et al.* Characterizing marijuana concentrate users: A web-based survey. *Drug Alcohol Depend* **178**, 399–407 (2017).

136. Braillon, A. & Bewley, S. ACOG committee opinion: Marijuana use during pregnancy and lactation. *Obstet. Gynecol.* **130**, e205–e209 (2017).

137. Behnke, M. & Smith, V. C. Prenatal Substance Abuse: Short- and Long-term Effects on the Exposed Fetus. *Pediatrics* **131**, e1009–e1024 (2013).

138. Westfall, R. E., Janssen, P. A., Lucas, P. & Capler, R. Survey of medicinal cannabis use among childbearing women: Patterns of its use in pregnancy and retroactive self-assessment of its efficacy against 'morning sickness'. *Complement. Ther. Clin. Pract.* **12**, 27–33 (2006).

139. Brown, Q. L. *et al.* Trends in marijuana use among pregnant and non-pregnant reproductive-aged women, 2002-2014 HHS Public Access Author manuscript. *JAMA* **317**, 207–209 (2017).

140. Cannabis Legalization and Regulation. (2019). Available at: https://www.justice.gc.ca/eng/cj-jp/cannabis/. (Accessed: 17th October 2019)

141. Habayeb, O. M. H., Taylor, A. H., Bell, S. C., Taylor, D. J. & Konje, J. C. Expression of the endocannabinoid system in human first trimester placenta and its role in trophoblast proliferation. *Endocrinology* **149**, 5052–5060 (2008).

142. Al-Zouabi, I., Stogner, J. M., Miller, B. L. & Lane, E. S. Butane hash oil and dabbing: Insights into use, amateur production techniques, and potential harm mitigation. *Subst. Abuse Rehabil.* **9**, 91–101 (2018).

143. Bow, E. & Rimoldi, J. The structure-function relationship of classical cannabinoids: CB1/CB2 modulation. *Perspect. Medicin. Chem.* **8**, 17–39 (2016).

144. Reggio, P. H. Endocannabinoid binding to the cannabinoid receptors: What is known and what remains unknown. *Curr. Med. Chem.* **17**, 1468–86 (2010).

145. Trost, B. M. & Dogra, K. Synthesis of (-)-Δ 9-trans-tetrahydrocannabinol-stereocontrol via mo-catalyzed asymmetric allylic alkylation reaction. *Org Lett* **9**, 861–863 (2007).

146. Parker, L. A., Rock, E. M. & Limebeer, C. L. Regulation of nausea and vomiting by cannabinoids and the endocannabinoid system. *Eur. J. Pharmacol.* **722**, 134–146 (2014).

147. Webb, C. W. & Webb, S. M. Therapeutic benefits of cannabis: A patient survey. *Hawai'i J. Med. Public Heal.* **73**, 109–11 (2014).

148. ElSohly, M. A., Mehmedic, Z., Foster, S., Gon, C., Chandra, S., Church, J. C. Changes in cannabis potency over the last 2 decades (1995-2014): Analysis of current data in the United States. *Biol. Psychiatry* **79**, 613–619 (2016).

149. Richardson, K. A., Hester, A. K. & McLemore, G. L. Prenatal cannabis exposure - The "first hit" to the endocannabinoid system. *Neurotoxicol. Teratol.* **58**, 5–14 (2016).

150. ElSohly, M. *et al.* Potency trends of delta9-THC and other cannabinoids in confiscated

marijuana from 1980-1997. *J. Forensic Sci.* **45**, 24–30 (2000).

151. Raikos, N. *et al.* Determination of δ9-tetrahydrocannabinolic acid A (δ9-THCA-A) in whole blood and plasma by LC-MS/MS and application in authentic samples from drivers suspected of driving under the influence of cannabis. *Forensic Sci. Int.* **243**, 130–136 (2014).

152. Adams, I. B. & Martin, B. R. Cannabis: Pharmacology and toxicology in animals and humans. *Addiction* **91**, 1585–1614 (1996).

153. Lucas, C. J., Galettis, P. & Schneider, J. The pharmacokinetics and the pharmacodynamics of cannabinoids. *Br. J. Clin. Pharmacol.* **84**, 2477–2482 (2018).

154. Johansson, E., Agurell, S., Hollister, L. E. & Halldin, M. M. Prolonged apparent half-life of Δ1-tetrahydrocannabinol in plasma of chronic marijuana users. *J. Pharm. Pharmacol.* **40**, 374–375 (1988).

155. Toennes, S., Ramaekers, J., Theunissen, E., Moeller, M. & Kauert, G. Comparison of cannabinoid pharmacokinetic properties in occasional and heavy users smoking a marijuana or placebo joint. *J. Anal. Toxicol.* **32**, 470–477 (2008).

156. Glaz-Sandberg, A. *et al.* Pharmacokinetics of 11-nor-9-Carboxy-Δ9-Tetrahydrocannabinol (CTHC) After Intravenous Administration of CTHC in Healthy Human Subjects. *Clin. Pharmacol. Ther.* **82**, 63–69 (2007).

157. Garrett, E. R. & Hunt, C. A. Pharmacokinetics of Δ9-tetrahydrocannabinol in dogs. *J. Pharm. Sci.* **66**, 395–407 (1977).

158. Bergamaschi, M. M. *et al.* Impact of prolonged cannabinoid excretion in chronic daily cannabis smokers' blood on per se drugged driving laws. *Clin. Chem.* **59**, 519–526 (2012).

159. Schwope, D. M., Karschner, E. L., Gorelick, D. A. & Huestis, M. A. Identification of recent cannabis use: Whole-blood and plasma free and glucuronidated cannabinoid

pharmacokinetics following controlled smoked cannabis administration. *Clin. Chem.* **57**, 1406–1414 (2011).

160. Hunault, C. C. *et al.* Delta-9-tetrahydrocannabinol (THC) serum concentrations and pharmacological effects in males after smoking a combination of tobacco and cannabis containing up to 69 mg THC. *Psychopharmacology (Berl).* **201**, 171–181 (2008).

161. Huestis, M. A., Henningfield, J. E. & Cone, E. J. Blood cannabinoids. I. Absorption of THC and formation of 11-OH-THC and THCCOOH during and after smoking marijuana. *J. Anal. Toxicol.* **16**, 276–282 (1992).

162. Karschner, E. L. *et al.* Predictive model accuracy in estimating last Δ 9-tetrahydrocannabinol (THC) intake from plasma and whole blood cannabinoid concentrations in chronic, daily cannabis smokers administered subchronic oral THC. *Drug Alcohol Depend* **125**, 313–319 (2012).

163. Lozano, J. *et al.* Prevalence of gestational exposure to cannabis in a Mediterranean city by meconium analysis. *Acta Paediatr. Int. J. Paediatr.* **96**, 1734–1737 (2007).

164. Kim, J. *et al.* Detection of in utero cannabis exposure by umbilical cord analysis. *Drug Test. Anal.* **10**, 636–643 (2018).

165. Isoherranen, N. & Thummel, K. E. Drug metabolism and transport during pregnancy: How does drug disposition change during pregnancy and what are the mechanisms that cause such changes? *Drug Metabolism and Disposition* **41**, 256–262 (2013).

166. Nahas, G., Paton, W. & Harvey, D. The Reims Symposium. in *Marihuana and Medicine* (eds. Nahas, G., Sutin, K., Harvey, D. & Agurell, S.) 13–19 (Humana Press, 1999).

167. Paton, W. Cannabis and its problems. *Proc. roy. Soc. Med* **66**, 718–721 (1973).

168. Meech, R. & Mackenzie, P. I. Brief review: Structure and function of uridine diphosphate glucuronosyltransferases. *Clin. Exp. Pharmacol. Physiol.* **24**, 907–915 (1997).

169. Maccarrone, M., Dainese, E. & Oddi, S. Intracellular trafficking of anandamide: New concepts for signaling. *Trends Biochem. Sci.* **35**, 601–608 (2010).

170. Pyszniak, M., Tabarkiewicz, J. & Łuszczki, J. J. Endocannabinoid system as a regulator of tumor cell malignancy – biological pathways and clinical significance. *Onco. Targets. Ther.* **9**, 4323–4336 (2016).

171. Pertwee, R. G. *et al.* International union of basic and clinical pharmacology. LXXIX. Cannabinoid receptors and their ligands: Beyond CB1 and CB2. *Pharmacol. Rev.* **62**, 588–631 (2010).

172. Fezza, F. *et al.* Endocannabinoids, related compounds and their metabolic routes. *Molecules* **19**, 17078–17106 (2014).

173. Muccioli, G. G. Endocannabinoid biosynthesis and inactivation, from simple to complex. *Drug Discov. Today* **15**, 474–483 (2010).

174. Kano, M., Ohno-Shosaku, T., Hashimotodani, Y., Uchigashima, M. & Watanabe, M. Endocannabinoid-mediated control of synaptic transmission. *Physiol Rev* **89**, 309–380 (2009).

175. Leung, D., Saghatelian, A., Simon, G. M. & Cravatt, B. F. *Inactivation of N-acyl phosphatidylethanolamine phospholipase D reveals multiple mechanisms for the biosynthesis of endocannabinoids*. *Biochemistry* **45**, (2006).

176. Chicca, A., Marazzi, J., Nicolussi, S. & Gertsch, J. Evidence for bidirectional endocannabinoid transport across cell membranes. *J. Biol. Chem.* **287**, 34660–34682 (2012).

177. Bisogno, T. *et al.* Cloning of the first sn1-DAG lipases points to the spatial and temporal regulation of endocannabinoid signaling in the brain. *J. Cell Biol.* **163**, 463–468 (2003).

178. Ueda, H., Kobayashi, T., Kishimoto, M., Tsutsumi, T. & Okuyama, H. A possible pathway

of phosphoinositide metabolism through EDTA-insensitive phospholipase A1 followed by lysophosphoinositide-specific phospholipase C in rat brain. *J. Neurochem.* **61**, 1874–1881 (1993).

179. Lipina, C., Irving, A. J. & Hundal, H. S. Mitochondria: A possible nexus for the regulation of energy homeostasis by the endocannabinoid system? *Am J Physiol Endocrinol Metab* **307**, 1–13 (2014).

180. Fowler, C. J. Transport of endocannabinoids across the plasma membrane and within the cell. *FEBS J.* **280**, 1895–1904 (2013).

181. Baggelaar, M. P., Maccarrone, M. & van der Stelt, M. 2-Arachidonoylglycerol: A signaling lipid with manifold actions in the brain. *Progress in Lipid Research* **71**, 1–17 (2018).

182. Fegley, D. *et al.* Anandamide transport is independent of fatty-acid amide hydrolase activity and is blocked by the hydrolysis-resistant inhibitor AM1172. *Proc. Natl. Acad. Sci. U. S. A.* **101**, 8756–8761 (2004).

183. Bisogno, T., De Petrocellis, L. & Di Marzo, V. Fatty acid amide hydrolase, an enzyme with many bioactive substrates. Possible therapeutic implications. *Curr. Pharm. Des.* **8**, 533–47 (2002).

184. Pertwee, R. G. Pharmacology of cannabinoid CB1 and CB2 receptors. *Pharmacol. Ther.* **74**, 129–180 (1997).

185. El-Talatini, M. R. *et al.* Localisation and function of the endocannabinoid system in the human ovary. *PLoS One* **4**, e4579 (2009).

186. Matsuda, L. A., Lolait, S. J., Brownstein, M. J., Young, A. C. & Bonner, T. I. Structure of a cannabinoid receptor and functional expression of the cloned cDNA. *Nature* **346**, 561–564 (1990).

187. Munro, S., Thomas, K. L. & Abu-Shaar, M. Molecular characterization of a peripheral receptor for cannabinoids. *Nature* **365**, 61–65 (1993).

188. Tuteja, N. Signaling through G protein coupled receptors. *Plant Signal. Behav.* **4**, 942–947 (2009).

189. McKallip, R. J., Lombard, C., Martin, B. R., Nagarkatti, M. & Nagarkatti, P. S. Delta(9)-tetrahydrocannabinol-induced apoptosis in the thymus and spleen as a mechanism of immunosuppression in vitro and in vivo. *J. Pharmacol. Exp. Ther.* **302**, 451–465 (2002).

190. Lojpur, T. *et al.* Δ9-Tetrahydrocannabinol leads to endoplasmic reticulum stress and mitochondrial dysfunction in human BeWo trophoblasts. *Reprod. Toxicol.* **87**, 21–31 (2019).

191. Hebert-Chatelain, E. *et al.* A cannabinoid link between mitochondria and memory. *Nature* **539**, 555–559 (2016).

192. Hermanson, D.J., Marnett, L. J. Cannabinoids, Endocannabinoids and Cancer. *Cancer Metastasis Rev* **30**, 599–612 (2011).

193. Harkany, T. & Horvath, T. L. (S)Pot on mitochondria: Cannabinoids disrupt cellular respiration to limit neuronal activity. *Cell Metab.* **25**, 8–10 (2017).

194. Sánchez, C., Velasco, G. & Guzmán, M. δ9-tetrahydrocannabinol stimulates glucose utilization in C6 glioma cells. *Brain Res.* **767**, 64–71 (1997).

195. Natale, B. V *et al.* Δ9-tetrahydrocannabinol exposure during rat pregnancy leads to symmetrical fetal growth restriction and labyrinth-specific vascular defects in the placenta. *Sci. Rep.* **10**, (2020).

196. Xie, H. *et al.* Silencing or amplification of endocannabinoid signaling in blastocysts via CB1 compromises trophoblast cell migration. *J. Biol. Chem.* **287**, 32288–32297 (2012).

197. Benevenuto, S. G. *et al.* Recreational use of marijuana during pregnancy and negative

gestational and fetal outcomes: An experimental study in mice. *Toxicology* **376**, 94–101 (2017).

198. Wasserman, E., Tam, J., Mechoulam, R., Zimmer, A., Maor, G., Bab, I. CB1 cannabinoid receptors mediate endochondral skeletal growth attenuation by Δ9-tetrahydrocannabinol. *Ann. N. Y. Acad. Sci.* **1335**, 110–119 (2015).

199. de Salas-Quiroga, A. *et al.* Prenatal exposure to cannabinoids evokes long-lasting functional alterations by targeting CB 1 receptors on developing cortical neurons. *Proc. Natl. Acad. Sci.* **112**, 13693–13698 (2015).

200. Panlilio, L. V. *et al.* Combined effects of THC and caffeine on working memory in rats. *Br. J. Pharmacol.* **165**, 2529–2538 (2012).

201. Campolongo, P., Trezza, V., Ratano, P., Palmery, M. & Cuomo, V. Developmental consequences of perinatal cannabis exposure: Behavioral and neuroendocrine effects in adult rodents. *Psychopharmacology (Berl).* **214**, 5–15 (2011).

202. Iversen, L. Cannabis and the brain. *Brain* **126**, 1252–1270 (2003).

203. Cecconi, S., Rossi, G., Castellucci, A., D'Andrea, G. & Maccarrone, M. Endocannabinoid signaling in mammalian ovary. *Eur. J. Obstet. Gynecol. Reprod. Biol.* **178**, 6–11 (2014).

204. Battista, N. *et al.* The role of endocannabinoids in gonadal function and fertility along the evolutionary axis. *Mol. Cell. Endocrinol.* **355**, 1–14 (2012).

205. Harris, A. L. & Okorie, C. S. Assessing Marijuana Use During Pregnancy. *Nurs. Womens. Health* **21**, 207–216 (2017).

206. Kleven, G. A. & Ronca, A. E. Prenatal behavior of the C57BL/6J mouse: A promising model for human fetal movement during early to mid-gestation. *Dev Psychobiol* **51**, 84–94 (2009).

207. Almada, M. *et al.* Anandamide interferes with human endometrial stromal derived-cell

differentiation: An effect dependent on inhibition of COX-2 expression and PGE2 release. *Biofactors* **42**, 277–286 (2016).

208. Scotchie, J. G., Savaris, R. F., Martin, C. E. & Young, S. L. Endocannabinoid regulation in human endometrium across the menstrual cycle. *Reprod. Sci.* **22**, 113–123 (2015).

209. Schuel, H. Tuning the oviduct to the anandamide tone. *J. Clin. Invest.* **116**, 2087–2090 (2006).

210. Maccarrone, M. Endocannabinoids: Friends and foes of reproduction. *Prog. Lipid Res.* **48**, 344–354 (2009).

211. Taylor, A. H., Ang, C., Bell, S. C. & Konje, J. C. The role of the endocannabinoid system in gametogenesis, implantation and early pregnancy. *Hum. Reprod. Update* **13**, 501–513 (2007).

212. Park, B., McPartland, J. M. & Glass, M. Cannabis, cannabinoids and reproduction. *Prostaglandins Leukot. Essent. Fat. Acids* **70**, 189–197 (2004).

213. Fügedi, G. *et al.* Increased placental expression of cannabinoid receptor 1 in preeclampsia: An observational study. *BMC Pregnancy Childbirth* **14**, 1–8 (2014).

214. Marchetti, D., Di Masi, G., Cittadini, F., La Monaca, G. & De Giovanni, N. Placenta as alternative specimen to detect in utero cannabis exposure: A systematic review of the literature. *Reprod. Toxicol.* **73**, 250–258 (2017).

215. Khare, M., Taylor, A. H., Konje, J. C. & Bell, S. C. Delta 9-Tetrahydrocannabinol inhibits cytotrophoblast cell proliferation and modulates gene transcription. *Mol. Hum. Reprod.* **12**, 321–333 (2006).

216. Chang, X. *et al.* Suppression of STAT3 signaling by Δ9-tetrahydrocannabinol (THC) induces trophoblast dysfunction. *Cell. Physiol. Biochem.* **42**, 537–550 (2017).

217. Ross, E. J., Graham, D. L., Money, K. M. & Stanwood, G. D. Developmental

consequences of fetal exposure to drugs: What we know and what we still must learn. *Neuropsychopharmacology* **40**, 61–87 (2015).

218. Wang, Y. & Walsh, S. W. Placental mitochondria as a source of oxidative stress in pre-eclampsia. *Placenta* **19**, 581–586 (1998).

219. Mayeur, S. *et al.* Maternal calorie restriction modulates placental mitochondrial biogenesis and bioenergetic efficiency: Putative involvement in fetoplacental growth defects in rats. *Am J Physiol Endocrinol Metab* **304**, 14–22 (2013).

220. Wakefield, S. L., Lane, M. & Mitchell, M. Impaired mitochondrial function in the preimplantation embryo perturbs fetal and placental development in the mouse. *Biol. Reprod.* **84**, 572–580 (2011).

221. Akhigbe, R. & Id, A. A. Testicular toxicity following chronic codeine administration is via oxidative DNA damage and up-regulation of NO/TNF-α and caspase 3 activities. *PLoS One* **15**, e0224052 (2020).

222. Mette Hoegh, A., Borup, R., Cilius Nielsen, F., Sørensen, S. & F Hviid, T. V. Gene expression profiling of placentas affected by pre-eclampsia. *J. Biomed. Biotechnol.* **2010**, 11 (2010).

223. Biri, A. *et al.* Investigation of free radical scavenging enzyme activities and lipid peroxidation in human placental tissues with miscarriage. *J. Soc. Gynecol. Investig.* **13**, 384–388 (2006).

224. Novakovic, B. *et al.* Wide ranging DNA methylation differences of primary trophoblast cell populations and derived-cell lines: implications and opportunities for understanding trophoblast function. *Mol Hum Reprod* **17**, 344–353 (2011).

225. Wheaton, W. W. *et al.* Metformin inhibits mitochondrial complex I of cancer cells to reduce tumorigenesis. *Elife* **3**, e02242 (2014).

226. Urra, F. A., Muñoz, F., Lovy, A. & Cárdenas, C. The mitochondrial complex(i)ty of cancer. *Front. Oncol.* **7**, 1–8 (2017).

227. Pryde, K. R. & Hirst, J. Superoxide is produced by the reduced flavin in mitochondrial complex I A SINGLE, UNIFIED MECHANISM THAT APPLIES DURING BOTH FORWARD AND REVERSE ELECTRON TRANSFER. *J. Biol. Chem.* **286**, 18056–18065 (2011).

228. Sarafian, T. A., Kouyoumjian, S., Khoshaghideh, F., Tashkin, D. P. & Roth, M. D. Delta-9-tetrahydrocannabinol disrupts mitochondrial function and cell energetics. *Am. J. Physiol. Lung Cell Mol. Physiol.* **284**, L298–L306 (2003).

229. Korge, P., Calmettes, G., Weiss, J. N., Biophys, B. & Author, A. Increased Reactive Oxygen Species Production During Reductive Stress: The Roles of Mitochondrial Glutathione and Thioredoxin Reductases HHS Public Access Author manuscript. *Biochim Biophys Acta* **1847**, 514–525 (2015).

230. Cassidy-Stone, A. *et al.* Chemical inhibition of the mitochondrial division dynamin reveals its role in bax/bak-dependent mitochondrial outer membrane permeabilization. *Dev. Cell* **14**, 193–204 (2008).

231. Gallily, R., Yekhtin, Z. & Hanuš, L. O. The anti-inflammatory properties of terpenoids from cannabis. *Cannabis Cannabinoid Res.* **3.1**, 282–290 (2018).

232. Ferber, S. G. *et al.* The "entourage effect": Terpenes coupled with cannabinoids for the treatment of mood disorders and anxiety disorders. *Curr. Neuropharmacol.* **18**, 87–96 (2019).

233. Lafaye, G., Karila, L., Blecha, L. & Benyamina, A. Cannabis, cannabinoids, and health. *Dialogues Clin. Neurosci.* **19**, 309–316 (2017).

234. Stith, S. S., Vigil, J. M., Brockelman, F., Keeling, K. & Hall, B. The association between

cannabis product characteristics and symptom relief. *Sci. Rep.* **9**, (2019).

235. Wice, B., Menton, D., Geuze, H. & Schwartz, A. L. Modulators of cyclic AMP metabolism induce syncytiotrophoblast formation in vitro. *Exp. Cell Res.* **186**, 306–316 (1990).

236. Pelekanos, R. A. *et al.* Isolation and expansion of mesenchymal stem/stromal cells derived from human placenta tissue. *J. Vis. Exp* **54204**, (2016).

237. Sullivan, M. Endocrine cell lines from the placenta. *Mol. Cell. Endocrinol.* **228**, 103–119 (2004).

238. Renaud, S. J. Strategies for investigating hemochorial placentation. in *Reproductive and Developmental Toxicology (Second Edition)* 1259–1273 (Elsevier, 2017).

APPENDICES: SUPPLEMENTARY FIGURES

APPENDIX A: ROTENONE INHIBITS INVASION OF HTR8/SVNEO CELLS
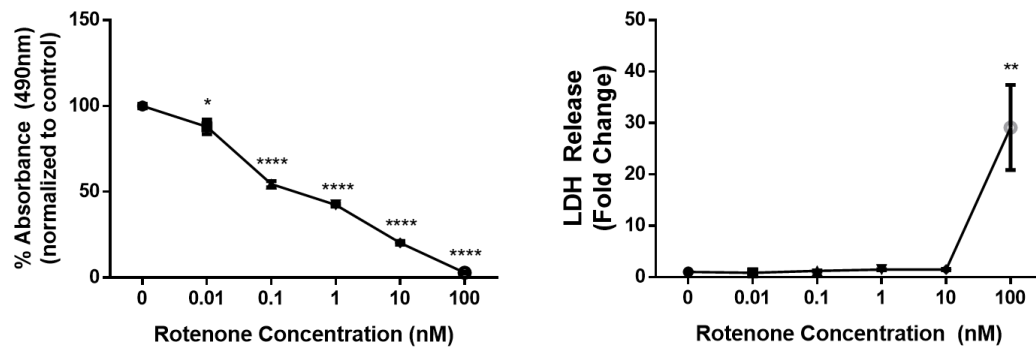

Figure A1.   0.1 nM rotenone negatively impacts proliferation of HTR8/SVneo cells without induction of cell membrane damage.
The trophoblast cells were treated with rotenone as indicated. Panel **A**: MTS data. Panel **B**: LDH data. Each data point represents the mean ± SEM of 3 replicates. Significant differences were determined by a one-way ANOVA followed by a Bonferroni post hoc test. * $P < 0.05$; ** $P < 0.01$; **** $P < 0.0001$.
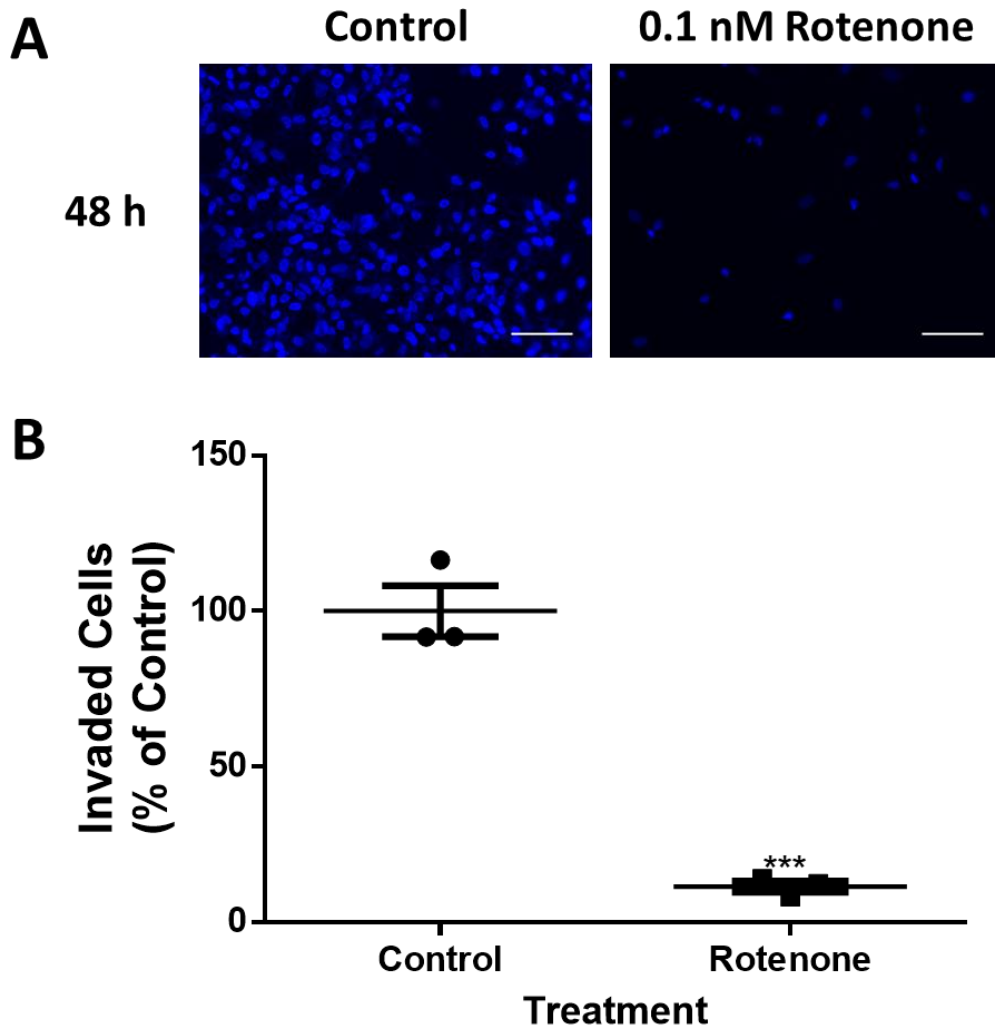
Figure A2. Rotenone inhibits transwell invasion of HTR8/SVneo cells.
HTR8/SVneo cells were added to Matrigel®-coated insert wells. The inserts were incubated for 48 hours with 0.1 nM rotenone, a mitochondrial complex I inhibitor. **(A)** Representative immunofluorescent images of invaded HTR8/SVneo cells are shown, with the nuclei staining blue, magnification 200x and scale bar indicates 100µm. **(B)** HTR8/SVneo cell invasion was quantified by counting the number of cells that invaded to the basal side of the porous polycarbonate membrane following fluorescent microscopy. Cell counts were performed, the average of which were calculated to determine the number of invaded cells relative to the vehicle control (DMSO). A summary histogram indicating the percentage of invaded cells relative to the control group is shown, with each data point representing the mean ± SEM (n = 3). Significant differences were determined by Student's t-test, *** $P < 0.001$ (B).
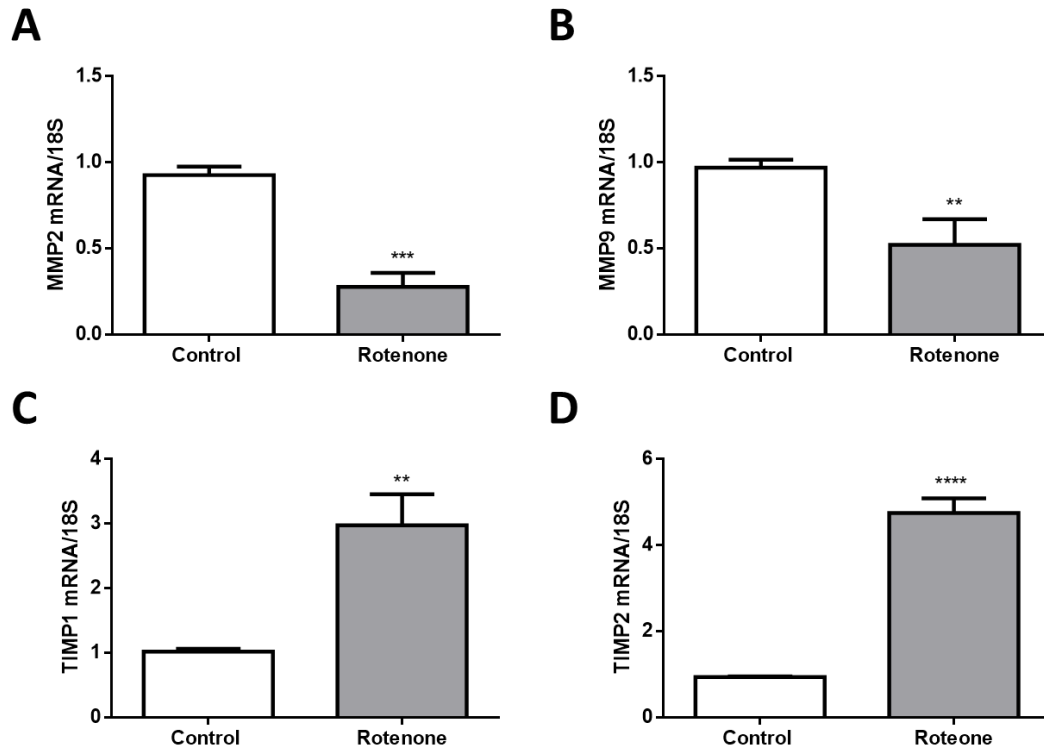
Figure A3. 0.1 nM rotenone alters the mRNA expression of degradative enzymes and their inhibitors.

HTR8/SVneo cells were treated as indicated for 48 hours. Total RNA was isolated from HTR8/SVneo cells and analyzed by RT-PCR (1 µg) with 18S used as the housekeeping gene. Summary histograms of relative MMP2 (**A**), MMP9 (**B**), TIMP1 (**C**), and TIMP2 (**D**) mRNA expression in each treatment group normalized to 18S, then compared to the gene in the vehicle control. Significant differences were determined by a student's t test. ** $P < 0.01$; *** $P < 0.001$; **** $P < 0.0001$.
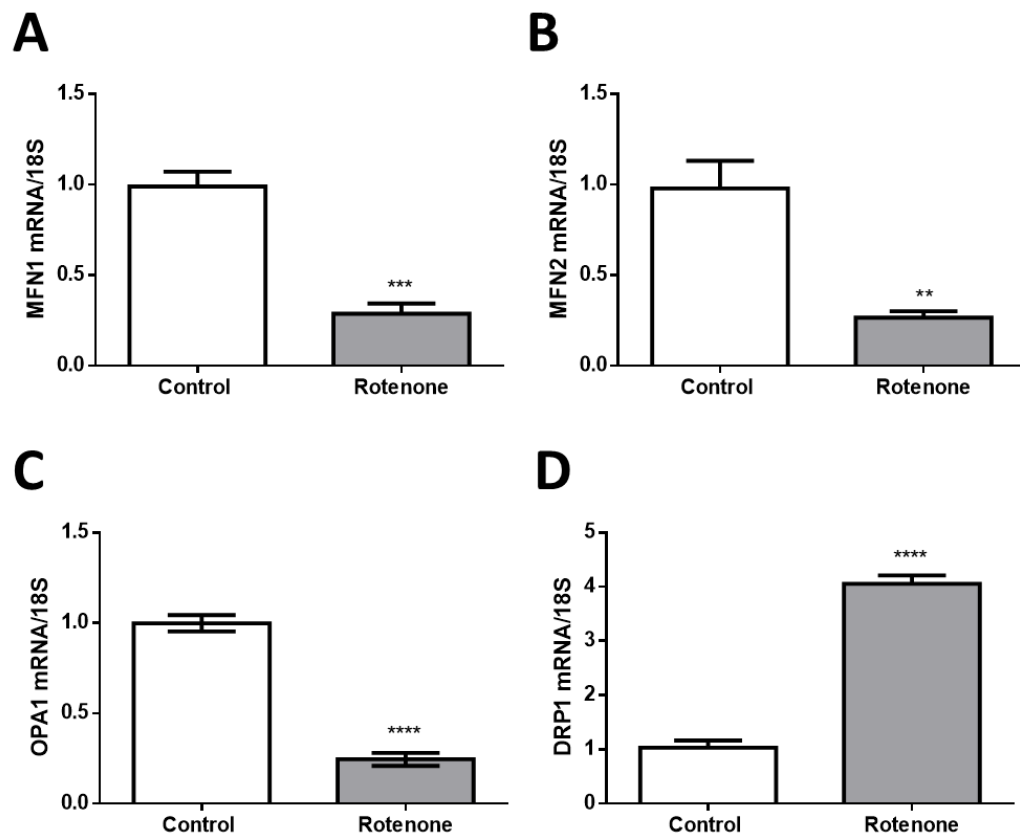
Figure A4. **Mitochondrial fusion and fission transcripts are altered in response to 0.1 nM rotenone in HTR8/SVneo cells.**
Summary histograms are shown of relative MFN1 (**A**), MFN2 (**B**) OPA1 (**C**) and DRP1 (**D**) mRNA expression in each treatment group were normalized to 18S, then compared to the gene in the vehicle control group. Significant differences were determined by student's t test. Data are presented as means ± SEM (n = 3). ** $P < 0.01$; *** $P < 0.001$; **** $P < 0.0001$.
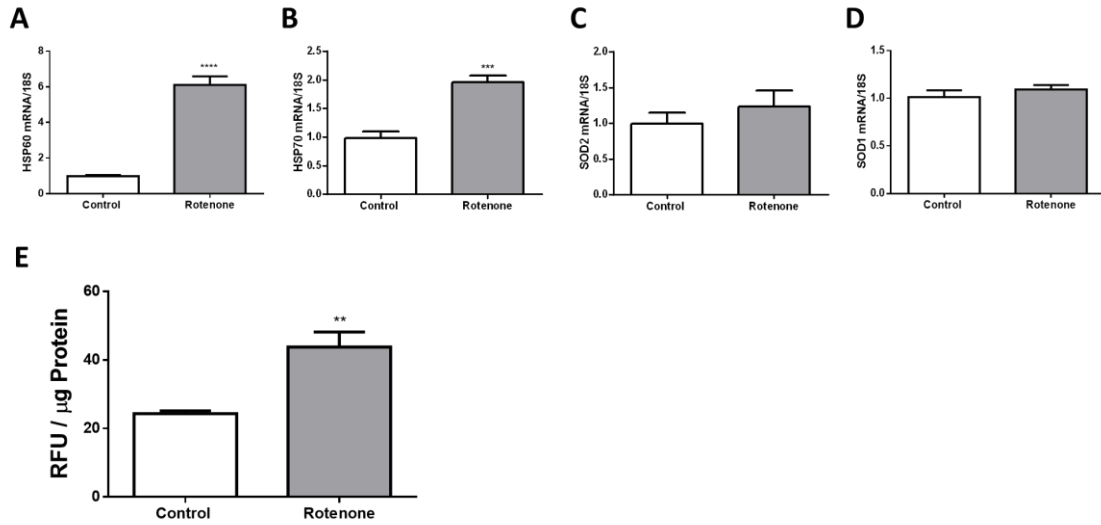
Figure A5. **Rotenone increases transcriptional markers of stress responses and ROS production in HTR8/SVneo cells without changing the intracellular defenses.**
Summary histograms are shown of relative HSP60 (**A**), HSP70 (**B**) SOD2 (**C**) and SOD1 (**D**) transcript expression in each treatment group were normalized to 18S, then compared to the gene in the vehicle control group. (**E**) DCFDA assays were performed to determine intracellular ROS levels following rotenone treatment. Tert-Butyl Hydrogen Peroxide (TBHP) solution (100 µM) was used as the positive control. Results were normalized to the protein content of cell lysates via the BCA assay, which enables the standardization of ROS production as a function of cell number (protein level). Significant differences were determined by student's t test. Data are presented as mean ± SEM (n = 3). ** $P < 0.01$; *** $P < 0.001$; **** $P < 0.0001$.

APPENDIX B: MITOCHONDRIAL RESPIRATION INDICES IN UNDIFFERENTIATED BEWO CELLS AND CANNABINOID RECEPTOR INVOLVEMENT
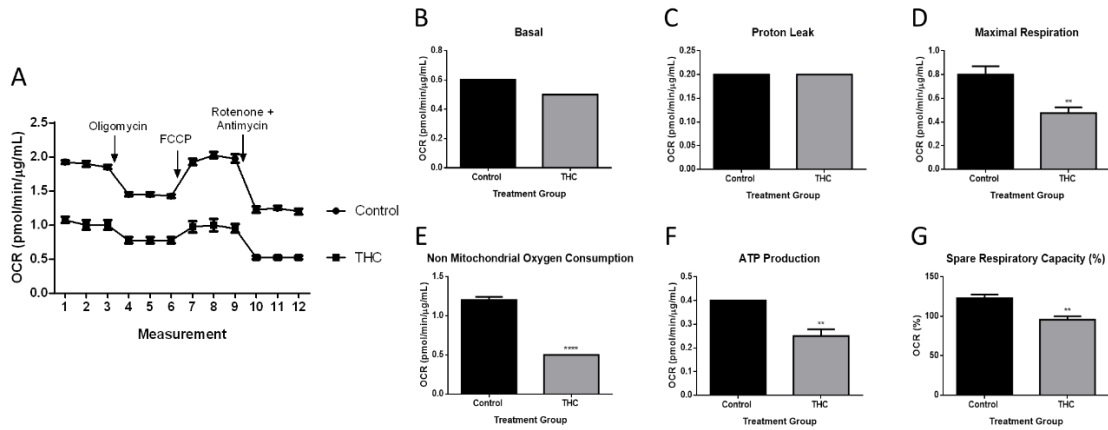
Figure B1. Mitochondrial respiration indices are impaired in CT cells upon exposure to THC.

(A) Representative mitochondrial profile. (B-G) Mitochondrial parameters as indicated. The detection of OCR was performed with 4 biological replicates per experiment, for each treatment condition, and repeated 3 more times. Group mean and SEM (A-G) are shown. Significance was assessed by Student's t-test (**P < 0.01, ****P < 0.0001).
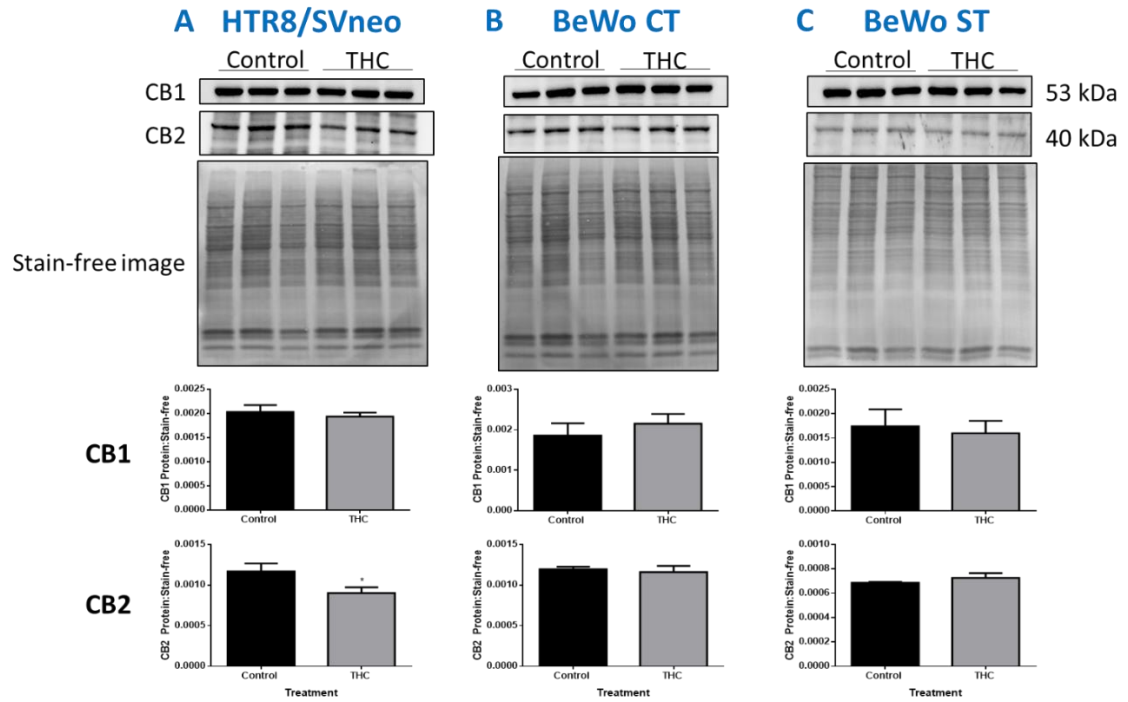
Figure B2. CB1 and CB2 expression in HTR8/SVneo and BeWo cells exposed to THC.
Cells were treated with vehicle or THC for 48 hours. Western blots, and graphs of CB1 and CB2 quantification are shown. Mean ± SEM, n=3, * P < 0.05 compared to vehicle control group (A).